# The ontogeny of inflammatory macrophages and monocyte-derived dendritic cells.

Menezes, Shinelle Geraldine

*Awarding institution:*
King's College London

KING'S College LONDON

# The ontogeny of inflammatory macrophages and monocyte-derived dendritic cells

By Shinelle G. Menezes

This thesis is submitted to King's College London for the degree of Doctor of Philosophy

September, 2016

# Abstract

Inflammation triggers the recruitment and differentiation of inflammatory monocytes into microbicidal phagocytes or monocyte-derived dendritic cells (moDCs). It is unclear if environmental inflammatory cues control the polarization of monocytes toward each of these fates or if specialized monocyte progenitor subsets exist prior to inflammation. Here I show that naïve monocytes are heterogeneous and contain an NR4A1- and Flt3L-independent, CCR2-dependent, $Flt3^{+}CD11c^{-}MHCII^{+}PU.1^{high}$ subset. This subset acts as a precursor for $Fc\gamma RII/III^{+}PD\text{-}L2^{+}CD209^{+}$, GM-CSF-dependent moDCs but is distal from the DC lineage as shown by fate mapping experiments using *Zbtb46*. By contrast, $Flt3^{-}CD11c^{-}MHCII^{-}PU.1^{low}$ monocytes differentiate into $Fc\gamma RII/III^{+}PD\text{-}L2^{-}CD209^{-}iNOS^{+}$ macrophages upon microbial stimulation. Importantly, *Sfpi1/Pu.1* haplo-insufficiency genetically distinguishes the precursor activities of monocytes toward moDCs or microbicidal macrophages. Indeed, $Sfpi1^{+/-}$ mice have reduced $Flt3^{+}CD11c^{-}MHCII^{+}$ monocytes and GM-CSF-dependent $Fc\gamma RII/III^{+}PD\text{-}L2^{+}CD209^{+}$ moDCs but generate $iNOS^{+}$ macrophages more efficiently. Therefore, intercellular disparities of PU.1 expression within naive monocytes segregate progenitor activity for inflammatory microbicidal macrophages or moDCs.

# Acknowledgements

I would like to thank Pierre for his guidance and advice on the project through my PhD. I am very grateful to Giorgio, Enric and Rajen for their help and support and their never-say-die attitude making life at the lab a memorable experience.

Thanks to Celine for ‘knowing all’, all the members of the CMCBI and my collaborators for being encouraging and helpful.

Life in London and surviving the biggest challenges of my PhD would not have been possible without my faith, Sandy, Adrian, Mum and Dad – I will always be grateful.

# Declaration

I declare that I have personally prepared this thesis, and that the work included is my own unless otherwise stated. All information sources included in this thesis are referenced accordingly.

Shinelle G. Menezes

September, 2016

# Table of Contents

# Table of Figures

# Table of Tables

# Abbreviations

BMDMs: Bone marrow -derived macrophages

cDC: Classical dendritic cell

CDP: Common DC precursor

CFU-S: Colony-forming-unit spleen

cMOP: common monocyte precursor

DC-SIGN: Dendritic cell- specific ICAM3- grabbing non-integrin

DEG: Differentially expressed genes

EAE: Experimental autoimmune encephalomyelitis

GFP: Green Fluorescent protein

GM-CSF: Granulocyte macrophage colony stimulating factor.

GM-DCs: GM-CSF induced dendritic cells

HDM: House dust-mite

iNOS: Inducible nitric oxide synthase

ITSM: immune-receptor tyrosine switch motif

JAK: Janus Kinase

*L.m.* : Listeria monocytogenes

LPS: Lipopolysaccharide

LyzM: Lysozyme

M-CSF: macrophage colony stimulating factor]

MDSCs: myeloid-derived suppressor cells

MHCII: Major Histocompatibility Complex Class II

Mo-DCs: Monocyte-derived dendritic cells

MOG: myelin oligodendrocyte glycoprotein

MPS: Mononuclear phagocyte system

NO: nitric oxide

PCA: Principle Component Analysis

PRRs: Pattern-recognition receptors

STAT: signal transducer and activator of transcription

TLR: Toll like receptor

TNF-α: Tumour necrosis factor alpha

WT: Wild type

*zDC*$^{DTR/DTR}$: Zbtb46-DTR

# 1 Introduction

## 1.1 A historical perspective of immunity

'There is at the end only one genuinely scientific treatment for all diseases, and that is to stimulate the phagocytes.' – *The Doctor's Dilemma.*

George Bernard Shaw's play was written in 1908, the same year the Nobel prize for Medicine was awarded to Ilya Metchnikoff for his discovery of phagocytosis. By the time of his discovery, the 'germ theory of disease' put forth by Robert Koch and Louis Pasteur was well accepted and Jenner's initial discovery of immunization against small pox (1796) had been used as the basis for the development of the first vaccines against rabies and anthrax. However, the exact mechanism by which the human body can develop this immunity to disease was unclear.

Metchnikoff attributed the purpose of phagocytosis to the clearance of dying cells, as well as the first line of defence against infection. Meanwhile, humoral biologists believed in the works of Paul Ehrlich, Von Behring and Kitasato who predicted the presence of immune entities (antibodies) in the humora that were elicited by specialized cells within the immune system (B and T lymphocytes) (Kaufmann, 2008). It was Paul Ehrlich who suggested that this function originates within 'hematopoietic tissue' (tissue responsible for the 'making' of 'blood components') and first proposed the concept of self vs non-self. These concepts were crucial to the discovery by George Snell and Peter Gorer of the genetic locus of major histocompatibility complex that determined the acceptance of grafts in mice. This in turn, led to the ground-breaking discovery of the interaction between the innate cellular immune cells and the specialized adaptive T cell by Peter Doherty and Rolf Zinkernagel in 1974. By carrying out an *in vitro* reaction with

lymphocytic choriomeningitis virus (LCMV) infected cells and T cells from other infected mice, they noted that the T cells killed only infected cells and those that came from a syngeneic donor. This seminal experiment described the MHC restriction of antigen presentation (Doherty and Zinkernagel, 1975; Zinkernagel and Doherty, 1974). The molecular structure of the MHC constituted immunological 'self'; the virus-infected cells of the same MHC identity constituted 'altered self'due to virus-induced changes of the MHC identity. T cells killed the altered-self cells while the non-infected self and infected non-self cells remained untouched by the T cells. This finding complemented Bretscher and Cohn's hypothesis of the need of a non-antigen-specific secondary signal to generate self-non-self discrimination. This secondary signal was required to decide between paralysis and activation of the T cells (Bretscher and Cohn, 1970).

Bretscher and Cohn's proposal was refined with the discovery of CD28 and CD40L co-stimulatory molecule expression on T cells that bound with cognate ligands on APCs (Bernard et al., 2002). These co-stimulatory molecules like the B7 family of molecules, are not present on resting monocytes but are induced upon activation of these cells and are present on more terminally differentiated myeloid cell types. Dendritic cells, first identified by Ralph Steinman in n 1973, specialize in priming T cells, (Steinman and Cohn, 1973; Steinman and Witmer, 1978) especially as they express co-stimulatory B7 molecules throughout their activation. This was a revolutionary finding on the role of phagocytic cells that Elie Matchinikoff had originally described almost 100 years before Steinman.

What remained to be understood then, was how T cells would learn to distinguish between non-self/altered self, and self, if they were only ever exposed to self-antigens in the thymus prior to their first encounter with non-self. It was Charles Janeway who proposed that the immune system recognized 'infectious self' through pattern recognition receptors (PRRs) on their surface. In 1997, Janeway and Medzhitov discovered the first PRR

namely Toll like Receptor (TLR) 4. Ectopic expression of this receptor induced the increased expression of pro-inflammatory cytokines and co-stimulatory molecules. Polly Matzinger then improved on the principle of Janeway in 1989 by suggesting that immune cells recognize danger signals in the form of dying or dead cells and proteins from necrotic cells. Indeed, it was found that the same receptors that recognized infectious self, recognized heat shock proteins from necrotic cells.

Thus, the main tenets of cellular immunology and innate and adaptive sensing have developed over 150 years. Exploration into the development of the various cell types and their role in the context of inflammation continues to intrigue researchers. This thesis will explore the origins of the phagocytes that characterise several inflammatory states.

## 1.2 The Hematopoietic System

Hematopoiesis is a complex and orchestrated process that results from the competition between master transcriptional regulators that decide on the fate of every hematopoietic stem cell (HSC). Progressively, sub-threshold levels of these transcription factors 'transcriptionally prime' a multipotent progenitor cell to express a multi-lineage expression pattern. Upon reaching the critical threshold level, transcriptional regulators like PU.1 interact with secondary regulators (factors that either co-operate or antagonise) to specify a lineage (Burda et al., 2010). Adult hematopoiesis originates from HSCs that differentiate into into non-self-renewing cells that may become committed to a specific cell lineage. These precursor cells include common myeloid progenitors (CMPs) (Akashi et al., 2000) and common lymphoid progenitors (CLPs) (Kondo et al., 1997). Although, the current understanding of hematopoietic development is more plastic than origically thought cells such as the CMP and CLP represent transitioning stages that are capable of amplification but not self-renewal and that differentiate into more specialized cell populations of granulocytes and precursors of monocytes, erythrocytes and lymphoid cells s (Kondo et al., 1997) (Notta et al., 2015).

There are specific phenotypic markers that help define pluripotent, multipotent and fully committed cells within the hematopoietic system. HSCs in murine and human bone marrow are contained entirely within a fraction of cells positive for the stem cell growth factor receptor (SCF-R) or cKit (CD117) (Sánchez et al., 1996). These $cKit^+$ populations are highly cycling and generate colonies of differentiated cells *in vitro* depending on the cytokines and growth factors available and the stage of commitment of the HSC. Differentiated cell populations express lineage-specific markers. In this thesis, I have focussed on the ontogeny of the mononuclear phagocytes namely dendritic cells (DCs), monocytes and macrophages.

## 1.3 The mononuclear phagocyte system

The mononuclear phagocyte system (MPS) is a collective term that includes phagocytic innate immune cells like macrophages, classical dendritic cells and their precursors. Each of these differentiated cell types are divided into sub-populations based on surface marker expression, function and anatomical location. While they may originate from a common branch of hematopoiesis, each cell type has been found to have unique progenitors (Akashi et al., 2000). The current section of this thesis will elaborate on the ontogeny of each of these cell populations, the transcription factors and growth factors that influence their development, as well as the specialized phenotype and function of each cell population that distinguishes them as members of the MPS.

### *1.3.1 Dendritic cells*

'Classical' or 'conventional' dendritic cells (cDCs) exhibit a stellate morphology (Steinman and Cohn, 1973) and rely on the growth factor fetal liver kinase-2 (flk-2/Flt3L) for their development (Karsunky et al., 2003; Waskow et al., 2008). cDCs are considered immature (expressing low levels of co-stimulatory molecules like CD80, CD86) before they are stimulated by non-self signals. Immature cDCs are very efficient at antigen capture via receptor-mediated uptake such as through the mannose receptor

(Mr1/CD206) in peripheral tissues while mature cDCs downregulate antigen uptake, upregulate their expression of co-stimulatory molecules, and increase antigen presentation to T cells (Caux et al., 1997; Mellman et al., 1998). Dendritic cells are divided into 2 sub-sets – cDC1 ($XCR1^{+}CD8\alpha^{+}$) and cDC2 ($CD11b^{+}CD8a^{-}$), the development and function of which is dependent on unique progenitor populations and the transcription factors that dictate their fate. Both cDC1 and cDC2 are required for the immune system to receive environmental signals within the tissue and convey these to T cells. cDC1 cells specialize in the cross-presentation and the stimulation of a Th1 response to viruses or cytosolic bacteria such as *Listeria monocytogenes, Salmonella typhi and Toxoplasma gondii* (Hildner et al., 2008; Mashayekhi et al., 2011; Torti et al., 2011). cDC2s present antigen via MHCII to $CD4^{+}$T cells and can stimulate a Th2 or Th17 response to infections with pathogens such as *Citrobacter rodentium* (Satpathy et al., 2013).

#### 1.3.1.1 *Ontogeny of cDCs*

Dendritic cells were established as a unique population of immune cells distinct from macrophages, lymphocytes and granulocytes with the seminal publication by Steinman and Cohn (Steinman and Cohn, 1973). Several studies have gone on to prove the independence of dendritic cells from other lineages with the most recent fate-mapping and bar-coding studies of hematopoietic progenitors (Naik et al., 2013; Schraml et al., 2013)

The earliest progenitor shown to be able to distinctly give rise to cDCs are the monocyte-DC progenitors (MDPs) (Auffray et al., 2009). Adoptive transfer of reporter-labelled MDPs into the spleen of WT recipient mice results in the production of cDC1s and cDC2s (Varol et al., 2007). The cDC2s include $CD4^{+}CD11b^{+}$ and $CD4^{-}CD11b^{+}$ cDCs. Dendritic cells rely on their expression of the receptor tyrosine kinase Flt3 which binds with its ligand Flt3L - a growth factor required for the homeostatic development of the common

dendritic cell precursors (CDPs) and all DC-lineage committed cells (McKenna et al., 2000; Waskow et al., 2008). CDPs give rise to pre-cDCs which have a lower proliferative capacity and are committed to the generation of cDCs, not plasmacytoid DCs (pDCs) (Liu et al., 2007). pDCs originate from a separate progenitor population identified within the $Lin^{-}ckit^{int/lo}CD115^{-}Flt3^{+}$ population that expresses high-levels of the transcription factor E2-2 (Onai et al., 2013) (**Figure 1-1**).

Until 2015, it was thought that pre-cDCs were homogeneously $Lin^{-}Flt3^{+}SIRP\alpha^{int}MHCII^{-}CD11c^{+}$ (Liu et al., 2007) and equally capable of giving rise to cDC1s and cDC2s. However, Grajales-Reyes et al and Schlitzer et al described the heterogeneity of this population and concurrently found that pre-DCs were pre-committed to the generation of either $CD4^{+}$ cDCs (pre-CD4 cDCs) or $CD8^{+}$ cDCs (pre-CD8 cDCs). These cells are phenotypically defined by their expression of Ly6C and SiglecH in the bone marrow and blood - $SiglecH^{-}Ly6C^{-}Zbtb46\text{-}GFP^{+}CD11c^{+}MHCII^{int}Flt3^{+}CD117^{int}$ pre-cDCs are committed to the generation of $CD24^{+}$ and $CD103^{+}$ cDC1s via the autoactivation of *Irf8* (Grajales-Reyes et al., 2015) while $SiglecH^{-}Ly6C^{+}Zbtb46\text{-}GFP^{+}CD11c^{+}CD115^{+}$ pre-cDCs are committed to $SIRP\alpha^{+}$cDC2s (Schlitzer et al., 2015). **Table 1-1** summarizes the surface markers used to delineate the populations of progenitor and differentiated cells of the cDC and monocyte lineages.

**Table 1-1: Surface marker expression of populations from the cDC and monocyte lineages**

| | Precursors | | | | | | Differentiated cells | | | | |
|---|---|---|---|---|---|---|---|---|---|---|---|
| **Population** | **CDP** | **Pre-DCs** | **Pre-cDC1** | **Pre-cDC2** | **MDP** | **cMop** | **cDC1** | **cDC2** | **pDC** | **Ly6Chi monocytes** | **Ly6Clo Monocytes** |
| cKit | + | lo/neg | - | lo/neg | + | - | - | - | - | - | - |
| Flt3 | + | + | + | + | + | - | + | + | + | - | - |
| M-CSFR | + | - | - | - | + | + | - | - | - | + | + |
| SIRPα | lo | lo | lo | lo | + | - | - | + | - | + | + |
| CD11b | - | - | - | - | - | - | - | + | - | + | + |
| Ly6C | - | - | - | - | - | + | lo | lo | + | + | - |
| MHCII | - | - | - | - | - | - | hi | hi | int | +/- | +/- |
| CD11c | - | + | + | + | - | - | + | + | + | - | +/- |
| DEC205 | - | - | - | - | - | - | + | - | - | - | - |
| CD24 | + | - | - | - | - | - | + | - | | - | - |
| XCR1 | - | - | - | - | - | - | + | - | - | - | - |
| ESAM | - | - | - | - | - | - | - | +/- | - | - | - |
| PDCA1 | - | - | - | - | - | - | - | - | + | - | - |
| CD45RA | - | - | - | - | - | - | - | - | + | - | - |
| SiglecH | - | + | - | - | - | - | - | - | + | - | - |
| Derived From: | MDP | CDP | CDP | CDP | LMPP | MDP | Pre-DC1 | Pre-DC2 | E2-2 hi precursor | cMop | cMop/Ly6C hi monos |

A number of comparisons have been drawn between non-lymphoid and lymphoid tissue cDCs. Non-lymphoid tissue cDCs consist of subsets that are described as either $CD24^{+}CD103^{+}$ or $CD11b^{+}$. In the gut, the 2 DC populations are $CD103^{+}CD11b^{-}$ and $CD103^{+}CD11b^{+}$ (Bedoui and Greyer, 2014; Ginhoux et al., 2009; Schreiber et al., 2013). $CD8\alpha^{+}$ cDCs in the spleen have a number of similar properties to $CD103^{+}$ cDCs in non-lymphoid tissues like the kidney, lungs and skin (Ginhoux et al., 2009; Schraml et al., 2013). These properties include high expression of MHCII in order to present antigen to $CD4^{+}$ T cells, and the dependence on the transcription factor Id2 and Irf8 (Ginhoux et al., 2009). Additionally, $CD103^{+}CD11b^{-}$ and $CD103^{+}CD11b^{+}$ lamina propria cDCs rely on Flt3l for their development as they originate from the CDP and pre-cDC (Bogunovic et al., 2009). Functionally, like $CD8\alpha^{+}$ cDCs, $CD103^{+}$ cDCs are specialized at cross-presentation (Bedoui and Greyer, 2014).

Despite their similarities in terms of ontogeny and functional capability, there are certain differences between $CD8\alpha^{+}$ and $CD103^{+}$ DCs. $CD103^{+}CD11b^{-}$ cells from the peripheral lymph nodes are more competent at the induction of a Th17 cell phenotype, express unique pattern recognition receptors and respond dramatically to GM-CSF as compared to $CD8\alpha^{+}$ cDCs (Greter et al., 2012; Jiao et al., 2014). Mice lacking either GM-CSF or its receptor have dramatically reduced levels of $CD103^{+}CD11b^{+}$ lamina propria and skin cDCs with minor changes in the cDC populations in lymphoid organs (Bogunovic et al., 2009; Kingston et al., 2009a; Varol et al., 2007). Additionally, there are $CD103^{-}CD11b^{+}CD64^{-}$ cells in the gut that exhibit Flt3L dependency, express CCR2, but are not derived from $Ly6C^{hi}$ monocytes (Scott et al., 2014) while certain DCs in the gut express CD103 and CD8α concomitantly (Fujimoto et al., 2011). These differences in phenotype and function indicate a change in transcriptional programme in response to the environment that cDCs are exposed to in spite of having a common origin.

#### 1.3.1.2 *Transcription factors involved in development of cDCs*

A number of transcription factors have been found to be critical for the development of distinct subsets of cDCs. ZBTB46, a small DNA-binding zinc-finger protein, was found to be the transcription factor that is uniquely expressed in cells committed to the cDC lineage (Meredith et al., 2012; Satpathy et al., 2012a). By creating a GFP reporter knock-in mouse model on *Zbtb46*, Satpathy et al were able to confirm microarray reports of the expression of Zbtb46 in the cDC lineage. cDCs in the spleen, resident and migratory cDCs in the skin-draining lymph node and resident cDCs in the tissues like the lamina propria and lung, as well as pre-cDCs in the BM expressed high levels of the reporter ZBTB46-GFP (Satpathy et al., 2012a).

The creation of a mouse strain that had the inducible diphtheria toxin (DT) receptor linked to a cherry reporter introduced between the 4$^{th}$ and 5$^{th}$ exons of the *Zbtb46* gene, allowed for both, monitoring of cellular expression of the transcription factor and induced depletion of the cells expressing it. These *zDC$^{DTR/DTR}$* mice when treated with diphtheria toxin had reduced levels of CDP, pre-cDCs and cDC subsets in the tissues as well as in the secondary lymphoid organs (i.e. skin draining lymph nodes and spleen) (Meredith et al., 2012). Moreover, the macrophages, monocytes and pDCs that are affected by DT treatment of the CD11c-DTR mice, remained consistent in the zDC-DTR mice (Meredith et al., 2012). Thus, Zbtb46 expression highlights cells that are committed to the cDC lineage of which pDCs and monocytes are not a part. Additionally, the *zDC $^{lSlDTR}$* mice when crossed onto the *Csf1r $^{Cre}$* mice have a dramatic reduction in the percentage of cDCs, and not monocytes, upon diphtheria injection (Loschko et al., 2016a). Thus far, the literature conclusively details the divergence of the DC lineage from the *Csf1r* expressing monocyte lineage.

cDC1s have distinct characteristics in that they are the only cDCs to express the chemokine receptor XCR1 (Bachem et al., 2010; Crozat et al., 2011; Dorner et al., 2009) and the lectin CLEC9a (Poulin et al., 2012) and serve the specialized function of cross-presentation (Gutiérrez-Martínez et al., 2015; del Rio et al., 2007). cDC2s are a heterogeneous population of cells that albeit are positive for the integrins CD11c and CD11b and major histocompatibility complex class II (MHCII) and do not distinctly express a cDC2-specific surface marker or transcription factor. Zbtb46 is the only transcription factor that uniformly characterizes cDC1 and cDC2s. The Zbtb46-GFP mouse model being a knock-in for the gene, caused a functional dysregulation of the gene. cDCs developed fully in the complete knock-in, indicating that the transcription factor was not specifically required for the development of the cells of the lineage. Instead, what was noticed was that these cells continued to express high levels of G-CSF-R and LIF-R which are usually reduced on fully mature cDCs. Additionally, overexpressing the gene resulted in a reduction in granulocyte potential (Satpathy et al., 2012a). The transcription factor could thus act to de-sensitize the DC lineage to other non-DC factors – a role played by a number of lineage-determining transcription factors in other cell lineages.

DNA-binding protein Inhibitor 2 (Id2) (Hacker et al., 2003), basic leucine zipper transcription factor ATF-like 3 (BatF3) (Hildner et al., 2008), NFIL3 (Kashiwada et al., 2011) and interferon regulatory factor 8 (Irf8) (Schiavoni et al., 2002), have all been found to be crucial to the development of cDC1s. Each of these transcription factors play a role at a different stage of development of the cell population. BatF3, for example, is required to induce maturation and differentiation of pre-CD8 cDCs into $CD24^{+}$cDCs (cDC1) but is dispensable for the development of the pre-cDCs from the CDP (Grajales-Reyes et al., 2015). Irf8 on the other hand, affects the development of $CD8\alpha^{+}$ cDCs from the progenitors and also influences their functional capabilities (Vander Lugt et al., 2014;

Tamura et al., 2005). These studies demonstrate the homogenous nature of the CD8α$^{+}$ cDCs.

Mice knocked out for Irf4, recombining binding protein suppressor of hairless (RBPJ) (Caton et al., 2007), RelB (Wu et al., 1998) and PU.1 (Guerriero et al., 2000) have severely reduced levels of cDC2s at steady state. The reduction of cDC2s however, is only partial demonstrating the heterogeneity of the population. Reizis and colleagues noted that the CD8α$^{-}$CD11b$^{+}$ cDCs are further divided based on their reliance on Notch2 signalling to become either CD4$^{+}$ T cell priming ESAM$^{hi}$ cDCs or cytokine producing ESAM$^{lo}$ cDCs (Lewis et al., 2011). Additionally, Tussiwand et al noted the developmental requirement of the transcription factor KLF4 in ESAM$^{lo}$ cDCs and their role in the induction of Th2 responses. ESAM$^{hi}$ cDC2s, on the other hand generate Th17 responses that are required for the clearance of pathogens like *Citrobacter rodentium* (Tussiwand et al., 2015).

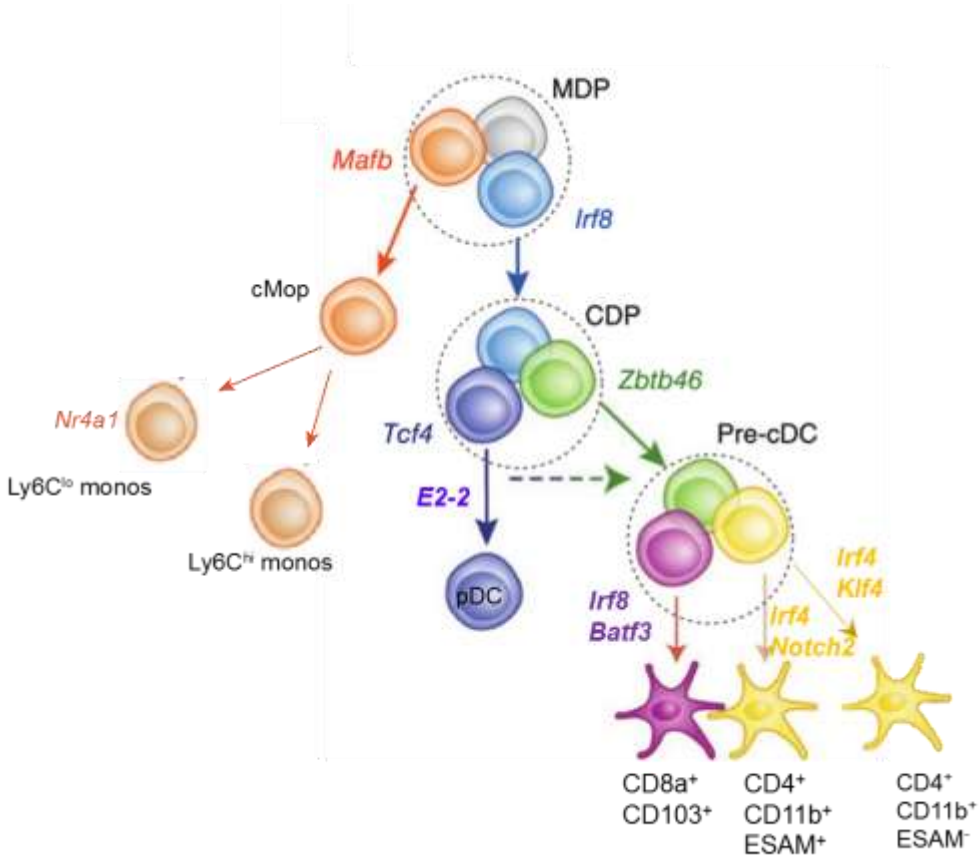

**Figure 1-1: cDC development**. Adapted from (Satpathy et al., 2012b). Irf8 drives the differentiation of MDPs to CDPs which then express Zbtb46 to develop the cDC lineage. Pre-cDCs are heterogeneous with some (green) being non-committed while others begin to express greater levels of lineage-specific transcription factors that determine their fate as either cDC1(Irf8, Batf3, Id2)(purple) or cDC2(Irf4)(yellow). cDCs are further differentiated into ESAM- and ESAM+ cDC2s.

### *1.3.2 Monocytes and Macrophages*

#### 1.3.2.1 *Ontogeny of monocytes and macrophages*

Ilya Metchnikoff's first description of phagocytes in starfish larvae *(Hydra)* and their phagocytic ability earned him the Nobel Prize in Physiology or Medicine in 1908 and the status of the 'Father of innate cellular immunity' (Kaufmann, 2008). Based on the properties of efficient phagocytosis, macrophages and monocytes were grouped within the reticuloendothelial system as it was thought that they shared a common origin with endothelial cells by Aschoff in 1924. However, increasingly, the differences in morphology and function indicated that they were in fact from different lineages and could not be grouped together (Davies et al., 2013).

Ralph van Furth, James G. Hirsch and Zanvil A. Cohn laid the foundation of the mononuclear phagocyte system (MPS)- a system which encompassed macrophages and their precursors- monocytes and bone marrow progenitors and excluded lymphocytes (van Furth et al., 1972). This was intriguing given the fact that the original discovery of macrophages had been made in lower form organisms which did not have any monocytes but did macrophages (van Furth et al., 1972; Kaufmann, 2008). Additionally, macrophages had already been found to have different principal sources (ie. either blood or tissue) and have distinct functions in various tissues (Sabin et al., 1925).

The understanding that the 'classification' of macrophages was a collection of cells of different origins came much later in the 20$^{th}$ century. It was originally thought that hematopoietic precursors arose within the yolk sac and then travelled to specific

hematopoietic organs for development into blood cells (Medvinsky and Dzierzak, 1996). However, such a concept made it difficult to understand how progenitors from the yolk sac until embryonic day 9 (E9) were unable to form definitive colonies of differentiated cells when injected into mouse spleens (called colony-forming-unit-spleen (CFU-S)) - yolk sac derived hematopoietic progenitors were not the precursors to adult blood cells. Hematopoietic progenitors from the yolk sac were able to differentiate into a number of blood cells *in vitro*, if provided with the appropriate cytokines and growth factors, namely, GM-CSF, M-CSF and Flt3L. On the other hand, it was found that hematopoietic progenitors from the aorta-gonad -mesonephros (AGM) from day E10.5 and 11 gave rise to substantially more CFU-S. It was thus concluded that there were 2 waves of blood cell development- one from the yolk sac at E9.5-10.0 and one from the AGM region at E10.5 - 11.0 (Medvinsky and Dzierzak, 1996).

More recent studies have shed light on the involvement of macrophage development in organogenesis. Geissmann and colleagues have categorized the presence of pre-macrophages (pMacs) that arise from erythro-myeloid precursors (E8.5) that come from the yolk sac. These cells colonize the whole embryo at E9.5 and begin to undergo differential transcriptional programmes that are responsible for varied organ-specific characteristics of each class of macrophage (Mass et al., 2016). Thus, yolk-sac derived macrophages colonize the embryo during organogenesis which gives rise to tissue resident macrophages seen postnatally. These cells are able to maintain themselves without the need for replenishment from circulating monocytes (Yona et al., 2013). The AGM-derived precursors are the pre-liver source of hematopoietic cells. Subsequently only the AGM-derived precursors continue to contribute to adult blood hematopoietic cells (Medvinsky and Dzierzak, 1996; Müller et al., 1994). Adult HSCs give rise to the macrophage dendritic cell progenitor (MDP) which is thought to be a dedicated progenitor capable of giving rise to monocytes and cDCs (Auffray et al., 2009). These

progenitors develop into committed precursor populations for monocytes- the common monocyte precursor (cMop) which is capable of giving rise to the 2 major populations of monocytes namely, Ly6C$^{hi}$ and Ly6C$^{lo}$ monocytes (Hettinger et al., 2013). Ly6C$^{hi}$ monocytes are recruited to tissues during inflammation where they differentiate into F4/80$^{lo}$ macrophages (Schulz et al., 2012).

Thus, macrophages in tissues originate in the yolk sac being sustained through self-renewal in situ. Circulating monocytes that arise from adult bone marrow, are recruited to sites of inflammation in tissues and develop a population of macrophages that are transcriptionally distinct to yolk-sac derived macrophages and have been broadly found to be F4/80$^{lo}$ (**Figure 1-2**).

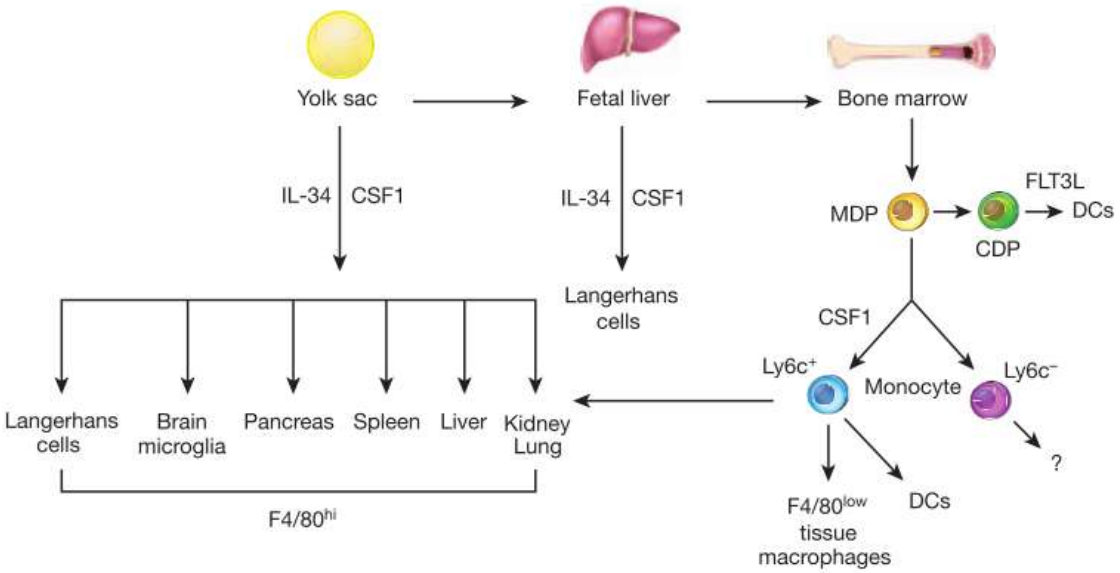


**Figure 1-2: A schematic of development of macrophages**. Reproduced from Wynn et al., 2013).Macrophages derive from 3 sources. The first is the yolk sac that derives the F4/80$^{bright}$ macrophages that populate the tissues during embryogenesis. The second is the fetal liver from which hemtopoiesis does occur but its generation of macrophages is less well-defined. The 3rd is the bone marrow which contains HSCs that derive from the fetal liver. Macrophages that originate from these progenitors are F4/80$^{low}$ and go through intermediate stages of development, i.e. the MDP and Ly6C$^{hi}$ monocytes.

#### 1.3.2.2 *Key transcription factors involved in monocyte and macrophage development*

A few transcription factors have been found to be critical for the development of macrophages from HSCs, which include PU.1, C/EBPα and Maf-B. Although dispensable for their origin, PU.1 is highly expressed in HSCs (Dakic, 2005) and remains at elevated levels in neutrophils, B cells and macrophages while gradually diminishing in cells that progress toward erythropoiesis (Lloberas et al., 1999). Overexpression of PU.1 instructs the development of the monocyte/macrophage lineage while simultaneously downregulating the development of other cell types such as granulocytes and erythrocytes (Burda et al., 2010). PU.1 exerts its role not only by direct binding to DNA elements in either antagonistically or synergistically with other transcriptional regulators to promote macrophage development, but also by binding to microRNAs. For instance, the ectopic expression of miRNA146a, a PU.1 target, in HSCs results in their differentiation into macrophages *in vivo* in the peritoneum (Ghani et al., 2011). Thus, PU.1 directs the development of HSCs into macrophages through multiple mechanisms.

PU.1 selectively drives differentiation towards macrophage development. Overexpressing it in bone marrow-derived mast cells results in the generation of macrophages (Ito et al., 2009). While HSCs are programmed toward a monocyte/macrophage lineage with increased expression of PU.1, the end-point phenotype of these cells has been documented to be DC-like. Pre-T cells ectopically expressing PU.1 have been re-programmed to generate DC-like cells while C/EBPα overexpression results in the generation of macrophages (Laiosa et al., 2006). Bakri et al, describe how constitutive expression of PU.1 results in the generation of DCs rather than macrophages while Maf-B is required for the induction of a macrophage phenotype (Bakri et al., 2005). Hematopoietically-derived DCs from both human and mouse have a much higher expression of PU.1 (Anderson et al., 2000).

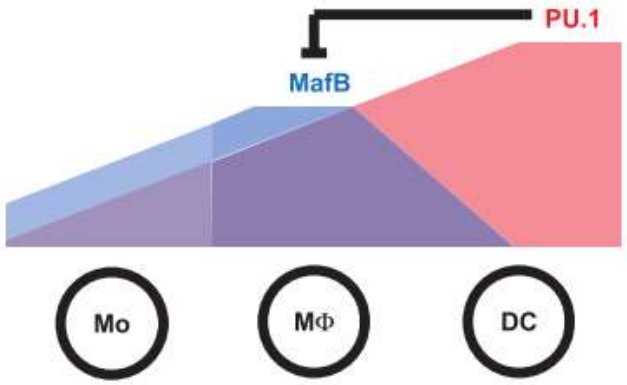


**Figure 1-3: Model of macrophage versus DC phenotype instructed by PU.1 and MafB**. (Reproduced from Bakri et al., 2005) PU.1 plays a crucial role in the development of the monocyte/macrophage lineage from multi-potent cells. Its role in the development of macrophage versus DC phenotype further to this is represented above. Elevated levels of PU.1 push toward a more DC phenotype while inhibiting the development of macrophage phenotypes by binding to MafB. If the levels of MafB are higher, the multi-potent cell or monocyte will develop into a macrophage.

The further downstream action of PU.1 in the phenotype and function of macrophages has also been discussed. PU.1 modulates the transcription of about 3000 genes and its binding sites are found near a number of macrophage-lineage specifying genes such as M-CSFR (Ross et al., 1998), GM-CSFR (Hohaus et al., 1995) but also close to phenotypic markers such as FcγRIb (Perez et al., 1994), CD11b , etc. PU.1 also mediates the steady state trans-activation of *Ciita* promoters pI and pIII (LeibundGut-Landmann et al., 2004; Yoon and Boss, 2010) as well as IFN-ɣ stimulated promoter *pIV* (Ito et al., 2009). PU.1 has also been reported to have a role in the alternative activation of macrophages towards an M2 phenotype, with conditional removal of PU.1 *in vivo* showing a dramatic reduction in M2-driven airway epithelial hypersensitivity (Qian et al., 2015).

Another crucial transcription factor involved in myelopoiesis, is NUR77 that is encoded by *Nr4a1*. Ly6C$^{lo}$ monocytes (Hanna et al., 2011) and a population of thymic macrophages (Tacke et al., 2015) are specifically dependent on *Nr4a1* for their development. The dependency of different cDC and monocyte populations on the various

transcription factors of what is known from the current literature is summarized in **Table 1-2.**

#### 1.3.2.3 *Phenotype and functions of monocytes and macrophages*

Monocytes are a major component of the circulating population of immune cells that form part of a lineage that is identified by its expression of M-CSFR (CD115) and lysozyme (*LyzM*). M-CSF-R is expressed from the earliest stages of yolk-sac macrophage development, while *LyzM* is expressed much later in liver hematopoiesis (Lichanska et al., 1999). Murine cells are insensitive to diphtheria toxin as they lack its receptor(Cha et al., 2003). Transgenic mice that are genetically manipulated to conditionally express the receptor to knock-out specific populations by DT treatment of the $LyzM^{cre}x\ Csf1r^{lslDTR}$ mice, which express a cre recombinase under the *LyzM* promoter along with promoting DTR sensitivity in *Csf1r* expressing cells, leads to the depletion of monocytes and macrophages, and not cDCs, in the BM, blood, spleen and tissues such as the lamina propria (Schreiber et al., 2013). Another crucial marker of differentiation between the subsets of monocytes is Ly6C. $Ly6C^{lo}$ monocytes patrol the vasculature (Auffray et al., 2009) and are dependent on the transcription factor NUR77 for their development (Hanna et al., 2011). $Ly6C^{hi}$ monocytes on the other hand circulate at steady state and are recruited by inflammatory mediators secreted by the $Ly6C^{lo}$ monocytes as well as other immune cells and endothelial cells to the site of inflammation. Monocyte subsets thus play distinct roles as sentinels of the immune system.

Macrophages reside in virtually every mammalian tissue (Wynn et al., 2013) and express both F4/80 and CSF-1R. F4/80 is often used to differentiate between populations of different origins- $F4/80^{bright}$ macrophages arise from the yolk sac and $F4/80^{low}$ macrophages originate from the erythro-myeloid progenitors that give rise to HSCs (Schulz et al., 2012). While these relative levels of F4/80 expression on macrophages is

not the clearest form of discrimination between different origins of the cells, the F4/80$^{bright}$ yolk-sac derived tissue-resident macrophages are also less proliferative as they are independent of the transcription factor crucial for maintaining the proliferative state of hematopoietic progenitors- c-Myb (Mucenski et al., 1991; Schulz et al., 2012) . In addition to this population, organs like the gut, dermis and heart are continually supplemented with monocyte-derived macrophages. Fate-mapping experiments in the dermis have shown that the F4/80$^{hi}$ macrophages are replenished by the CCR2-dependent Ly6C$^{hi}$ monocytes that give rise to an intermediate population of F4/80$^{lo}$ macrophages which progressively acquire an F4/80$^{hi}$ phenotype (Bain et al., 2016; Tamoutounour et al., 2013). The heart is one of the few organs that exhibit considerable numbers of the yolk-sac derived macrophages in adulthood but also have CCR2-dependent monocyte-derived macrophage populations especially after cardiac inflammation (Epelman et al., 2014). CD103$^{-}$CD11b$^{+}$ macrophages in the gut are continually replenished by recruited monocytes (Bain et al., 2013; Varol et al., 2007). This difference in origin could contribute to the phenotypic and functional differences observed in the many macrophage populations in these tissues.

By large, macrophages act to maintain homeostasis in a tissue-specific manner. Each tissue-specific macrophage differs from the others in form and function depending on the tissue of residence. For example, red pulp macrophages in the spleen digest and recycle heme to maintain systemic iron levels (Chow et al., 2013) while microglia prune synapses during development (Paolicelli et al., 2011). These differences would appear to arise from changes in the transcriptional programme of macrophages which result from the microenvironment in which they reside (Gosselin et al., 2014; Lavin et al., 2014; Okabe and Medzhitov, 2014). Additionally, macrophages continually change their transcriptional profile with chronic insults like fibrosis, obesity and cancer, converting to a more ‘metastable’ phenotype in response to various tissue-specific stimuli (Wynn et al.,

2013). This in turn, makes it more difficult to classify all macrophages within defined groups. Increasingly, published reports are pointing toward a need for a deeper, more diverse classification of the various sub-types of macrophages found at steady-state and during inflammation (Wynn et al., 2013).

Thus, tissue resident myeloid populations at steady state constitute cDC1s, cDC2s, yolk-sac derived macrophages and monocyte-derived macrophages. The key transcription factor *Zbtb46* can be used to discriminate cDCs (both immature and mature) from monocytes and macrophages. Macrophages derived from HSCs are discriminated by the expression of transcription factors c-Myb (Schulz et al., 2012) and Id3 (Mass et al., 2016).Thus by the use of transcription factors, the lineages of steady-state myeloid populations can be distinguished from each other

Table 1-2: Comparison of transcription factors

| | | CDP | Pre-cDC1 | Pre-cDC2 | cDC1 | cDC2 | pDC | cMop | Ly6Chi monocytes | Ly6Clo Monocytes |
|---|---|---|---|---|---|---|---|---|---|---|
| Developmental Requirement | Irf4 | - | - | + | - | + | lo | | - | - |
| | Irf8 | + | + | - | + | - | + | | + | + |
| | Zbtb46 | - | - | - | - | - | - | - | - | - |
| | Batf3 | | - | - | + | - | - | - | - | - |
| | E4BP4 | - | - | - | + | + | | | - | - |
| | LyzM | | | | | +/- | | | + | + |
| | E2-2 | - | - | - | - | - | + | - | - | - |
| | Id2 | - | - | + | + | - | - | | | |
| | Nr4a1 | - | - | - | - | - | - | - | - | + |
| | Klf4 | - | - | + | | | | | + | |
| Expression | | **CDP** | **Pre-cDC1** | **Pre-cDC2** | **cDC1** | **cDC2** | **pDC** | **cMop** | **Ly6Chi monocytes** | **Ly6Clo Monocytes** |
| | Irf4 | - | - | + | - | + | + | | - | |
| | Irf8 | + | + | - | + | - | + | + | lo | lo |
| | Zbtb46 | - | + | + | + | + | - | - | - | - |
| | Batf3 | - | - | | + | + | | - | - | - |
| | E4BP4 | + | - | - | - | - | - | - | - | - |
| | LyzM | | | | - | +/- | | | + | + |
| | E2-2 | - | - | - | - | - | + | - | - | - |
| | Id2 | - | - | + | + | + | - | | - | - |
| | Nr4a1 | - | - | - | - | + | - | - | - | + |
| | Klf4 | lo | - | + | - | + | | lo | + | + |

(Abram et al., 2014; Clausen et al., 1999; Hettinger et al., 2013; Hildner et al., 2008; Meredith et al., 2012; Satpathy et al., 2012a; Tamura et al., 2005; Tussiwand et al., 2015)

(Hettinger et al., 2013)

## 1.4 Growth factors at steady state and inflammation

A number of growth factors play a crucial role in the development of both the monocyte and cDC lineages. These include GM-CSF, Flt3L and M-CSF. To understand the role that each growth factor plays in the ontogeny and function of each myeloid population, I shall discuss each in the next sub-section.

### *1.4.1* Flt3L

Flt3 (fmo-like tyrosine kinase-3) or flk-2 (fetal liver kinase-2) was originally discovered in populations enriched for stem cells (Matthews et al., 1991). 60% of $Lin^{-}Sca\text{-}1^{+}c\text{-}kit^{+}$ cells are $Flt3^{+}$ (Adolfsson et al., 2001). The expression of Flt3 on hematopoietic progenitors is transient. *Flt3l*$^{-/-}$ mice have reduced populations of lymphocytes and neutrophils in addition to a fall in the GM-dependent precursors (McKenna et al., 2000). Administration of supra-physiological levels of FLT3L however, does not influence the relative amounts of lymphoid cells in circulation or in the bone marrow (Waskow et al., 2008).

The cell populations most dramatically affected within the *Flt3l*$^{-/-}$ mice are the $CD8\alpha^{+}$ and $CD8\alpha^{-}$ spleen cDCs (McKenna et al., 2000). Importantly, *Flt3l*$^{-/-}$ cDCs induce similar levels of T cell stimulation as their *Flt3l*$^{+/+}$ counterparts (McKenna et al., 2000). *Flt3*$^{-/-}$ and *Flt3l*$^{-/-}$ mice have reduced cellularity in the bone marrow and spleen and show a particularly low level of cDCs and cDC-committed precursors (MDP, CDPs, Pre-DCs) in the BM (McKenna et al., 2000; Waskow et al., 2008) indicating a requirement of FLT3 for their development. Additionally, exposure to super-physiological levels of Flt3L increased MDPs and peripheral cDCs and pDCs. Expression of the receptor FLT3 was also required for the peripheral expansion and maintenance of $CD11c^{hi}MHCII^{+}$ cDCs as

mixed adoptive transfer experiments of *Flt3*$^{-/-}$ and WT MDPs into WT recipients showed increased amounts of CFSE dilution in the WT donor CD11c$^{+}$ cells (Waskow et al., 2008). Thus, Flt3 is required for the development of cDCs from MDPs and for their peripheral expansion (**Figure 1-4**).

In the case of inflammation due to an infection, Flt3L is released in the serum of infected mice at high concentrations, for e.g. in *Plasmodium chabaudi* infections (Guermonprez et al., 2013). Released by mast cells due to increased type I IFN receptor signalling in the case of *P.chabaudi* infection, the elevated levels of Flt3L causes elevated levels of CD8α$^{+}$ and CD8α$^{-}$ cDCs in the spleen. However, the levels of FLT3 are highly regulated as over expression during infection can lead to detrimental outcomes (Alaniz et al., 2004).

### *1.4.2 M-CSF*

Macrophage colony-stimulating factor (M-CSF) or *Csf1* was originally isolated from human urine and used as a constituent in solid-state culture medium to grow macrophage colonies that also contained granulocytes (Stanley et al., 1975) However, later on L929-cell conditioned medium (from the cell line named L cells) was used as a source of potently active M-CSF (Stanley and Heard, 1977) which Stanley and Heard later renamed Colony stimulating factor-1 (CSF-1).

CSF-1 is produced by several cell types including macrophages, osteoblasts, stromal cells and endothelia and its main contribution to hematopoiesis has largely been attributed to the development of macrophages - *Csf1*$^{-/-}$ and *Csf1r*$^{-/-}$ mice lack macrophages in a number of tissues, including osteoclasts-a loss that leads to an osteopetrotic phenotype in the *Csf1*$^{-/-}$ mice (Witmer-Pack et al., 1993; Yoshida et al., 1990). While studies have also found that the cytokine is required for the development of Langerhans cells at steady state (Ginhoux et al., 2006) and plays a role in cDC development *in vivo* (MacDonald et al., 2005). Administration of CSF-1 results in the increase in pDC and cDC numbers (Fancke et al., 2016).

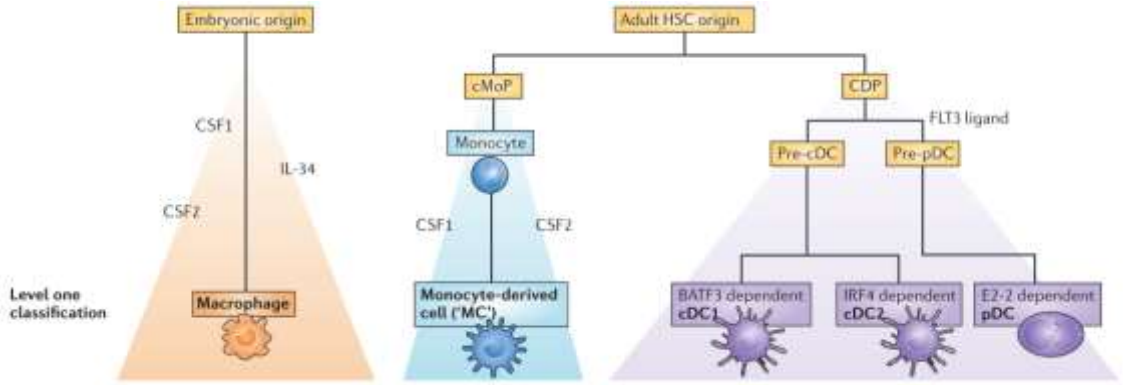


**Figure 1-4: Ontogeny of the mononuclear phagocyte system**:Adapted from Guilliams et al, 2014. Classification system of various cells of the MPS. Macrophages rely on M-CSF(CSF1), IL-34 and GM-CSF (CSF-2) to develop into macrophages from the embryonic stage. Under steady state, monocytes remain in circulation or replenish only certain tissue macrophages such as that of the gut, but differentiate in response to inflammation into macrophages or dendritic cells. At this point they are called 'monocyte-derived' to distinguish them from embryonically or hematopoietically-derived macrophages or dendritic cell

### *1.4.3 GM-CSF*

First identified as a growth factor involved in the generation of granulocyte and macrophages colonies *in vitro*, GM-CSF (or *Csf2*) has proved to have a key role during inflammation. At steady state, mice lacking the *Csf2r* or *Csf2* show relatively little difference in the development of myeloid populations. However, in several disease states in humans and in disease models in mice, GM-CSF appears to have a pathogenic role, inducing heightened pathology in arthritis, experimental autoimmune encephalomyelitis (EAE) and asthma to name a few (Hamilton, 2002). Its relevance at steady state is not clear given that *Csf2r-/-* mice display little to no differences in the numbers of tissue resident macrophage (except alveolar macrophages), circulating monocytes or lymphoid tissue resident cDCs (Wynn et al., 2013). The one population GM-CSF does appear to influence is the non-lymphoid tissue cDCs.

#### *1.1.1.1 GM-CSF on c-DCs:*

GM-CSF (CSF2) plays a crucial role in the development of cDCs at steady state. A study by Shortman and colleagues utilized GM-CSF-R$^{-/-}$ (*Csfr2b*$^{-/-}$) or GM-CSF$^{-/-}$ (*Csf2*$^{-/-}$) mice have normal numbers of both sub-populations of cDCs in the spleen, i.e., cDC1 and cDC2 but a decrease in both the subsets in the lymph nodes (Vremec et al., 1997). Although it was not clearly outlined in the study, the threefold reduction in the lymph node cDCs was possibly a reflection more of the migratory than the resident populations of cDCs (Vremec et al., 1997). Indeed, Merad and colleagues later showed that the migratory cDC1 (CD103$^{+}$) subset in the draining lymph nodes of the lung, skin and gut were all reduced several fold in the *Csf2rb*$^{-/-}$*Csf2rb2*$^{-/-}$ double knockout mice (Greter et al., 2012) emphasizing a specific reliance of cDCs from non-lymphoid tissue cDCs on GM-CSF. *Csf2r-β*$^{-/-}$ mice when injected with Flt3L have increased levels of cDC1s but not cDC2s (Daro et al., 2000). This shows a dependency of the cDC2s or a fraction of them on CSF-

2R. Although, pre-cDCs rely on Flt3L to differentiate into terminally differentiated cDCs in secondary lymphoid organs, they appear to rely on ligand binding of CSF-2R to differentiate into $CD103^+CX_3CR1^-$ lamina propria DCs (Bogunovic et al., 2009). Administration of GM-CSF at supra-physiological levels results in the expansion of cDCs in the spleen and thymus (Daro et al., 2000; Vremec et al., 1997). Thus, GM-CSF contributes to the development of non-lymphoid tissue cDCs at steady state and aids in further expansion of cDCs in secondary lymphoid organs which might prove useful during inflammation when there is an increase in the growth factor.

Del Rio et al also reported the need for GM-CSF in culture to derive $CD103^+$ cDCs (Rio et al., 2008). By contrast, Murphy and colleagues noted that although the $CD103^+CD24^+CD11b^-CD11c^+$ cells were reduced in the lung and the inguinal lymph nodes of *Csf2rb*$^{-/-}$ mice, they were not completely removed in the *Batf3*$^{-/-}$ mice but simply have reduced expression levels of CD103 (Edelson et al., 2011; Hildner et al., 2008). *In vitro* studies in this paper show that the addition of GM-CSF to a *Flt3l* culture of BM cells results in the generation of CD103 expression on the $CD24^+MHCII^+$ cells in culture which do not appear in a similar culture of *Csf2rb*$^{-/-}$ BM (Mayer et al., 2015). Thus, the expression of CD103 on the migratory DCs is dependent on GM-CSF and these migratory cDCs are partially dependent on GM-CSF for their development.

GM-CSF not only increases the numbers of $CD11b^+$ cDCs in the spleen but also increases their antigen degradation capacity (Daro et al., 2000). GM-CSF is also capable of promoting development of additional immune cells. For instance GM-CSF and TNF-α exposed $CD34^+$ human cord blood cells generate $CD14^+$-derived DCs that are capable of

inducing immature B cells to differentiate into IgM-producing cells in response to CD40 ligation and IL-2 (Caux et al., 1997).

Whole bone marrow cultured in GM-CSF will derive cells that have a cDC-like phenotype and transcriptomic signature (Inaba et al., 1992). Culture in GM-CSF alone results in approximately 75% of Zbtb46-GFP$^{+}$ cells while GM-CSF + IL-4 promotes 96% Zbtb46-GFP expression among the resulting progeny (Satpathy et al., 2012a). However, *Flt3*$^{-/-}$*Csf2r*$^{-/-}$ mice also have similar levels of splenic cDCs as the *Flt3*$^{-/-}$ mice (Waskow et al., 2008). Thus, although GM-CSF supplemented cultures paved the way for research in DC biology by promoting amplification of DC cell numbers *in vitro*, GM-CSF-R signalling plays a limited role in the development of cDCs in secondary lymphoid organs.

**Table 1-3: Requirement of various growth factors for DC lineage development**

| | **CDP** | **Pre-cDC1** | **Pre-cDC2** | **cDC1** Lymphoid tissue resident | **cDC2** Lymphoid tissue resident | **cDC1** Non-lymphoid tissue resident | **cDC2** Non-lymphoid tissue resident | **pDC** |
|---|---|---|---|---|---|---|---|---|
| GM-CSF | × | × | × | × | × | ✓ | ✓ | × |
| M-CSF | × | × | × | × | × | × | × | × |
| Flt3L | ✓ | ✓ | ✓ | ✓ | ✓ | ✓ | ✓ | ✓ |

#### *1.1.1.2 MHCII$^{+}$ cells are induced by elevated levels of GM-CSF*

A number of *in vitro* and *in vivo* studies have demonstrated that GM-CSF induces the expression of MHCII on myeloid cells (Daro et al., 2000; Hanada et al., 1996). This increase in MHCII is seen on both monocytes and dendritic cells (Daro et al., 2000; Randolph et al., 1999). GM-CSF, upon engaging with its receptor, brings about the activation of specific signalling pathway intermediates - STAT5 in a Janus JAK2-dependent manner (Van De Laar et al., 2012). This activation of STAT5 initiates a

signalling cascade leading to the activation of CIITA (Choi et al., 2009), the transcription factor that drives the expression of MHC class II (LeibundGut-Landmann et al., 2004).

The increase in $MHCII^+$ cells is not only seen in response to excessive levels of GM-CSF but also in response to infectious agents like *Leishmania*, *Listeria* and Lipopolysaccharide (LPS) (Greter et al., 2012; Meredith et al., 2012; Olekhnovitch et al., 2014).

Upregulated MHCII expression is seen particularly within the cDC population. Inducing an increase in circulating GM-CSF by either administration of recombinant protein, recall response to mBSA or by an established tumour engineered to produce GM-CSF constitutively (Dranoff et al., 1993; Naik et al., 2006), results in an increased number of $CD11b^+$ c-DCs in the spleen as compared to controls, with enhanced expression of MHCII (Hanada et al., 1996; Storozynsky et al., 1999; Vremec et al., 1997). $Ly6C^{hi}$ monocytes are recruited to the site of GM-CSF production and the draining lymph nodes and then convert into a population that is DC-like in its expression of co-stimulatory molecules in CD80, CD86 and MHCII (León et al., 2007). These DC-like cells have the highest levels of MHCII in a culture with GM-CSF and IL-4, as compared to cultured macrophages and $CD11b^+Ly6G^-Ly6C^{hi}$ inflammatory cells (Xu et al., 2007). Indeed, monocytes cultured in GM-CSF and IL-4 generate cells that are $Zbtb46^+$ (Briseño et al., 2016). Distinguishing these cells from cDCs is challenging. Thus, with increased levels of GM-CSF, the relative contributions of different types of DCs is manipulated.

#### *1.1.1.3 GM-CSF in inflammation.*

Inflammation is characterized by the generation and accumulation of a number of inflammatory factors such as cytokines IL-1β, TNF-α, IFN-γ, IL-10, chemokines and growth factors GM-CSF and *Flt3l* (Guermonprez et al., 2013; Serbina et al., 2003; Zhan et al., 2011) that induce the recruitment of immune cells. These are crucial at the site of

inflammation as they act on myeloid cells to induce co-stimulatory marker expression like CD40, CD80 and CD86, which are collectively required to promote T cell stimulation. The role of GM-CSF specifically, is context-dependent. It has been reported to have both tolerogenic roles (Mortha et al., 2014) and inflammatory roles (Cook et al., 2004; Croxford et al., 2015). From the several studies on GM-CSF, it appears that its role is possibly indirect and context-dependent. Furthermore, GM-CSF has been found to induce the generation of DCs and macrophages both - *in vitro* (Inaba et al., 1992) and *in vivo* (Vremec et al., 1997), and during inflammation (Cook et al., 2004; Croxford et al., 2015; Daro et al., 2000).

In comparison with DCs that were expanded in *Flt3l*-treated mice, DCs expanded with GM-CSF showed very similar levels of $CD4^+$ and $CD8^+$ T cell activation indicating no difference in their ability to present antigen. However, they showed a significant increase in their ability to take up antigen and process it as evidenced by the degradation of fluorescently trackable DQ-OVA (Daro et al., 2000).

*In vivo* models used to study the effect of GM-CSF include a recall response to methylated bovine serum albumin (mBSA). Such models have also shown an increase in the production of $CD11b^+CD11c^+MHCII^+$ cells in the spleen in response to elevated levels of GM-CSF (Cook et al., 2004; Naik et al., 2006).

### 1.5 Induction of mo-DCs and iNOS-producing cells

As described earlier, macrophages and DCs are highly heterogeneous. Furthermore, during inflammation, $Ly6C^{hi}$ monocytes are recruited to sites of inflammation and differentiate into macrophages and DCs (Sprangers et al., 2016). The resultant cells are widely termed inflammatory macrophages and inflammatory DCs that have unique properties that distinguish them from their steady state counterparts. Inflammatory macrophages have been found to generate a strong pro-inflammatory response by

secreting various cytokines such as TNF-α and reactive oxidative species in the presence of parasites as well as anti-inflammatory responses via the production of IL-10 and TGF-β during conditions of stress such as cardiac overload (Lavine et al., 2016; Liaskou et al., 2013; Nahrendorf et al., 2010). In such cases the distinction between the origin of the macrophages is of great consequence (Lavine et al., 2016). Inflammatory DCs or mo-DCs have been reported to have anti-inflammatory responses in the case of viral infections (Ohyagi et al., 2013) while promoting the pathogenic Th2 immune reponses to house dute-mite allergen (Plantinga et al., 2013) depending on the conditions of inflammation (Sprangers et al., 2016). These divergent outcomes from MPS development point toward characteristics of plasticity or heterogeneity in the progenitor cell populations, namely, monocytes.

### *1.5.1 Monocyte-derived cells*

Monocytes are recruited in large numbers to the site of inflammation, outnumber both macrophages and cDCs present in the tissue (Geissmann et al., 2003; Randolph et al., 1999). Ly6C$^{hi}$ monocytes can differentiate into macrophages or DCs (Askenase et al., 2015). However, classification of these cells are challenging as to the lack of markers at steady state to clearly differentiate between cells that have expanded *in situ* and those that have been recruited and differentiated from monocytes. During inflammation, markers such as CD11b, CD11c and MHCII that are classically expressed on all myeloid cells, are upregulated. Additionally, these monocyte-derived cells could acquire similar functions to macrophages (improved phagocytosis, killing of pathogens etc.) or DCs (improved antigen presentation) depending on the site at which they develop, making classification of these cells difficult due to redundancy in immune function and surface marker expression.

### *1.5.2 Phenotype of Mo-DCs*

MoDCs are phenotypically similar to $CD11b^+$ cDCs in that they are $CD11b^+CD11c^+$ (Daro et al., 2000) and are present in the spleen (Naik et al., 2006) and lymph nodes (Davidson et al., 2013; Plantinga et al., 2013) during inflammation. These phenotypic markers are not unique enough to distinguish them from other myeloid populations such as macrophages ($CD11b^+CD11c^+F4/80^+$) and $CD8\alpha^-$ cDCs ($CD11b^+CD11c^+MHCII^+$).

Sallusto and Lanzavecchia first documented the expression of the mannose receptor (CD206) on human DCs and DCs derived from peripheral blood cultured in the presence of GM-CSF and IL-4. These GM-CSF induced DCs utilize CD206 to selectively uptake particulate antigens, process and present them onto MHCII (Sallusto and Lanzavecchia, 1994a). CD209a or DC-specific ICAM3 grabbing non-integrin (DC-SIGN) was also documented to be expressed on GM-CSF-induced-DCs by day 7 of differentiation from human monocytes and found to specifically bind to ICAM3 on T cells with greater affinity than to LFA-1 (Geijtenbeek et al., 2000). When Mo-DCs were described *in vivo*, Cheong et al. defined them based on their expression of a combination of CD206 and CD209a (DC-SIGN) in response to administration of LPS. This expression correlated to the *in vitro* expression of these markers on monocyte-derived DCs i.e. the result of cultures in GM-CSF (Geijtenbeek et al., 2000). Additionally, mo-DCs have also been found to express markers like FcεRI in the lung (Plantinga et al., 2013) and CD64 in the lung and gut (Plantinga et al., 2013; Tamoutounour et al., 2012). However, a common marker expressed on these cells in all tissues and all systems of inflammation is lacking

Mo-DCs display several characteristics resembling cDCs, such as the ability to illicit T cell proliferation and IFNɣ production *ex vivo*. Mo-DCs are found in the T cell areas of the lymph nodes, are CCR7-dependent, and are phenotypically and anatomically different from the sub-capsular and medullary macrophages that express CD206 and CD209b (SIGN-R1) at steady state (Cheong et al., 2010). Intriguingly, mo-DCs were found also

to be Flt3-independent, express CD14 and dramatically reduced in the *LyzM$^{CRE}$ x iDTR* mouse model (Cheong et al., 2010) indicating that they were more closely associated with the myeloid lineage.

These markers have since been used to define mo-DCs that arise in response to LPS. However, not all markers are used for identification and a combination of one (CD209a, CD206 or CD14) with high expression of CD11c, MHCII and CD11b continue to be used as a phenotypic description of 'Mo-DCs' (Meredith et al., 2012). This has led to confusion surrounding these cells, specifically regarding their origin from either the monocyte or DC lineage, their phenotypic definition, and their correlation to macrophages and cDCs and to other inflammatory progeny of the mononuclear phagocyte system. Thus, there is currently no consensus on the definition of mo-DCs.

### *1.5.3 Ontogeny of Mo-DCs*

Mo-DCs have been described in various models of inflammation, including pathologies in the lung such as asthma (Plantinga et al., 2013), in the gut in models of colitis (Tamoutounour et al., 2012; Zigmond et al., 2012), and in secondary lymphoid organs like the spleen and lymph nodes in infectious models with *Listeria* (Greter et al., 2012) and *Leishmania* (León et al., 2007). Mo-DCs are also widely identified from inflammatory fluids from patients with tumour ascites or rheumatoid arthritis (Segura et al., 2013)

Largely, mo-DCs were thought to arise from Ly6C$^{hi}$ monocytes, but there are conflicting results from different studies. Using the *Flt3$^{-/-}$* mouse models, Cheong et al. showed that the CD11c$^{+}$MHCII$^{+}$CD209a$^{+}$CD206$^{+}$ cells that arose in response to LPS, did not rely on Flt3 expression indicating that they were distinct from the cDC lineage (Cheong et al., 2010). *Flt3l$^{-/-}$* mice administered with house dust mite allergen (HDM) have similar levels

of mo-DCs (FcεR1$^{+}$CD64$^{+}$) cells as WT controls (Plantinga et al., 2013). LPS- injected WT and Zbtb46-DTR (*zDC$^{DTR/DTR}$*) mixed bone marrow chimeras had reduced levels of zDC-DTR CD14$^{+}$CD11c$^{+}$MHCII$^{+}$ cells in the skin draining lymph nodes. This showed that these cells were dependent on the cDC- lineage (Meredith et al., 2012). The use of genetic models and stringent gating strategy without a common phenotypic definition, might be the reason for this confusion.

The expression of Ly6C on mo-DCs differs with each study. A careful examination of the various studies shows that the expression of Ly6C is context-dependent and also relies on whether the researcher includes populations that are iNOS/TNFα$^{+}$ or cells that are MHCII$^{hi}$ and arise in response to inflammation. iNOS/TNFα$^{+}$ cells are found to be Ly6C$^{hi}$ (Serbina et al., 2003) while the MHCII$^{hi}$ CD11b$^{+}$CD11c$^{+}$ gated mo-DCs are Ly6C$^{lo}$ (Cheong et al., 2010; Plantinga et al., 2013). I could thus speculate that Ly6C$^{lo}$MHCII$^{hi}$ cells might be transcriptionally and phenotypically different to inflammatory cells that produce iNOS and arising from a unique precursor.

### *1.5.4 Function of Mo-DCs*

Mo-DCs are better at antigen uptake and processing than cDCs (Daro et al., 2000). *In vitro* culture of B and T cell-depleted murine bone marrow in GM-CSF results in the development of DC aggregates that are efficient at induction of MHCII-restricted T cell activation (Inaba et al., 1992). House dust-mite (HDM) allergen sensitized mo-DCs, and not tissue DCs, when adoptively transferred into naïve mice that were then given a booster dose of allergen, respond with a strong Th2 mediated immune reaction with eosinophil infiltration into the lung indicating the central role of mo-DCs in the uptake and presentation of antigen to T cells *in vivo* (Plantinga et al., 2013). Within this model, migration of mo-DCs to draining lymph nodes in the case of Th2 immune responses have been found to be largely CCR7 dependent (Plantinga et al., 2013). By eliciting a number of pro-inflammatory cytokines such as IL-1β and IL-6 (Cook et al., 2004) and chemokines

like CCL2, CCL7 (Plantinga et al., 2013), mo-DCs gain the capacity to recruit other immune cells to the site of inflammation. Ly6C$^{hi}$CCR2$^{+}$ mo-DCs rely on GM-CSF to exert their effect in certain pathologies such as EAE (Croxford et al., 2015). *Ccr2$^{cre}$ x Csf2r$^{fl/fl}$* mice when injected with myelin oligodendrocyte glycoprotein (MOG) peptide developed Ly6C$^{hi}$MHCII$^{+}$ Mo-DCs but did not develop EAE as it was noted that their expression of IL-1β was greatly diminished (Croxford et al., 2015). Human monocytes when cultured in GM-CSF, also produced much higher levels of IL-1β than controls (Croxford et al., 2015). Thus, GM-CSF appears to control the functional role of mo-DCs in regards to their capacity for antigen presentation and the production of inflammatory cytokines.

### *1.5.5 iNOS expression by monocyte-derived cells*

Inducible nitric oxide synthase (iNOS) is an enzyme that is induced upon inflammation in macrophages (Beckerman et al., 1993). The enzyme aids in the production of nitric oxide (NO) that carries out bactericidal activity and has been considered toxic to the cell producing it in excessive amounts. *Nos2$^{-/-}$* mice are more susceptible to infection by *Listeria monocytogenes* (*L.m.*) iNOS expression by activated monocytes was first documented by Pamer and colleagues (Serbina et al., 2003) who coined the term Tip-DCs for TNF-α and iNOS-producing DCs to describe the cells that resulted from the activation of CCR2-dependent Ly6C$^{hi}$ monocytes in response to an *L.m.* infection. Supporting the notion of their origin from Ly6C$^{hi}$ monocytes, *LyzM$^{cre}$x Csf1r$^{lslDTR}$* mice upon infection with *L.m.* have a significantly reduced level of iNOS$^{+}$ TNFα$^{+}$ cells in the spleen (Schreiber et al., 2013). Other than iNOS expression this phenotype of MHCII$^{+}$CD11c$^{+}$CD11b$^{+}$matches that of mononuclear phagocytic cells that arise under conditions of elevated levels of GM-CSF. As a results iNOS$^{+}$ cells have been considered a type of GM-CSF induced mo-DC (Greter et al., 2012; Naik et al., 2006). Zigmond et

al. examined the role of iNOS$^{+}$ cells *in vivo* in a mouse model of colitis and reported that Ly6C$^{hi}$ monocytes give rise to iNOS$^{+}$ cells, a phenotype which is followed by a DC-like phenotype at a later time point (Zigmond et al., 2012). This report will examine the relationship of iNOS$^{+}$ cells and mo-DCs in greater detail.

## 1.6 Objectives and overall aims

### *1.6.1 Rationale of the study*

Mo-DCs and iNOS-producing cells are considered to be part of the same population of cells despite the lack of convincing evidence other than concomitant expression of MHCII, CD11c and CD11b (Naik et al., 2006). Studied in various organs with different models of inflammation, various markers have been used to phenotype these cells, the most selective so far being Fcεr1 and CD64 in the lung and gut (Plantinga et al., 2013; Segura and Amigorena, 2013; Tamoutounour et al., 2012) during allergic asthma and colitis, respectively. But whether these markers appear in other models of inflammation, for example in response to LPS where they have been phenotyped as $CD209a^{+}CD206^{+}$ remains to be determined. Another aspect that remains to be deciphered is the origin of mo-DCs. While $iNOS^{+}$ cells are thought to derive from $Ly6C^{hi}$ monocytes, the question of whether mo-DCs belong to the monocyte or DC lineage remains unanswered.

### *1.6.2 Objectives of this study*

This study aimed to answer the following questions

- Is there a distinct precursor population for mo-DCs and $iNOS^{+}$ cells?
- Are mo-DCs and $iNOS^{+}$ cells the same?
- Can mo-DCs and $iNOS^{+}$ cells be distinguished from other myeloid populations at the site of inflammation?
- If there is a distinct precursor population, does it belong to the monocyte or the cDC lineage?

# Thesis Outline

Chapter 2 will discuss the material and methods used during this thesis including mouse models used and the various techniques used to transcriptionally define the cell populations discussed.

Chapter 3 will describe the phenotype of a novel precursor population of Ly6C$^{hi}$ monocytes that bear at steady state, the characteristic of mo-DCs. Their association with the monocyte and cDC lineages will be addressed.

Chapter 4 will address the cell types that arise in response to GM-CSF given its central role in the derivation of mo-DCs.

Chapter 5 will interrogate the ontogeny of iNOS$^{+}$ cells and will compare these to cells that arise in response to GM-CSF.

Chapter 6 will be a discussion of the results obtained and their wider implications.

# Chapter 2:
# Materials and methods

# 2 Materials and Methods

## 2.1 Animal models: Mice

C57Bl/6 mice were bought from Charles River Laboratories, UK. All mice used were between 6-12 weeks old and age- and sex- matched for all experiments. Genetically modified mice are described in Supplemental Procedures. They were maintained under specific pathogen-free conditions in accordance with the UK Animals (Scientific Procedures) Act, 1986.

### *2.1.1 Genetic knockouts*

### *2.1.2 $Ccr2^{-/-}$ mice:*

Generated as previously described by Boring et al, $Ccr2^{-/-}$ mice were a gift from Prof. Frederic Geissmann (Boring et al., 1997).

### *2.1.3 $Nr4a1^{-/-}$ mice:*

Generated by Lee et al (Lee et al., 1995), these mice were housed within King's College London by the laboratory of Prof. Frederic Geissmann. Littermate controls and knock-outs were generaously provided by Frederic Geissmann.

### *2.1.4 $Sfpi1^{+/-}$ mice:*

Generated by McKercher et al, $Sfpi1^{+/-}$ (C57Bl/6**)** breeders were generously provided by Prof. Frederic Geissmann (McKercher et al., 1996). $Sfpi1^{+/-}$ mice were bred within the conventional unit of King's College London and used from matings of $Sfpi1^{+/-}$ males with C57BL/6 females.

### *2.1.5 Zbtb46-GFP mice (Satpathy et al., 2012)*

Originally described by Murphy and colleagues, Zbtb46-GFP mice (C57BL/6) were housed at the animal facility at Queen Mary, University of London and were a kind gift from Dr. Maria Longhi.

### *2.1.6 pIII $^{+}$pIV$^{-/-}$, pIV$^{-/-}$, pI$^{-/-}$ and Ciita$^{-/-}$ mice:*

Various knockouts for the promoters of *Ciita – pIII $^{+}$pIV$^{-/-}$* mice (C57BL/6) (LeibundGut-Landmann et al., 2004), *pIV$^{-/-}$* (C57BL/6)(Waldburger et al., 2001), *pI$^{-/-}$* (C57Bl/6) (Dubrot et al., 2014) were generated as described before and were housed at Geneva Medical School, Switzerland within the lab of Dr. Stephanie Hugues. Maintenance and experimentation on these mice were carried out by Dr. Juan Dubrot Armendariz of the same laboratory.

### *2.1.7 Zbtb46$^{Cre}$x ROSA$^{loxSTOPloxYFP}$ mice*

*Zbtb46$^{Cre}$* mice were generated by Loschko *et al* (Loschko et al., 2016b) and were crossed onto a mouse expressing the transcriptional STOP element flanked by loxP sites (that are recognized by Cre recombinase) within the ubiquitously expressed ROSA locus – the *ROSA $^{loxSTOPlosYFP}$* mice (Jakob Loshko, 2016). This provided a conditional knockout specifically in cells that expressed *Zbtb46*. *Zbtb46$^{Cre}$x ROSA$^{lSlYFP}$* were housed within the The Rockefeller University, New York, USA. Bone marrow from these mice was provided by Prof. Michel Nussenzweig, transported on dry ice to our laboratory and used to re-constitute age- and sex-matched lethally irradiated C57BL/6 mice. Mice were allowed to completely re-constitute their hematopoietic system whist in quarantine for 8-12 weeks before use.

### *2.1.8 zDC$^{DTR/DTR}$ mice*

Generated as described before (Meredith et al., 2012), *zDC$^{DTR/DTR}$* mice were housed within The Rockefeller University, New York, USA. Bone marrow from these mice was provided by Prof. Michel Nussenzweig, transported on dry ice to our laboratory and used to re-constitute age- and sex-matched lethally irradiated C57BL/6 mice. Mice were allowed to completely re-constitute their hematopoietic system whist in quarantine for 8-12 weeks before use. In order to knock out cells expressing Zbtb46, 20ng of diphtheria

toxin /g weight of the mouse was administered intra-peritoneally 20 hours prior to sacrifice.

### *2.1.9 Nos2$^{Tomato\text{-}Cre}$xROSA$^{loxSTOPloxtdTomato}$*

*Nos2$^{Tomato\text{-}Cre}$* mice were created in the Institut Clinique de la Souris (Illkirch, France)

The tdTomato-ires-Cre cassette was inserted by homologous recombination into the RP23-341J22 bacterial artificial chromosome (BAC) within the 2$^{nd}$ exon of the *Nos2* gene with the ATG of the tdTomato replacing the endogenous ATG. This was done through the collaboration with Gregoire Lauvau (Albert Einstein College of Medicine, New York ,USA) and Frederic Geissmann (King's College London, UK).

These mice were then crossed onto *Rosa26-$^{tdTomato}$* mice (Madisen et al., 2012) to generate a fluorescence within the 585 channel in order to fate map iNOS$^{+}$ cells (Bechade et al., 2014). The cross is called *Nos2$^{Tomato\text{-}Cre}$xROSA$^{loxSTOPloxtdTomato}$* and were housed within Institut de Biologie de l'Ecole Normale Superieure, Paris, France.

Bone marrow from these mice was provided by Dr. Alain Bessis, transported on dry ice to our laboratory and used to re-constitute age- and sex-matched lethally irradiated C57BL/6 mice. Mice were allowed to completely re-constitute their hematopoietic system whist in quarantine for 8-12 weeks before use.

### *2.1.10 Flt3L$^{-/-}$*

Generated as described before (McKenna et al., 2000), the *Flt3L$^{-/-}$* mice (C57BL/6) were maintained within the Francis Crick Institute, London, UK and were generously donated by Prof. Caetano Reis e Sousa.

### *2.1.11 Bone marrow Chimeras:*

8-10 week old C57bl/6 mice were hematopoietically-lethally irradiated at 11Gy; bone marrow from *Zbtb46-Cre-loxSTOPloxYFP* (Loshko *et al*, 2016) , *Zbtb46-iDTR* mice (Meredith et al., 2012) or *NOS2-$^{Tomato\text{-}Cre}$xROSA$^{loxSTOPloxtdTomato}$* (Bechade et al., 2014)was

injected intravenously at a dose of 5 x $10^6$ cells in100µl into these irradiated recipients. To allow full reconstitution, the mice were used at 8-16 weeks after transplantation. *Ccr2*$^{-/-}$ (CD45.2$^+$) and WT (CD45.1$^+$) mixed bone marrow chimeras were produced in hematopoietically-lethal irradiated (11Gy) CD45.1$^+$ recipients by transplanting them with CD45.1$^+$ WT and *Ccr2*$^{-/-}$ (CD45.2$^+$) bone marrow in equal parts. CD45.1$^+$ recipients that received 100% CD45.2$^+$ C57Bl/6 bone morrow were used as a control for the complete replacement of recipient bone marrow with donor-derived bone marrow.

## 2.2 Genotyping

### *2.2.1 DNA Isolation*

Genomic DNA was isolated by digesting ear biopsies of animals in a digestion buffer with ProteinaseK at 56$^o$C for 2 -14 hours before being centrifuged to remove debris and placed on ice. Supernatants containing the DNA were then mixed with equal volumes of 100% cold isoproponal to allow the DNA to fall out of solution. Upon centrifugation, the pellets were washed with cold 70% ethanol. Pellets were allowed to dry with only a small volume of supernatant left before 100µl of water was used to dissolve the DNA. Samples were stored at 4$^o$C until required for analysis.

### *2.2.2 Genotyping protocol for Sfpi*$^{+/-}$ *mice*

Single reaction for 2 PCR products was carried out using the HotStartTaq kit (Qiagen). Each reaction contained 2µl of genomic DNA (prepared as mentioned above), 0.5µl of each primer, 12.5µl of HotStartTaq reagent (Qiagen), 2.5µl of CoralLoad DNA loading buffer (Qiagen) and DNase free water to perform a 25ul PCR reaction. Primers used for the genotyping of the *Sfpi1*$^{+/-}$ mice were:

Forward: 5'- GCC CCGGAT GTGCTT CCC TTA TCA AAC-3'
Reverse Neo: 5'CGC ACG GGT GTT GGG TCG TTT GTT CGG-3'
Reverse WT: 5'TGC CTCGGC CCT GGG AAT GTC -3'
Expected band width:

Wt band:1170bp

Knock-out band: 980bp

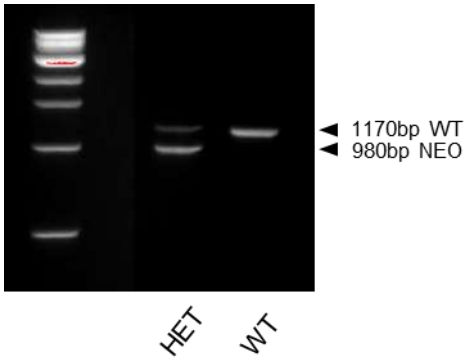


**Figure 2-1: *Sfpi1* genotyping gel** of a WT and heterozygous mouse against a 1kb ladder.

The PCR reaction was run for 30 cycles of the following temperatures and time intervals:

Denaturation at 95$^{o}$C for 45s, annealing at 60$^{0}$C for 45s and elongation at72$^{o}$C for 90s after an initial hold of 95$^{o}$C for 15mins.

Post-PCR reactions were run on 1.5% agarose gels made with TBE buffer (Life technologies) and containing ethidium bromide (Santa Cruz Biotechnology) alongside a 1kb DNA ladder (NEB). PCR products were visualized using Bio-Rad Gel Doc EZ System.

## 2.3 Preparation of cell suspensions from various tissue

### *2.3.1 Preparation of mouse bone marrow cell suspension*

Murine bone marrow was obtained from both tibia and femurs from each mouse. The ends of each bone were cut and the bone flushed using a 23G syringe with cold FACS buffer into centrifuge tubes. Cell suspensions were maintained on ice. After centrifugation at 320rcf for 4mins at 4$^{o}$C, cell pellets were resuspended in Ack RBC lysis buffer (Life technologies) and incubated at RT for 2 mins before being diluted with FACS buffer and pelleted again. The resulting pellets were resuspended in fresh FACS buffer and left on ice until stained with appropriate antibody cocktails.

### *2.3.2 Preparation of mouse blood cells*

Murine blood was obtained by cardiac puncture after exposure to an increasing gradient of $CO_2$. Blood was collected using a 23G syringe coated on the inside with 2000IU/ml (10x) Heparin (Sigma Aldrich) and deposited in microcentrifuge tubes containing 100ul of 100mM EDTA (Life technologies) and 10ul of 20,000 IU/ml (100x) Heparin on ice. This mixture was then added to 1.5ml of Ack RBC lysis buffer and incubated on ice for 7 mins. Cell suspensions were centrifuged at 320rcf for 4mins at 4$^{o}$C and Ack lysis was repeated. After centrifugation, cell pellets were resuspended in fresh FACS buffer and left on ice until stained with appropriate antibody cocktails.

### *2.3.3 Preparation of mouse splenocytes*

Mouse spleens were collected in Digestion buffer (HBSS$^{+}$1%FBS), cut into small pieces and incubated with CollagenaseD (0.375U/ml) and DNaseI (10µg/ml) for 20 mins at 37$^{o}$C. The reaction was stopped by placing the spleens on ice and adding EDTA at a final concentration of 2mM. Spleens were then smashed through 100um filters and the cell suspensions centrifuged at 320rcf for 4mins at 4$^{o}$C. Ack lysis at RT for 5mins was stopped by dilution with FACS buffer. Cell suspensions were centrifuged and cell pellets resuspended in fresh FACS buffer.

## 2.4 Flow cytometry

### *2.4.1 Enrichment of cells for fluorescence assisted cell sorting*

For experiments requiring the sorting of specific cell populations or enrichment of Ly6C$^{hi}$ monocytes for *in vitro* cultures, cell suspensions that were prepared as detailed above, were incubated with biotin-labelled antibodies for the lineage (containing anti-CD3ε, anti-CD19, anti- NK1.1, anti-CD45RA, anti-Ter119, anti-ckit, anti-Ly6G) for 20 mins on ice. Cells were washed to remove excess antibody and incubated with MACS beads (30µl

beads/200µl buffer/80-100x $10^6$ cells) for 20 mins in the fridge. Cells were then centrifuged and resuspended in FACS buffer to be passed through a pre-washed depletion (LD) column (Miltenyi). The flow-through was collected and 2ml of FACS buffer was passed through the column to retrieve any non-lineage cells that may have adhered to the column. The flow through was then centrifuged and the pellet resuspended in FACS buffer for staining with appropriate antibody cocktails.

### *2.4.2 Flow cytometry reagents*

Fluorochrome or biotin- conjugated antibodies were used to stain single cell suspensions for flow cytometry. that were bought from eBioscience (Hatfield, UK) and Biolegend (London, UK).

| Marker | Clone |
|---|---|
| CD19 | MB19-1 |
| Ly6G | 1A8 |
| CD3ε | 145-2C11 |
| NK1.1 | PK136 |
| CD45RA | HI100 |
| ckit | 2B8 |
| MHCII I-A/I-E | M5/114. 15.2 |
| Ly6C | HK1.4 |
| CD11b | M1/70 |
| CD115 | AFS98 |
| CD16/32 | 93 |
| CD209 | LW206 |
| CD135 | A2F10 |

| | |
|---|---|
| CD172a | P84 |
| CD11c | N418 |
| CD273 | TY25 |
| CD274 | 10F.9G2 |
| Ter119 | Ter119 |
| | |

### *2.4.3 Intracellular FACS staining*

For staining intracellular levels of iNOS, cells were fixed and permeabilized using BD Cytofix/Cytoperm Fixation kit as per manufacturer's instructions and stained with anti-iNOSA488 or -iNOS-PE (clone: CXNFT) purchased from eBioscience. For staining PU.1, cells were fixed and permeabilized using FoxP3/ Transcription factor staining buffer set (eBioscience) according to manufacturer's instructions. Anti-PU.1 rabbit monoclonal antibody (clone: 9G7) and the corresponding isotype were purchased from Cell Signaling Technology (New England Biolabs (UK) Ltd).

## 2.5 Adoptive Transfer experiments

### *2.5.1 Adoptive transfer of FACS sorted cells*

For adoptive transfer of FACS sorted cells, cell suspensions of whole organs were made (see earlier). Cell suspensions were exposed to Ack lysis and further enriched using MACS beads and a depletion column (LD column)(Miltenyi) (see above). Cells were then stained with appropriate fluorochromes and sorted using the BD FACSAria II. 3.3 x $10^5$ cells of each population were sorted into complete RPMI, centrifuged and resuspended in RPMI alone to be injected *i.v.* into CD45.1$^+$ congenic recipients, in a total volume of 120µl per mouse.

### *2.5.2 Adoptive transfer of whole bone marrow*

For whole bone marrow transfers, single cell suspensions of bone marrow (prepared as above) were depleted of red blood cells by exposure to Ack RBC lysis buffer (Life technologies) and counted. 40 x $10^6$ whole bone marrow cells from *Sfpi1*$^{+/+}$ or *Sfpi1*$^{+/-}$ mice were transferred into B16-GM-CSF treated congenic CD45.1$^+$ mice on day9 and analyzed on day11 after tumor injection; For *L.m.* infected recipients, 20x$10^6$ whole bone marrow cells were transferred into congenic CD45.1$^+$ recipients 6 hours before *L.m.* infection *i.v.*.

### *2.5.3 Reagents:*

Complete medium used for cell culture was RPMI with Glutamax, (Life technologies) and 10% FBS (Life technologies) and 50uM beta-mercaptoethanol (Sigma). FACS buffer used was made of PBS (Life Technologies) with 1% bovine serum albumin (Apollo Scientific) and 2mM EDTA (Life technologies).

### *2.5.4 Cell Isolation and fluorescence-activated cell sorting.*

Single-cell suspensions of the bone marrow of each mouse were prepared by flushing the bones of both hind limbs (2 tibia and 2 femurs) with ice cold FACS buffer (PBS (Life technologies) with 1% BSA (Apollo Scientific Ltd) and 2mM EDTA (Life Technologies)). Spleens were collected, cut into small pieces and incubated with Collagenase D (Roche) and DNaseI (Roche) in HBSS (PAA) $^+$ 5% Fetal Bovine Serum (Life technologies) for 20 mins. They were then smashed through 100um cell strainers (BD Falcon) to obtain cell suspensions. To lyse the red blood cells, bone marrow suspensions were pelleted and resuspended in 2ml of Ack lysis buffer (Life technologies), incubated for 2 mins at room temperature and then diluted with FACS buffer. After centrifugation at 320rcf for 4 mins at 4$^o$C, cells were either re-suspended in antibody

cocktail in FACS buffer or permeabilized/fixed for intracellular staining. Cells were analysed using BD LSR Fortessa. For sorting, bone marrow or spleen cells were resuspended to an approximate concentration of 7000cells/µl. They were then sorted on a BD FACS Aria (special order machine) fitted with 405nm, 488nm, 561nm, 633nm lasers and sorted through 100µm nozzle with 4-way purity. Purity checks were run on samples used for microarrays and were used when purity was found to be >95%.

Both instruments were housed at the Biomedical Research Centre Flow Core Facility (Guy's and St Thomas' NHS Foundation Trust and King's College London). Flow cytometry analysis was done using FlowJo software (TreeStar).

## 2.6 Giemsa Staining

Cytospins of FACS sorted R1, R2, R3 and P were fixed with methanol for 5 mins, stained with 1:20 Giemsa stain in deionized water for 45 mins and then washed and air dried. Slides were imaged on Motic AE2000 with 40x magnification. Images were modified for brightness with ImageJ (NIH).

## 2.7 In vitro culture experiments

### *2.7.1 In vitro GM-CSF Cultures*

Total BM or $10^4$ sorted $Ly6C^{hi}CD115^+$ monocytes (total or R1, R2, R3 subsets) cells were cultured in 20ng/ml of GM-CSF in complete RPMI with 6000 live MS-5 cells or whole bone marrow congenically marked, as indicated per experiment, as 'feeders', plated on the same day. Cells analysed were pre-gated to be $DAPI^-$ and $CD45^+$.

### *2.7.2 In vitro L.m. infections:*

*In vitro* cultures of primary sorted cells with *Listeria monocytogenes* (*L.m.)* was done overnight at an MOI of 0.01 or 0.1 as indicated in complete RPMI1640 medium supplemented with MCSF (20ng/ml) (Peprotech), GM-CSF(3ng/ml) (Peprotech) and

human Flt3L(100ng/ml) (CellDex). BMDMs were derived from *Sfpi1*$^{+/-}$ or *Sfpi1*$^{+/+}$ BM cultured for 8-10 days in DMEM medium (Life technologies) supplemented with 10% FBS and 10% MCSF containing L-929 cell culture supernatant. These were re-plated as 0.45 x $10^6$ cells/well in a 24-well non-tissue culture treated plate to be stimulated with LPS (1µg/ml) or *L.m.* at MOI 1 or 10 for 16 hours. Cells were collected, stained with fluorochrome conjugated antibodies and analysed by FACS.

### 2.8 B16-GM-CSF tumor experiments

Melanoma cell lines B16 and B16 expressing GM-CSF (B16-GM-CSF)(Dranoff et al., 1993) were maintained in RPMI1640 medium supplemented with Glutamax (Life technologies), 10% fetal bovine serum (Life technologies), 1% penicillin-streptomycin (Life Techonologies) and 50uM beta-mercaptoethanol (Sigma) and used from between passages 4 and 10. Cells were checked for viability with Trypan Blue and 1.5-3 x $10^5$ live cells were injected subcutaneously in sterile RPMI 1640 medium alone.

### 2.9 Infection

*Listeria monocytogenes* or the ΔActA mutant of the same (ΔActA *Listeria)* were grown and sub-cultured in brain heart infusion broth at $37^0$C until an $OD_{600}$ value of 0.12-0.15 was obtained to use bacteria in their exponential growth phase. 4 – 5 x $10^3$ wild type CFU (Listeria) or $10^6$ ΔActA mutant CFU of *L.m.* were injected intravenously in sterile PBS.

### 2.10 Microarray processing and analysis:

The NuGEN Ovation Pico WTA v2 kit was used to process 1ng RNA per sample into SPIA amplified cDNA. The Encore Biotin Module (NuGEN) was used to fragment and biotin-label the cDNA. Hybridisation cocktails were prepared as recommended by NuGEN and hybridised to Affymetrix Mouse Gene 1.0 ST arrays overnight. Arrays were washed and stained using Affymetrix Fluidics Station FS450 and GeneChip Hybridisation Wash Stain kit and scanned in GCS3000 7G scanner with Autoloader. Raw

data files (DAT and CEL) were generated in Affymetrix GeneChip Command Console software (AGCC).

Affymetrix CEL files were converted into gct files using the ExpressionFileCreator Module within Gene Pattern Software (Broad Institute) (Reich et al., 2006). The RMA algorithm withquantile normalization and background correction was used. No thresholds or filters were applied for assessing the relative expression of all genes assayed on the microarray. Heat maps were generated with this data on Gene-E software (https://software.broadinstitute.org/GENE-E/). Heat maps show relative raw expression values for each gene, comparing one sample to the others. Colour bars therefore indicate highest to lowest values for each gene.

To create the Volcano plots, MutiplotPreprocess Module within the Gene Pattern Software (Broad Institute) was used to derive fold change and p-values from the expression dataset of the aforementioned microarrays to be used in the MultiplotVisualizer Module. This latter module was used to highlight the genes more highly expressed in R2 or R3 above a threshold of p-value set at 0.05 and fold change of 1.2. These selected genes were then overlaid on comparisons done between R1 and R2, and R1 and R3 to obtain the plots shown in Fig.1F.

### 2.11 PCA analysis and hierarchical clustering:

Microarray data of R1, R2 and R3 were compared with ST1.0 array data available on ImmGEN for Pre-DCs (GSE68590) (Tussiwand et al., 2015)and CDP (GSE 15907) (www.immgen.org) on Qlucore Omics Explorer (Sweden) and plotted as 2D plots on Prism (Graphpad). Hierarchical clustering of data sets was performed using Gene-E software (Broad Institute).

### 2.12 qPCR on bulk sorted populations

Cells were sorted as described and centrifuged. Supernatant was removed

and cells were resuspended in RLT buffer from the RNeasy kit (Qiagen). mRNA was extracted using the columns as per manufacturer's instructions. mRNA was resuspended in RNase-free water and the concentration and quality measured by nanodrop (Thermo Scientific). Equal amounts of mRNA (between 0.1ng – 5µg) from each sample were taken to produce cDNA using the manufacturer's First Strand cDNA synthesis protocol with the RevertAid™ H minus Reverse Transcriptase (Thermo Scientific). Random Primers (Oligo dT primers) were mixed with template RNA and incubated at 65$^{o}$C for 5 mins and Ribolock (Thermo Scientific), dNTP mix, Reaction buffer (5x) and mMulV reverse transcriptase enzyme were added and incubated at RT for 10 mins, 42$^{o}$C for 1hr and at 70$^{o}$C for 5 mins to inactivate the enzyme. A 1 in 10 dilution of this cDNA was used to perform qPCR with Sensimix™SYBR® (Bioline) as per manufacturer's instructions. Primers used for testing Zbtb46 were: Forward 5'- AGA GAG CAC ATG AAG CGA CA-3', Reverse: 5'-CTG GCT GCA GAC ATG AAC AC-3'. Results were normalized against Actin B levels for each sample. Primers used for Actin-B were: and Forward: 5'-ATG CTC CCC GGG CTG TAT-3' and Reverse: 5'-CAT AGG AGT CCT TCT GAC CCA TTC-3'.

### 2.13 Multidimensional reduction analysis:

Automated t-distributed stochastic non-linear embedding (t-SNE) algorithm was used to visually (viSNE) analyse (Amir el et al., 2013) bone marrow monocytes acquired by FACS for 7 fluorochromes. The online (web-based) software implementation of viSNE (Cytobank) (Kotecha et al., 2010) was used to analyse the presence of different populations within the Ly6C$^{hi}$CD115$^{+}$ BM monocytes. No *a priori* gating was used and an unbiased automated analysis was conducted. The resulting viSNE maps were overlaid with each monocyte population, R1, R2 and pre-DC R3 that were gated separately by

conventional FACS analysis. The colour scheme for all four viSNE maps was adjusted to represent the Flt3 expression – blue colour denoting lower levels and red – higher.

### 2.14 Single cell qPCR

Single cells were FACS sorted from bone marrow into 9ul of Cell Direct pre-Amp master mix in 96-well qPCR plates. Complementary DNA synthesis and specific target amplification of 45 genes (including 3 housekeeping genes- Hprt, ActB, Gapdh) was performed using CellsDirect One Step qRT-PCR kit (Invitrogen) with 48 Taqman assays (Life technologies) at 0.2x. Reverse transcription was performed within the same plates using the following cycle: 40$^{o}$C for15 mins, 50$^{o}$C for 15 mins, 60$^{o}$C for 15 mins. Enzyme inactivation was done at 95$^{o}$C for 2mins followed by 22x (95$^{o}$C for 15s, 60$^{o}$C for 4mins). cDNA was then diluted 1 in 5 in low EDTA TE buffer. Samples were stored at -20$^{o}$C until used in the BioMark. 81 cells of R2, and 44 cells of R1 and R3 each were compared along with control well including 10 cells and no cell controls and dilutions of cDNA from $10^5$ cells to 1 cells to check for primer viability. 5µl of diluted cDNA + Taqman mastermix+ Sample loading reagent and 5 µl of each Taqman assay + Assay loading reagent were loaded into their respective wells on 4 M48.M48 Dynamic Arrays. Samples and Assays were then loaded into the reaction chambers of the Dynamic Array using the IFC ControllerMX(Fluidigm), and then transferred to the BioMark HD for qPCR (95$^{o}$C for 10 min; 40 cycles of 95$^{o}$C for 15 s and 60$^{o}$C for 60 s). Data obtained from the 'Real time PCR analysis' software (Fluidigm) was analysed using Gene-E software.

The following Taqman probes were tested on all samples:

**Table 2-1: List of primers used for single-cell qPCR**

| Gene | Primers |
|---|---|
| Adamts3 | Mm00625880_m1 |
| Cd209a | Mm00460067_m1 |
| Cd209c | Mm00652419_m1 |
| Cd209d | Mm00459972_m1 |
| Cd209e | Mm00459980_m1 |
| Cd74 | Mm01262763_m1 |
| Ciita | Mm00482914_m1 |
| Clec10a | Mm00546124_m1 |
| Clec4a2 | Mm00488795_m1 |
| Clec4g | Mm01212425_m1 |
| Clec5a | Mm01131766_m1 |
| Clec7a | Mm00490960_m1 |
| Clec9a | Mm00554956_m1 |
| Csf1r | Mm01266652_m1 |
| Csf2ra | Mm00438331_g1 |
| Csf2rb | Mm00655745_m1 |
| Csf3r | Mm00432735_m1 |
| Ctsb | Mm01310506_m1 |
| CtsG | Mm00456011_m1 |
| Cybb | Mm01287743_m1 |
| Fcgr2b | Mm00438879_m1 |
| Fcgr3 | Mm00438882_m1 |

| | |
|---|---|
| Fcgr4 | Mm00519988_m1 |
| Flt3 | Mm00439016_m1 |
| H2-Aa | Mm00439211_m1 |
| H2-Ab1 | Mm01271199_m1 |
| H2-dma | Mm04337015_m1 |
| H2-dMb2 | Mm00783707_s1 |
| Id2 | Mm00711781_m1 |
| Irf8 | Mm00492567_m1 |
| Klrb1f | Mm04211785_m1 |
| Klrd1 | Mm00495182_m1 |
| Kmo | Mm01321343_m1 |
| Mgl2 | Mm01250813_m1 |
| Mpo | Mm01298424_m1 |
| Mrc1 | Mm00485155_m1 |
| Ms4a3 | Mm00460072_m1 |
| Nfil3 | Mm00600292_s1 |
| Sfpi1 | Mm00488140_m1 |
| Spib | Mm03048233_m1 |
| Tcfec | Mm01161234_m1 |
| zbtb46 | Mm00511327_m1 |

These genes were selected for their discriminating capacity based on the PCA analysis between sorted populations of R1, R2 and R3 along with genes with previously described expression in monocytes and DCs. Below is a heat map of the microarray data on sorted populations R1, R2 and R3, of all the genes assayed in the single-cells analysis. Genes highlighted in red are those that feature in the variables list from the PCA (**Figure 2-2**).

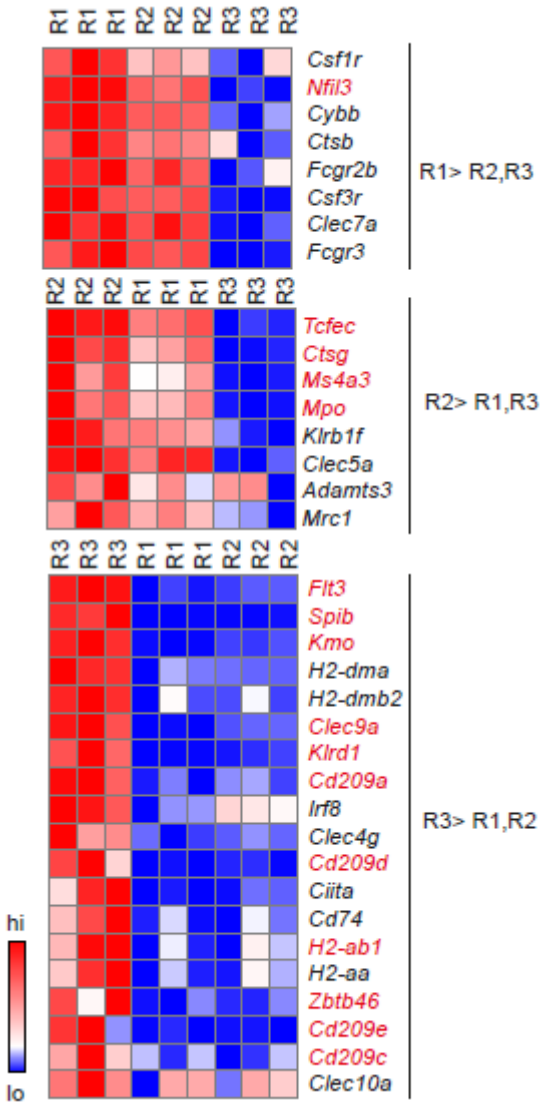


**Figure 2-2: Heat map of gene expression on R1, R2 and R3**. Microarray analysis of bulk-sorted populations R1, R2 and R3 of the genes that were most differentially expressed among R1, R2 and R3 in a PCA analysis (red) and genes of functional interest (black).

## 2.15 Statistical Analysis

Data was analysed for statistical significance by unpaired Student's t-test. Differences were considered significant for $p<0.05$. *$p<0.05$, **$p<0.005$, ***$p<0.0005$, ****$p<0.00005$, ns= not significant.

# Chapter 3:
# Heterogeneity of Ly6C$^{hi}$ monocytes

# 3 Heterogeneity of Ly6C$^{hi}$ monocytes

## 3.1 Introduction and Objectives

### *3.1.1 Introduction*

#### 3.1.1.1 *The role of monocytes and cDCs in the development of 'mo-DCs'*

cDCs and monocytes arise from distinct progenitors and represent members of distinct lineages that are characterised by elevated expression of transcription factors (*e.g. Zbtb46 for cDCs* (Meredith et al., 2012; Satpathy et al., 2012a), *LyzM* in monocytes (Cross et al., 1988)). During steady-state hematopoiesis, the development of monocytes and pre-cDCs arise from unique precursors such as cMop and CDP respectively. cDCs are classically characterized as cells that are reliant on Flt3L for their development (McKenna et al., 2000). Interestingly, 'Mo-DCs' have been reported to be both Flt3L-independent (Bogunovic et al., 2009; Croxford et al., 2015; Plantinga et al., 2013) and Flt3L-dependent (Meredith et al., 2012) suggesting that mo-DCs may arise from a heterogeneous population of precursor cells. It is important to note that each report had a slightly different gating strategy to characterize their target cell population. For example, Plantinga et al utilized CD11c$^{+}$MHCII$^{+}$CD11b$^{+}$MAR-1$^{+}$CD64$^{+}$cells (Plantinga et al., 2013) while Meredith et al. described mo-DCs as CD11b$^{+}$CD11c$^{+}$MHCII$^{hi}$CD14$^{+}$ cells (Meredith et al., 2012) which further complicates the matter and requires clarification.

Other studies also allude to the origin of mo-DCs from the cDC lineage. cDC lineage deleting *zDC$^{DTR/DTR}$* mice allow the induced depletion of all cells expressing Zbtb46. Meredith et al. noted that mixed bone marrow chimeras of WT and zDC-DTR mice did not have mo-DCs (defined as CD11b$^{+}$CD11c$^{+}$MHCII$^{hi}$CD14$^{+}$). This would suggest that mo-DCs originate from the cDC lineage (Meredith et al., 2012).

During inflammation, Ly6C$^{hi}$ monocytes are recruited in large numbers to the inflamed tissue where they differentiate into macrophage or DC-like cells (Askenase et al., 2015).

The local tissue-resident macrophages and cDCs also become activated and express higher levels of co-stimulatory molecules. Dependent on the conditions of inflammation, such as the type of pathogen involved (*Listeria, Leishmania,* etc.) (Segura and Amigorena, 2013; Serbina et al., 2008), the dose of antigen (Cook et al., 2004) and the cytokines present in the microenvironment, recruited Ly6C$^{hi}$ monocytes can develop into cells capable of producing iNOS and TNFα (Serbina et al., 2003) (referred to as Tip-DCs) or have a more regulatory role by producing TGF-β and IL-10 (Bain et al., 2013). Additionally, they contribute to the population of MHCII$^{hi}$ cells within tissues that are capable of presenting antigen to T cells (Cheong et al., 2010). These MHCII$^{hi}$ cells are referred to as monocyte-derived dendritic cells or 'mo-DCs'. Thus, Ly6C$^{hi}$ monocytes exhibit plasticity in response to various stimuli.

Cheong et al. described mo-DCs as cells that were CD209a$^{+}$CD206$^{+}$ which migrate to the lymph nodes in response to LPS stimulation *in vivo*. Interestingly, these cells were absent in *Ccr2*$^{-/-}$ mice and bore CD14 (Cheong et al., 2010) – 2 characteristics of murine monocytes (Geissmann et al., 2003). This suggests that the CD209$^{+}$CD206$^{+}$ MoDCs indeed come from Ly6C$^{hi}$ monocytes. Additionally, Murphy and colleagues elaborated on the distinction between LPS-induced DCs and CD11c$^{int}$CD11b$^{+}$Ly6C$^{hi}$ Tip-DCs; cDC lineage reporting *Zbtb46*$^{gfp/+}$ mice highlighted that the Tip-DCs found in the spleens of *Listeria monocytogenes (L.m)* infected mice were ZBTB46-GFP$^{-}$ indicating that they did not belong to the cDC lineage (Satpathy et al., 2012a). Conversely, the administration of LPS induced DCs in the spleen which were defined as CD11b$^{+}$MHCII$^{hi}$CD206$^{+}$ cells, were ZBTB46-GFP$^{+}$ (Satpathy et al., 2012a). This suggested that there are 2 DC-like inflammatory populations, of which one belongs to the DC lineage and one does not.

The *Zbtb46*$^{gfp/+}$ and *zDC*$^{DTR/DTR}$ mice provide a snapshot of the cells that are currently expressing *Zbtb46* but do not indicate the lineage that the cells originate from. The strongest evidence supporting the notion that cells of monocyte origin can differentiate

into DCs comes from the transcriptional profiling of mo-DCs in a model of colitis carried out by Jung and colleagues (2012). Mo-DCs were found to express Zbtb46 and Flt3 among other DC signature genes and were absent from *Ccr2*$^{-/-}$ mice (Zigmond et al., 2012). Interestingly, the DC-like phenotype followed from an iNOS-producing stage. However, experiments such as *ex vivo* analysis of the iNOS$^{+}$ cells for the expression of Zbtb46 and Flt3 was not done in this study, leaving questions open as to whether the Ly6C$^{hi}$ monocytes that become iNOS$^{+}$ evolved into DC-like cells with time or whether the DC-like phenotype appeared from distinct Ly6C$^{hi}$ cells.

Another hypothesis for the diverse phenotypes associated with Ly6C$^{hi}$ monocytes during inflammation is a previously uncharacterised heterogeneity within the population. I hypothesized that this heterogeneity might be represented by populations that have a pre-destined role in the development of either more macrophage features or more DC-like features. The discrepancies in the origin and phenotypic description of mo-DCs requires further clarification and is addressed in the present chapter.

### *3.1.2 Objectives*

Classically, Ly6C$^{hi}$ monocytes have been considered to be a homogenous population which leads to the development of macrophages and DCs during inflammation. A major aim of my thesis is to investigate the possibility of a novel population of Ly6C$^{hi}$ monocytes that could be responsible for the development of cells with DC-like features during inflammation. In order to achieve this, phenotypic and genetic features commonly associated with monocytes and/or dendritic cells were tested at steady state in the bone marrow, blood and spleen. In particular, the specific aims addressed in this chapter are:

- To investigate the heterogeneity of Ly6C$^{hi}$ monocytes.
- To establish the precursors for mo-DCs and inflammatory macrophages.
- To describe at a genetic level the specific function of these precursors.

- To establish the developmental precursors to mo-DCs and inflammatory macrophages

.

## 3.2 Results

### *3.2.1 Ly6C$^{hi}$ monocytes are a heterogeneous population*

#### 3.2.1.1 *Ly6C$^{hi}$ monocytes contain Flt3$^{+}$ subsets*

Ly6C$^{hi}$ monocytes do not have any unique transcription factors by which to distinguish them from other populations. The best way to identify Ly6C$^{hi}$ monocytes is by using characteristic surface markers analysed by flow cytometry. Conventional gating strategies for Ly6C$^{hi}$ monocytes require the use of the M-CSFR (CD115/CSF-1R) and SIRPα (CD172α) or the integrin CD11b after the exclusion of all other lineages (T cells, B cells, NK cells, RBCs, pDCs). This allows the selection of Ly6C$^{hi}$ and Ly6C$^{lo}$ monocytes. However, upon a closer examination of the expression of Flt3 and CD11c on these cells, it could be noted that Ly6C$^{hi}$ monocytes are in fact divisible into 3 sub-populations- Flt3$^{-}$CD11c$^{-}$ cells, Flt3$^{+}$CD11c$^{-}$ and Flt3$^{+}$CD11c$^{+}$ cells. These were named R1, R2 and R3 respectively for the purpose of our study (**Figure 3-1**).

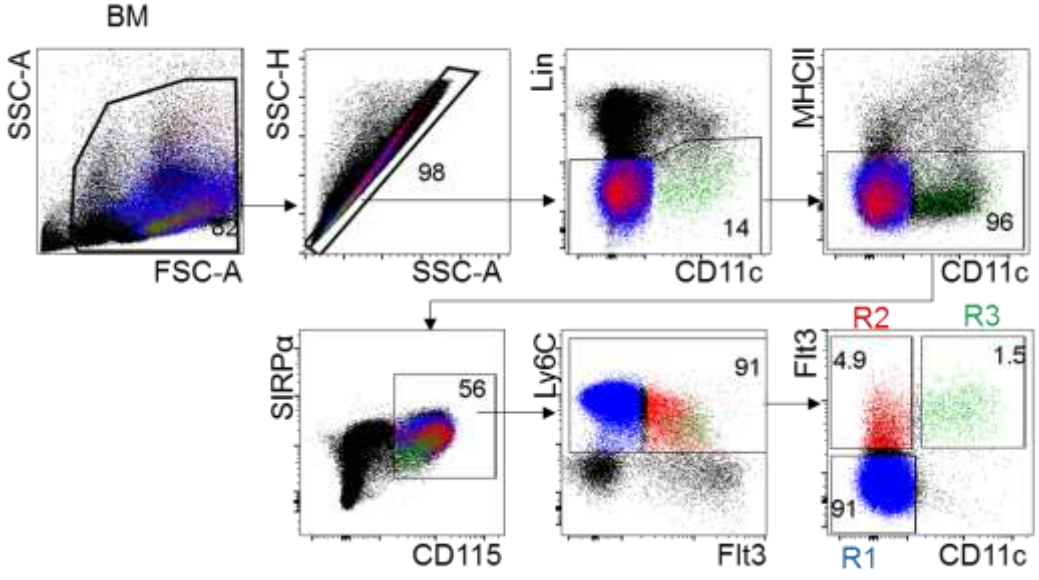


**Figure 3-1: Ly6C$^{hi}$ monocyte heterogeneity revealed using Flt3 and CD11c**. WT Ly6C$^{hi}$ monocytes were gated after the exclusion of CD19$^{+}$CD3e$^{+}$NK1.1$^{+}$Ter119$^{+}$CD45RA$^{+}$Ly6G$^{+}$ckit$^{+}$ cells (Lineage). The MHCII$^{-}$SIRPα$^{+}$CD115$^{+}$cells display 2 main levels of Ly6C expression. DC-related marker- Flt3 and CD11c were assessed on Ly6C$^{hi}$ monocytes. R1 (blue), R2 (red), and R3 (green) were overlaid on all previous hierarchical gates.

I next investigated the heterogeneity of the Ly6C$^{hi}$ monocytes in circulation. Indeed, Flt3$^{+}$ cells were visible within the Ly6C$^{hi}$ monocytes in the blood and spleen and in similar proportions as in the bone marrow **(Figure 3-2)**

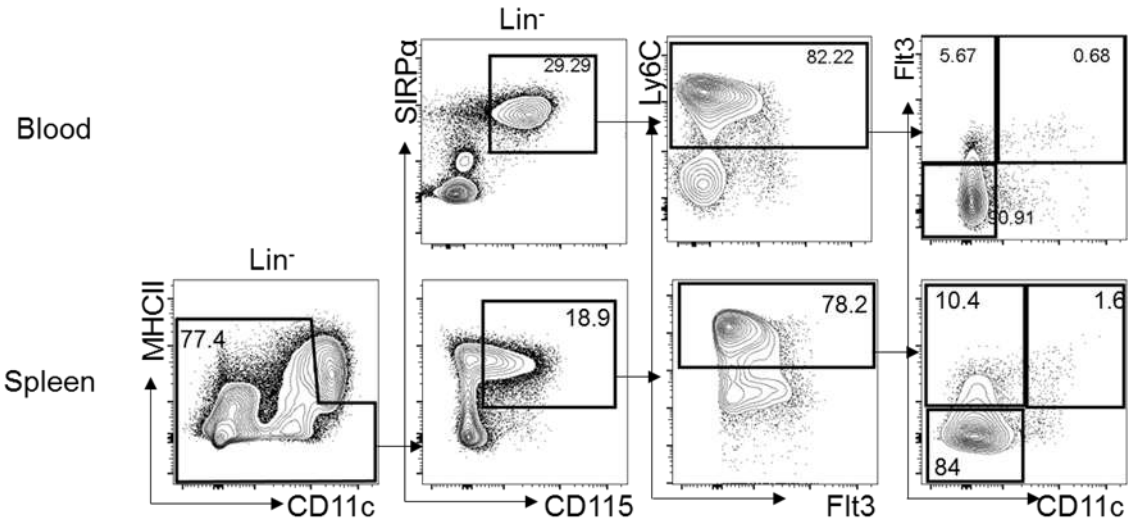


**Figure 3-2: Ly6C$^{hi}$ monocyte heterogeneity is perpetuated in the blood and spleen** WT blood Ly6C$^{hi}$ monocytes were gated on Lineage$^{-}$ (CD19$^{-}$CD3ε$^{-}$NK1.1$^{-}$Ter119$^{-}$CD45RA$^{-}$Ly6G$^{-}$ckit$^{-}$) SIRPα$^{+}$CD115$^{+}$ cells. WT spleen monocytes were gated after the exclusion of CD11c$^{+}$MHCII$^{hi}$ cDCs.

### 3.2.1.2 *Does the R3 population of Ly6C$^{hi}$ cells belong to the cDC lineage?*

Pre-cDCs are commonly gated as Lin$^{-}$MHCII$^{-}$CD11c$^{+}$Flt3$^{+}$ cells in the bone marrow and blood (Liu et al., 2007) and are thought to be the immediate precursors of differentiated cDCs. R3, albeit gated within the Ly6C$^{hi}$ monocyte gating strategy, fit the pre-cDC definition of cells. An overlay of the R3 on the gating strategy set out by Liu et al showed that R3 was in fact a CD115+ pre-cDC population (Liu et al., 2007) and was a contaminating population within conventionally gated Ly6C$^{hi}$ monocytes (Lin$^{-}$CD115$^{+}$SIRPα$^{+}$Ly6C$^{hi}$ cells) (Nascimento et al., 2014; Yona et al., 2013) (**Figure 3-3**). Ginhoux and colleagues also described the use of Ly6C and SiglecH in determining sub-populations within the Flt3$^{+}$SIRPα$^{lo}$ total pre-DCs that are either non-lineage primed

or are primed towards either cDC1 or cDC2 commitment (Schlitzer et al., 2015). R3 mostly overlapped with the SiglecH$^{-}$Ly6C$^{hi}$ cells indicating that they were the cDC2-committed pre-cDCs with a small proportion of non-lineage primed pre-cDCs that did not overlap with the CD115- pre-DCs, P **(Figure 3-3).**

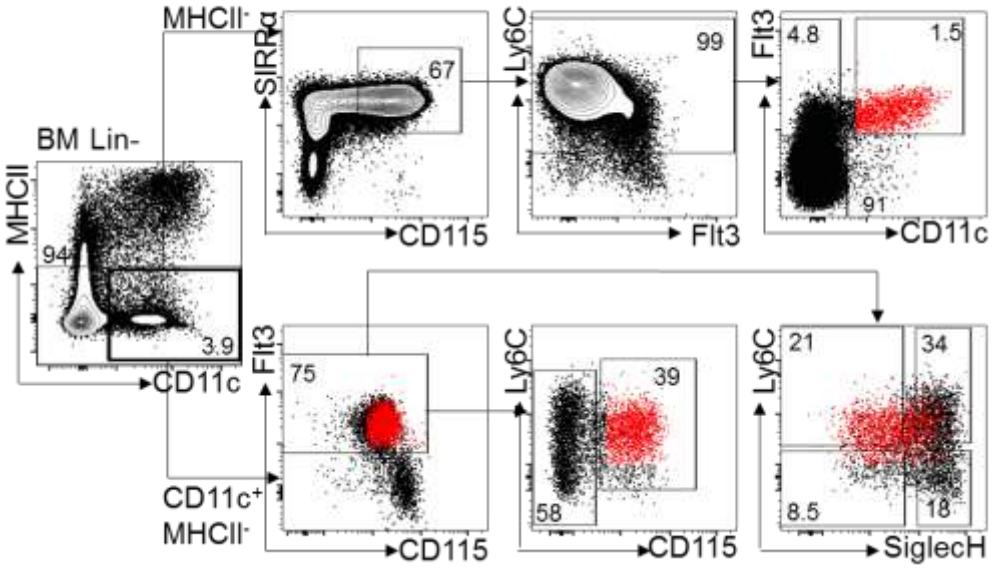


**Figure 3-3: Correlation of R3 with pre-DC populations**. MHCII$^{-}$CD115$^{+}$SIRPα$^{+}$Ly6C$^{+}$Flt3$^{+}$CD11c$^{+}$ R3 cells (red) were overlaid on the conventional gating strategy for pre-DCs (Liu et al., 2007)(lower gating panel) as well as the more refined delineation of the cDC1 and cDC2 subset-primed pre-DC populations (Schlitzer et al., 2015).

### 3.2.1.3 *R2 and R3 cells are not precursors*

Double positive expression of Flt3 and CD115 is seen on non-committed progenitor populations in the BM. It was thus important to test if the R2 population was indeed a progenitor cell population. cKit is expressed on all hematopoietic progenitor populations-half of which co-express lineage-specific markers (Matthews et al., 1991; Ogawa et al., 1991). I thus tested for the Ly6C$^{hi}$ monocyte heterogeneity within cKit$^{-}$ cells. The percentages of these populations were unaffected after removal of cKit$^{+}$ cells (**Figure 3-4)**. I thus concluded that R2 and R3 were lineage-committed non-precursor cells.

Nonetheless, I maintained the use of cKit in all further experiments as part of the lineage exclusion gate.

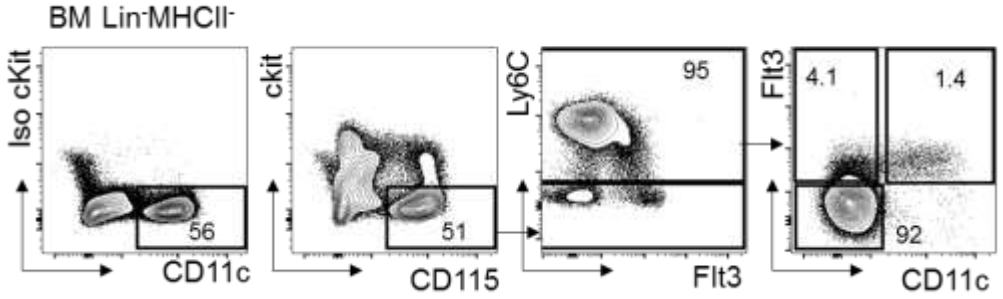


**Figure 3-4: Flt3$^{+}$CD115$^{+}$ cells are not cKit$^{+}$.** Comparison of anti-cKit staining and isotype control on BM Lineage$^{-}$MHCII$^{-}$ cells prior to analysing Ly6C$^{hi}$ monocytes with respect to Flt3 and CD11c.

### *3.2.2 The relationship between R2 and Ly6C$^{hi}$ monocytes*

#### 3.2.2.1 *R2 cells are CCR2-dependent.*

A salient feature of Ly6C$^{hi}$ monocytes is their dependence on CCR2 for egress from the bone marrow into the blood (Geissmann et al., 2003; Kurihara et al., 1997). Phenotyping of R1 and R2 monocytes and R3 and P pre-DCs showed that CCR2 was expressed highly on R1 and R2 in contrast to the R3 or P populations (**Figure 3-5**a).

To test the requirement of CCR2 on Flt3$^{+}$ monocytes, I analysed the BM and blood of *Ccr2*$^{-/-}$ mice. R1 and R2 were dramatically reduced while total pre-DCs remained at similar levels in *Ccr2*$^{-/-}$ mice as compared to their WT counterparts in the blood **(Figure 3-5b**).

To ensure a cell-intrinsic role of CCR2 in the egress of BM R2 cells I tested the presence of R1 and R2 in the BM and blood of *Ccr2*$^{-/-}$ and *Ccr2*$^{+/+}$ mixed BM chimeras. The percentage of CCR2-sufficient R2 cells in the blood far exceeded CCR2-deficient cells. R3 and P pre-DCs maintained equal proportions of both genotypes in the BM and blood

**(Figure 3-5c).** I therefore concluded that R2 is a *Ccr2*-dependent Ly6C$^{hi}$ monocyte subset, distinct from the cDC lineage.

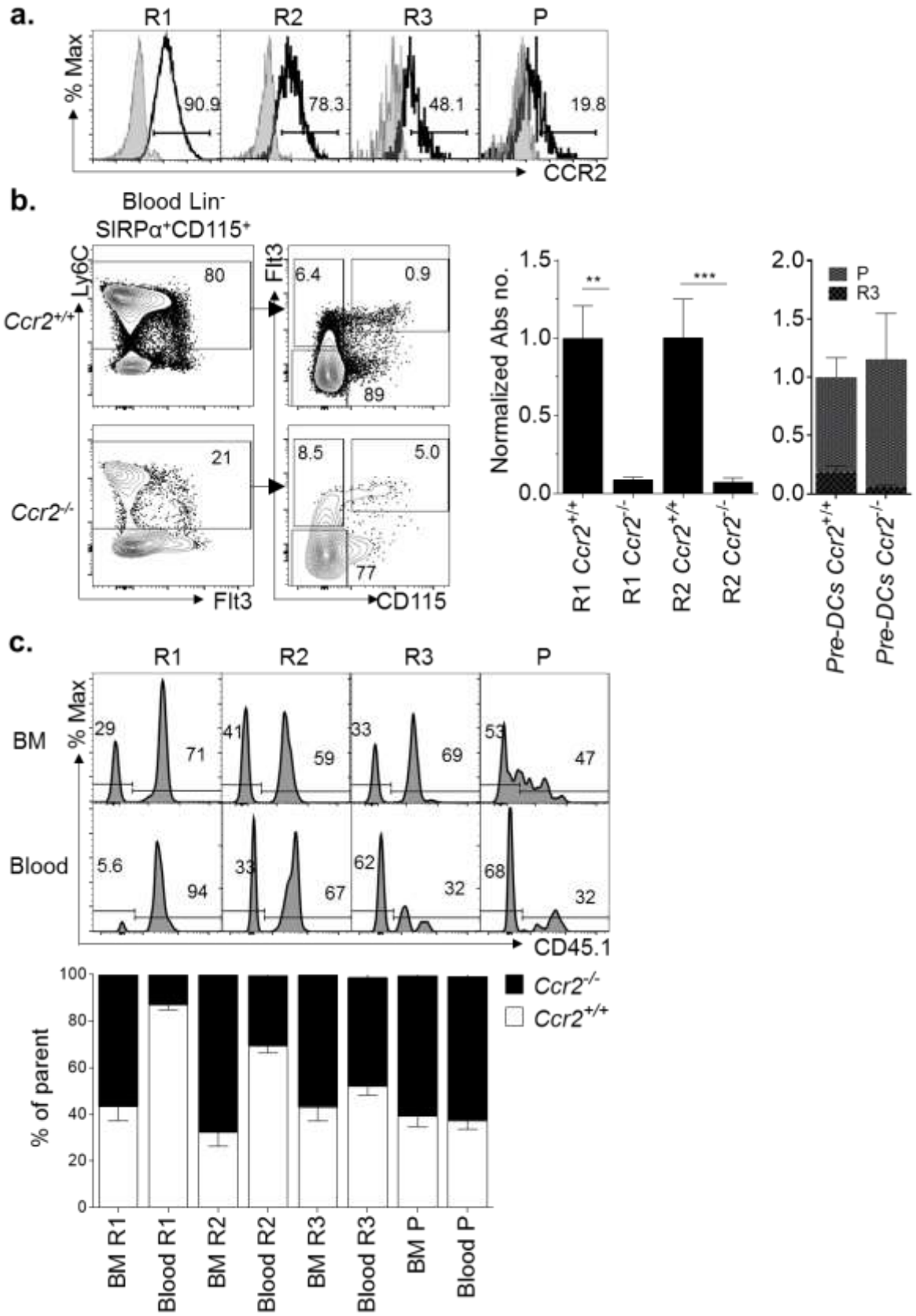

**Figure 3-5: R2 cells are CCR2-dependent**. a.) Bone marrow monocytes R1 and R2, and pre-cDCs R3 and P, were tested for Ccr2 expression. b) *Ccr2*$^{+/+}$ and *Ccr2*$^{-/-}$ blood were assessed for the presence R1 and R2 Ly6C$^{hi}$ monocytes, and R3 and P pre-cDCs. Graphs shows absolute numbers of cells from Ccr2$^{-/-}$ or Ccr2$^{+/+}$ blood normalized to the absolute number of Ccr2$^{+/+}$ cells. c.) Ccr2: WT bone marrow chimeras. R1, R2, R3 and P from the BM and blood of Ccr2$^{-/-}$ (CD45.2) and WT (CD45.1) mixed bone marrow chimeras assessed for the percentage of congenic (CD45.1) marker expression. Graphs show mean ± SEM; n=4-6, **p<0.005, ***p<0.0005, ns= non-significant; Student's t-test.

### 3.2.2.2 *R1, R2 and R3 are independent of Nr4a1-dependent lineage*

To test the relationship, if any, of R1, R2 and R3 to the *Nr4a1*-dependent Ly6C$^{lo}$ monocytes, *Nr4a1*$^{-/-}$ mice were assessed for any modifications to the R1, R2, R3 and P populations. As has been previously reported (Hanna et al., 2011), Ly6C$^{lo}$ monocytes do not develop in *Nr4a1*$^{-/-}$ mice as compared to WT controls. In our analysis of the *Nr4a1*$^{-/-}$ mice, R1, R2, R3 and P were not affected (**Figure 3-6**).

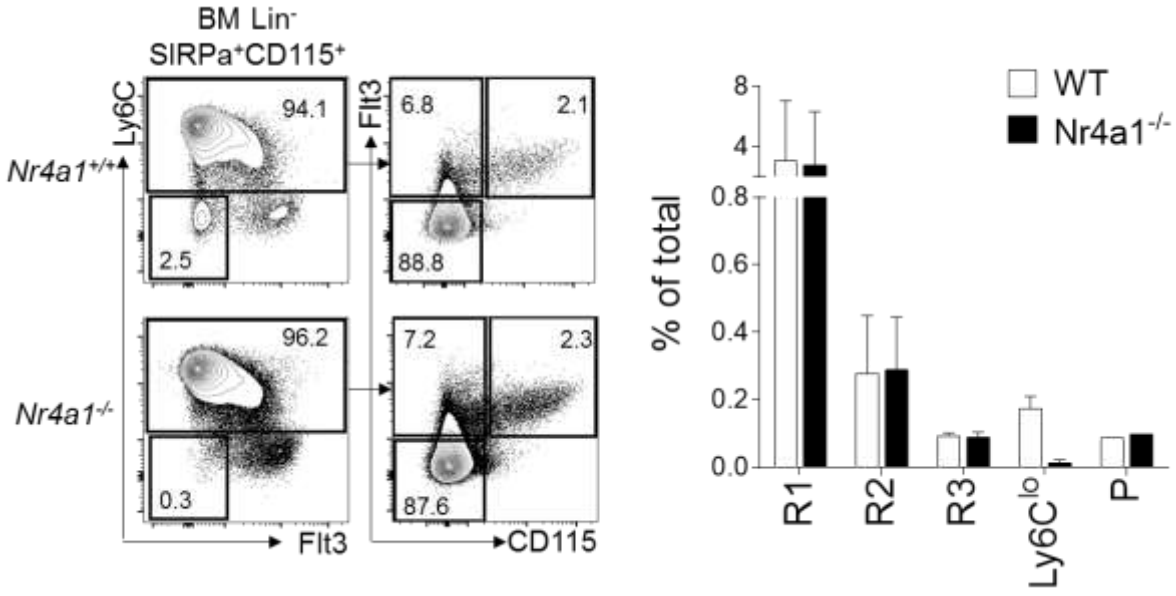


**Figure 3-6: R2 and R3 are not influenced by NR4A1** Nr4a1$^{-/-}$ mice were compared to WT controls and percentages of each Ly6C$^{hi}$ monocyte population, Ly6C$^{lo}$ monocytes (Ly6C$^{lo}$) and pre-cDC populations R3 and P were analysed. n=2.

#### 3.2.2.3 *R2 cells resemble Ly6C$^{hi}$ monocytes*

**T**ranscriptional analysis of R1, R2 and R3 by the use of microarrays on each population showed that R1 expressed the macrophage signature while R3 expressed the cDC signature very strongly (**Figure 3-7**a). R2 exhibited an intermediate phenotype but expressed a stronger macrophage signature than that of cDCs. To phenotypically assess the similarity of R2 cells to Ly6C$^{hi}$ monocytes or R3 pre-DCs, a Giemsa stain of cytospin samples of FACS sorted populations R1, R2, R3 and P revealed the typical horse-shoe shaped nuclei characteristic of monocytes in R1 and R2. R3 and P had irregular nuclei as is characteristic of cDCs (**Figure 3-7b**).

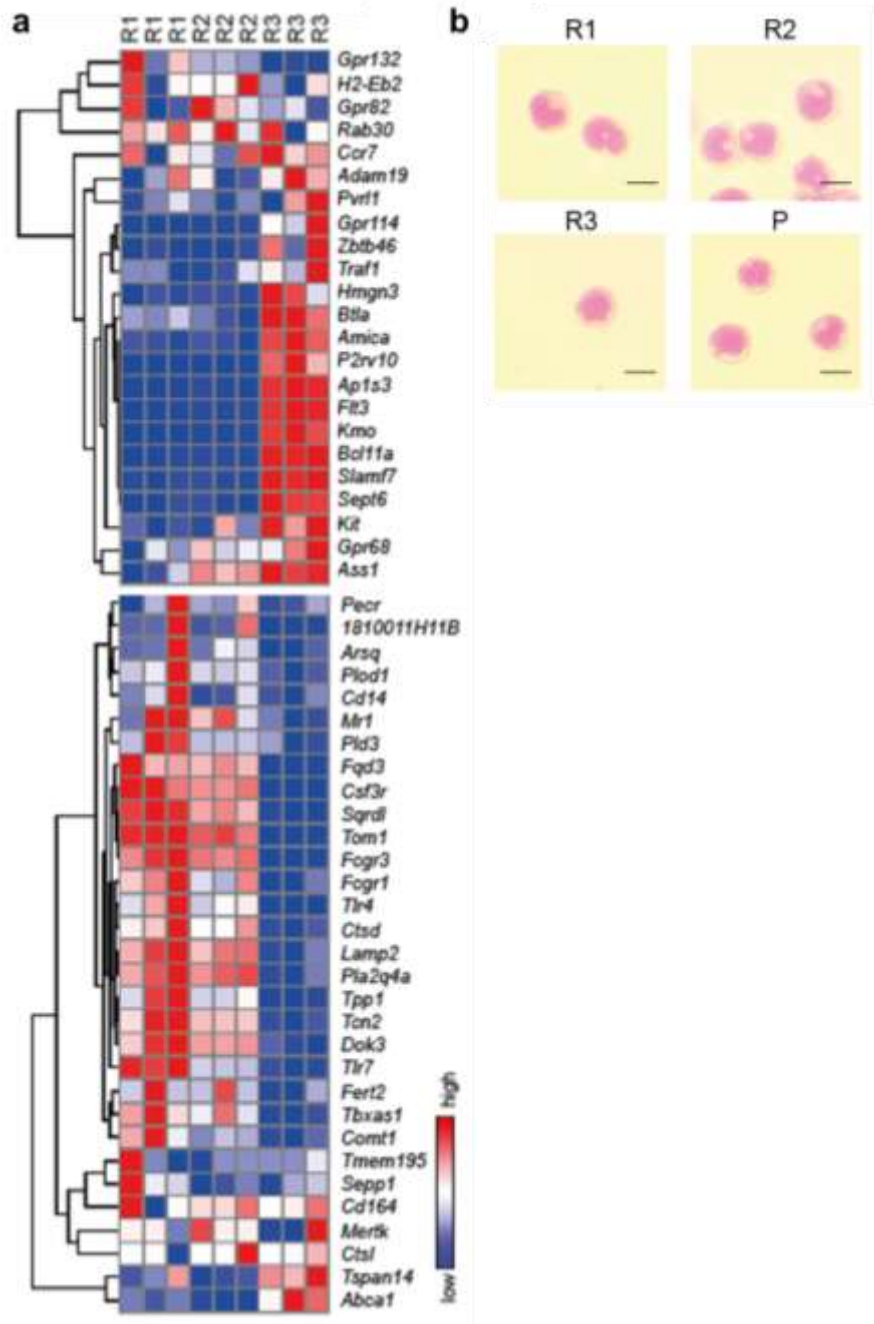


**Figure 3-7:R2 cells resemble monocytes** a) DC and macrophage gene signature in R1, R2 and R3 from 3 biological replicates sorted in 3 separate experiments. Microarray data of R1, R2 and R3 showing their relative mRNA expression of genes that belong to the cDC (upper panel) and macrophage (lower panel) gene signatures obtained from ImmGen. b) Giemsa stain of R1, R2 monocytes and R3 and P pre-cDCs. Cytospin samples of flow-cytometrysorted R1, R2, R3 and P were fixed and stained with Giemsa stain and photographed at 400x. Scale bar=10µm

### *3.2.3 Ly6C$^{hi}$ monocytes and the cDC lineage*

#### 3.2.3.1 *Dependence of R2 and R3 on Flt3L*

One of the key features of the DC lineage is its dependence on Flt3L for development (Karsunky et al., 2003). Flt3 is widely expressed on a number of hematopoietic progenitors (McKenna et al., 2000). With progressive differentiation, Flt3L-dependency is restricted to the DC lineage (McKenna et al., 2000). *Flt3l*$^{-/-}$ mice are deficient in pre-cDCs in the BM and blood as well as terminally differentiated cDCs in the spleen (Liu et al., 2007). In order to determine Flt3 dependence of the Flt3$^{+}$ Ly6C$^{hi}$ cells (R2), *Flt3l*$^{-/-}$ mice were assessed for cell numbers of R1, R2, R3 and P. R1 and R2 remained at much the same levels as WT counterparts, while R3 and P cells were dramatically reduced (**Figure 3-8**). This showed that while R3 and P were DC-committed, the expression of Flt3 on R2 did not indicate commitment to the DC lineage.

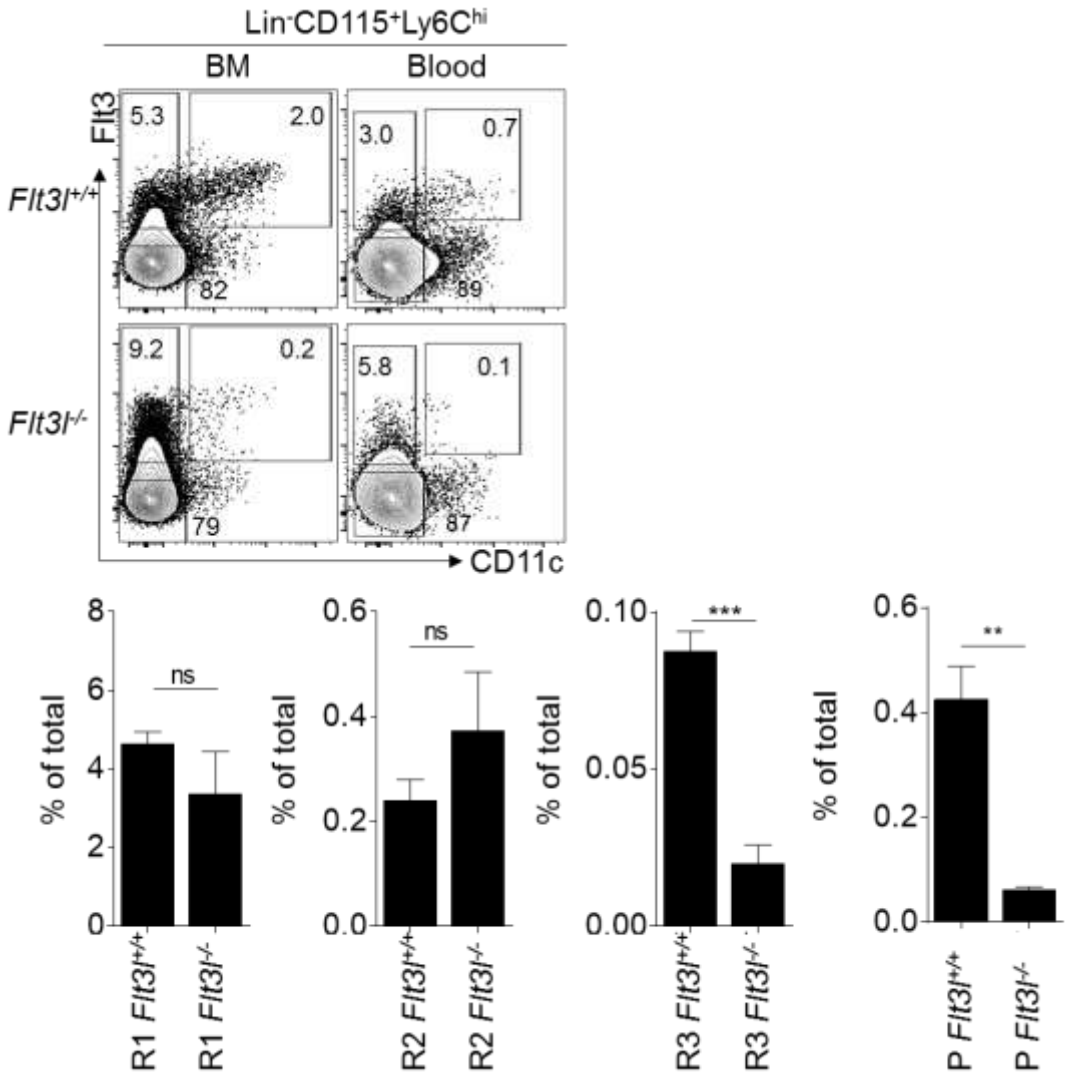


**Figure 3-8: R2 cells are Flt3L-independent:** WT and *Flt3l*$^{-/-}$ bone marrow and blood were assessed for the presence of R1, R2 and R3 within Lineage$^{-}$SIRPα$^{+}$CD115$^{+}$Ly6C$^{hi}$ cells. Graphs show mean ± SEM of R1, R2, R3 and P in WT and *Flt3l*$^{-/-}$ blood; n=4-5, **p<0.005, ***p<0.0005, ns= non-significant; Student's t-test.

### 3.2.3.2 *Zbtb46 is not expressed in R2 cells.*

Another technique used to accurately determine the ontogeny of a cell population, is fate mapping. The *Zbtb46*$^{Cre}$*x ROSA*$^{lSlYFP}$ mice conditionally and then permanently label any cell and its daughters upon expression of the transcription factor ZBTB46. This highlights any cell that originated within the cDC lineage. Phenotypic analysis of the BM and blood showed that Ly6C$^{hi}$ monocytes- R1 and R2, as well as pre-cDCs- R3 and P, showed very low background staining with YFP (**Figure 3-9a**). In the spleen however, R3 and P pre-

DCs expressed 25-30% of YFP, while R1 and R2 continued to express background levels of the fluorescent molecule (**Figure 3-9a**). This showed that even after egress from the bone marrow, R1 and R2 did not express sufficient levels of the cDC-specific transcription factor ZBTB46.

The analysis of the spleen showed that these mice have a rather stringent labelling of cells given that cDC1s that had previously been found to be homogeneously derived from the cDC lineage (Hildner et al., 2008; Tamura et al., 2005; Waskow et al., 2008) – was only 50% positive for YFP (**Figure 3-9**b). I also noted that $CD11b^{+}ESAM^{+}$ cells had a higher proportion of $YFP^{+}$ cells than $ESAM^{-}$ cells corroborating data from Reizis and colleagues that showed that the $ESAM^{+}$ cells bear a stronger DC phenotype than the $ESAM^{lo}$ $CD11b^{+}$ cDCs (Lewis et al., 2011).

Murphy and colleagues constructed a reporter mouse that introduced an IRES-GFP reporter gene in the place of the 2nd exon of the *Zbtb46* gene (Satpathy et al., 2012a). This construct allows for the reporting of the expression of *Zbtb46* within a cell and unlike the $Zbtb46^{Cre}$ *x* $ROSA^{lslYFP}$ mice, does not fate map the daughter cells of a Zbtb46 expressing cell. The Zbtb46-GFP mice provide a 'snapshot' of the $Zbtb46^{+}$ cells.

R1 and R2 monocytes did not express higher than background levels of GFP while the pre-cDCs R3 and P expressed much higher levels (~ 84-90% positive) (**Figure 3-9**c). This showed conclusively that R1 and R2 did not express *Zbtb46*.

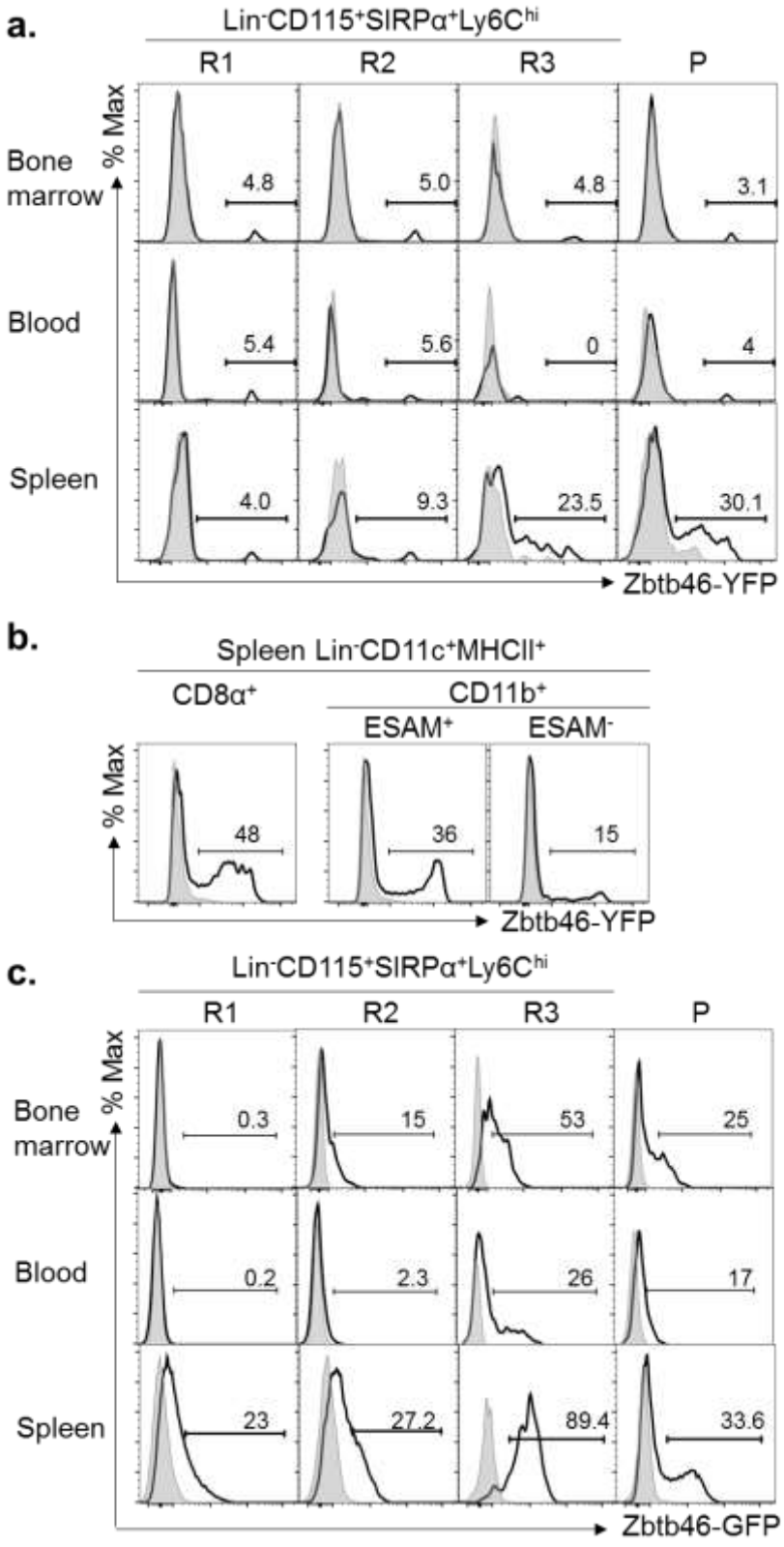


**Figure 3-9: Zbtb46 labelling in R1, R2 monocytes and R3 and P pre-DCs**. Bone marrow, blood and spleen of R1, R2, R3 and P were analysed for reporter expression in *Zbtb46*$^{CRE}$ *x ROSA*$^{lslYFP}$ mice (a,) and Zbtb46$^{gfp/+}$ (c) bone marrow, blood and spleen. b) CD8α$^{+}$, ESAM$^{hi}$CD11b$^{+}$ and ESAM$^{lo}$CD11b$^{+}$ cDCs in the spleen of *Zbtb46*$^{CRE}$ *x ROSA*$^{lslYFP}$ mice were assessed.

While reporter mice can provide insight into lineage commitment of a given cell populations, I also wanted to accurately address the mRNA levels of Zbtb46. In addition, I also tested the mRNA levels of $CD8\alpha^+$ cDC-specific lectin receptor - Clec9a (Poulin et al., 2012). CLEC9a is known to be expressed in committed progenitors of the $CD8\alpha^+$ cDCs. I wondered whether this might provide insight into whether there was a difference in the pre-commitment of R3 and P pre-cDCs to $CD8a^+$ cDCs (cDC1) or $CD11b^+$ cDCs (cDC2). I found that R1 and R2 expressed negligible levels of both markers while R3 expressed high levels of *Zbtb46* and *Clec9a (***Figure 3-10***)*.

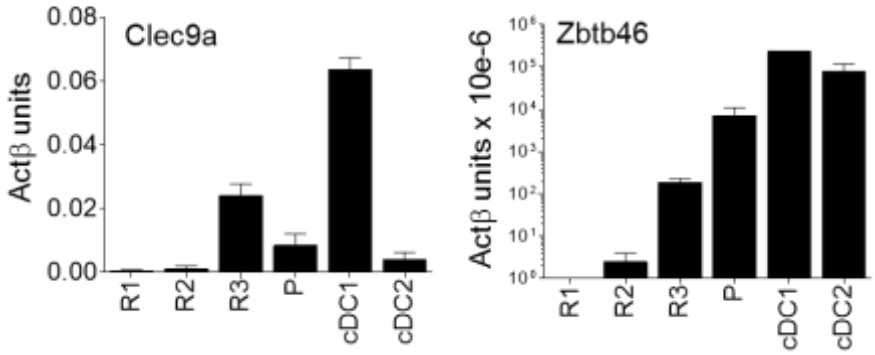


**Figure 3-10: qRT-PCR analysis for Zbtb46 and Clec9a**. mRNA from FACS-sorted R1, R2, R3 and P along with cDC1 and cDC2, was tested for cDC1 specific Clec9a and cDC1 and cDC2- specific Zbtb46. Data of R1, R2, R3 and P is representative of 3 experiments while cDC1 and cDC2s were tested as controls in 1 experiment.

### 3.2.3.3 *Influence of Irf8 on the development of R1 and R2 monocytes.*

The interferon response factors IRF4 and IRF8 have an overlapping role in the stimulation of DC development while also having individual roles in the stimulation of cDC subset specific gene expression (Tamura et al., 2005). Irf8 has been found to control the development of the cDC1s and to a certain extent the pDCs (Tamura et al., 2005). IRF4 controls the development of the $CD4^+$ DCs (cDC2s) while the double negative ($CD4^-CD8a^-$) DCs are influenced by both Irf4 and Irf8 (Tamura et al., 2005).

Additionally, Irf8 plays an important role in the myeloid cell lineage selection as is seen by controlling the development of terminally differentiated macrophages from bipotent myeloid cell progenitors in *in vitro* cultures of Irf8 overexpressing cell lines (Tamura et al., 2000).

*Irf8*$^{-/-}$ mice are immune-deficient and develop chronic myelogenous leukemia-like disease (Holtschke et al., 1996). In order to test the reliance of both the monocytes, R1 and R2 on this transcription factor, the *Irf8*$^{-/-}$ mice were phenotyped for relative numbers of the monocytes in the bone marrow and blood. *Irf8*$^{-/-}$ mice had dramatically reduced levels of both monocyte subsets as well as of Ly6C$^{hi}$ pre-cDCs, R3 (**Figure 3-11)**. This indicated a possible role of the transcription factor IRF8 on the development of Ly6C$^{hi}$ monocytes as well as the cDC2- committed pre-cDCs, R3, albeit this role might not be cell-intrinsic given the systemic effect on the mice. It also does not help discriminate between the 2 monocyte subsets.

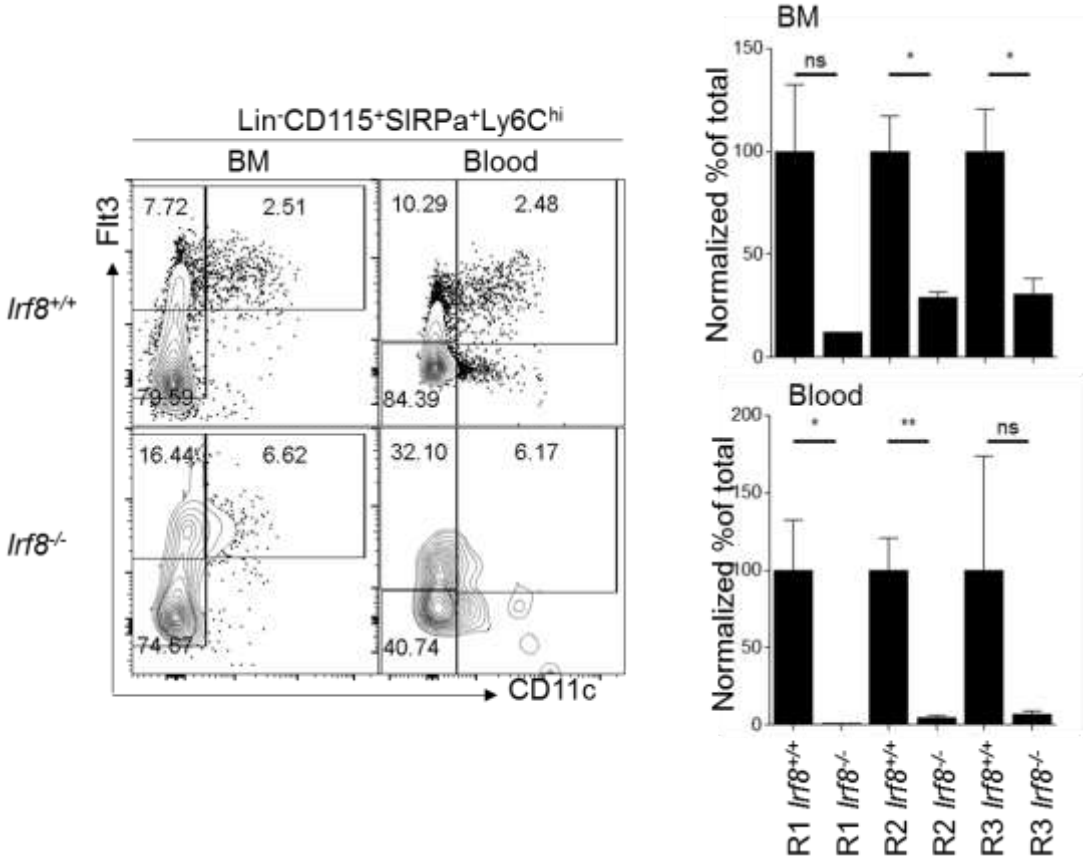

**Figure 3-11: *Irf8*$^{-/-}$ mice exhibit reduced levels of R1, R2 and R3**. Bone marrow and blood of *Irf8*$^{+/+}$ and *Irf8*$^{-/-}$ mice were analysed for the presence of R1, R2 and R3. Graphs show mean ± SEM of R1, R2, R3 in WT and *Irf8*$^{-/-}$ blood; n=4, *p<0.05, **p<0.005, ns= non-significant; Student's t-test. This experiment was performed by Dr. Hannah Garner.

### *3.2.4 Phenotypic and transcriptomic description of Flt3$^{+}$Ly6C$^{hi}$ monocytes*

#### 3.2.4.1 *Transcriptomic analysis*

Microarray analysis of R1 and R2 monocytes with R3 pre-cDCs provided a basis for transcriptomic analysis of the 3 populations along with comparisons of published data on other populations (such as pre-cDCs and CDPs). A hierarchical clustering of the data shown in **Figure 3-12** shows that R1 and R2 cluster very close together while R3 clusters separately. In addition, total pre-cDCs and CDPs cluster under separate branches (**Figure 3-12**). Analysing these populations by a PCA analysis also showed that R1 and R2 cluster close to each other (**Figure 3-12b)**

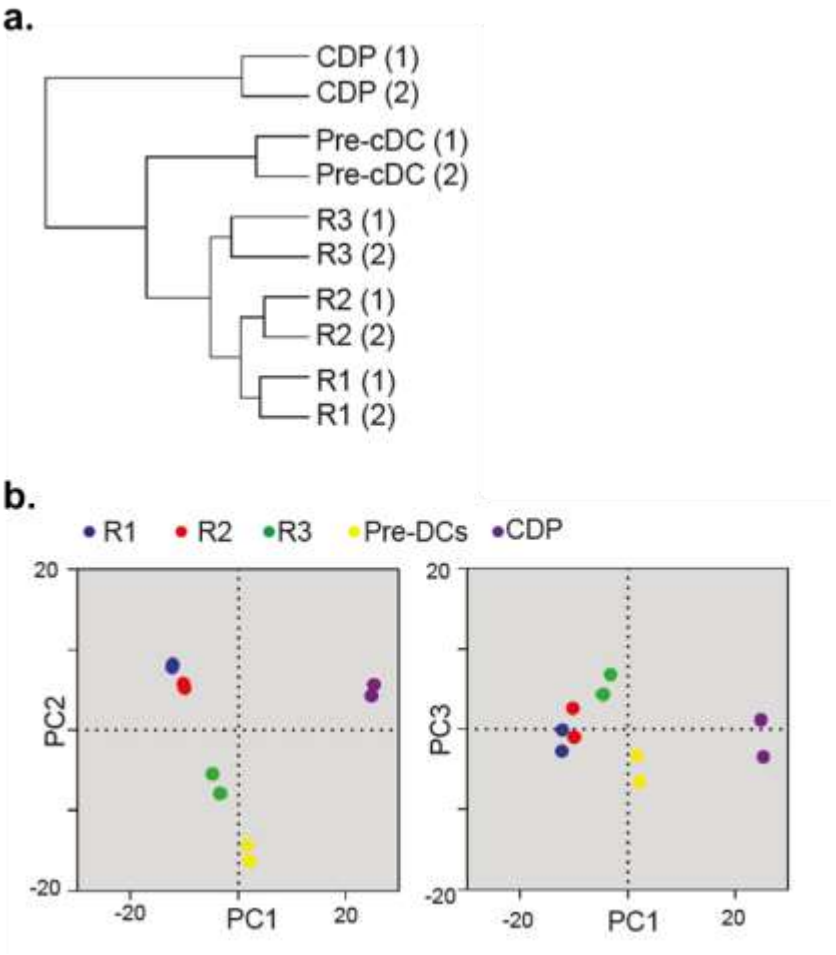

**Figure 3-12: Clustering analysis of R1 and R2 monocytes with cDC precursors**. a) Hierarchical clustering of 2 samples each of R1, R2 and R3 along with CDP and pre-DC populations using One-minus Pearson Correlation. b) Principle component analysis of the above populations along principle components PC1 (72%), PC2 (24%), and PC3 (2%). Microarrays were performed by the King's Genomics Centre, Waterloo, London.

A volcano plot analysis of microarray data also helps with 2 aspects of understanding the dynamics of these populations. Firstly, the similarity in gene expression and secondly, the differentially expressed genes between the populations. With regards to the first aspect, **Figure 3-13**a shows that R1 and R2 have very similar gene expression patterns with most genes exhibiting less than 2-fold change in expression. R3 however, had a distinctly different gene expression pattern to both R1 and R2, albeit having a closer relationship to R2 than R1 (**Figure 3-13**a).

Volcano plots are also useful in the identification of differentially expressed genes (DEGs). Using a threshold value of 2-fold change and a p-value $< 0.05$, I listed genes that were uniquely expressed in R1 or R2 or R3 in comparison to the other 2 populations. For clarity, genes expressed highly in R2 are highlighted in blue while those more highly expressed in R3 are highlighted in red. Overlaying these genes on comparisons of each population with R1 shows their relative similarity to R1 in terms of mRNA expression. Interestingly, R2 DEGs are more strongly expressed in R1 than in R3. Furthermore, R3 DEGs are more strongly expressed in R2 than in R1 (**Figure 3-13**a).

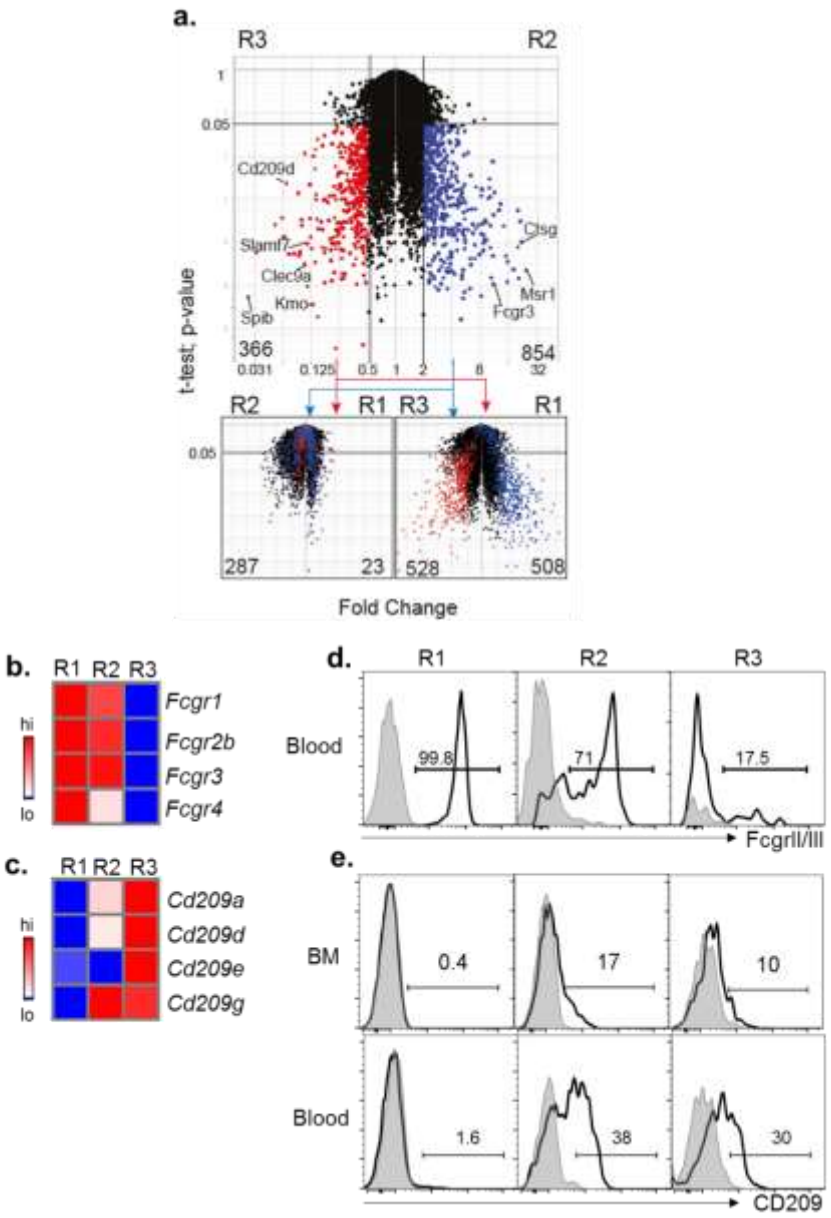


**Figure 3-13: Differential gene expression in R2 cells** a) Differential gene expression analysis of fold change versus statistical t-test p-value on microarray data of R1, R2 and R3. Top panel highlights genes most differentially expressed in a comparison between R2 and R3 with R2-specific genes highlighted in blue and R3- specific one in red (fold change>2, $p<0.05$). Candidate genes are marked on either side. The same highlights have been applied to comparisons of R1 and R2 (left) and R1 and R3 (right). Numbers in the bottom corners of each plot indicate the numbers of genes most highly upregulated in the population indicated above it for the indicated comparison. b and c). Microarray data of R1, R2 and R3 (average of 3 replicates) for members of FcγR family (b) and CD209 (c) that were expressed above baseline. d and e) flow cytometry analysis of FcγRII/III (d) and CD209a (e) (black lines) on steady state R1, R2 and R3 in the blood as compared to isotype control (grey shaded).

Given that the identification of monocytes and cDCs relies on a combination of surface markers that are widely expressed within the myeloid population (*eg*. CD11b, CD11c, MHCII), I wished to find other surface markers that would not only distinguish these Ly6C$^{hi}$ monocytes from other myeloid cells but also from each other.

I searched within the differentially expressed genes to identify markers that can be associated with each population. I found that R1 highly expressed the family of FcγRs in comparison to the R3 population. R2 showed an intermediate expression level of FcɣRIIb and FcγRIII between R1 and R3 (**Figure 3-13b)**. Among the genes most highly expressed in R3 as compared to R1 were several lectin receptors. Of these *Cd209a* was particularly well expressed in R3 while R2 had an intermediate phenotype and R1 showed minimal expression of *Cd209a* (**Figure 3-13c).** CD209a analysis in the bone marrow proved futile as no expression was observed, possibly because surface expression does not occur until the cells have left the BM.

Reasoning that mRNA expression within the populations in the BM might lead to surface expression in the blood, I tested for the markers on R1, R2 and R3 in the blood. CD209a was highly expressed in R3 and R2 while R1 did not express it. FcγRII/III was detected on R1 and R2 but not R3 **(Figure 3-13 d,e).** Thus R2 cells were distinguished by their co-expression of FcγRII/III and CD209a.

#### 3.2.4.2 *R1 cells express inflammatory genes at steady state.*

In assessing the transcriptional profile of the R1, R2 and R3, it was noted that several inflammation-associated genes were upregulated in R1 (**Figure 3-14**). These included vATPases (eg. lysosomal markers (eg., TLRs (*Tlr1, Tlr2*), Nod-like receptors (NLRs) (eg. *Nod1, Nod2*) and interferon-stimulated genes (eg. *Cxcl10, Isg20*). These were at

much higher expression intensities than R2 monocytes or R3 pre-DCs. This indicated that R1 is genetically pre-disposed to develop an inflammatory response as compared to R2.

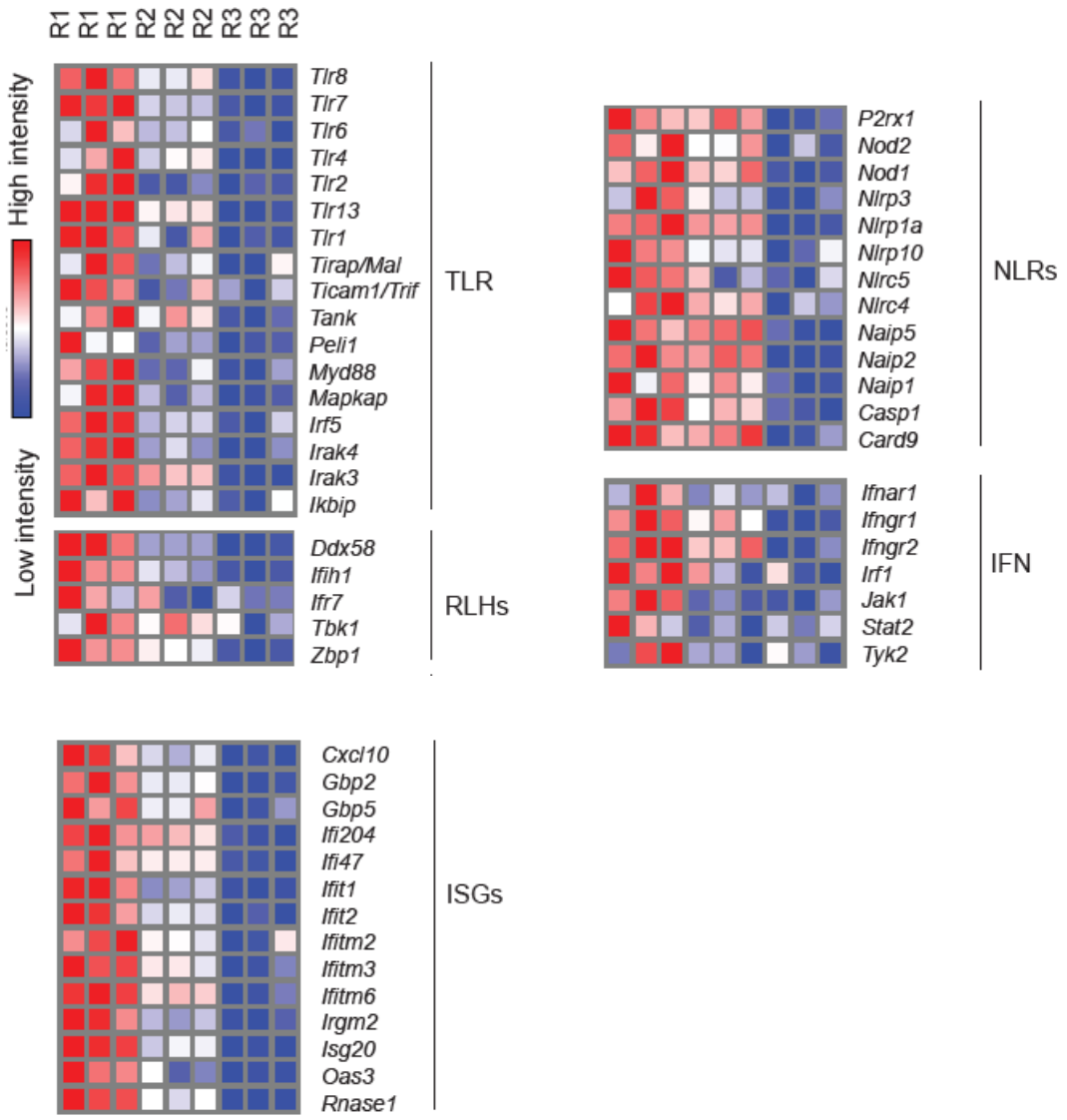


**Figure 3-14: Transcriptomic analysis of R1, R2 and R3 for inflammatory markers**. Microarray analysis of R1, R2 and R3 in 3 biological replicates from 3 independent experiments for genes associated with inflammatory signals. TLR- Toll-like receptors, RLHs – RIG like Helicases, ISGs: Interferon stimulated genes, NLRs- NOD like receptors, IFN: Interferon associated genes. High and low intensity..

### *3.2.5 MHCII expression on Flt3$^+$Ly6C$^+$CD115$^+$ cells*

#### 3.2.5.1 *R2 upregulates MHCII surface expression in the blood*

Within the BM, it is crucial to exclude macrophages from the myeloid populations when gating on Ly6C$^{hi}$ monocytes. In order to do this, I excluded the MHCII$^+$ cells in the gating strategy of R1, R2 and R3 in the bone marrow. as they were found to be predominantly Ly6C$^{int}$F4/80$^{hi}$ cells, i.e. macrophages (**Figure 3-15**).

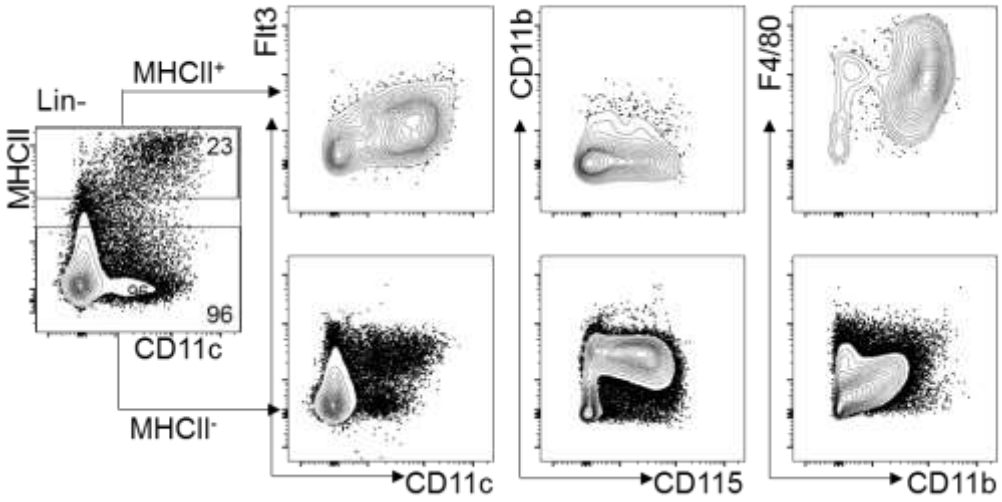


**Figure 3-15: MHCII$^+$ BM are macrophages**. Flow cytometry analysis of MHCII$^+$ cells for Flt3, CD11c, CD11b, CD115 and F4/80 within Lineage$^-$cells from the BM of C57Bl/6 mice.

In the blood however, MHCII could be expressed on a number of APCs which cannot be excluded from analysis. Upon inclusion of the MHCII$^+$ cells, I corroborated previous results of there being an MHCII$^+$ population within Ly6C$^{hi}$ monocytes (Jakubzick et al., 2013)(**Figure 3-16a**). These MHCII$^+$ cells contained some cells that were CD11c$^+$ but were 50% Flt3$^+$. I could thus conclude that the Flt3$^+$Ly6C$^{hi}$ cells were predominantly MHCII$^+$, *i.e.*, R2 monocytes. R3 pre-DCs contribute to at least half of the MHCII$^+$ CD115$^+$Ly6C$^+$ cells. Intriguingly there appeared to be a trend toward increased levels of MHCII expression in Ly6C$^{lo}$ monocytes (**Figure 3-16b**). This could be due to gradual loss in Ly6C expression

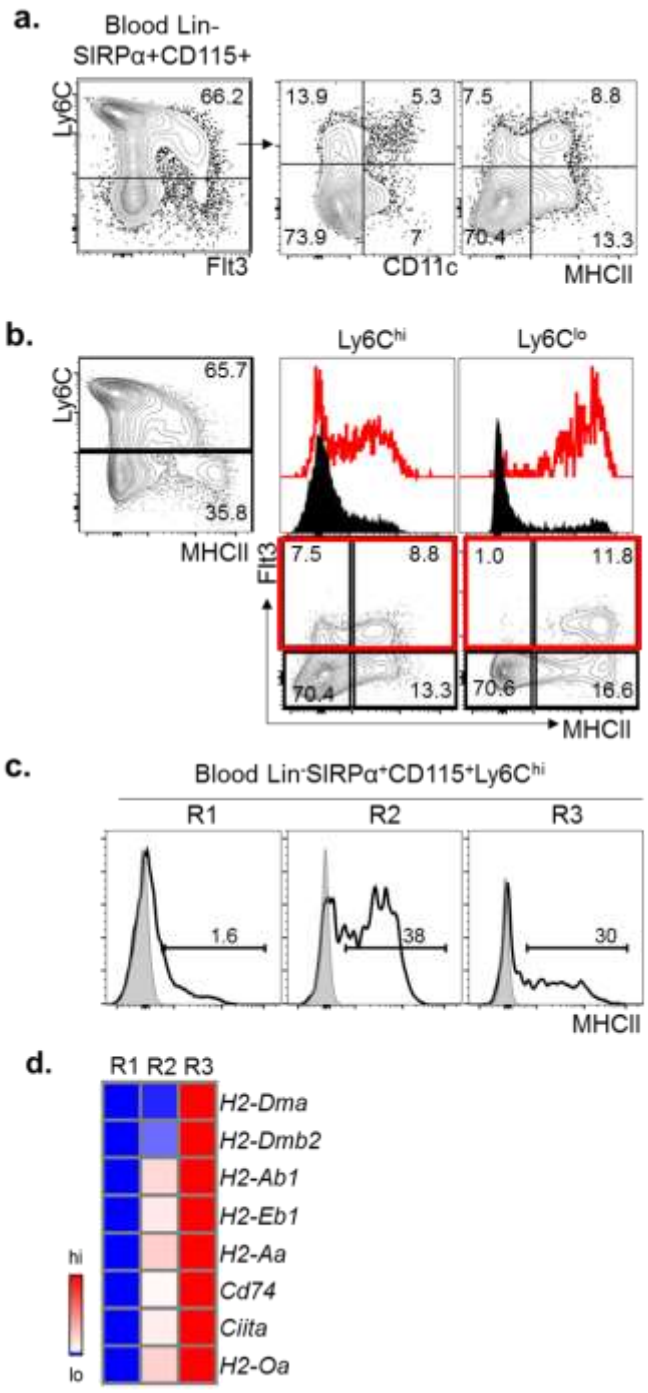


**Figure 3-16: Flt3+ R2 cells are enriched for MHCII expressing cells in the blood,** .a). Lin$^{-}$CD115$^{+}$SIRPa$^{+}$Ly6C$^{hi}$ cells analysed for Flt3, MHCII and CD11c expression. b) Analysis of the percentage of MHCII$^{+}$cells within the Flt3$^{+}$Ly6C$^{hi}$ monocyte gate. c) Percentage of MHCII$^{+}$ cells within R1, R2 and R3. d) Average relative mRNA expression of MHCII-associated genes in R1, R2 and R3.

with increased expression of MHCII in the blood. The Flt3$^{+}$ cells within the Ly6C$^{lo}$ monocytes were all MHCII$^{+}$. It is difficult to ascertain whether these cells are R2 and R3 populations that are gradually losing their expression of Ly6C.

Gating for each population within the Ly6C$^{hi}$ monocytes and analysing the MHCII levels on each of these populations showed that R2 had approximately 40% MHCII$^{+}$ cells while R3 was about 30% MHCII$^{+}$ **(Figure 3-16c).** R1 had less than 2% MHCII$^{+}$ cells. This was reflected in the microarray analysis of the MHCII associated genes as well (**Figure 3-16d**). R2 therefore relates to the MHCII$^{+}$ population previously described in the blood and spleen (Randolph et al., 1999).

### 3.2.5.2 *MHCII is upregulated on R2 in in vitro culture overnight*

I next tested the upregulation of MHCII in R2 cells after leaving the BM by flow cytometry sorted monocytes and pre-DCs following *ex vivo* culture in complete media overnight. R2 monocytes upregulated similar levels of MHCII as was seen in the blood. R3 also upregulated MHCII while R1 monocytes did not (**Figure 3-17**). This showed that R2 was distinctly capable of cell-intrinsically upregulating MHCII.

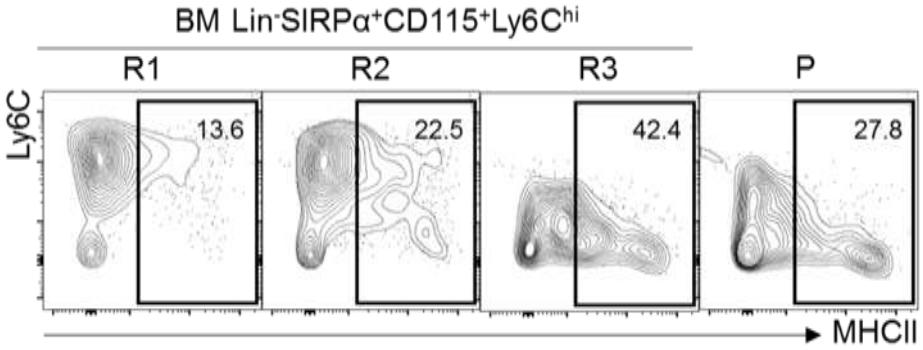


**Figure 3-17: MHCII is upregulated on R2 monocytes and R3 pre-DCs**. Representative plots of overnight cultures of fluorescence assisted cell sorted R1, R2 R3 and P representative of 2-3 independent cultures.

### 3.2.5.3 *pI promoter of Ciita is responsible for the expression of MHCII*

The expression of MHCII on a cell is driven by the transcription factor CIITA. It has been previously reported that the promoter regions of CIITA are activated in a cell-specific manner. pI has been reported to be activated in macrophages, monocytes and cDCs, *pIII*

in B cells and *pIV* is activated in response to IFNɣ (Kitamura et al., 2012; Yoon and Boss, 2010).

In order to identify the promoter responsible for the upregulation of MHCII on R2, I analysed the *pI*$^{-/-}$, *pIII*$^{-/-}$ and *pIII*$^{-/-}$*pIV*$^{-/-}$ mice along with WT and *Ciita*$^{-/-}$ mice as controls. Using intracellular staining for MHCII in the BM and surface staining in the blood, it was observed that the *pI* promoter was uniquely responsible for the expression of MHCII on R2 as expression levels were reduced as compared to those of *Ciita*$^{-/-}$ mice (**Figure 3-18**). MHCII expression on all cells was unaffected in the WT, *pIII*$^{-/-}$ and *pIII*$^{-/-}$*pIV*$^{-/-}$ mice. This shows that the expression of MHCII on R2 is due to steady state upregulation via the pI promoter.

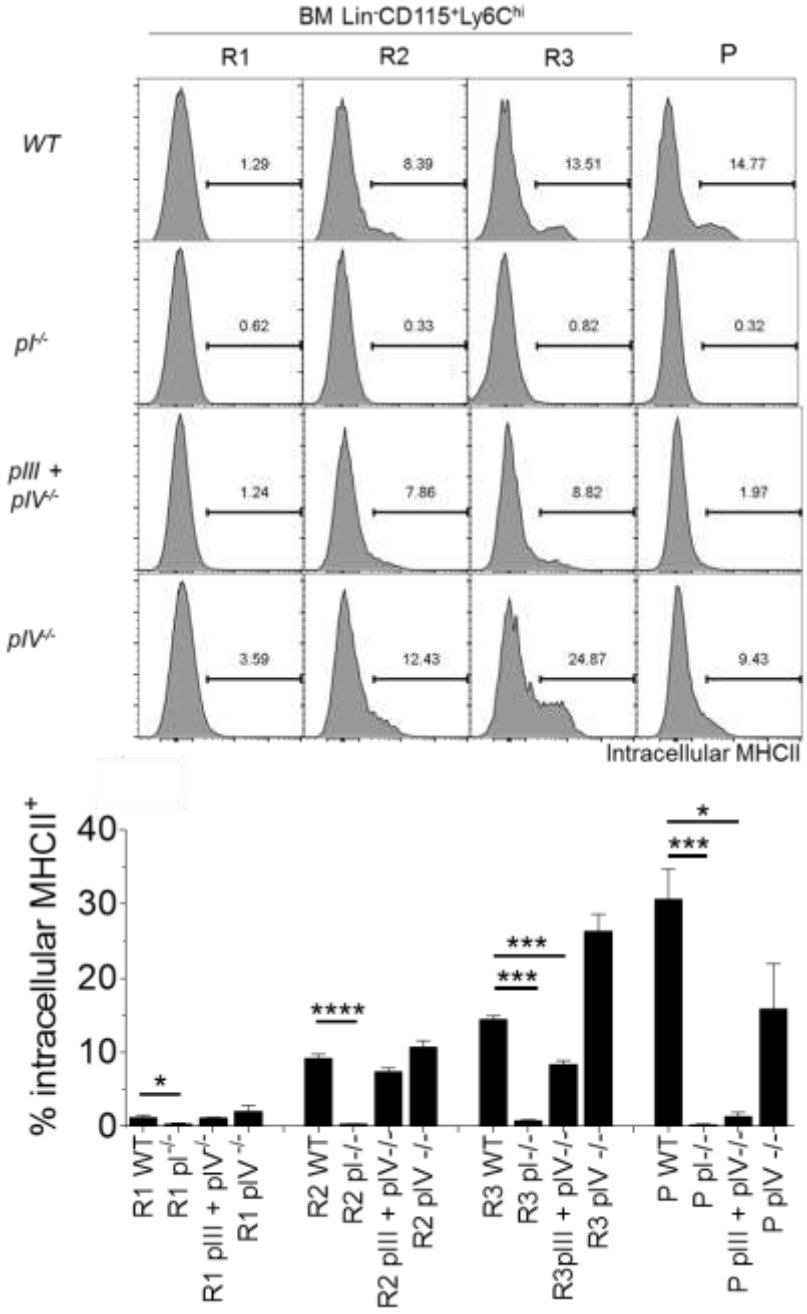


**Figure 3-18: Expression of intracellular MHCII is pI-dependent** *p1*$^{-/-}$, *pIV*$^{-/-}$ and *pIII*$^{-/-}$*pIV*$^{-/-}$ bone marrow was compared with WT controls for the expression of intracellular MHCII on R1, R2, R3 and P. Graph shows mean ± SEM of the percentage of intracellular MHCII staining within the indicated parent population; n=4, *p<0.05, ***p<0.0005; Student's t-test. Comparisons that were not show significant differences were left blank. This experiment was performed by Dr. Juan Dubrot Armendariz.

### *3.2.6 Transcriptional regulation of Ly6C$^{hi}$ monocytes*

#### 3.2.6.1 *The role of PU.1 in the development of R2 monocytes*

After assessing the differences in the transcriptional phenotype of the Ly6C$^{hi}$ monocytes-R1 and R2, their differentiation, and surface expression of MHCII in the blood, it became

clear that each population was primed for divergent functions. I therefore questioned if a specific transcription factor was responsible for the generation of functionally distinct populations.

PU.1 is known to be a master transcriptional regulator in the development of macrophages (McKercher et al., 1996). The decision at the MDP stage between development into monocytes or cDCs is made by the competition between Maf-B and PU.1 with PU.1 determining a more DC lineage commitment and Maf$^{-}$B, macrophage commitment (Bakri et al., 2005). Thus, I wondered if PU.1 might regulate the DC-like phenotype of R2 (*eg.* pI regulated MHCII expression, C-type lectin- CD209a, expression). Intra-nuclear staining for PU.1 versus isotype controls, showed minimal differences in the bone marrow (**Figure 3-19**). This difference was more evident within the blood. Furthermore, R2 (and also pre-DC R3) expressed much higher levels of PU.1 than R1 (**Figure 3-19**).

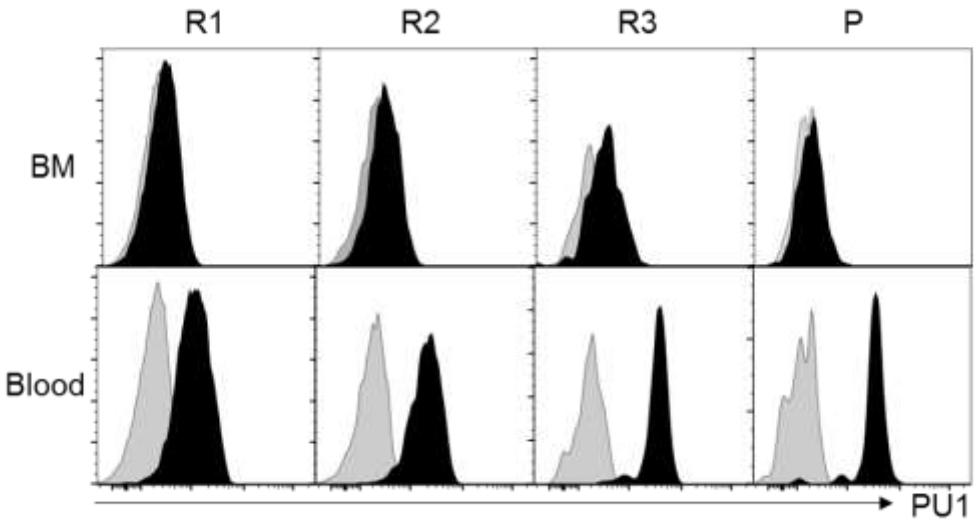


**Figure 3-19: PU.1 expression in R1, R2, R3 and P**. BM and blood R1, R2, R3 and P were stained for PU.1 (Black shaded) and compared against isotype controls (shaded grey).

### 3.2.6.2 *PU.1 hemizygosity results in the diminution of PU.1$^{hi}$ cells-R2 and R3.*

To test if R2 and R3 rely on PU.1 for their development, I analysed the steady state levels of these populations in the bone marrow, blood and spleen of *Sfpi1*$^{+/-}$ mice versus WT littermate controls. Our study was limited to the use of *Sfpil*$^{+/-}$ mice as the *Sfpi1*$^{-/-}$ mice

die in utero or shortly after birth (McKercher et al., 1996; Scott et al., 1994). Firstly, I noted there was a reduction in the number of Ly6C$^{lo}$ cells in the BM and blood **(Fig. 3-20a)** of the *Sfpi1*$^{+/-}$ mice while the relative percentage of Ly6C$^{hi}$ monocytes remained the same.

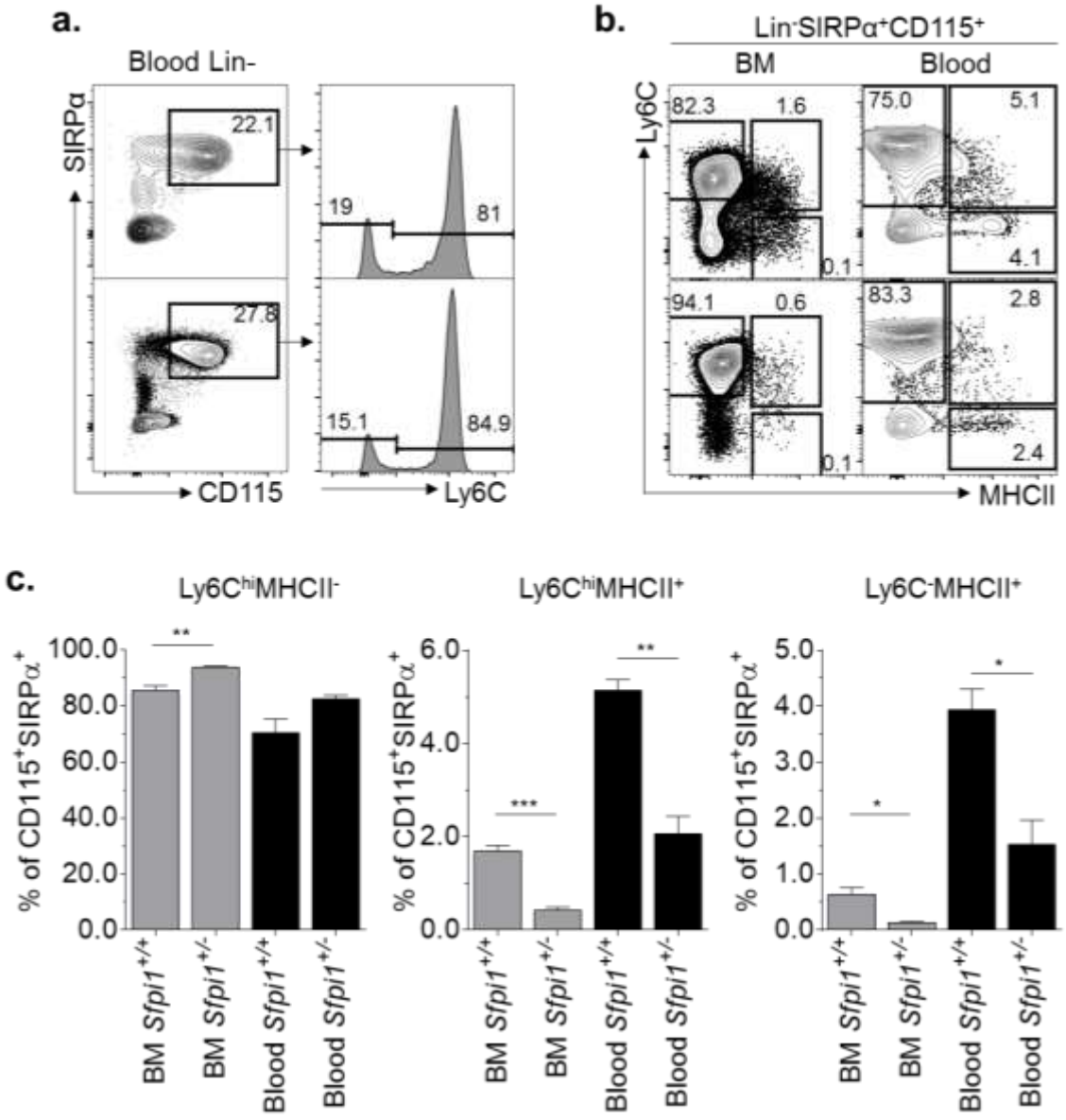


**Figure 3-20: MHCII$^{+}$ cells are reduced in BM and Blood in *Sfpi1*$^{+/-}$ mice.** Phenotypic analysis of Ly6C$^{hi}$MHCII$^{+}$, Ly6C$^{hi}$MHCII$^{+}$ and Ly6C$^{-}$MHCII$^{+}$ cells in BM and blood of *Sfpi1*$^{+/+}$ and *Sfpi1*$^{+/-}$ mice. Grey bars indicate intraceullular staining for MHCII. Graphs show mean±SEM of n=3,representative of 3 experiments. *p<0.05, **p<0.005, p<0.0005; Student's t-test.

Furthermore, the MHCII$^{+}$ cells in the bone marrow (intracellular) and blood (extracellular) were vastly reduced in the *Sfpi1*$^{+/-}$ mice as compared to their wild type controls **(Figure 3-20 b,c)**. This was expected as PU.1 is known to transcriptionally control the expression of MHCII (Kitamura et al., 2012). Finally, within the Ly6C$^{hi}$ monocyte populations, R2 and R3 were greatly diminished in the bone marrow and R2 even more so in the blood **(Figure 3-21)**. This showed that R2 and R3 rely on PU.1 for their development in the bone marrow.

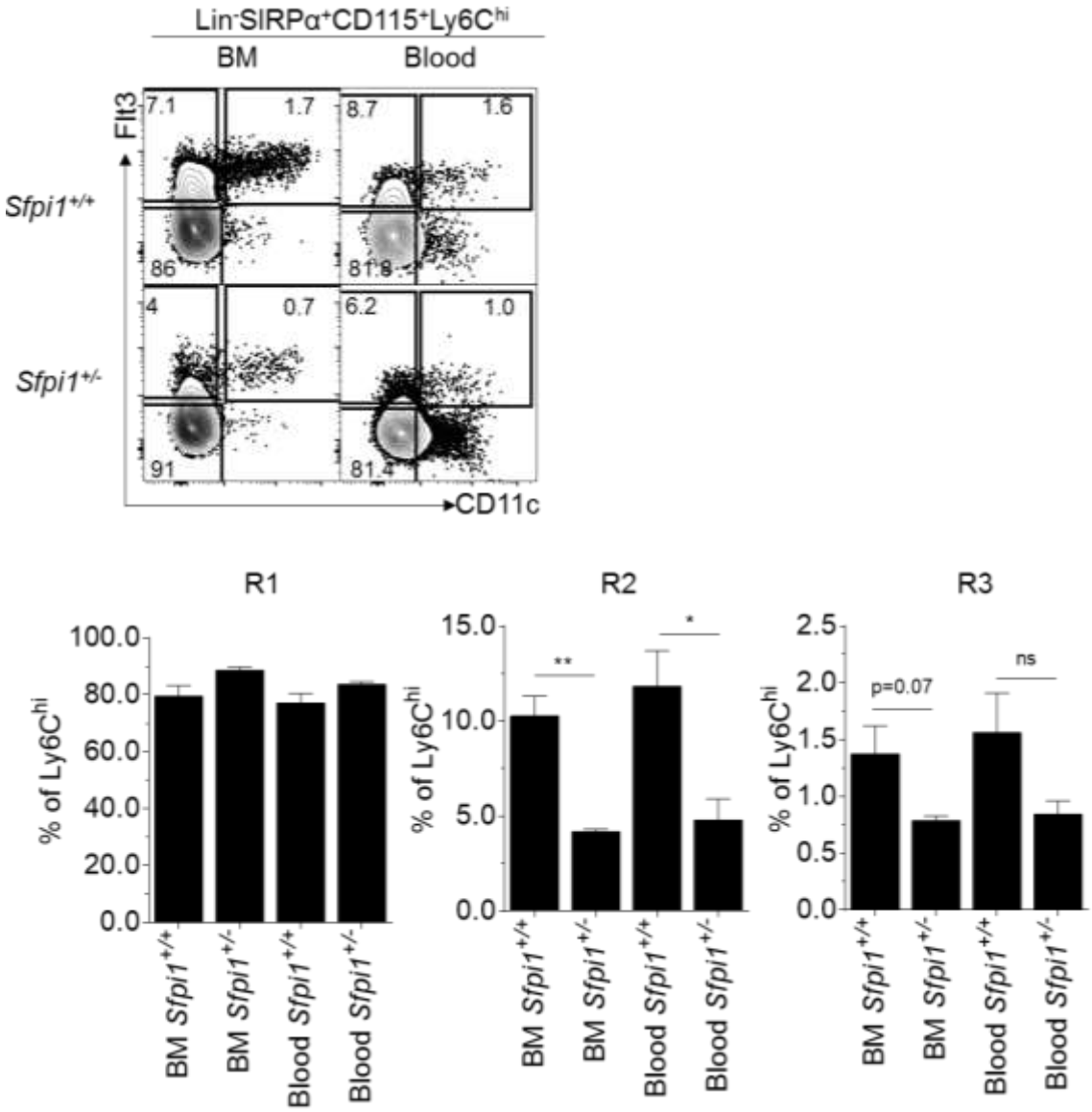


**Figure 3-21: R2 and R3 rely on PU.1 for their development *in vivo*.** *Sfpi1*$^{+/+}$ and *Sfpi1*$^{+/-}$ mice were assayed for the presence of R1, R2 and R3 in the bone marrow and blood. Graphs show mean ± SEM for n=3 for 3 experiments with identical results.

### *3.2.7 R2 is a heterogeneous population*

Throughout our analysis of the 3 populations, R2 always presented an intermediate phenotype between R1 and R3. Additionally, finding surface markers that were distinctly expressed in R2 alone proved impossible. Phenotyping experiments showed that the population of R2 was heterogeneous for markers such as CD11b, CD209a, or FcγRII/III. It thus became evident that R2 was in fact a heterogeneous population.

In order to test this, I used another approach to study the FACS data of Ly6C$^{hi}$ monocytes in the BM. Multi-dimensional reduction approach using the t-SNE algorithm, allows a 2-dimensional visualization of all 7 parameters (Lineage, MHCII, SIRPa, CD115, Flt3, CD11c, Ly6C) used to analyse every acquired cell without any *a priori* information regarding the gating strategy of each population. An overlay of the separately gated cell populations, on the unbiased clustering obtained through t-SNE, showed that R3 clustered separately from R1 and R2 (**Figure 3-22**). Additionally, based on just these 7 markers, R2 could be differentiated into 3 populations that clustered with R1, one of which clustered on the edge indicating a more distinct expression pattern to R1 (**Figure 3-22**)

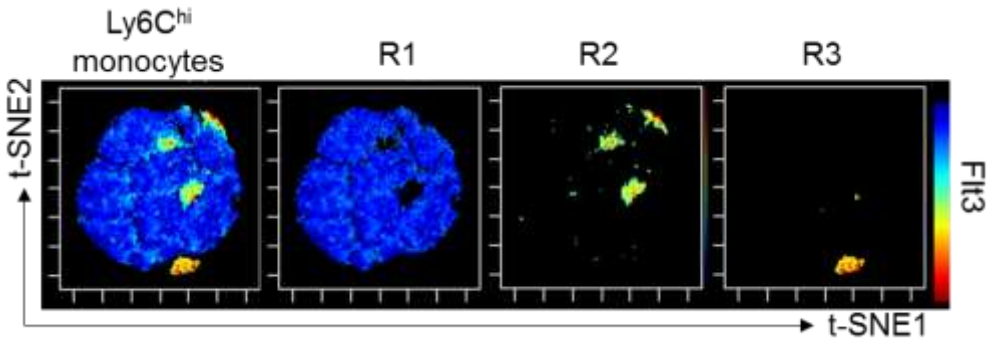


**Figure 3-22: Multi-dimensional reduction analysis of Ly6C$^{hi}$ monocytes**. t-SNE analysis of bone marrow Ly6C$^{hi}$ monocytes previously gated on Lin$^{-}$CD115$^{+}$SIRPa$^{+}$ cells. Overlay of separately gated R1, R2 and R3 on t-SNE analysis of total Ly6C$^{hi}$ monocytes reveals single-cell expression and clustering within each monocyte population.

To further analyse the heterogeneity in the R2 populations, a single-cell qPCR analysis for 45 genes on 44 single cells of the R1 and R3 populations, and 82 cells of the R2

population was performed. This experiment was performed by Thibaut Perchet and was analysed by myself. This experimental approach provided an unsupervised analysis of R2 to (i) determine how the population clusters with R1 monocytes and R3 pre-DCs, (ii) to determine if there is a unique population within R2 that might be the precursor population to mo-DCs and (iii) for the identification of a unique gene expression pattern to identify these cells. The genes assayed were among those that most highly discriminated by microarray data of FACS-sorted populations R1, R2 and R3 in a PCA analysis (**Figure 3-23**). Additionally, some transcription factors (*e.g. Irf8, Sfpi1*) were added to the list in the interest of finding any further evidence of a different transcriptional profile between the clusters of single cells.

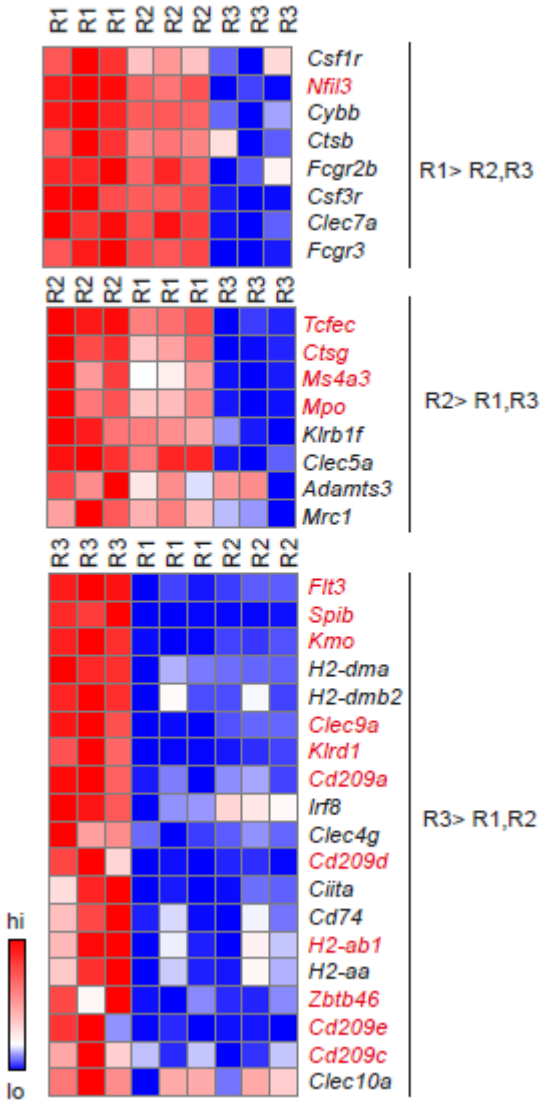


**Figure 3-23:List of most highly discriminating genes between R1, R2 and R3**. Heat map showing the relative expression pattern of genes most highly upregulated in FACS sorted populations R1, R2 and R3 over the others. Genes in red indicate those that resulted from PCA analysis of the same. Genes in black were tested due to previous experimental analysis.

Unsupervised clustering of the genes showed that specific monocyte-related (eg. *FcγR2b, Fcγr3*) or DC-related genes (eg. *Irf4, Sfpi1, Kmo*) clustered together and apart from the other (**Figure 3-24**).

Unsupervised clustering analysis of all the cells assayed showed that R2 was indeed heterogeneous (**Figure 3-24**). A majority of cells (60%) of R2 clustered with R1 indicating the strong transcriptional relationship between the 2 populations which mirrored the volcano plot analysis of the sorted populations (**Figure 3-13**). 30% of R2 clustered with

R3 (**Figure 3-24**). This cluster of cells was unique to only R2 indicating that there was a population within R2 that exhibited the properties of a precursor to mo-DCs (**Figure 3-24**, **Figure 3-25a,b**). Intriguingly, about 10% of R2 clustered separately from the other populations having a unique transcriptional profile of co-expression of Fcγr3 and CD209a along with being Zbtb46$^{-}$ (Cluster 3) (**Figure 3-24**, **Figure 3-25c**).

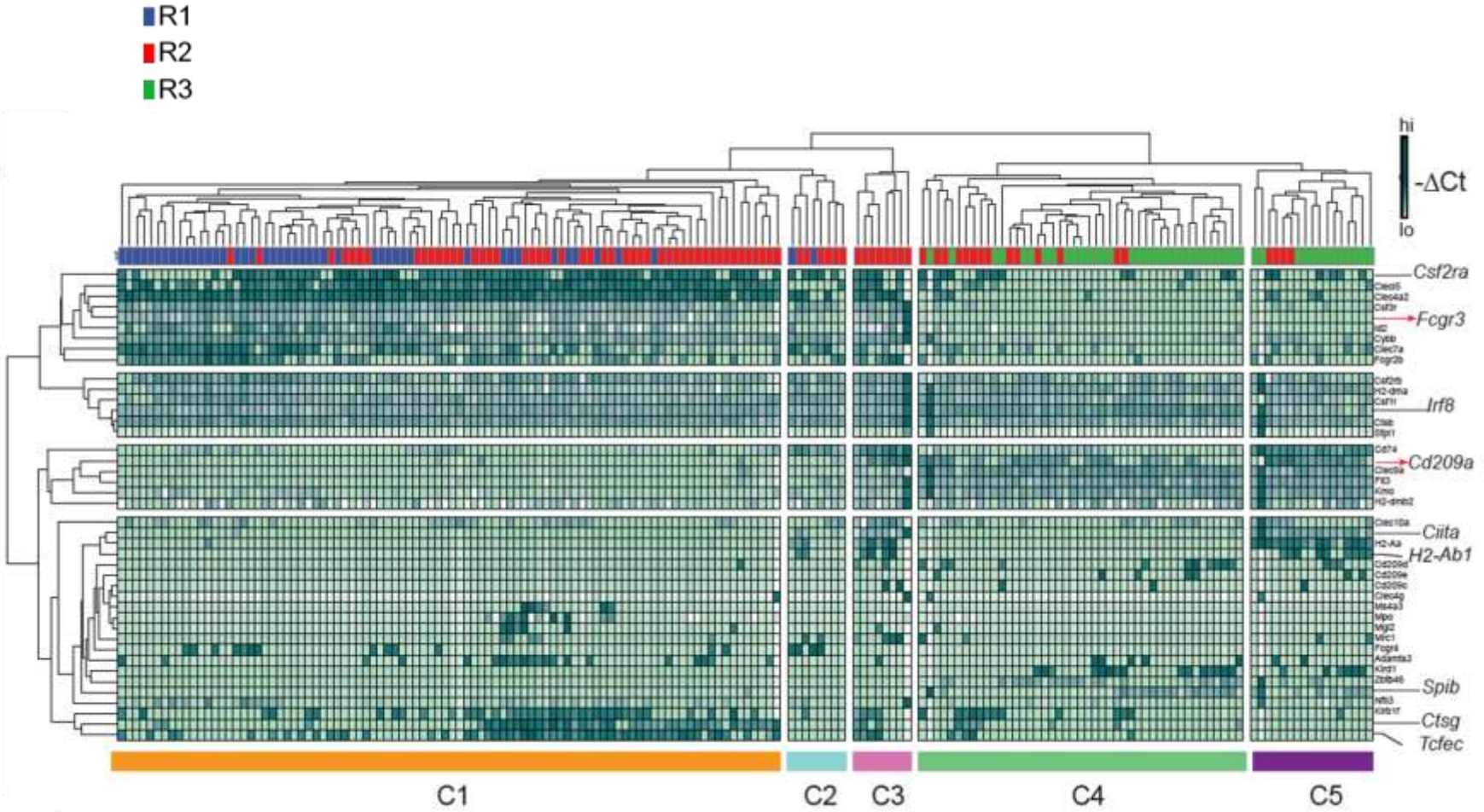
R1
R2
R3
hi
-ΔCt
lo
Csf2ra
Fcgr3
Irf8
Cd209a
Ciita
H2-Ab1
Spib
Ctsg
Tcfec
C1
C2
C3
C4
C5

**Figure 3-24: Heterogeneity in the R2 population**. Hierarchical clustering dendogram (top and left margins) derived from -ΔCt values from single-cell multiplex qPCR analysis of 44 R1 (Blue), 81 R2 (red) and 44 R3 (green) single cells for 42 genes and 3 housekeeping genes (not shown). Resulting clusters are indicated at the bottom as C1, C2, C3, C4 and C5. Dendogram displays the hierarchical clustering based on Euclidean distance between each cell based on its mRNA expression.

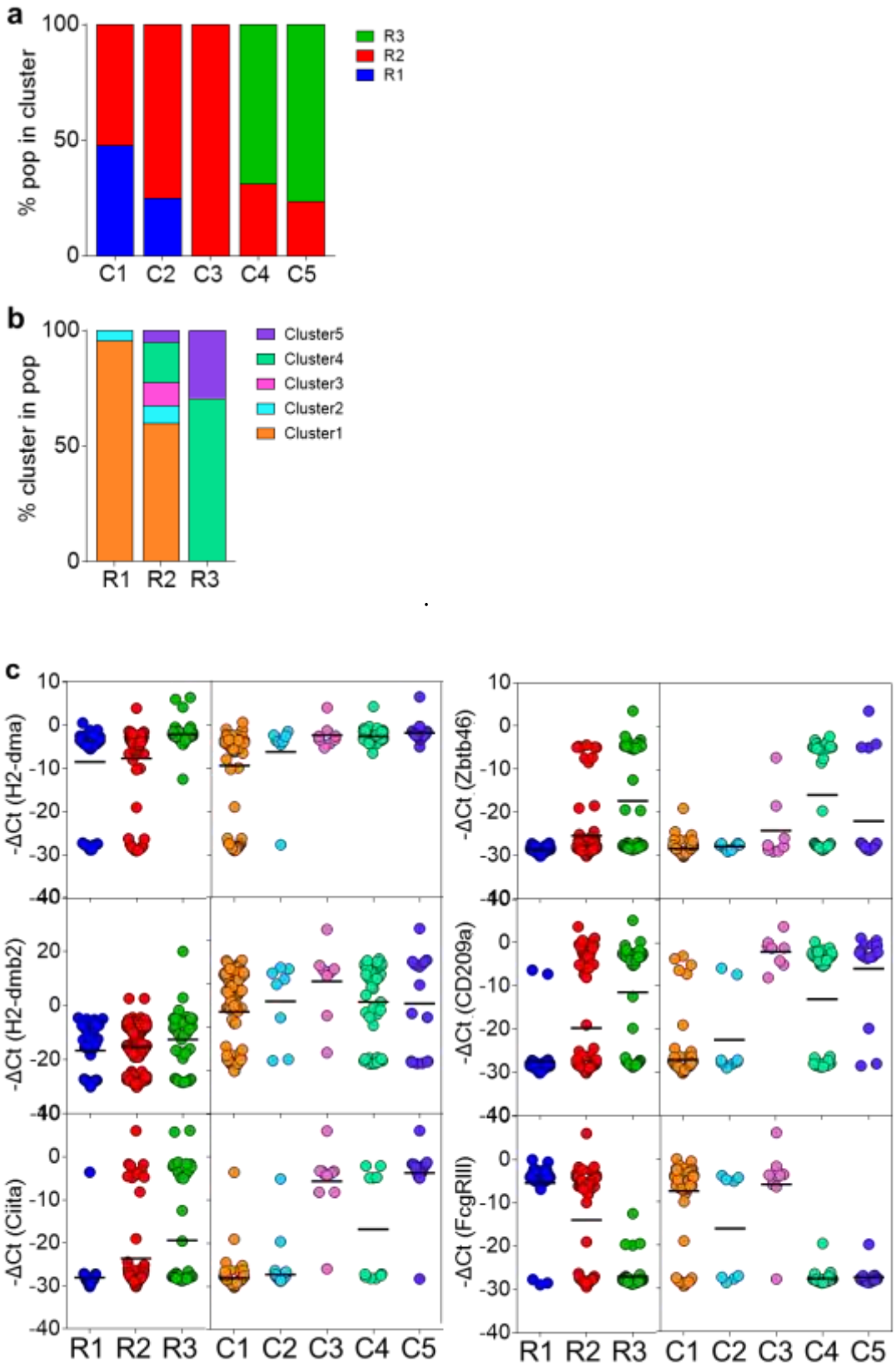


**Figure 3-25: Quantitative analysis of single cell qPCR data on populations and clusters within Ly6C$^{hi}$CD115$^{+}$ cells**. a ) Representation in percentage of R1, R2 and R3 populations within the 5 clusters defined in fig.3-21. b) Representation in percentage of the 5 clusters within R1, R2 and R3 populations.c) Single-cell expression of MHCII-

related genes, Zbtb46, FcγR3, CD209a in R1-R3 populations or C1-5 clusters. Each dot represents the -ΔCt value of a single cell.

Given that the protein expression of CD209a could not be seen within the BM, I could not use these markers to define R2 when analysing the cells by FACS and so continued to use Flt3 and CD11c to gate out R2 and R3 for functional experiments.

### 3.3 Discussion and chapter overview

Excluded from discussions on the development of monocytes and cDCs, monocyte-derived DCs or mo-DCs have been left under a branch of their own. Left incomplete with contradictions on their origin (Cheong et al., 2010; Meredith et al., 2012; Satpathy et al., 2012a) and broad definition, the term 'monocyte-derived DCs' has loosely defined a population of cells induced upon inflammation. This chapter has attempted to bring clarity to the field by considering the presence of a novel dedicated precursor.

$CX_3CR1^{int}CD11b^+$ cells had been found to be capable of generating both $iNOS^+$ cells as well as $MHCII^{hi}$ cells that expressed the DC specific transcription factor ZBTB46 after adoptive transfer into a mouse model of colitis (Zigmond et al., 2012). This study, along with others showing that mo-DCs were *Ccr2*-dependent provided a certain amount of certainty that the precursors of monocyte-derived DCs originated within the $Ly6C^{hi}$ monocyte population. By looking for DC-related marker expression (Flt3, CD11c) I were able to identify 2 populations within conventional $Ly6C^{hi}$ monocyte gating that had not been documented before. $Flt3^+CD11c^+$ R3 cells that I found to be a pre-cDC contamination within $Ly6C^{hi}$ monocytes could explain the appearance of the dendritic cell phenotype arising from widely gated $Ly6C^{hi}$ monocytes used in adoptive transfer experiments such as the one referenced above (Biswas et al., 2015; Zigmond et al., 2012).

$Flt3^+CD11c^-$ R2 cells were an entirely novel population identified in this study. Being $Flt3^+CD115^+$, it was intriguing to find that they were neither progenitor cells ($cKit^-$) nor belonging to the cDC lineage (*Flt3l*-independent, $Zbtb46^-$). This *Ccr2*-dependent, *Nr4a1*-independent population stood apart from $Ly6C^{lo}$ monocytes and identified transcriptionally and phenotypically with $Flt3^-CD11c^-Ly6C^{hi}$ monocytes. Very few genes were exclusively expressed within the R2 population making its identification a challenge. By identification of a combination of markers, namely FcγRII/III and CD209a, that could be stained on the surface of the cells in the blood, I were able to establish a

phenotypic characterisation of this novel population. As a consequence, I were able to distinguish the R2 population from Flt3$^{-}$CD11c$^{-}$ Ly6C$^{hi}$ monocytes as well as from pre-cDCs.

An additional point of interest is the enrichment of MHCII$^{+}$ cells within the R2 population. Ly6C$^{hi}$ monocytes had been documented previously as being able to transfer antigen to draining lymph nodes while they upregulated MHCII (Jakubzick et al., 2013). Very little was known about these MHCII$^{+}$Ly6C$^{hi}$ monocytes at steady state (Kingston et al., 2009b). In this chapter, I have assessed the relative percentages of the MHCII$^{+}$Ly6C$^{hi}$ monocytes, and report that they account for 65% of the Flt3$^{+}$ population (which encompasses R2 and R3) and only 17% of the Flt3$^{-}$ population (R1). Thus characterising R2 allows for the study of the Ly6C$^{hi}$ monocytes that upregulate MHCII in the blood.

Understanding the mechanism that drives the derivation of a cell population is critical to understanding its origin. I found that the transcription factor PU.1 plays a central role in the promotion of Flt3$^{+}$ R2 cells over Flt3$^{-}$ R1 cells in the BM and blood. PU.1 regulates the transcription of a number of target genes which include Flt3 and the transcription factor that drives MHCII expression – CIITA, via promoters *pI* and *pIII* at steady state (Kitamura et al., 2012; Yoon and Boss, 2010). Given that *pI*$^{-/-}$ mice lacked the MHCII$^{+}$Ly6C$^{hi}$ monocyte population, our study suggests that PU.1 could control the MHCII$^{+}$ R2 cells via the *pI* promoter.

While gating for Flt3 expression within the Ly6C$^{hi}$CD11c$^{-}$ monocyte population allows for the study of a population of MHCII-enriched, Ccr2-dependent cell population that upregulated CD209a and FcγRII/III in the blood, it was not possible to ignore the fact that all phenotypic analyses of the cells showed heterogeneity (CD209a, FcγRII/III, CD11b and MHCII expression, Ccr2-dependency). It appeared that the FACS-based

identification of these cells may not be accurate enough to identify the single unique population within R2 that might act as a precursor to Mo-DCs.

Single-cell analysis showed that 10% of R2 formed a unique cluster with its own transcriptional profile, unique from that of $Flt3^{-}CD11c^{-}$ R1 monocytes and $Flt3^{+}CD11c^{+}$ pre-cDCs. I could not find specific markers to identify this sub-population. This was possibly due to the fact that the single-cell qPCR tested genes were selected based on those that had the highest fold change in a PCA analysis of bulk-sorted R1, R2 and R3. This ensured that genes that were most highly upregulated in R1 or R3 and most co-expressed in R2 topped the list and the genes tested were not comprehensive. In order to find a specific marker exclusively expressed on the unique cluster within R2 cells in the future I would need to perform RNA-seq analysis or a multiplex FACS analysis of all the known surface-expressed CD markers on $Ly6C^{hi}$ monocytes from the BM and/or blood. Within, the scope of this study however, I noted by microarray, FACS and single-cell qPCR analysis that FcγRII/III and CD209a provided a strong means of identification of cluster 3 within R2.

# Chapter 4

# The influence of GM-CSF on R1 and R2 monocytes

# 4 The influence of GM-CSF on R1 and R2 monocytes

## 4.1 Introduction

### *4.1.1 The role of GM-CSF in MPS development*

Granulocyte-macrophage colony stimulating factor (GM-CSF) was originally discovered as the culture constituent required to stimulate the production of colonies of granulocytes and macrophages from mouse bone marrow in solid agar cultures (Bradley and Metcalf, 1966; Pluznik and Sachs, 1966). Subsequent *in vivo* experiments demonstrated the critical role of GM-CSF in early myeloid development. GM-CSF is required for the development of tissue cDCs (Greter et al., 2012) and monocytes precursors within the bone marrow (Van De Laar et al., 2012). GM-CSF also influences the expression of $CD103^+$ on migratory cDCs and the ability of cells to engage in cross-presentation (Zhan et al., 2011). Furthermore, the heterogeneity in cell type and activation state observed in such cultures is testament to the wide effects of GM-CSF on the myeloid populations in murine BM (**Figure 4-1**).

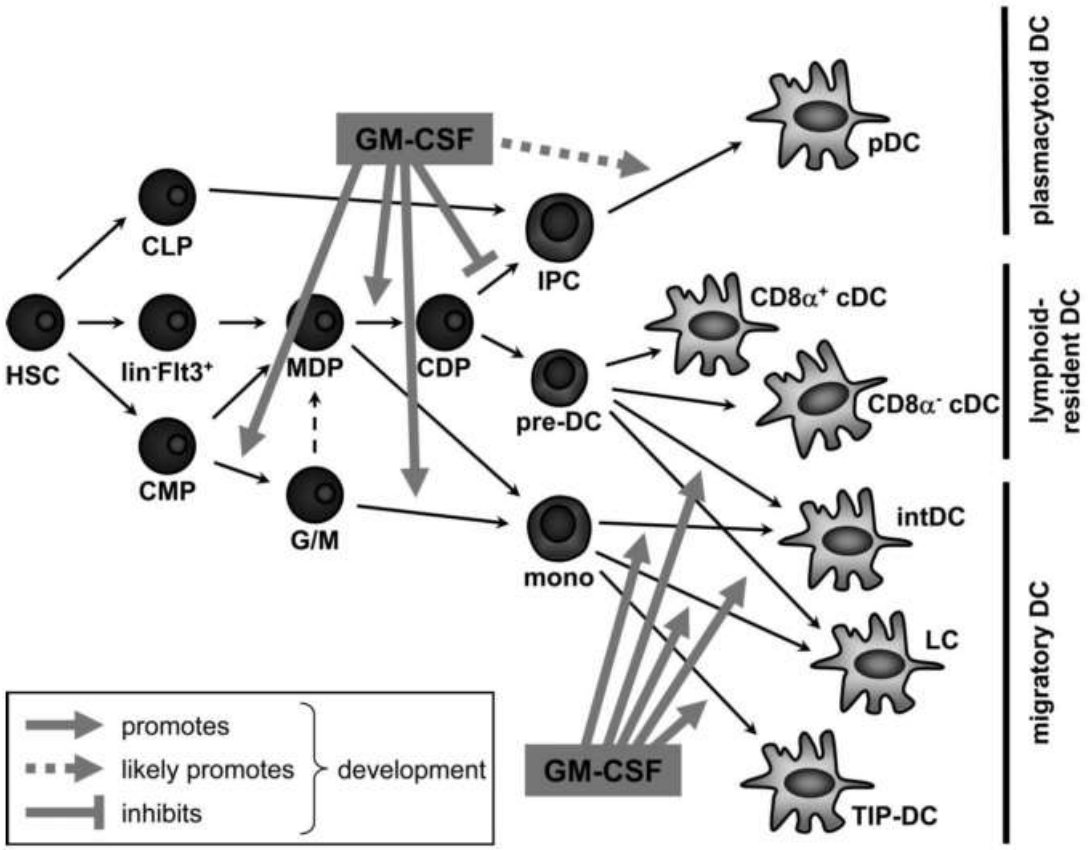


**Figure 4-1: The influence of GM-CSF on myeloid development.** Reproduced from Van de Laar et al, 2012. GM-CSF strongly influences the development of DCs and monocytes from the early hematopoietic developmental stage. Additionally, it has an important role in the development of cDCs at later stages of development especially in the context of inflammation such as in the formation of of iNOS-producing cells (in this figure referred to as Tip-DCs)

### *4.1.2 Influence of GM-CSF on the generation of mo-DCs*

Unlike M-CSF and Flt3L, steady state levels of circulating GM-CSF are low. This is because the developmental requirement of the growth factor is low due to the high biological activity (Barreda et al., 2004). Pathogens and other inflammatory mediators bring about systemic increase in GM-CSF (Hamilton, 2002) while *in vivo* administration promotes the expansion of $CD11b^+$ DCs in the spleen (Daro et al., 2000). In the presence of either GM-CSF alone (Inaba et al., 1992) or in combination with IL-4 (Sallusto and Lanzavecchia, 1994b), monocytes from murine bone marrow or human peripheral blood are able to generate large numbers of $CD11c^+MHCII^+$ cells *in vitro* that are able to prime

T cells (Daro et al., 2000). Recent studies have utilized additional markers of differentiation to better characterize resulting progeny of GM-CSF supplemented cultures. A study by Reis e Sousa and colleagues has demonstrated that a culture of total murine bone marrow with GM-CSF yields both macrophage-like cells ($CD11b^{+}MHCII^{int}PD^{-}L2^{+}CD64^{+}CD115^{+}CD14^{+}$) and DC-like cells ($CD11b^{+}MHCII^{hi}PD\text{-}L2^{hi}CD135^{+}CD14^{+}$) (Helft et al., 2015). Gao et al. divided the murine bone marrow progeny on the basis of their activation states and expression of PD-L2. The $PD\text{-}L2^{lo}$ cells were capable of differentiating into $PD\text{-}L2^{hi}$ cells upon LPS stimulation, with a transcriptional profile that fit that of an activated cell type (Gao et al., 2013). Due to the generation of a DC-like phenotype from monocytes *in vitro*, the resulting progeny of GM-CSF supplemented cultures is often referred to as mo-DCs (monocyte-derived dendritic cells) or GM-DCs (GM-CSF induced DCs).

The current functional understanding of mo-DCs is that they are required within the tissue as antigen-presenting cells (APCs) able to take up and process antigen far better than their $CD11b^{+}$ cDC counterparts (Daro et al., 2000; Plantinga et al., 2013) . However, *in vitro* co-culture assays for antigen-specific T cell proliferation detected no differences between the T cell activation elicited by mo-DCs versus $CD11b^{+}$cDCs (Cook et al., 2004; Daro et al., 2000). Although, their specialized role in an immune response remains elusive, mo-DCs are very responsive to inflammatory stimuli such LPS, TNF-α and recombinant-CD40L (Caux et al., 1997; Zhong et al., 2009),. In comparison to cDCs derived from Flt3L-supplemented bone marrow cultures (Fl-DCs), GM-DCs have greater immunogenicity- capable of producing inflammatory mediators like NO, TNF-α, IL10 and CCL2, upon TLR activation (Xu et al., 2007). Thus, iNOS-producing cells fall within the classification of monocyte-derived inflammatory cells. Additionally, mo-DCs can be derived from $CD11b^{+}Ly6C^{hi}Ly6G^{-}$ monocytes while Fl-DCs cannot (Xu et al., 2007). The aforementioned *in vitro* studies provide evidence of the origin of mo-DCs and iNOS-

producing cells from monocytes in response to GM-CSF. *In vivo* evidence for the existence of mo-DCs relies largely on experiments utilizing *Ccr2*$^{-/-}$ *mice* which do not develop mo-DCs in response to an inflammatory stimulus (Croxford et al., 2015; Greter et al., 2012). Thus, the definition of 'Mo-DCs' has become that of an inflammatory population of cells reliant on GM-CSF and derived from *Ccr2*-dependent monocytes.

### *4.1.3 Phenotypic distinction between Mo-DCs, cDCs and macrophages*

Mo-DCs that arise in response to exogenous GM-CSF *in vivo* were originally defined as CD11b$^{+}$CD11c$^{+}$ and MHCII$^{hi}$ (Daro et al., 2000). More recently, using models of systemic LPS administration, 'mo$^{-}$DCs' have been described with more specific markers such as CD206 and CD209 (Cheong et al., 2010; Greter et al., 2012) in the spleen, FcεR1 and CD64 in the lung (Plantinga et al., 2013) and in models of colitis have been characterised as expressing CD64 in the gut (Tamoutounour et al., 2012). These markers are crucial to distinguish them from other myeloid populations that express CD11b and CD11c to a similar extent, namely the tissue$^{-}$resident macrophages and cDCs.

There is a need to characterize specific surface markers on mo-DCs that can distinguish them from other myeloid populations to better characterize this specific population of cells in the context of steady state and inflammation. The distinction between mo-DCs and 'inflammatory macrophages' *in vivo* is unclear. Largely they are considered within the mo-DC classification but are not phenotypically distinguished from them. *In vivo* inhibition of GM-CSF results in the reduction of CD115$^{+}$Ly6C$^{+}$F4/80$^{+}$ inflammatory macrophages in models of antigen-induced peritonitis and lung inflammation (Lenzo et al., 2012). Thus, both 'mo-DCs' and 'inflammatory macrophages' are reliant on GM-CSF.

One possible method of better characterising these inflammatory cells is by accurately determining the lineage to which they belong *in vivo*. Defining the mo-DCs as

$CD14^{+}CD11b^{+}CD11c^{+}MHCII^{hi}$, Meredith et al. showed that mo-DCs were absent from LPS treated *Flt3l*$^{-/-}$ mice and DT-treated mixed bone marrow chimeras of WT and *zDC*$^{DTR/DTR}$ bone marrow (Meredith et al., 2012). Given the dependency of cDCs on Flt3L and *Zbtb46* for development, Meredith et al inferred that 'mo-DCs' derived from the cDC-lineage. Conversely, a number of studies detail the requirement of *Ccr2* to develop mo-DCs in different inflammatory settings such as LPS administration, EAE, and colitis (Cheong et al., 2010; Croxford et al., 2015; Zigmond et al., 2012). These studies are testament to the heterogeneity within the 'Mo$^{-}$DC' definition.

It is unclear whether all Ly6C$^{hi}$monocytes have the capacity to become iNOS$^{+}$ cells or dendritic cells or if a subset within this wider definition is specialized to produce each of these in response to GM-CSF. This will be addressed in the current chapter of this thesis.

### *4.1.4 Objectives of Chapter 4*

Given the complexity in macrophage, cDC and mo-DC development in response to elevated levels of GM-CSF, it might also be considered that these GM-CSF-dependent cell populations are ontogenically distinct, arising from unique monocyte or DC precursors. I hypothesized that the previously described heterogeneity within the Ly6C$^{hi}$ monocyte population in the bone marrow, blood and spleen, could help explain this. The focus of this chapter will be to study the cells among the precursor monocyte subsets that respond to GM-CSF described in Chapter 1.

The objectives of this chapter are the following:

- To investigate the influence of GM-CSF on each Ly6C$^{hi}$ monocyte population- R1 and R2
- To study the role, if any, of PU.1 on the generation of mo-DCs
- To distinguish mo-DCs from cDCs.
- To establish a phenotypic definition of mo-DCs and discriminate between them and inflammatory macrophages.

## 4.2 Results

### *4.2.1 Impact of GM-CSF on Ly6C$^{hi}$ monocytes in vitro*

#### 4.2.1.1 *Phenotype of GM-CSF-induced progeny of Ly6C$^{hi}$ monocytes*

As discussed previously, the culture of murine bone marrow in GM-CSF results in heterogeneous progeny- macrophages and GM-DCs, that are largely monocyte-derived and yet display distinct phenotypic outcomes (Gao et al., 2010; Helft et al., 2015). In this chapter, I address the possibility that the heterogeneity in GM-CSF induced progeny arises from heterogeneity within Ly6C$^{hi}$ monocytes, i.e. that either R1 or R2 is capable of generating more DC-like features while the other generates macrophages.

Bone marrow Lin$^-$MHCII$^-$Ly6C$^{hi}$ monocytes were sorted for their expression of Flt3 and CD11c into R1 (Flt3$^-$CD11c$^-$) and R2 (Flt3$^+$CD11c$^-$) monocytes and Lin$^-$MHCII$^-$ cells were sorted into R3 (CD115$^+$Flt3$^+$CD11c$^+$) and P (CD115$^-$Flt3$^+$CD11c$^+$) pre-cDCs. Equal numbers of each population were plated in the presence of 20ng/ml of GM-CSF along with $10^5$ cells of congenically labelled whole bone marrow as feeder cells for 7 days. R2 responded to GM-CSF to a greater degree than pre-DCs or R1 monocytes with a trend toward greater numbers of CD11c$^+$ CD45.1$^+$ cells (**Figure 4-2**).

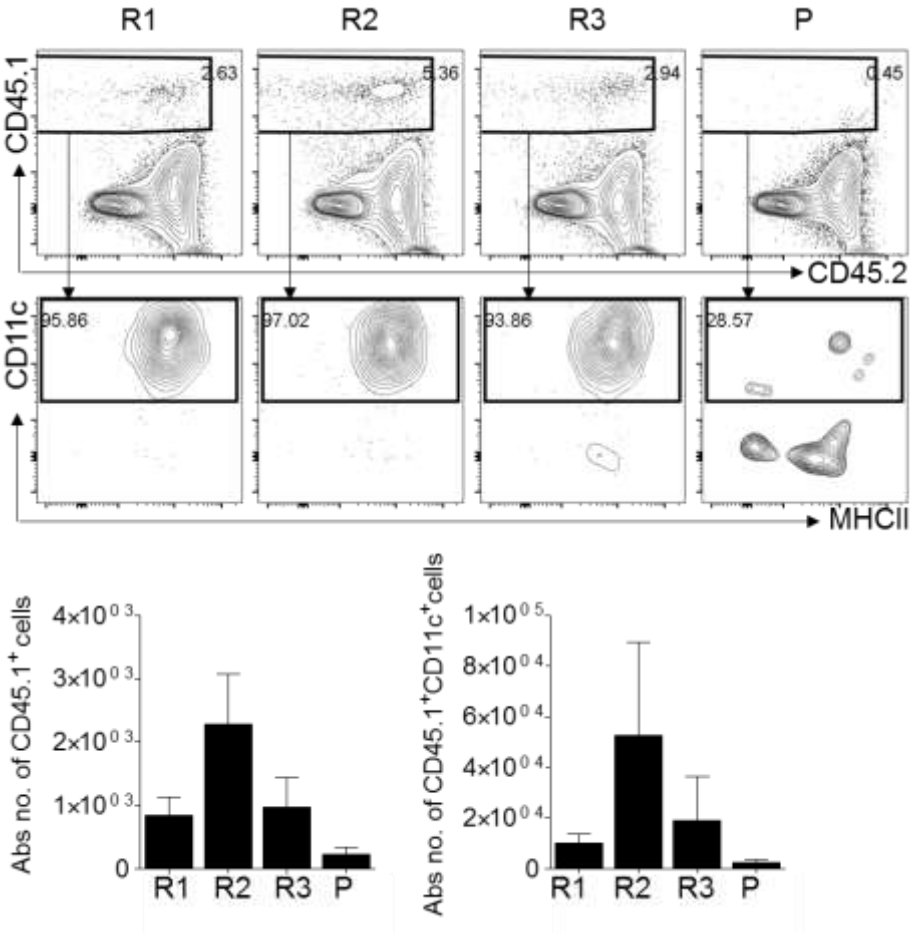


**Figure 4-2: *In vitro* GM-CSF culture of R1, R2, R3 and P.** 10,000 flow cytometry sorted CD45.1$^+$ Ly6C$^{hi}$ R1 and R2 monocytes, alongside CD115+ R3 and CD115- P pre-cDCs were cultured in GM-CSF for 7 days. They were plated with whole bone marrow from congenically marked CD45.2$^+$ mice acting as feeder cells. Absolute numbers of recovered cells were counted from DAPI$^-$ cells and quantified as shown. Flow cytometry data is representative of 3 experiments with similar results. Graphs show mean ± SEM from grouped data of all 3 experiments(n=3).

Although there was a greater response to GM-CSF by R2, the numbers obtained following 7 days in culture were greatly diminished, possibly due to cell death *in vitro* as only 2000 cells were retrieved in comparison to the input of 10,000 cells. Thus, I attempted shorted culture periods with GM-CSF.

Medzhitov and colleagues reported the use of PDL2 and CD86 to define cell populations within a monocyte-derived BM culture that were phenotypically and functionally distinct (Gao et al., 2013). I therefore tested FACS-sorted R1 and R2 monocytes alongside pre-cDCs as controls, for PDL2 and CD86 (Gao et al., 2013). Most recently, Helft et al determined that these cells were in fact a mixture of macrophage cells (Flt3$^-$ PDL2$^{lo}$) and

DC-like cells ($Flt3^{+}PDL2^{hi}$) (Helft et al., 2015) differently able to stimulate T cells in the context of MHC-I and MHC-II.

I incubated the sorted cells for 5 days in 20ng/ml of recombinant GM-CSF (rGM-CSF). Using the total cells in culture ($CD45.2^{+}$ and $CD45.1^{+}$) as a control for equal culture conditions in all wells, I noted that R2 produced the highest levels of $PDL2^{+}CD86^{+}$ cells as compared to the other monocyte or pre-DC populations in a 5-day culture with GM-CSF (**Figure 4-3**).

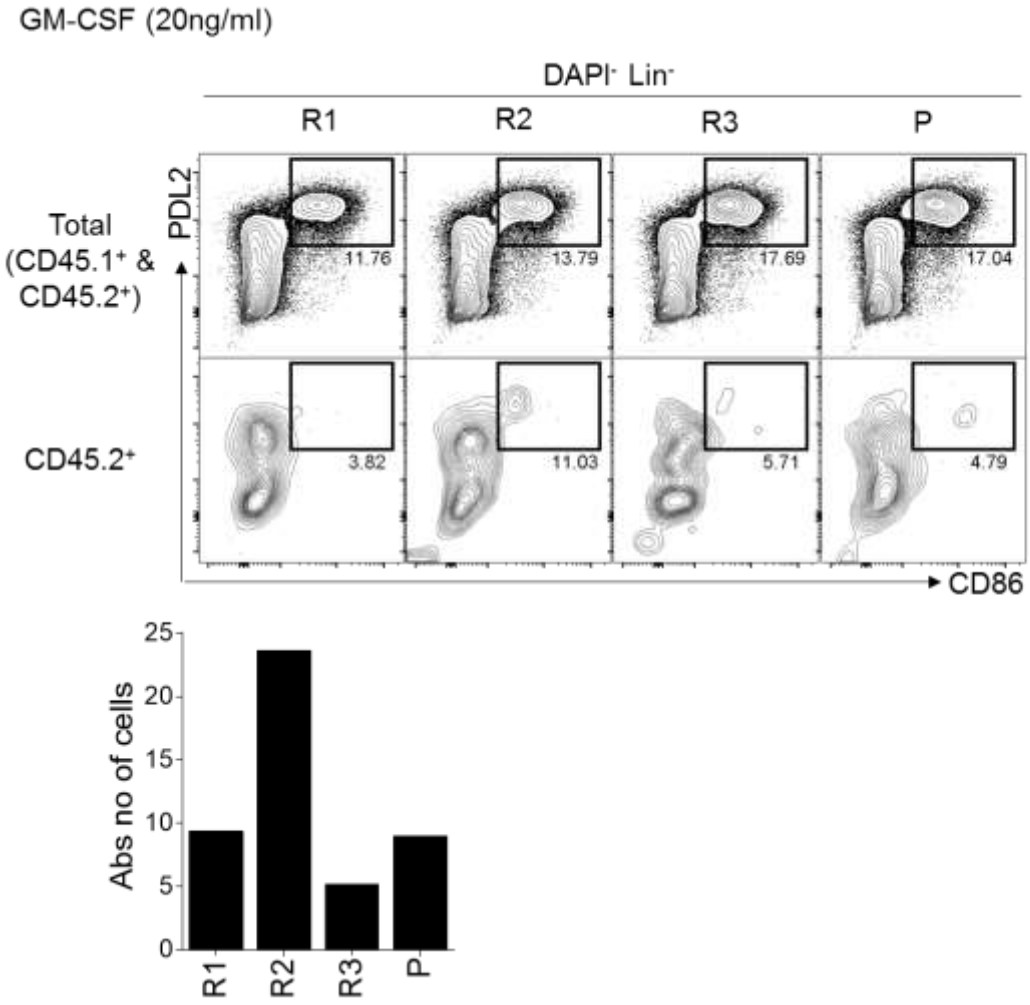


**Figure 4-3: R2 is responsible for the production of $PDL2^{+}CD86^{+}$ cells.** 10,000 FACS sorted $CD45.2^{+}$ R1, R2, R3 and P cells were plated with $CD45.1^{+}$ feeder whole bone marrow cells in 20ng/ml GM-CSF. Upper panel shows the total percentage of $PDL2^{+}CD86^{+}$ cells obtained in culture after 5 days. The progeny of $CD45.2^{+}$ sorted cells are shown in the bottom panel. n=1

#### 4.2.1.2 *Role of PU.1 in the generation of PDL2$^{+}$CD86$^{+}$ cells*

Having shown that R2 was capable of generating PDL2$^{+}$ CD86$^{+}$ cells in culture, I hypothesized that these cells would also rely on the master transcription factor, PU.1. *Sfpi1*$^{+/-}$ mice have half the alleles for PU.1 than WT mice. If PDL2$^{+}$CD86$^{+}$ cells derived exclusively from PU.1$^{hi}$ R2 cells, it could be expected that *Sfpi1*$^{+/-}$ BM cultures would not develop PDL2$^{+}$CD86$^{+}$ cells as *Sfpi1*$^{+/-}$ bone marrow has far fewer R2 monocytes (Chapter 3).

In order to improve the numbers of cells that survive in culture with GM-CSF, I replaced the CD45.1$^{+}$ bone marrow with the MS-5 cell line as feeder cells. MS-5 is a mouse stromal cell line that has been found to aid in murine and human progenitor cell survival and proliferation (Issaad et al., 1993) via uncharacterized soluble molecules (Kobari et al., 1995) and a cell-contact dependent mechanism via the expression of neuropilin-1 (Tordjman et al., 1999). Additionally, I tested the expression of cell surface markers at day5 instead of day7 to test for earlier cell differentiation and the upregulation of activation markers like PDL2 and CD86. The culture resulted in the production of PDL2$^{+}$CD86$^{+}$ cells that were MHCII$^{hi}$. A large number of cells also remained PDL2$^{lo}$CD86$^{lo}$ and were the same in both *Sfpi1*$^{+/+}$ and *Sfpi1*$^{+/-}$ cultures (**Figure 4-4**). However, the numbers of PDL2$^{+}$CD86$^{+}$ cells were greatly diminished in *Sfpi1*$^{+/-}$ BM culture as compared to the *Sfpi1*$^{+/+}$ counterpart. Thus, PDL2$^{+}$CD86$^{+}$ cells are a PU.1-dependent population.

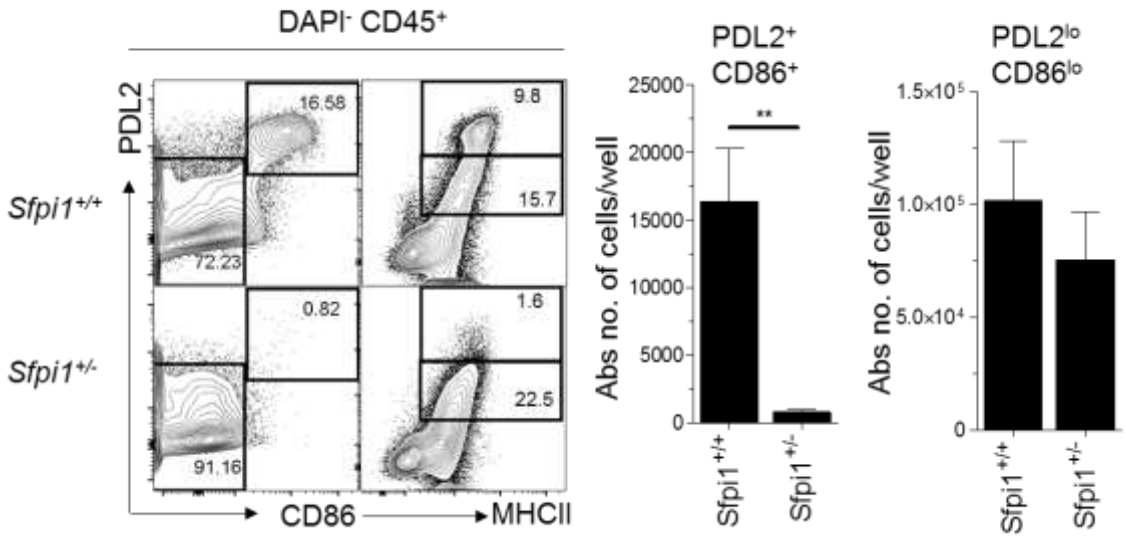


**Figure 4-4: Role of PU.1 in the development of PDL2$^{+}$CD86$^{+}$ cells *in vitro*.** *Sfpi1*$^{+/-}$ and *Sfpi1*$^{+/+}$ whole bone marrow cells were cultured with MS$^{-}$5 cells in 20ng/ml GM-CSF for 5 days. Absolute numbers of PDL2$^{+}$CD86$^{+}$ cells and PDL2$^{lo}$CD86$^{lo}$ cells were counted from the recovered progeny and are depicted in the graphs alongside. Flow cytometry data is representative of 4 independent cultures and cumulative numbers are depicted in the graphs.n=4 **p<0.005; Student's t-test.

#### 4.2.1.3 *FcγRII/III and CD209a expression on in vitro progeny of R1, R2 and R3*

Having found that PU.1-dependent R2 was capable of giving rise to sufficient numbers of PDL2$^{+}$CD86$^{+}$ cells in our feeder culture system with GM-CSF, I wondered whether these cells could be defined based on highly expressed markers as revealed by the mRNA levels in the bone marrow and as a surface phenotype in the blood on R1, R2 and R3 (Chapter3), such as CD209a and FcγRII/III. This would allow us to define surface markers that can be used to distinguish these cells at steady state and in response to GM$^{-}$CSF.

Since in previous experiments, R3 and P pre-cDCs gave similar results in surface marker expression in response to GM-CSF, I focused on phenotyping R2 in comparison with R1 Ly6C$^{hi}$ monocytes and R3 CD115+ pre-DCs. R1, R2 and R3 were cultured in 20ng/ml of

GM-CSF with MS-5 feeders. The culture was carried out for 2 days as I speculated that with such small numbers of cells sorted by flow cytometry, shorter time points would ensure survival and a sufficient amount of differentiation. The progeny were assessed for the expression of FcγRII/III, CD209a as well as PDL2 and CD86 to relate to the $PDL2^{+}CD86^{+}$ cells described previously to derive from R2 (**Figure 4-4**) (Gao et al., 2013).

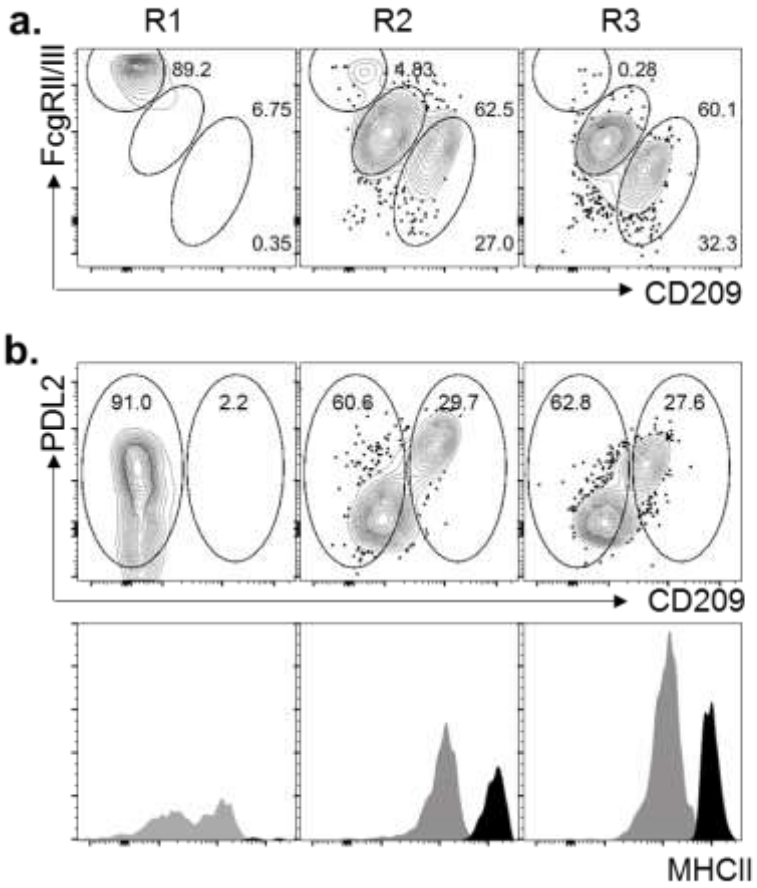


**Figure 4-5: R2 cells generate *FcγRII/III*$^{+}$CD209$^{+}$PDL2$^{+}$MHCII$^{+}$ cells**a., b.)10,000 FACS sorted cells were cultured in GM-CSF for 2 days and assayed for expression for *FcγRII/III*, CD209a, PDL2 and MHCII. Representative FACS plots of 4 independent cultures are shown. b) Grey histograms indicate the $CD209a^{-}$ population while $CD209a^{+}$cells are depicted in black histograms as gated in FACS plots above.

The progeny showed distinct expression levels of FcγRII/III, CD209a and PDL2. R1 generated $FcγRII/III^{+}CD209^{-}$ cells while R3 generated $CD209a^{+}$ cells that were

FcγRII/III$^{int-neg}$. R2 generated all three populations but the progeny were predominantly CD209$^{+}$ FcγRII/III$^{int}$ (~60%) (**Figure 4-5a**).

R1 generated a large number of CD209a-PDL2+ cells while R2 generated cells that were both PDL2$^{+}$CD209$^{+}$ as well as PDL2$^{+}$CD209$^{-}$ cells. The level of MHCII expression on the PDL2$^{+}$CD209$^{+}$ cells was much higher than in the CD209a$^{-}$ counterparts (**Figure 4-5b**). Intriguingly, R3 also produced PDL2$^{+}$CD209$^{+}$ MHCII$^{+}$ cells but these were in fewer numbers and of a lower MFI in CD209 than those generated by R2. This provided us with some insight on characterizing R1, R2 and R3 populations using the surface markers FcγRII/III, CD209a and PDL2.

#### 4.2.1.4 *PDL2$^{+}$MHCII$^{hi}$cells rely on PU.1 for their development in vitro*

To test the reliance of the PDL2$^{+}$MHCII$^{hi}$cells on PU.1, *Sfpi1$^{+/+}$* and *Sfpi1$^{+/-}$* bone marrow monocytes were cultured in GM-CSF for 2 days. Wild type controls gave rise to the FcγRII/III$^{+}$PDL2$^{+}$MHCII$^{hi}$CD209$^{+}$ cells (red) while the *Sfpi1$^{+/-}$* monocytes developed mainly into FcγRII/III$^{+}$PDL2$^{+}$MHCII$^{-}$CD209$^{-}$ cells (blue) (**Figure 4-6**). This showed the relative dependence of the FcγRII/III$^{+}$CD209$^{+}$ and FcγRII/III$^{-}$CD209$^{+}$ cells on PU.1 *in vitro*.

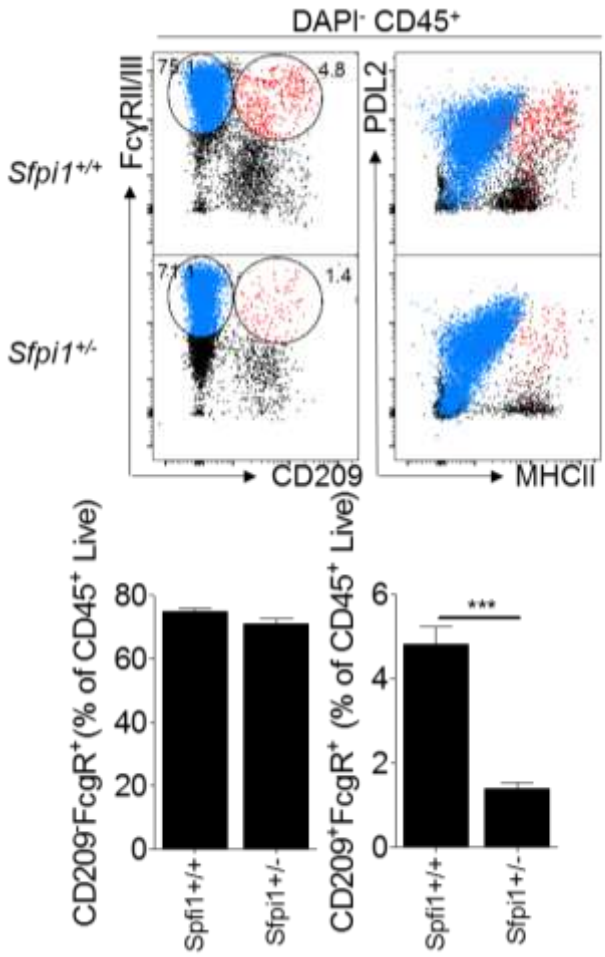


**Figure 4-6: *FcγRII/III*$^{+}$CD209$^{+}$cells are PU.1 dependent**. Whole bone marrow from *Sfpi1*$^{+/+}$ or *Sfpi1*$^{+/-}$ mice were cultured *in vitro* with 20ng/ml GM-CSF on MS$^{-}$5 feeder cells. FACS plots for CD209, *FcγRII/III*, PDL2 and MHCII expression are shown. *FcγRII/III*$^{+}$CD209$^{-}$ cells (blue) and *FcγRII/III*$^{+}$CD209$^{+}$ cells (red) are overlaid on an analysis of the same cells for expression of PDL2 and MHCII. Graphs show data from 4 independent cultures. n=4

### *4.2.2 The impact of GM-CSF on monocytes R1 and R2 in vivo*

In order to study the influence of GM-CSF on the myeloid population *in vivo*, I used a B16 melanoma cell line, that is engineered to constitutively produce GM-CSF (B16-GM). The cells must be at approximately 75% confluency to be injected in order to get a sizeable tumour by day12-14 (Dranoff et al., 1993). A single sub$^{-}$cutaneous injection of $10^5$ cells results in the development of a visible tumour by 9 days which enlarges gradually until the end$^{-}$point of 13 days. As controls, naïve C57Bl/6 mice and C57Bl/6 mice injected with B16 control cells that lack expression of GM-CSF, were used.

#### 4.2.2.1 *Blood MHCII$^{+}$Ly6C$^{+/-}$ cells in blood expand in response to GM-CSF*

As an initial approach to understanding the overall outcome of *in vivo* exposure to GM-CSF, the cells of the bone marrow, blood and spleen of mice treated with B16-GM or B16 cells, were phenotyped for their expression of monocyte markers CD11b, CD115 and Ly6C as well as for MHCII **(Figure 4-7)**. MHCII$^{+}$ monocytes presented a 'waterfall' of Ly6C$^{+}$ to Ly6C$^{-}$ cells in mice treated with B16-GM tumours. A clear increase in numbers as well as in percentage of MHCII$^{+}$ cells (both Ly6C$^{+}$ and Ly6C$^{-}$ cells) was observed in circulation in response to GM-CSF (**Figure 4-7)**

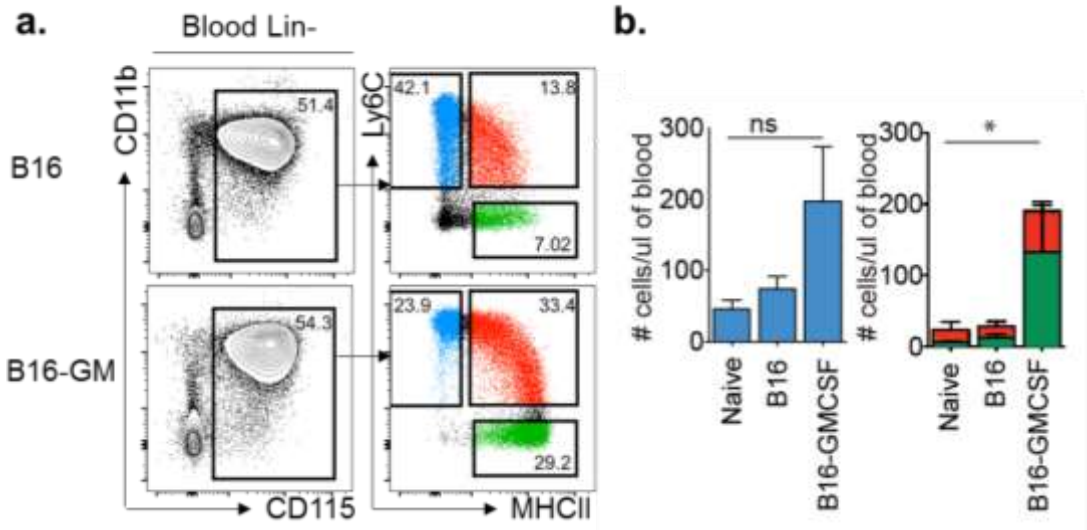


**Figure 4-7: Phenotyping blood monocytes in B16$^{-}$GM treated mice**. Gating strategy and analysis of blood from B16$^{-}$GM$^{-}$ versus B16 – treated mice on d13 after sub$^{-}$cutaneous injection of live melanoma cells. Lin$^{-}$ (CD19$^{-}$CD3e$^{-}$Ter119$^{-}$Ly6G$^{-}$CD45RA$^{-}$ckit$^{-}$NK1.1$^{-}$) cells were gated for CD115/ M$^{-}$CSF$^{-}$R expression and further divided into Ly6C$^{hi}$MHCII$^{-}$ (blue), Ly6C$^{+}$MHCII$^{+}$ (red) and Ly6C$^{lo}$MHCII$^{+}$ (green) cells (a.). These are quantified in b. in absolute number of each cell population /mouse.

#### 4.2.2.2 *B16$^{-}$GM treated mice show an increase in MHCII$^{+}$Ly6C$^{-}$ splenocytes*

In a similar way to the blood, an increase in MHCII$^{+}$ myeloid population was observed in the spleen (**Figure 4-8**). In the gating strategy for splenocytes, cells negative for all other lineage markers (Ter119: RBCs, CD3ε : T cells, CD19: B cells, NK1.1: NK cells, ckit: progenitor cells, CD45RA: pDCs) were gated for CD11b, Ly6C and MHCII to gate

on myeloid cells. Although it could be assumed that these CD11b$^{+}$Ly6C$^{int\text{-}lo}$MHCII$^{+}$ cells are the same as those in the blood, the surface markers used to characterize these cells in the spleen could foreseeably be confused with that of CD11c$^{+}$CD11b$^{+}$ cDCs. In fact, an overlay of the CD11b$^{+}$Ly6C$^{int\text{-}lo}$ MHCII$^{+}$ cells on conventional gating of splenic cDCs shows this gate includes the CD11b$^{+}$ DCs (Lin$^{-}$CD11c$^{+}$MHCII$^{+}$) (**Figure 4-8**)

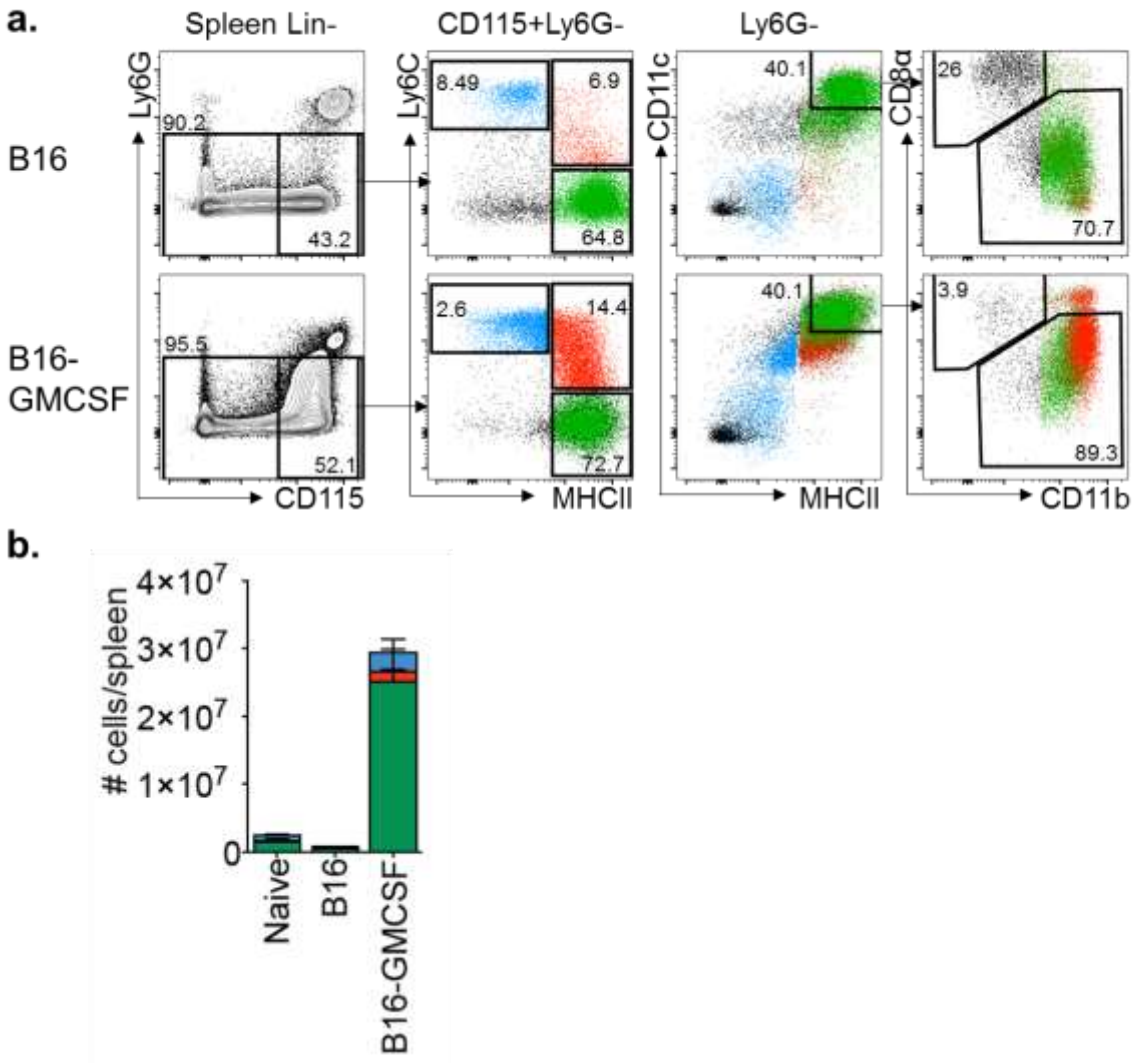


**Figure 4-8: Phenotyping spleen cells in B16-GM treated mice.** Gating strategy and analysis of lineage$^{-}$ (CD19$^{-}$CD3e$^{-}$Ter119$^{-}$ CD45RA$^{-}$ckit$^{-}$NK1.1$^{-}$) cells in the spleens of B16 and B16-GM-CSF treated mice by FACS (a). Ly6C$^{hi}$MHCII$^{-}$(blue), Ly6C$^{+}$MHCII$^{+}$ (red) and Ly6C$^{lo}$MHCII$^{+}$ (green) cells are gated on Lin$^{-}$CD11b$^{+}$ cells quantified in absolute number per treated spleen (b). An overlay of the Ly6C$^{hi}$MHCII$^{-}$(blue), Ly6C$^{+}$MHCII$^{+}$ (red) and Ly6C$^{lo}$MHCII$^{+}$ (green) cells is shown on Lin$^{-}$Ly6G$^{-}$ conventional cDC gating (a).

Although there was a pronounced increase in the number of MHCII$^+$ cells in the spleen, I wanted to confirm that this was not due to increase of the CD4$^+$ (CD11c$^+$MHCII$^+$CD11b$^+$) cDCs. In fact, previous reports showed that they reduced (Naik et al., 2006). An initial conventional gating of the cells showed there was an increase in what could be thought to be CD11b$^+$ cDCs in response to B16-GM injection **(Figure 4-9).**

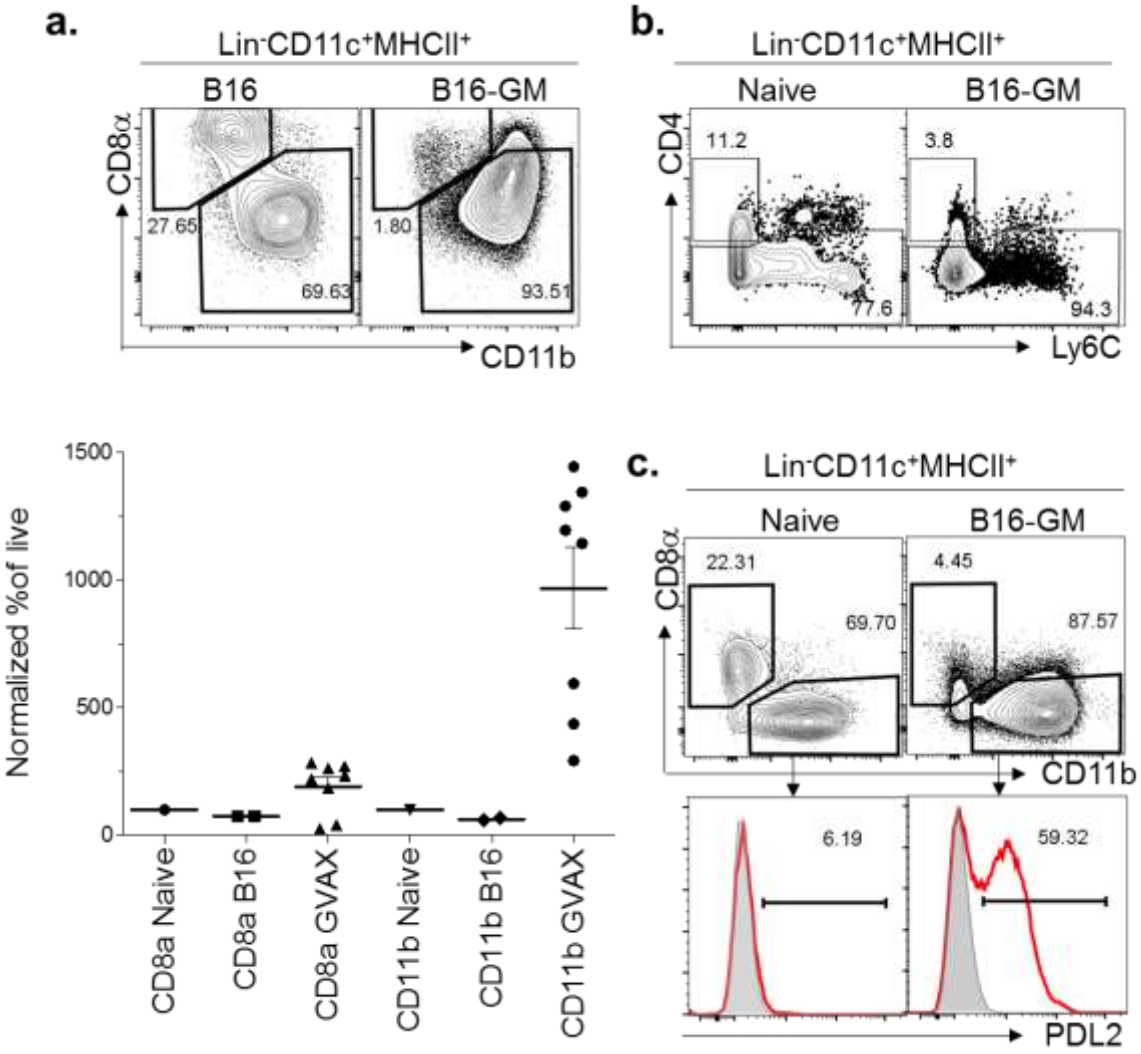


**Figure 4-9: cDCs decrease in response to elevated *in vivo* levels of GM-CSF**. a) Representative FACS analysis of CD8a$^+$ (cDC1) and CD11b$^+$(cDC2) cDCs in the spleens of naïve versus B16-GM-CSF treated mice. Graph shows the cumulative data of 3 experiments normalized to the naïve for the respective population. n=3 b) Analysis of CD4$^+$ cells in Lin$^-$CD11b$^+$MHCII$^+$ cells in B16 versus B16-GM-CSF treated mice. c) Analysis of PDL2$^+$ population (Red line) within the Lin$^-$CD11c$^+$MHCII$^+$CD11b$^+$ cells versus isotype control (grey shaded).

However, upon a more careful examination of the GM-CSF induced $CD11b^+$ myeloid cells, I noted that the $Lin^-MHCII^+CD11c^+CD11b^+CD4^+$ cells did in fact decrease (**Figure 4-9a,b**). Additionally, I also tested these GM-induced $CD11b^+$ cells for a GM-DC marker-PDL2 (Gao et al., 2013), that had previously only been discussed in the context GM-CSF cultures. I found that 60% of GM-CSF-induced $CD11b^+$ cells were $PDL2^+$ (**Figure 4-9**c). This provided evidence of the similarity between the GM-CSF induced cells derived *in vitro* and *in vivo*.

#### 4.2.2.3 *Phenotypic description of $MHCII^+$ cells*

The increase in $MHCII^+$ cells in response to GM-CSF *in vivo*, has been reported in previous studies using models of recall antigen with adjuvant (Naik et al., 2006) and with tumours expressing GM-CSF (Lesokhin et al., 2012). In order to test if these cells were an expansion of the reported monocyte populations documented in Chapter 1, a phenotypic analysis of these $MHCII^+$ cells as compared to $Ly6C^{hi}MHCII^-$ cells was performed. It was noted that these cells were heterogeneous for their expression of macrophage markers CD115 and CD206 (Sallusto and Lanzavecchia, 1994a) as well as for GM-DC-specific markers like CD209a (Geijtenbeek et al., 2000) and activation markers like PDL2 (Gao et al., 2013) (**Figure 4-10**).

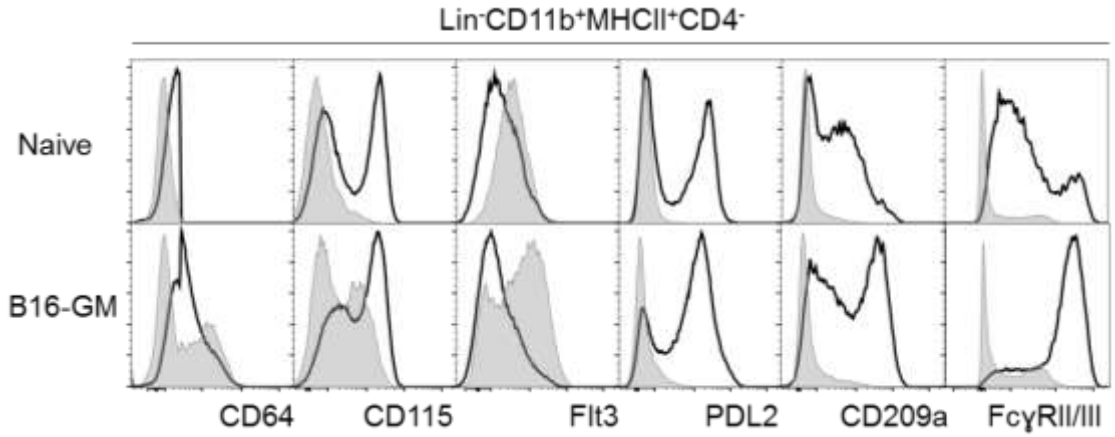


**Figure 4-10:Characterization of MHCII$^+$CD11b$^+$ cells**. FACS analysis of Lin$^-$ CD11b$^+$MHCII$^+$CD4$^-$ splenocytes for CD64, CD115, Flt3, PDL2, CD209 and *FcγRII/III* (black lines) against isotype controls (grey shaded) in naïve and B16-GM treated mice.

### *4.2.3 Phenotypic characterization of GM-induced MHCII$^+$ cells*

The phenotype of the MHCII$^+$ cells made it evident that this GM-induced expanding population was heterogeneous. I sought to segregate mo-DCs and inflammatory macrophage subsets within it, using markers that have been described on monocytes and cDCs but that were also found among genes that were highly expressed on the monocyte subsets described in this report at steady state.

Firstly, in order to ensure that the MHCII$^+$CD11b$^+$ cells did not include cDCs, I excluded the CD4$^+$ population. Of the markers tried so far I found that FcγRII/III and CD209a formed distinct subsets of cells within the MHCII$^+$CD11b$^+$CD4$^-$ population. B16-GM-CSF, and not B16, generated 2 distinct populations that were FcγRII/III$^+$ and either CD209$^+$ or CD209$^-$ (**Figure 4-11**).

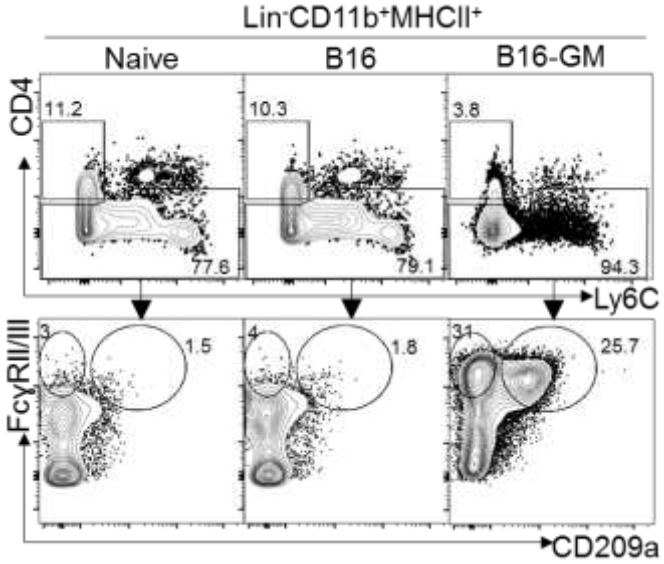


**Figure 4-11: GM-CSF induces MHCII$^+$ *FcγRII/III*$^+$CD209$^{+/-}$ cells *in vivo*.**

Spleens from mice injected with B16, B16$^-$GM or PBS, were analysed 13 days after injection. Lin$^-$CD11b$^+$MHCII$^+$CD4$^-$ cells were phenotyped for *FcγRII/III* and CD209. Quantification of *FcγRII/III*$^+$CD209$^{+/-}$ cells in B16-GM-CSF treated versus naïve control mice. n=5.

The spleens of B16- treated mice phenotypically resembled that of the naïve mice. B16 tumours did not elicit the generation of FcγRII/III$^+$CD209$^{+-}$ and FcγRII/III$^+$CD209$^-$ cells (**Figure 4-11**). Therefore, I used naïve mice as controls for the B16-GM tumour recipients.

#### 4.2.3.1 *FcγRII/III$^+$CD209$^+$ and FcγRII/III$^+$CD209$^-$ cells are CCR2-dependent.*

A salient feature of any cell type originating from Ly6C$^{hi}$ monocytes is their reliance on CCR2 for their egress from the bone marrow (Geissmann et al., 2003; Kurihara et al., 1997). In order to test the reliance of the CD4$^-$CD11b$^+$MHCII$^+$FcγRII/III$^+$CD209$^{+/-}$ cells on CCR2, I treated *Ccr2*$^{-/-}$ and control mice with B16$^-$GM-CSF tumours to study the recruitment of the FcγRII/III$^+$CD209$^{+/-}$ cells to the spleen. The spleens from B16$^-$GM-CSF-treated *Ccr2*$^{-/-}$ mice showed a dramatic reduction in both the FcγRII/III$^+$CD209$^+$ and FcγRII/III$^+$CD209$^-$ cells (**Figure 4-12**).

Although, the FcγRII/III$^{-}$ cells were present in the naïve and B16-treated mice, there was a possibility that they could be replenished by recruited monocytes that did not then express FcγRII/III. Analysis of the FcγRII/III$^{-}$CD209$^{+/-}$ cells showed that they were unaffected, indicating an independence from Ly6C$^{hi}$ monocytes.

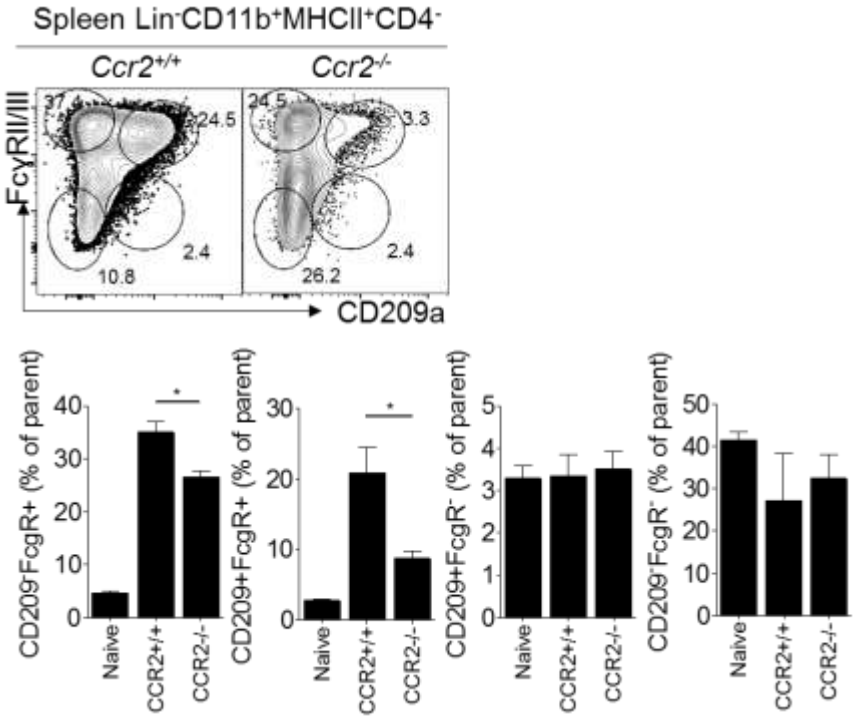


**Figure 4-12: FcγRII/III$^{+}$CD209$^{+/-}$ cells rely on CCR2.** Representative flow cytometry analysis of Lin$^{-}$CD11b$^{+}$MHCII$^{+}$CD4$^{-}$ B16-GM treated spleens of *Ccr2*$^{-/-}$ and WT mice. Graphs depict mean±SEM of percentage of each population within the Lin$^{-}$ MHCII$^{+}$CD11b$^{+}$ cells of n=5; *p<0.05, Student's t-test.

#### 4.2.3.2 *B16-GM induced FcγRII/III$^{+}$CD209$^{+/-}$ cells have a monocytic phenotype.*

I next wondered if each FcγRII/III$^{+}$ population could represent distinct macrophages or dendritic cell populations. To comprehensively analyse the Lin$^{-}$CD11b$^{+}$MHCII$^{+}$ cells, I tested the FcγRII/III$^{+}$CD209$^{+}$ and FcγRII/III$^{+}$CD209$^{-}$ cells for the expression of previously described macrophage and DC markers. Using CD4$^{+}$ cDCs as a control, FcγRII/III$^{+}$CD209$^{+}$ and FcγRII/III$^{+}$CD209$^{-}$ were found to be CD115$^{+}$ and Flt3$^{-}$ against appropriate isotype controls. This corroborated previous data on Mo-DCs from Cheong et al (**Figure 4-13**) (Cheong et al., 2010).

An interesting aspect with regards to the MHCII expression was that the FcγRII/III$^{+}$CD209$^{+}$ cells had the highest expression of MHCII indicating that these cells could be the most capable or most primed for MHCII-restricted T cell activation (**Figure 4-13**).

Another aspect of differentiation between the cells was PDL2 and PDL1. It has been previously noted that PDL1 is expressed highly on cDCs at steady state while PDL2 is expressed on macrophages during inflammation in a murine model of allergic asthma (Singh et al., 2011). The FcγRII/III$^{+}$CD209$^{+/-}$ cells were PDL2$^{+}$ while the CD4$^{+}$cDCs were PDL1$^{+}$ as compared to isotype controls (**Figure 4-13**). Given the distinct role of PD-1 ligands- PDL1 and PDL2, in polarizing T cell responses toward Th1 or Th2, respectively (Akbari et al., 2010), it might be important to note the differential expression of these ligands on GM-CSF induced myeloid cells and CD4$^{+}$ cDCs.

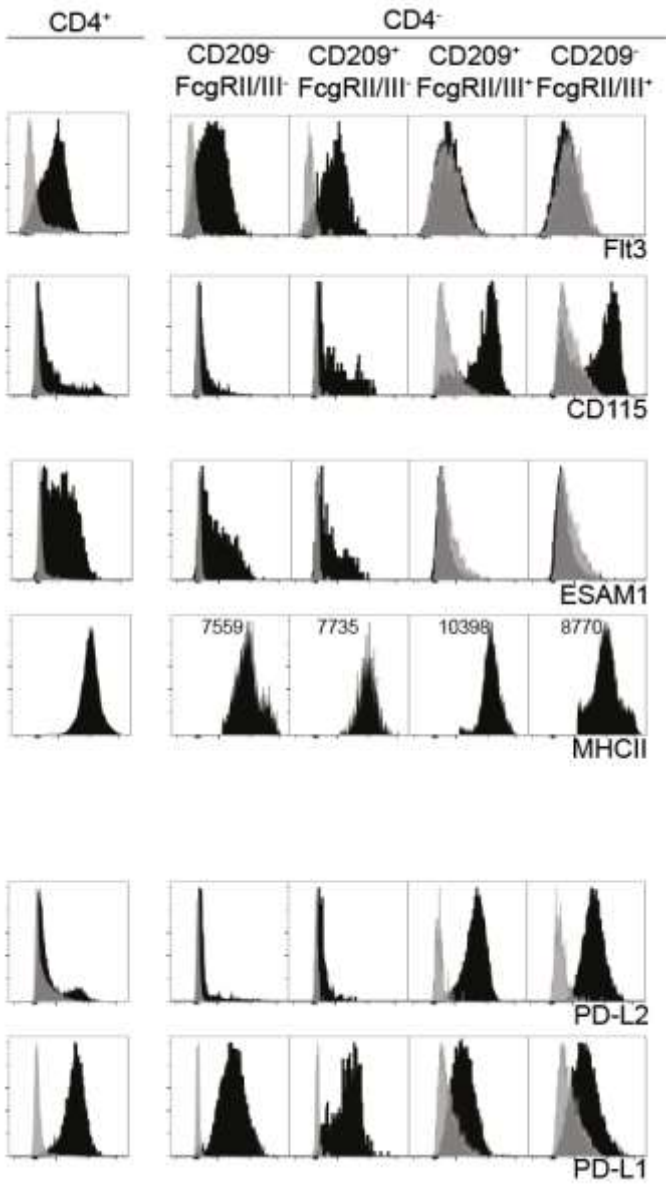


**Figure 4-13: Phenotype of *FcγRII/III*$^{+/-}$ and CD209$^{+/-}$ MHCII$^{+}$ cells** FACS analysis for Flt3,CD115, ESAM1, MHCII, PD-L2 and PD-L1 (shaded black) against isotype controls (shaded grey) on *FcγRII/III*$^{+}$CD209$^{-}$, FcγRII/III$^{+}$CD209$^{+}$, FcγRII/III$^{-}$CD209$^{+}$ and FcγRII/III$^{-}$CD209$^{-}$ and CD4$^{+}$ cells from Lin$^{-}$CD11b$^{+}$MHCII$^{+}$ splenocytes from mice treated with B16-GM for 13 days. Numbers adjacent to *his*tograms indicate the mean fluorescent intensity (MFI) of the indicated marker on each population.

The FcγRII/III$^{+}$CD209$^{+/-}$ cells expressed a number of macrophage markers such as FcγRI (CD64) and Mertk as well as markers that have been previously attributed to mo-DCs-FcεR1 (Plantinga et al., 2013) and CD206 (Cheong et al., 2010) (**Figure 4-14**). There was not much difference in the levels of expression of these markers between the

FcγRII/III$^{+}$CD209$^{+}$ and FcγRII/III$^{+}$CD209$^{-}$ cells (**Figure 4-14**). Additionally, they expressed similar levels of CCR2 (**Figure 4-14**)

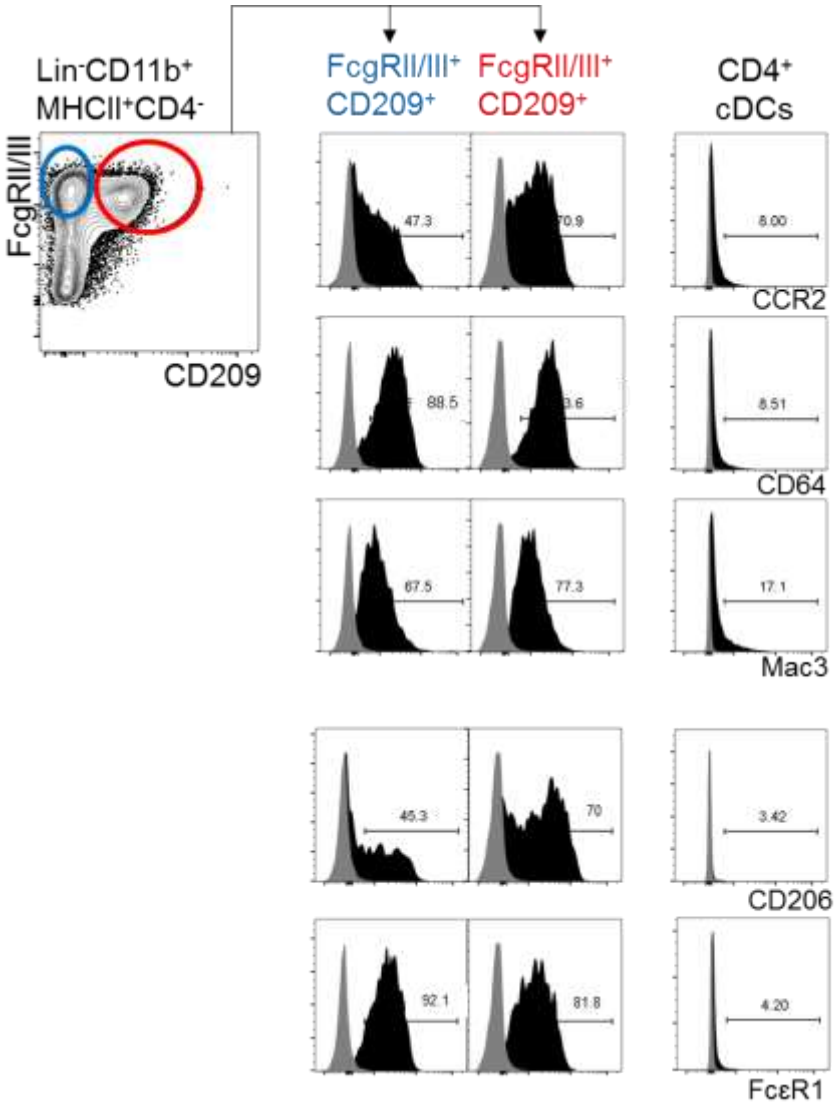


**Figure 4-14: Monocyte and 'Mo$^{-}$DC' markers on *FcγRII/III*$^{+/-}$CD209$^{+/-}$ cells** Lin$^{-}$ CD11b$^{+}$MHCII$^{+}$ cells were gated into *FcγRII/III*$^{+/-}$and CD209$^{+/-}$ cell populations. Monocyte and Mo$^{-}$DC markers were assayed on each of the populations in comparison with CD4$^{+}$ cDCs (Lin$^{-}$CD11b$^{+}$MHCII$^{+}$).

Thus, B16-GM induced FcγRII/III$^{+}$CD209a$^{+}$ and FcγRII/III$^{+}$CD209a$^{-}$ cells exhibited a monocyte/macrophage phenotype and also resembled previous reports of 'Mo-DCs'. The one distinction that stood between them was the expression of CD209a.

#### 4.2.3.3 *DC lineage and FcγRII/III$^{+}$CD209a$^{+/-}$ cells.*

Although the FcγRII/III$^{+}$CD209$^{+/-}$ cells express a number of monocyte markers and displayed a reliance on CCR2, it could not be excluded that these cells belonged to the DC lineage. To investigate this using the best lineage tracing method currently available for cDCs, I analysed the expression of YFP in the these GM-induced populations in *Zbtb46$^{CRE}$ x ROSA$^{loxSTOPloxYFP}$* mice (*Zbtb46$^{CRE}$xROSA$^{lslYFP}$)* (Loschko et al., 2016a). YFP expression was close to background levels in the FcγRII/III$^{+}$ cells as compared to the 54% positive expression levels seen in CD4$^{+}$cDCs (**Figure 4-15**).

The *Zbtb46$^{CRE}$xROSA$^{lslYFP}$* mice had a very stringent YFP expression pattern and this turned out to be similar to that described by the Nussenzweig and colleagues (Loschko et al., 2016a). I wondered if with a reporter mouse, I might obtain a representation of the levels of expression of the transcription factor expressed by the FcγRII/III$^{+}$ cells I thus used the *Zbtb46$^{gfp/+}$* mice.

GFP was strongly expressed in the cDCs as had been previously reported (Satpathy et al., 2012a). However, the FcγRII/III$^{+}$CD209$^{+/-}$ cells had much lower levels of GFP expression. Although the percentage of GFP$^{+}$ cells within the FcγRII/III$^{+}$CD209$^{+}$ cells was slightly higher than in the FcγRII/III$^{+}$CD209$^{-}$ cells, this difference was not significant (**Figure 4-15**). This showed that the FcγRII/III$^{+}$CD209$^{+/-}$ cells were not part of the DC lineage as they did not express the transcription factor ZBTB46.

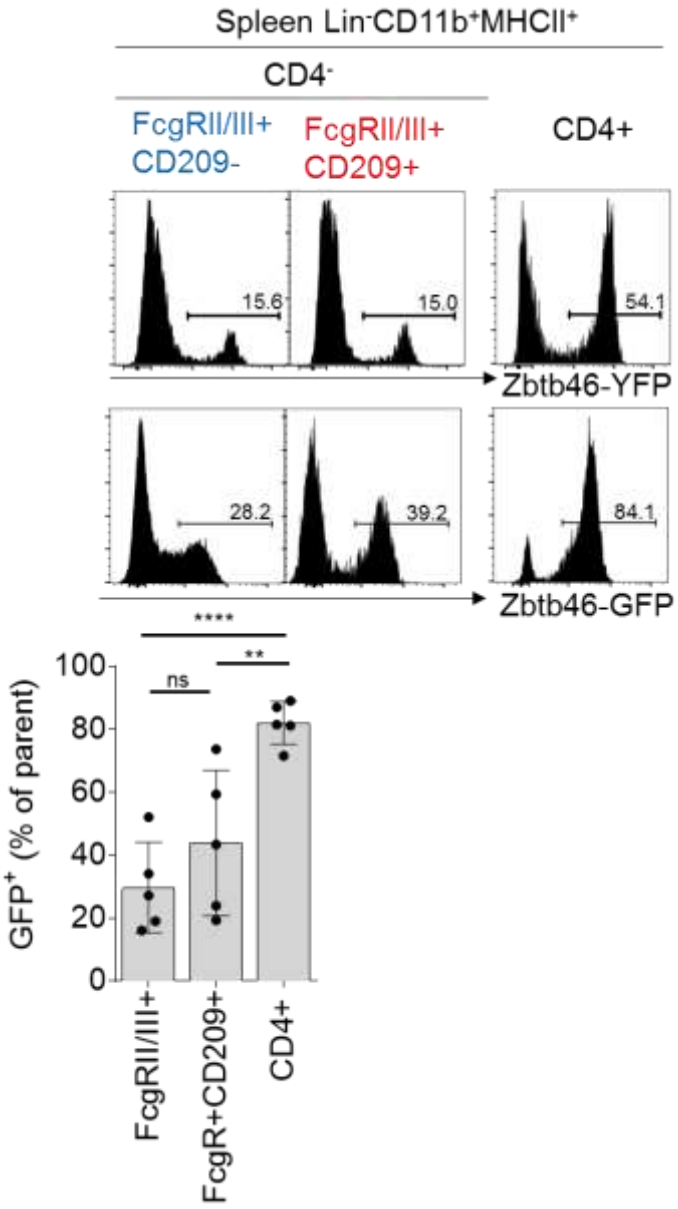


**Figure 4-15: FcγRII/III$^{+}$CD209$^{+/-}$ cells do not express Zbtb46**. FACS analysis of the FcγRII/III$^{+}$CD209$^{+/-}$ cells and CD4$^{+}$ cDCs of the Lin$^{-}$CD11b$^{+}$MHCII$^{+}$ splenocytes for YFP expression in *Zbtb46$^{Cre\ x}$ ROSA$^{lslYFP}$* and GFP expression in *Zbtb46$^{gfp/+}$* mice. Mice were injected with B16$^{-}$GM 14 days prior to analysis. Graph shows data from 5 *Zbtb46$^{gfp/+}$* mice. n=5

### *4.2.4 Reliance of FcγRII/III$^{+}$CD209a$^{+/-}$ cells on the transcription factor PU.1*

#### **4.2.4.1** *Sfpi1$^{+/-}$ mice display a reduction in FcγRII/III$^{+}$CD209$^{+}$ cells.*

FcγRII/III$^{+}$CD209$^{+}$ and FcγRII/III$^{+}$CD209$^{-}$ cells had thus far proven to be of similar origin and phenotype. I next wondered if they had any difference in their reliance on PU.1- the transcription factor found to play a role in the development of CD209a$^{+}$ cells

*in vitro* (Fig.1-7). The spleens of B16-GM-CSF treated *Sfpi1*$^{+/-}$ and *Sfpi1*$^{+/+}$ mice showed that PU.1 hemizygocity dramatically reduced the FcγRII/III$^{+}$CD209$^{+}$ cells. The FcγRII/III$^{+}$CD209$^{-}$ cells, on the other hand, remained equivalent to controls (**Figure 4-16**a). FcγRII/III$^{+}$CD209$^{+}$ cells thus relied on PU.1 for their development.

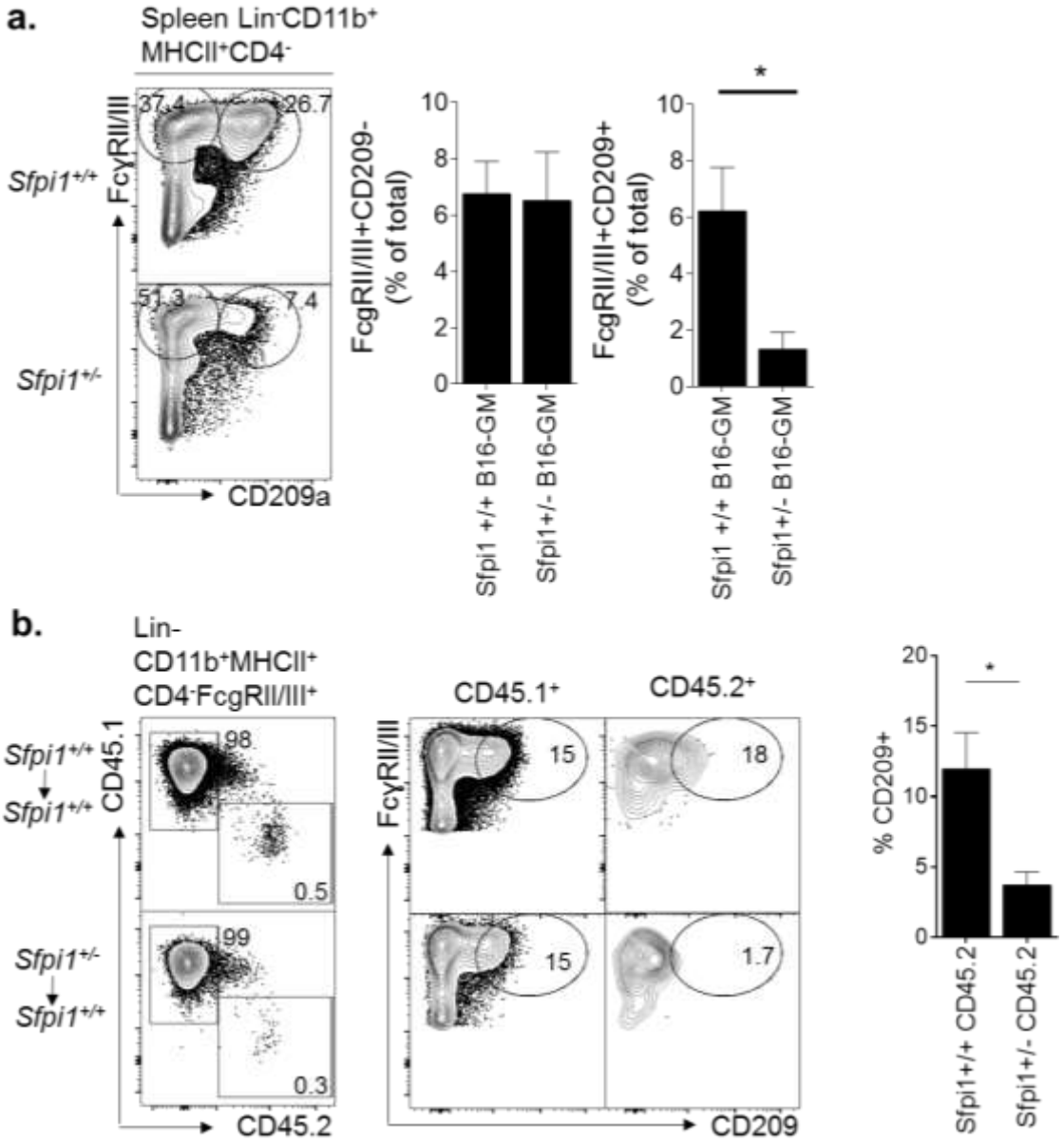


**Figure 4-16: PU.1 positively regulates GM-induced FcγRII/III$^{+}$CD209$^{+}$ cells.** a) Lin$^{-}$ CD11b$^{+}$CD4$^{-}$ splenocytes in *Sfpi1*$^{+/+}$ and *Sfpi1*$^{+/-}$ cells were analysed for the presence of FcγRII/III$^{+}$CD209$^{-}$ and FcγRII/III$^{+}$CD209$^{+}$ cells. b) Representative FACS analysis of spleens from congenic recipient B16-GM treated *Sfpi1*$^{+/+}$ mice adoptively transferred with either *Sfpi1*$^{+/+}$ *or Sfpi1*$^{+/-}$ (CD45.2$^{+}$) bone marrow. Graph shows mean ± SEM of n=6; *p<0.05; Student's t-test.

To test for the cell-intrinsic requirement of PU.1 on FcγRII/III$^{+}$CD209$^{+}$ cells, I performed an adoptive transfer experiment of *Sfpi1*$^{+/-}$ or *Sfpi1*$^{+/+}$ whole bone marrow into congenically marked B16-GM-CSF-treated recipients. FcγRII/III$^{+}$CD209$^{+}$ cells were absent from donor *Sfpi1*$^{+/-}$ cells **above (Figure 4-16b).** The FcγRII/III$^{+}$CD209$^{-}$ cells, on the other hand, were not influenced by the lack of PU.1. This showed a cell intrinsic requirement for PU.1 in the FcγRII/III$^{+}$CD209$^{+}$ cells- a feature that distinguished it from FcγRII/III$^{+}$CD209$^{-}$ cells.

#### 4.2.4.2 *Origin of FcγRII/III$^{+}$CD209$^{+/-}$ cells.*

Having noted the strong expression of monocyte/macrophage markers, the reliance on CCR2, and the difference in reliance on PU.1, the FcγRII/III$^{+}$CD209$^{+/-}$ cells were tested for their distinct origin from the 2 Ly6C$^{hi}$monocyte populations described in Chapter 3. I performed an adoptive transfer experiment of Ly6C$^{hi}$Flt3$^{-}$CD11c$^{-}$ R1 cells and Ly6C$^{hi}$Flt3$^{+}$CD11c$^{-}$ R2 cells into B16-GM-treated mice. An analysis of the spleens of the recipients showed that R1 was capable of generating FcγRII/III$^{+}$CD209$^{-}$ cells alone. R2, on the other hand, was capable of generating FcγRII/III$^{+}$CD209$^{+}$ cells in addition to CD209a$^{-}$ cells (**Figure 4-17**).

In addition to firmly establishing that R2 acts as the precursor Ly6C$^{hi}$ monocyte population to FcγRII/III$^{+}$CD209a$^{+}$ cells, this experiment also emphasized the heterogeneity of R2 (ref. Chapter 3).

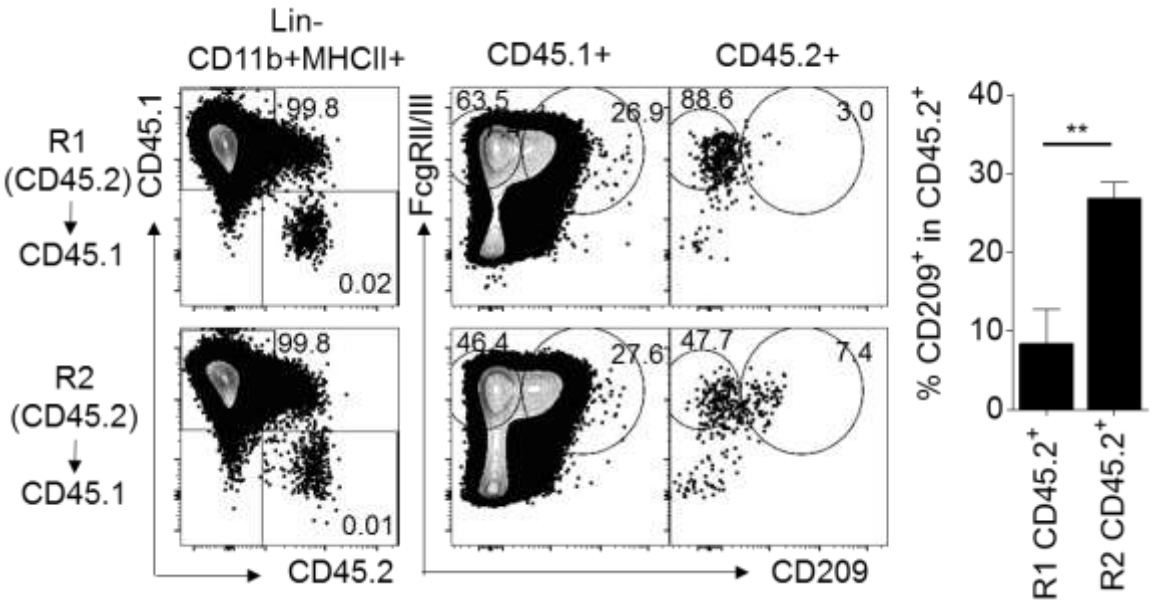


**Figure 4-17: *FcγRII/III*$^{+}$ CD209a$^{+}$ cells derive from PU1$^{hi}$Flt3$^{+}$CD115$^{+}$CD11c$^{-}$ (R2) cells**Representative FACS analysis of spleens from recipient B16$^{-}$GM- treated CD45.1$^{+}$ mice adoptively transferred with 3.3 x $10^{5}$ cells of R1 or R2 from congenically labelled wild-type mice. Graph shows the percentage of CD209a$^{+}$ cells within the CD45.2$^{+}$ donor population. Graph shows mean ± SEM of n=5, **p<0.005; Student's t-test.

## 4.3 Discussion and overview of Chapter 4

The increase in GM-CSF during inflammation has previously been shown to give rise to inflammatory populations of macrophages and DCs. In this chapter, I have characterised these inflammatory populations both *in vitro* and *in vivo*, providing phenotypic descriptions of the same and an ontogenic basis for their differences.

By culturing sorted populations of ($Flt3^{-}CD11c^{-}$) R1 and ($Flt3^{+}CD11c^{-}$) R2 monocytes or *Sfpi1*$^{+/+}$and *Sfpi1*$^{+/-}$ bone marrow with GM-CSF, I determined that *Sfpi1*-dependent R2 cells can generate of $PDL2^{hi}CD86^{+}$ cells. Additionally, the use of FcγRII/III and CD209a to characterize these progenies showed that R2 responded to GM-CSF by upregulation of both receptors. I were thus able to explain the heterogeneity in GM-CSF cultures described previously (Gao et al., 2013; Helft et al., 2015; Inaba et al., 1992)and in the context of their origin. The $PDL2^{lo}CD86^{lo}$ population found in these cultures were produced by R1 cells. I further characterised them as being $FcγRII/III^{+}CD209a^{-}MHCII^{lo}$ and independent of PU.1 for their development. I would therefore describe these cells as 'inflammatory macrophages' (Inf-Macs).

In addition to studying the response of these cells *in vitro* to GM-CSF, I studied their phenotypic characterisation *in vivo* in response to systemically elevated levels of GM-CSF. B16 cells are a C57BL/6 melanoma cell line that eventually metastasizes to the lung. By sacrificing the mice at a relatively early time point of 12-14 days, I could analyse the spleens of mice that showed localized expansion of the melanoma and no other obvious pathology. B16-GM melanomas induced splenomegaly accompanied by an influx of myeloid cells.

Phenotypically, the expanded myeloid population expressed high levels of MHCII and could be divided based on their expression of FcγRII/III and CD209a. Extensive phenotyping of these cells showed that $FcγRII/III^{+}CD209a^{-}$ and $FcγRII/III^{+}CD209a^{+}$

cells were equally PDL2$^{+}$CCR2$^{+}$Flt3$^{-}$ESAM1$^{-}$PDL1$^{-}$CD115$^{+}$ with similar levels of previously described mo-DC attributed markers like CD206 and Fcεr1. Fate-mapping and genetic reporting of Zbtb46 expression also showed that these cells did not originate from the cDC lineage nor did they acquire a cDC transcriptional programme. They proved to be CCR2-dependent indicating that they derived from Ly6C$^{hi}$ monocytes.

A critical point of difference between the FcγRII/III$^{+}$CD209a$^{-}$ and FcγRII/III$^{+}$CD209a$^{+}$ cells was that the FcγRII/III$^{+}$CD209a$^{+}$ cells were PU.1-dependent being reduced dramatically in B16-GM treated *Sfpi1*$^{+/-}$ mice. This became apparent when adoptive transfer experiments of *Sfpi1*$^{+/+}$ or *Sfpi1*$^{+/-}$ BM into B16-GM treated recipients showed that PU.1 was required for the generation of FcγRII/III$^{+}$CD209a$^{+}$ mo-DCs but not FcγRII/III$^{+}$CD209a$^{-}$ Inf-macs.

The response to GM-CSF both *in vitro* and *in vivo* of the Ly6C$^{hi}$ monocyte populations showed that while R1 and R3 produced homogenous progeny, R2 consistently generated a mixed population of cells, *i.e.,* FcγRII/III$^{+}$CD209a$^{-}$ and FcγRII/III$^{+}$CD209a$^{+}$ cells. Adoptively transferring R2 into B16-GM-treated recipients caused the differentiation of R2 cells into FcγRII/III$^{+}$CD209a$^{-}$, FcγRII/III$^{+}$CD209a$^{+}$ and FcγRII/III$^{-}$CD209a$^{-}$ cells. The FcγRII/III$^{+}$CD209a$^{+}$ cells generated by R2 were approx. 10% of the progeny of the total transferred cells. This frequency was similar to the frequency within R2 that displayed dual mRNA expression of FcγRII/III and CD209a by single-cell analysis (refer Chapter 3, **Figure 3-24**). Thus I can conclude that by the use of Flt3 and CD11c to denote R2 at steady state, I can isolate the fraction of Ly6C$^{hi}$ monocytes that contain the precursors to mo-DCs.

Thus, the findings in this chapter allow a clearer phenotypic description of the GM-CSF-induced mo-DCs and inf-macs and an ontogenic perspective for their development.

# Chapter 5:

# The development of iNOS-producing inflammatory macrophages

# 5 The development of iNOS-producing inflammatory macrophages

## 5.1 Introduction and objectives

An effective defence against pathogens like viruses, bacteria and parasites requires the efficient activation of innate cells. Monocytes mount prompt responses to pathogenic invasion. Amongst their many defence mechanisms, production of inflammatory factors such as tumour necrosis factor a (TNF-α), nitric oxide (NO) and hydrogen peroxide ($H_2O_2$) and are essential for the clearance of pathogens (Sprangers et al., 2016).

### *5.1.1 iNOS-producing cells are important for pathogen control*

Nitrate biosynthesis was originally studied in the context of stomach cancer and the role of nitrosamines in causing it (Cuello et al., 1976). The carcinogenicity of N-nitroso compounds had been found to occur across 39 species and was being investigated in man (Bogovski and Bogovski, 1981). Nitrates and nitrites, thought to be synthesized through metabolic breakdown by gut microbes, were thought to bind with exogenously acquired amines forming the carcinogenic nitrosamines. However, further investigation with germ-free mice, showed that nitrate biosynthesis was initiated through a mammalian mechanism (Green et al., 1981). Peritoneal macrophages were found to carry out nitrate metabolism of L-arginine when stimulated with LPS *in vitro* and *in vivo,* inhibiting the proliferation of fungi (Granger et al., 1990). *Nos2*$^{-/-}$ (iNOS$^{-/-}$) mice are more susceptible to infections like that of *Trypanosoma cruzi* infections and sepsis (Cobb et al., 1999; Huang et al., 1999) as well as autoimmune conditions like EAE (Fenyk-Melody et al.,

1998). NO thus plays a crucial role in clearance of bacterial pathogens and a pathogenic role in autoimmunity.

The production of NO is crucial to the clearance of several pathogens such as *Listeria* (Serbina et al., 2003) and *Leishmania* (Liew et al., 1990; De Trez et al., 2009; Xie et al., 1993). As NO diffuses through the cell membrane of iNOS-producing cells, it acts in a tissue-wide manner (Olekhnovitch et al., 2014) playing a critical bactericidal role against intracellular bacteria (*e.g. Listeria monocytogenes*, *Mycobacterium tuberculosis* and *Salmonella*) and defence against parasites (e.g. *Leishmania, Trypanosoma brucei*). Other than the production of NO during infection, $iNOS^+$ cells also carry out antigen transfer, harbouring of pathogens and priming of T cells to initiate an immune response depending on the infectious agent (Jiao et al., 2002). These functions are however, redundant with that of cDCs and macrophages in the inflamed tissue (Serbina et al., 2003) and occur in response to some infections and not others (De Trez et al., 2009) . Mice depleted of DCs, have a higher resistance to infections like *Yersinia enterocolitica* (Autenrieth et al., 2012) and others like *Listeria* due to increased infiltration of phagocytes that perform enhanced levels of phagocytosis and bactericidal activity mainly through the increased production of ROS and TNF-a (Kang et al., 2008).

The generation of TNF-α and reactive oxygen species by $Ly6C^{hi}$ cells in response to infection with *Listeria* is not only crucial in a primary immune defense against the pathogen, but is also required in secondary response for bactericidal activity. During a secondary infection, these cells are activated in an antigen-independent manner by CCL3, which is secreted by memory $CD8^+$ T cells (Narni-Mancinelli et al., 2007). Thus, understanding the exact precursors, the transcriptional regulation and a phenotypic description that distinguishes $iNOS^+$ cells from other inflammatory and steady state myeloid populations is crucial to further studies. This thesis addresses these critical aspects.

### *5.1.2 The induction of iNOS$^+$ cells is dependent on its microenvironment*

The production of iNOS has been attributed largely to macrophages in response to pathogens. Macrophages are generated *in vitro* from bone marrow progenitors in the presence of growth factors like M-CSF or GM-CSF. Each of these cultures generate macrophages with slightly different characteristics. As alluded to in previous chapters, GM-CSF cultures of BM progenitors results in a mixture of macrophage and DC-like cells (Inaba et al., 1992)- of which the macrophages upon exposure to LPS are able to produce NO resulting in the elimination of the pathogen (Xu et al., 2007). Flt3L supplemented BM cultures do not generate cells capable of NO production indicating that cDCs are not capable of producing the inflammatory mediator (Xu et al., 2007). It could be inferred, therefore, that GM-CSF induces the generation of macrophages that are required for the clearance of pathogens via the production of NO. However, *Csf2rb*$^{-/-}$ *Csf2rb2*$^{-/-}$ (GM-CSF-R$^{-/-}$) mice efficiently control infection with *Listeria monocytogenes* (*L.m.*) as there are no differences in the numbers of TNF-α and iNOS-producing macrophages generated (Greter et al., 2012). Thus, the role of GM-CSF in the development of iNOS-producing cells may be redundant acting more to promote the expansion of these cells. In fact, Greter et al noted that *Csf1r* (M-CSF-R) was indispensable for the generation of iNOS$^+$ cells instead.

The functional and phenotypic characteristics of these cells is determined by the presence of a number of other inflammatory factors at the site of inflammation. For instance, regulatory factors such as IL-10 controls the production of iNOS and TNF-α from CD11c$^+$CD11b$^+$Ly6G$^-$ splenocytes in a *Trypanosoma brucei* infection (Guilliams et al., 2009). The reduction in iNOS$^+$ cells reduces the levels of inflammatory chemokines and cytokines like CXCL9, CXCL10 and CXCL11 released, thus reducing the numbers of other recruited inflammatory cells (Guilliams et al., 2009). TGF$^-$β is also a potent inhibitor

of iNOS and its presence was found to be the reason for increased susceptibility to *Leishmania major* infection in Balb/c mice over the resistant C57Bl/6 strain in spite of no differences in inflammatory macrophage-inducing-IFN-ɣ at the site of infection (Stenger et al., 1994). $CX_3CR1$-deficient mice have reduced numbers of recruited inflammatory $Ly6C^{hi}$ monocytes due to the reduction in $Ly6C^{lo}$ ($CX_3CR1$) monocytes and thus a lack of iNOS-, TNFα- and ROS- producing inflammatory cells This leads to increased susceptibility to *L.m.* (Auffray et al., 2009).. $iNOS^+$ cells thus form an important part of an inflammatory network of cells.

### *5.1.3 Characterisation of the precursors to iNOS⁺ cells*

Studies addressing the source of key inflammatory mediators such as NO, $H_2O_2$ and TNF-α show an inflammation-induced population of myeloid cells that play a key role in the destruction of pathogens. In particular, these cells have been described to be $CD11c^{int-high}CD11b^+Mac\text{-}3^+$ cells that express high levels of co-stimulatory molecules such as MHC-II, CD80 (B7-H1), CD86 (B7-H2) and are found in a variety of infectious settings (Guilliams et al., 2014; Serbina et al., 2003; De Trez et al., 2009). Unfortunately, this description defines a rather broad population of myeloid cells. Thus, Guilliams et al. set out to determine the population that is responsible for pathogen elimination in a parasitic model of infection. It was found that a sub-set of these $CD11b^+CD11c^+Ly6C^+Ly6G^-$ cells produced TNF-α (Guilliams et al., 2009) of which some also expressed iNOS - a function critical for pathogen control regardless of an effective T cell response to the pathogen (Serbina et al., 2003). Due to the use of these widely expressed markers, $iNOS^+$ cells are called macrophages in some studies while they are called DCs in others (Serbina et al., 2003; De Trez et al., 2009). Thus there is a requirement to clearly define inflammatory cell populations from those resident at steady state.

The expression of iNOS is a useful marker for myeloid cells that are inflammatory. However, using an inflammatory factor such as iNOS does not define all the cells that

are, in fact, capable of producing iNOS. This could be aided by the knowledge of their cellular lineage from progenitor cells. Studies addressing the cell lineage of $iNOS^+$ cells have produced conflicting results. $iNOS^+$ cells are often referred to as DCs since they are cDC-like in their co-stimulatory molecule expression and the ability to prime T cells in an allogeneic reaction *in vitro* (Serbina et al., 2003). However, most myeloid cells will upregulate co-stimulatory molecules and mice lacking $iNOS^+$ cells are fully capable of priming CD4 and CD8 T cells in response to infection. Additionally, it is noted that $iNOS^+$ cells are still present in *Flt3l*$^{-/-}$ mice (Greter et al., 2012),which lack a critical growth factor required for the development of cells in the cDC lineage. In contrast, iNOS-producing cells were reported to be CCR2 dependent and *Csf1r*-dependent (Greter et al., 2012; Serbina et al., 2003) indicating that they belong to the monocyte lineage. Despite their dependence on growth factors associated with monocyte development, these $iNOS^+$ inflammatory cells continue to be called 'dendritic cells'.

I wished to decipher a clear distinction between iNOS producing cells and other populations at the site of inflammation.

### *5.1.4 Objectives and aims*

The overall objectives of this chapter will be the following:

- To characterize $iNOS^+$ cells using distinct phenotypic marker expression to delineate these cells from different subsets of $Ly6C^{hi}$ monocytes.
- To investigate lineage specific transcription factors to distinguish iNOS-producing cells from tissue-resident macrophages and cDCs.
- To determine the dependence of the transcription factor PU.1 on the expression of iNOS in macrophages

## 5.2 Results:

### *5.2.1 iNOS production in vitro*

#### 5.2.1.1 *Titration of Listeria for the generation of iNOS$^+$ cells in vitro*

In order to be able to study the production of iNOS by Ly6C$^{hi}$ monocytes, the precursors of iNOS$^+$ cells and the result of their terminal differentiation, I set up an in vitro model of infection with *Listeria monocytogenes* (*L.m.*) and LPS. This was done by taking total Ly6C$^{hi}$ monocytes enriched by MACS sorting from WT C57BL/6 BM and culturing these cells overnight with varying concentrations of either virulent *L.m.* or LPS. Analysis of the cultures showed an increase in iNOS$^+$ cells when exposed to *L.m.*at an MOI 0.01, 0.1 and LPS in comparison to isotype controls for anti-iNOS staining., At higher MOIs, there was no increase in iNOS producing cells as many of the MACS-sorted cells died of infection (**Figure 5-1**).

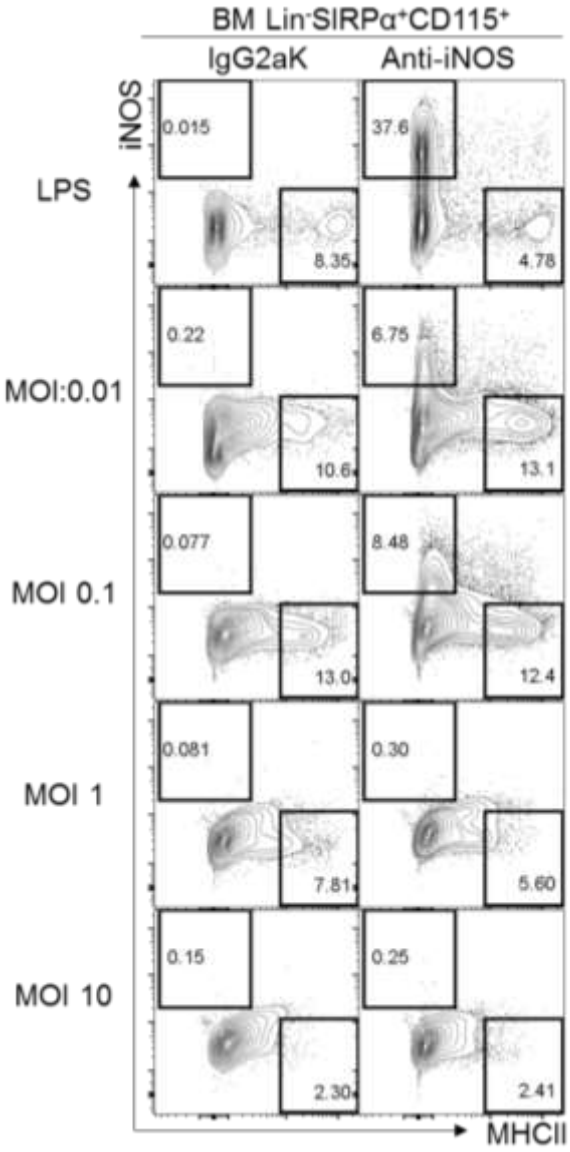


**Figure 5-1: iNOS producing cells differentiate from bone marrow monocytes following microbial stimulation.** 100,000 SIRPa$^{+}$CD115$^{+}$ MACS-enriched bone marrow monocytes were plated in complete medium with 1ug/ml LPS or *Listeria monocytogenes* at a multiplicity of infection (MOI) of 0.01, 0.1, 1 and 10. After an overnight incubation cells were stained with either isotype or anti-iNOS antibody and anti$^{-}$MHCII. This was done with 3 technical replicates.

### 5.2.1.2 *Requirement for IFN-ɣ in the expression of MHC-II on iNOS$^{+}$ cells*

*In vivo* generated iNOS$^{+}$ cells are MHCII$^{+}$ (Kang et al., 2008). In the previous experiment, I showed that iNOS$^{+}$ cells were MHCII$^{-}$. This could be expected as it has been previously reported that the presence of MHCII$^{+}$iNOS$^{+}$ cells among activated macrophages is dependent on IFN-ɣ generated by NK cells (Kang et al., 2008). Since our experimental

protocol was devoid of any IFNɣ, I do not expect to see expression of MHCII in the iNOS producing cells. In order to confirm that the lack of MHCII expression is due to the absence of IFN-ɣ, an *in vitro* culture of MACS-sorted BM monocytes was carried out with *L.m.*, in the presence or absence of IFNɣ. Cultures containing IFN-ɣ showed an increase in the MHCII$^+$ expression on the iNOS$^+$ cells (**Figure 5-2**).

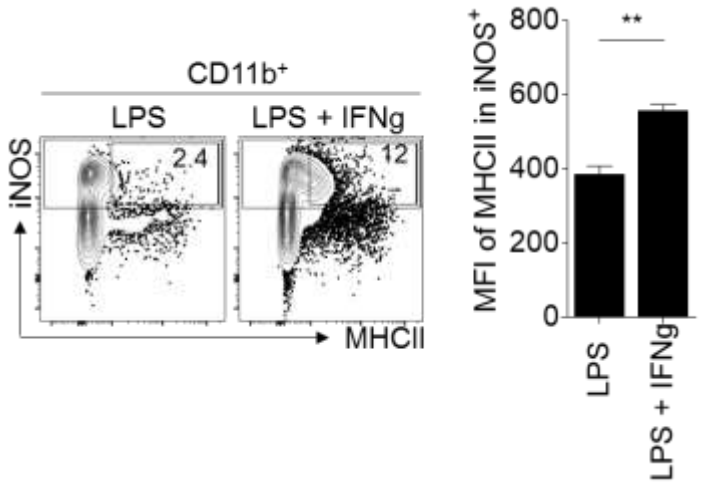


**Figure 5-2: IFN-ɣ is required for the intermediate expression of MHCII on iNOS$^+$ cells.** Enriched BM monocytes cultured overnight in the presence or absence of IFN-ɣ. Cells were then analysed by flow cytometry by gating onto CD11b$^+$ cells and assessing the expression of iNOS. The number within each gate is indicative of the percentage of cells within total iNOS$^+$ cells. Graphs shows the mean ± SEM of n=3; **p<0.005;Student's t-test.

#### 5.2.1.3 *R1 cells are the precursors to iNOS$^+$ cells*

Previous reports have distinctly shown that iNOS$^+$ cells arise from a Lin$^-$ CD11b$^+$MHCII$^+$Ly6C$^{hi}$ population *in vivo*. However, iNOS$^+$ cells whether identified by reporter labelling with $CX_3CR1$ or antibody staining always appears to be only a small sub-population of Ly6C$^{hi}$ monocytes (Serbina et al., 2003; Zigmond et al., 2012). I thus wanted to test the ability of each of the Ly6C$^{hi}$ subsets of monocytes discussed in Chapter 3, to give rise to these iNOS$^+$ cells. This was done in comparison with the pre-cDC population R3.

FACS sorted R1, R2 and R3 cultured with *L.m.* showed that R1 was the most efficient at generating $iNOS^+$ cells. These $iNOS^+$ cells were $MHCII^-$ as was expected given that the culture did not have any IFN-ɣ present. Additionally, R3 generated cells that were $iNOS^-$ and $MHCII^+$. R2 was able to generate $MHCII^+$ progeny to a greater extent than R1 (**Figure 5-2)**.

A similar experiment was performed with LPS overnight at a concentration of 1µg/ml. Here, the FACS sorted R1 were the only cells capable of producing iNOS. R2 and R3 populations generated $MHCII^+$ cells (**Figure 5-3**b). Thus, using 2 different types of microbial stimulation, I could conclude that R1 $Ly6C^{hi}$ monocytes have the strongest predilection for iNOS production.

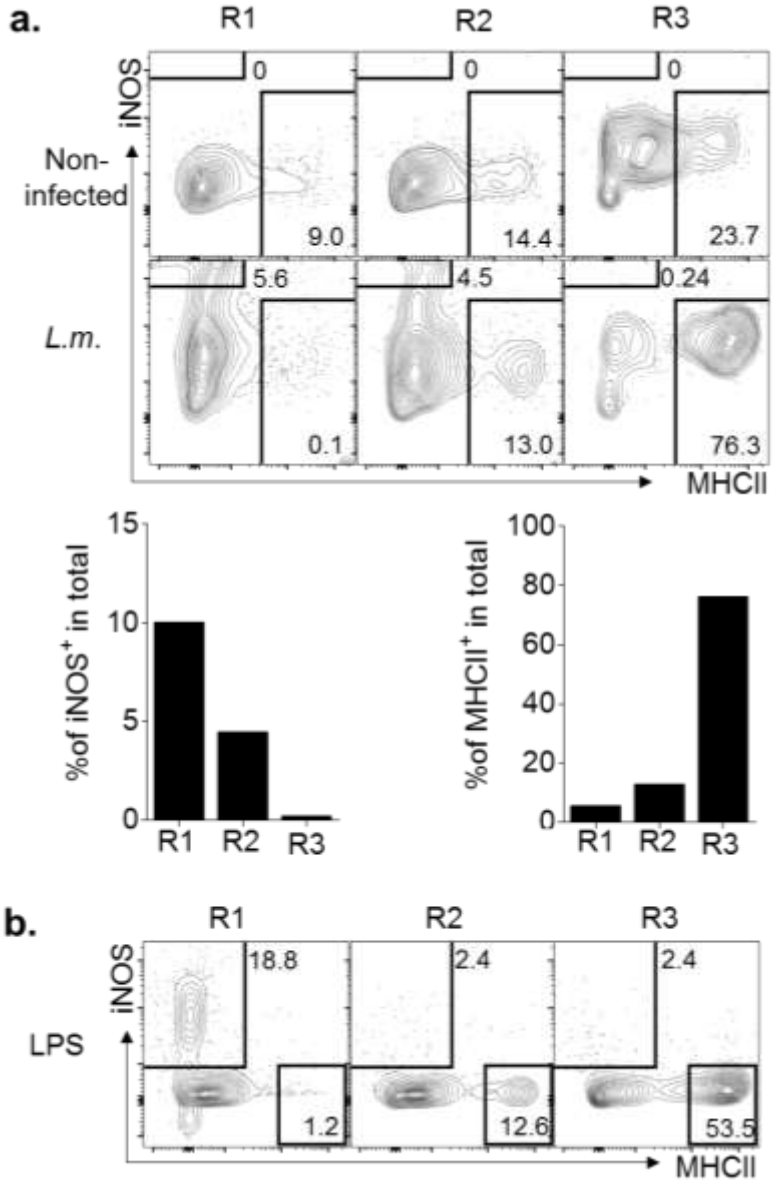


**Figure 5-3: R1 generates iNOS$^+$ cells in-vitro.** R1, R2 and R3 were sorted by flow cytometry and cultured in complete RPMI supplemented with 3ng/ml GM$^-$CSF, 100ng/ml Flt3L and 20ng/ml M-CSF.(a) Listeria was added at MOI 0.01 and cells cultured overnight. Representative FACS analysis of MHCII and either anti$^-$iNOS or isotype control is shown. (b) Cells were cultured overnight with 1ug/ml LPS. Graphs reflect the mean of 2-3 independent cultures.

### *5.2.2 In vivo production of iNOS$^+$ cells in response to Listeria*

With the initial discovery of iNOS production by macrophages (Stenger et al., 1994), a novel mechanism for bactericidal action had been found. Furthermore it was found that there was a specific subset of myeloid cells that were CD11b$^+$CD11c$^+$ and MHCII$^{hi}$ that were able to produce iNOS in response to cytosolic bacteria such as *Listeria* (Serbina et

al., 2003,) and parasites such as *Leishmania* (Guilliams et al., 2009; De Trez et al., 2009); These cells were labelled as 'monocyte-derived dendritic cells' due to their reliance on CCR2 and subsequent high expression of MHCII (Serbina et al., 2003; De Trez et al., 2009). However, in order to understand if these $iNOS^+$ cells were in fact the same as those that arise in response to GM-CSF (that are also called monocyte-derived dendritic cells) as had been previously assumed (Naik et al., 2006; Zigmond et al., 2012), I wanted to phenotype $iNOS^+$ cells for the same markers as studied in *in vivo* models of increased levels of GM-CSF. To do this I used an *in vivo* model system of *L.m.* infection and assessed the presence of $iNOS^+$ cells in the spleen.

#### 5.2.2.1 *Setup of Listeria monocytogenes infection model*

Experiments performed previously in the literature indicated 2-4 x $10^3$ Listeria CFU/ mouse was sufficient to generate an immune response that peaked at approximately 2 days after infection (Serbina et al., 2003). I thus used 2.5 x $10^3$ CFU/mouse and tested for anti-iNOS antibody staining. I were able to discern a clear population of $Lin^-CD11b^+$ cells that were expressing iNOS. These $iNOS^+$ cells were $MHCII^+$ and $Ly6C^{hi}$. This was in agreement with previous studies on $iNOS^+$ cells (Kang et al., 2008; De Trez et al., 2009). I also noted an increase in granulocytes ($CD11b^{high}Ly6C^{int}MHCII^-$) that can be expected in an immune response to pathogenic bacteria (**Figure 5-4**).

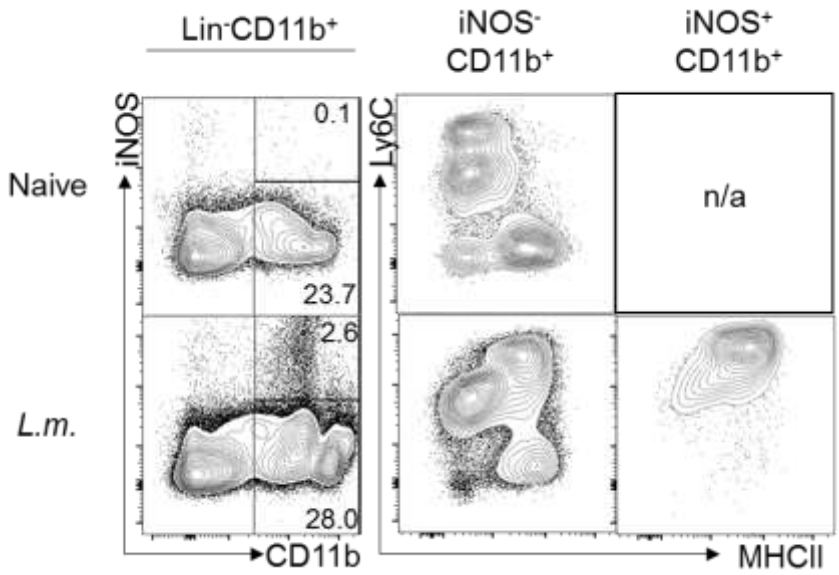


**Figure 5-4: *L.m.* induces the production of iNOS$^+$ cells *in vivo*.** WT mice were injected with 2500 CFU/mouse *i.v.* Mice were culled 2 days after infection and spleens assessed for iNOS$^+$ cells among Lin$^-$CD11b$^+$ cells and analysed for Ly6C, CD11b and MHCII.

### 5.2.2.2 *Fate mapping of iNOS$^+$ cells*

Next, I wished to address the fate of iNOS$^+$ cells. A number of studies on iNOS$^+$TNF$\alpha^+$ cells have noted that they are Ly6C$^{hi}$. Jung and colleagues tracked adoptively transferred *Cx3cr1$^{gfp/+}$* cells in a model of colitis and noted at later time points, that CX$_3$CR1$^{gfp/+}$ cells lose Ly6C expression to gain a more DC-like phenotype after an initial iNOS$^+$ stage (Zigmond et al., 2012). To accurately determine the fate of iNOS$^+$ cells I used an improved fate mapping mouse model; The *Nos2$^{CreTomato}$ x ROSA$^{lslTomato}$* system undergoes stable recombination in cells that express iNOS resulting in permanent expression of the fluorescent molecule Tomato.

*Listeria* infected mice were culled 2 days after infection. Splenocytes were stained with anti-iNOS antibody to assess the percentage of cells that were currently expressing iNOS (anti-iNOS$^+$) and compare these to any cells that had previously done so (Tom$^+$). I reported a slightly lower percentage of Tom$^+$ cells than anti-iNOS$^+$ cells indicating that the model might display a more conservative iNOS reporter expression than is actually

present (**Figure 5-5**a). Both anti-iNOS$^{+}$ and Tom$^{+}$ cells expressed high levels of Ly6C (**Figure 5-5**a). An overlay of iNOS-tomato labelled cells (Tom$^{+}$) over anti-iNOS antibody stained cells (anti-iNOS$^{+}$) showed that staining with anti-iNOS captured approximately 65% of the total cells that had produced iNOS in response to the infection (**Figure 5-5**b).

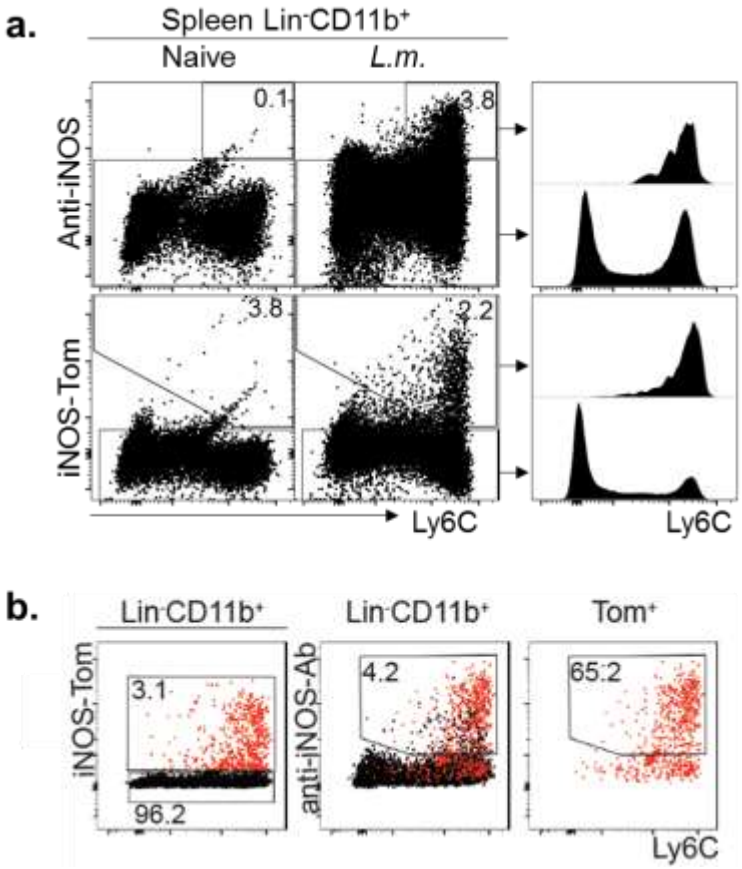


**Figure 5-5: L.m. induced iNOS$^{+}$ cells are Ly6C$^{hi}$.** *Nos2$^{creTomato}$ x ROSA$^{lslTomato}$* and C57Bl/6 controls were infected with *L.m.* Spleens were harvested 2 days after infection. Cells were either permeabilized to intracellularly stain with anti-iNOS antibody (anti-iNOS) or left non-permeabilized to ensure reporting of Tomato$^{+}$ cells (iNOS$^{-}$Tom). Graph shows mean ± SEM from 4 mice. Lower panel shows an overlay of iNOS$^{-}$Tom$^{+}$ cells over anti-iNOS stained splenocytes (red dots).

The study of iNOS production in response to bacterial infection is often done with live bacteria. In the previous experiment done *in vitro*, I noted that infections with higher MOIs resulted in the death of the cells in culture. This is because as fully virulent bacteria, *L.m.* evades host immune responses by directing the polymerization of actin filaments in order exit the host lysosome to then enter the cytosol which is its site of multiplication

(Poussin and Goldfine, 2010). A mutated strain of *L.m.* that has a deletion in the virulence factor ActA (ΔActA *Listeria*) is unable to direct actin polymerization. This results in lysosomal clearance of the pathogen by the infected cell. The induction of iNOS production in macrophages is equivalent in infection with the WT and the ΔActA strains of *L.m.*. Thus, using ΔActA *L.m.* infection allows the study of iNOS producing cells without overwhelming host cells with bacterial burden.

The spleens of mice infected with ΔActA *L.m* were tested for Tomato expression as well as anti-iNOS antibody staining within the $Lin^{-}CD11b^{+}$ population. The peak in Tomato and $anti^{-}$iNOS antibody staining appeared at day2. Most of the $Tomato^{+}$ cells were stained with anti-iNOS antibody indicating most of the cells were actively expressing iNOS at the time. By day 4, the number of cells stained for iNOS either by tomato expression or anti-iNOS antibody staining had reduced dramatically albeit there was a small number of cells still expressing Tomato that were not stained by the antibody. This indicated that most of the cells that expressed iNOS in response to the infection, had died. Furthermore, whether at day 2 or day 4, the iNOS-$tomato^{+}$ cells were always $Ly6C^{hi}$ even when they they were no longer expressing iNOS as indicated by the lack of anti-$iNOS^{-}$antibody staining (**Figure 5-6**). I could thus conclude that $iNOS^{+}$ cells are in fact terminally differentiated cells that arise in response to bacterial infection, express MHCII *in vivo* and do not lose Ly6C expression.

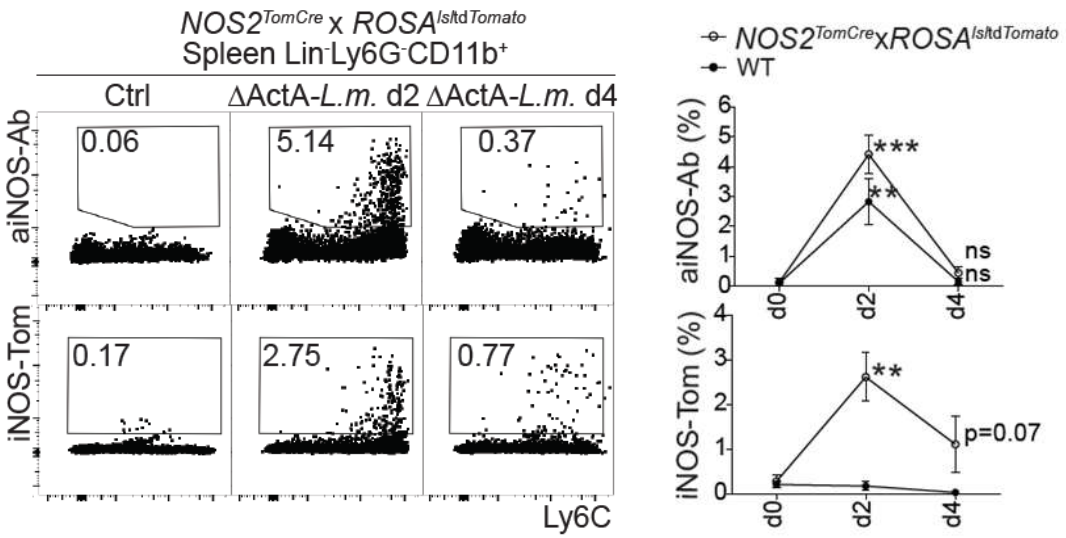


**Figure 5-6: iNOS$^+$ cells are an end-stage population.** Analysis of iNOS$^+$ by intracellular anti-iNOS antibody staining and labelling with Tomato expression, in the spleens of *NOS2$^{creTomato}$ x ROSA$^{lstdTomato}$* mice at days 2 and 4 after *L.m.* infection. Percentage of Ly6Chi cells within each population is quantified as mean ± SEM of the percentage of iNOS-Tom$^+$ or iNOS$^-$Ab$^+$ within total cells is shown in the graphs; n=3; **p<0.005, ***p<0.0005, ns=not significant; Student's t-test. This experiment was performed in collaboration with Daisy Melandri.

### 5.2.2.3 *Phenotype of iNOS$^+$ cells*

Given the ability of R1 cells to generated iNOS$^+$ cells, I wondered if iNOS$^+$ cells would have a similar phenotype to R1. Previous reports have found iNOS$^+$ cells to be F4/80$^{int}$ MHCII$^{int}$CD11c$^+$CD11b$^+$Ly6C$^{hi}$ (Guilliams et al., 2009; Serbina et al., 2003). These markers are not distinctive among the myeloid lineage and are expressed on other cell types such as tissue-resident macrophages and cDCs as well. I therefore performed FACS analysis for the markers that I noted were differentially expressed among the Ly6C$^{hi}$monocytes by mRNA expression in the BM and by surface expression in the blood (refer Chapter 3). I found that iNOS$^+$ cells were Ly6C$^{hi}$MHCII$^{int}$ and distinctly separate from an iNOS$^-$Ly6C$^{lo}$ MHCII$^+$ population (**Figure 5-7**a).

FACS analysis of the iNOS$^+$ cells against specific isotype controls showed that they were FcγRII/III$^+$CD209$^-$Flt3$^-$CD115$^-$ (**Figure 5-7b**). Additionally, they were PDL2$^+$ and PDL1$^-$

. This phenotype was similar to that of Inf-Macs generated by R1 monocytes when exposed to high levels of GM-CSF.

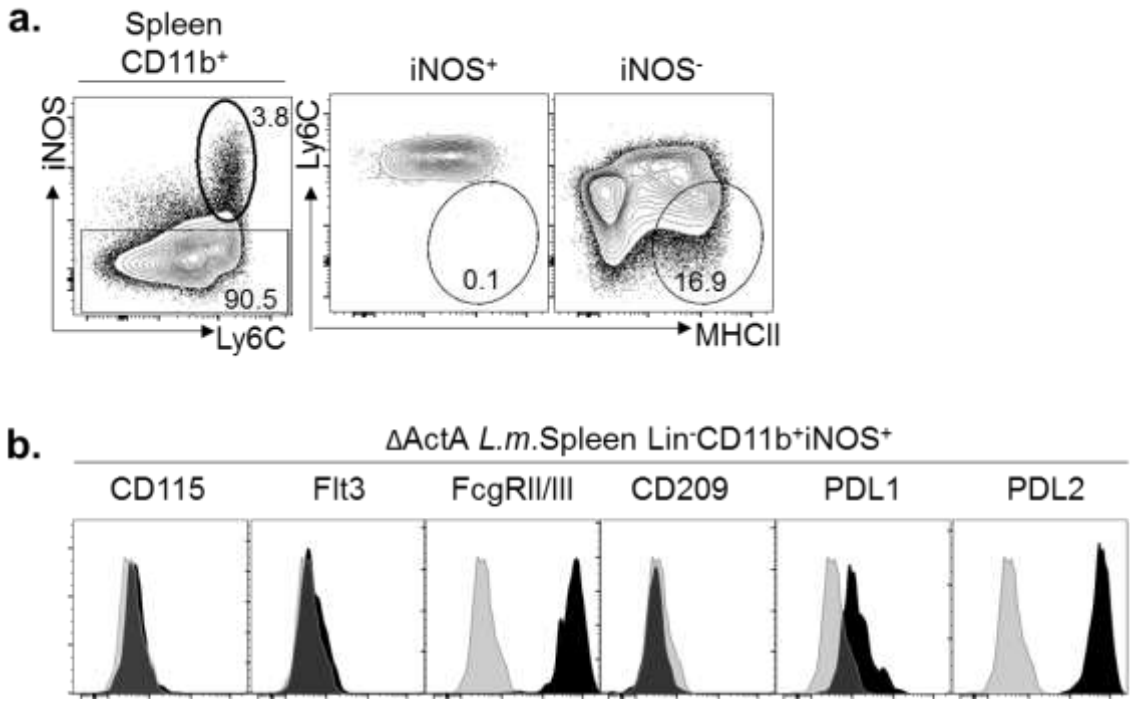


**Figure 5-7: iNOS$^+$ cells have a similar phenotype to GM-induced inflammatory macrophages**. (a) Representative FACS analysis of spleens from WT. *L.m.* infected mice 2 days after infection. (b) iNOS $^+$ cells were assayed for CD209a (DC-SIGN), FcγRII/III (CD16/32), Flt3(CD135), CD115 (MCSF-R), PDL1 (CD274) and PDL2 (CD273) (black shaded) against isotype control (grey shaded). n=3

I could thus conclude that iNOS$^+$ cells had a phenotype similar to inflammatory macrophages and not inflammatory DCs. Additionally, iNOS$^+$ cells had a phenotype that was distinct from the MHCII$^{hi}$Ly6C$^{lo}$ population that resembled the inflammatory DC phenotype.

#### 5.2.2.4 *Fate-mapping reveals iNOS$^+$ cells do not belong to the cDC lineage*

Previous literature suggests the conversion of CX3CR1$^{int}$ cells that produce iNOS within the first 24-48 hrs that then begin to describe a more DC phenotype expressing DC-specific markers such as Zbtb46 and Flt3 (Zigmond et al., 2012). Using a recent model for fate mapping of DC lineage cells with the *Zbtb46$^{CRE}$ x ROSA$^{lslYFP}$* mice, I attempted

to assess whether the Ly6C$^{hi}$CD11b$^{+}$iNOS$^{+}$ cells belonged to the DC lineage (Loschko et al., 2016a). Infection of *Zbtb46$^{CRE}$ x ROSA$^{lslYFP}$* mice with *L.m.* resulted in the generation of iNOS$^{+}$ cells that expressed minimum background levels of YFP while this was far higher in the positive control CD4$^{+}$ cDCs (cDC2s) (20%) (**Figure 5-8).** Collectively, I found that iNOS$^{+}$ cells did not arise from a cDC lineage.

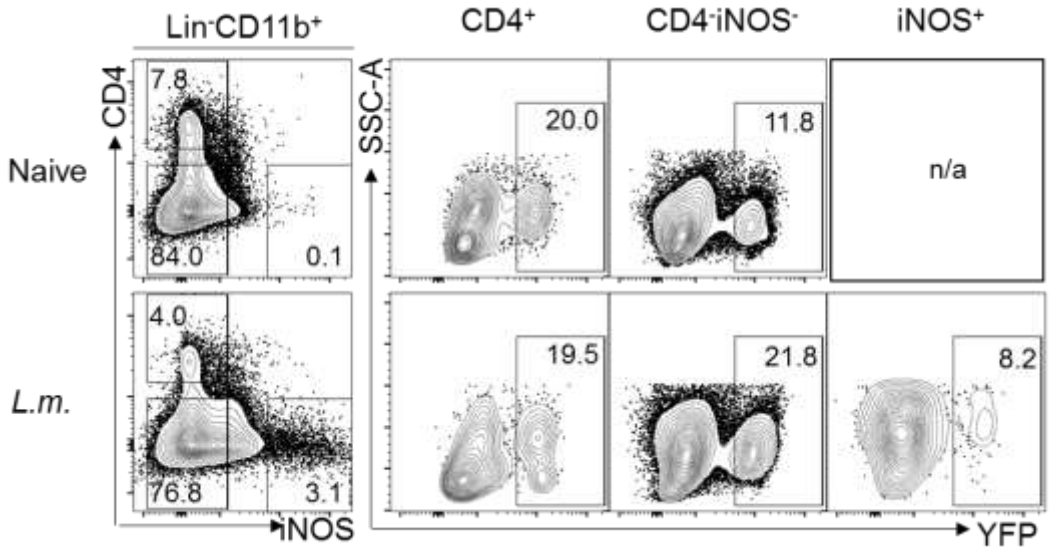


**Figure 5-8: iNOS$^{+}$ cells are Zbtb46$^{-}$YFP negative.** Representative flow cytometry analysis of *L.m.* infected or naïve *Zbtb46$^{CRE}$ x ROSA $^{lslYFP}$* mice. iNOS$^{+}$ cells, iNOS$^{-}$ CD11b$^{-}$ and CD4$^{+}$CD11b$^{+}$ cells were analysed for their expression of YFP.

### *5.2.3 Role of PU.1 in the generation of iNOS$^{+}$ cells*

#### 5.2.3.1 *Listeria infection in Sfpi1$^{+/-}$ mice leads to elevated production of iNOS*

As described in Chapter 3, R1 has far lower levels of PU.1 than R2 monocytes or R3 pre-DCs. I therefore wondered if PU.1 might play an inhibitory role on the functions of R1, *i.e* in the production of iNOS. *Sfpi1$^{+/-}$* mice were injected alongside wild type controls with ΔActA *L.m.*. At day 2, splenocytes were harvested and assayed by FACS for their expression of iNOS. I found that *Sfpi1$^{+/-}$* mice had increased numbers of CD11b$^{+}$Ly6C$^{hi}$iNOS$^{+}$ cells than their wild type counterparts (**Figure 5-9**). However, it

should be noted that there was an increase in the number of total splenic Lin$^-$ CD11b$^+$Ly6C$^{hi}$cells. Within Lin$^-$CD11b$^+$Ly6C$^{hi}$cells, the percentage of iNOS$^+$ cells was also increased. This data suggested that iNOS expression was negatively regulated by PU.1.

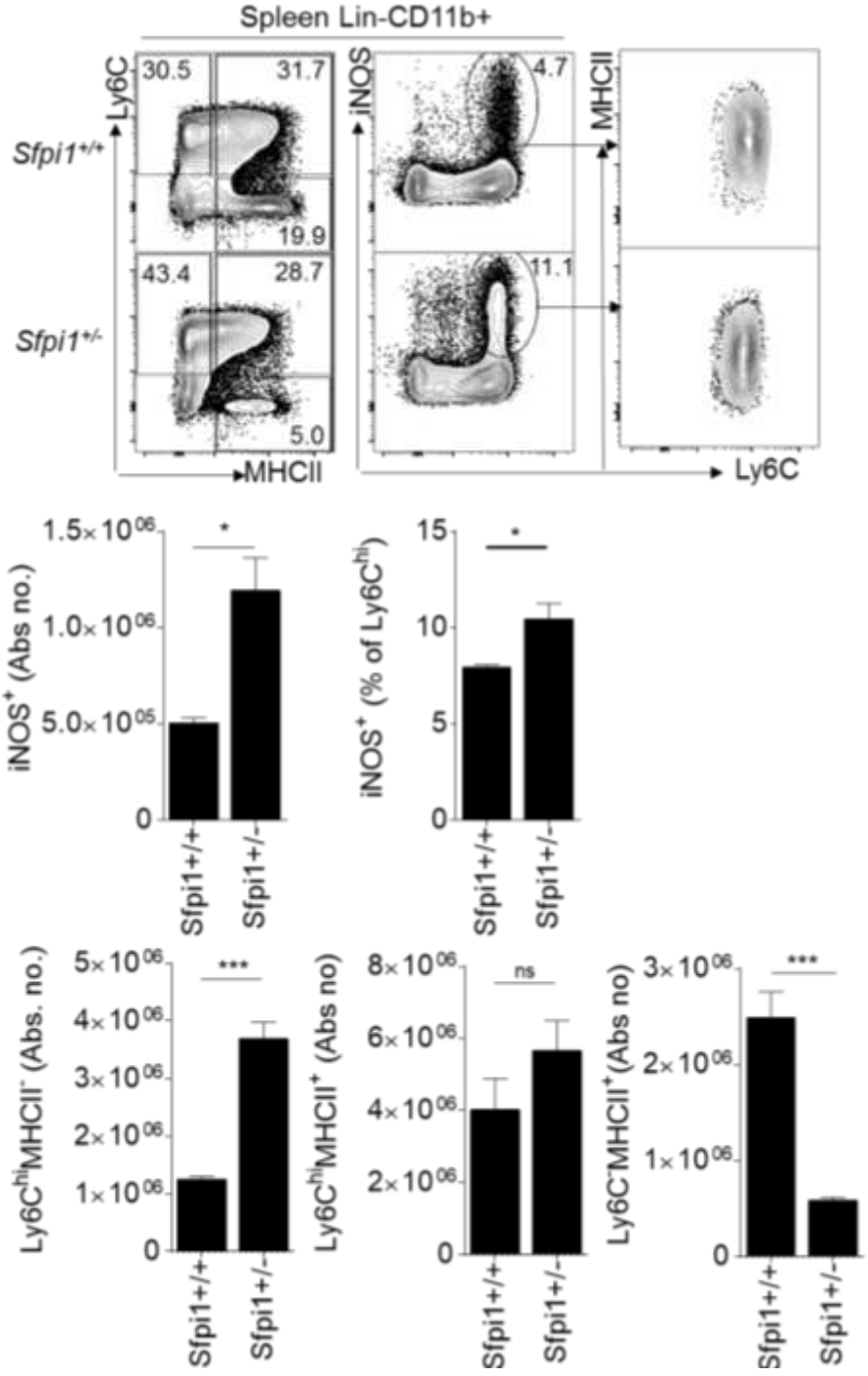


**Figure 5-9*: Sfpi1*$^{+/-}$ mice have increased levels of iNOS production than WT controls**.

*Sfpi1*$^{+/-}$ and *Sfpi1*$^{+/+}$ mice were injected with WT Listeria and sacrificed 2 days later. Representative FACS plots show the expression of iNOS among Lin$^-$CD11b$^+$ splenocytes

in mice of each genotype as well as the corresponding MHCII levels of the iNOS$^+$ cells. Graphs show mean ± SEM data from 1 of 2 experiments with similar results; n=3; *p<0.05, ***p<0.0005, ns=not significant; Student's t-test.

#### 5.2.3.2 *Sfpi$^{+/-}$ bone marrow derived macrophages exhibit higher levels of iNOS*

The role of PU.1 in the generation of macrophages and DCs was discussed previously. I have found that PU.1 plays a crucial role in the development of R2 monocytes and R3 pre-DCs. Additionally, I found that hemizygosity rendered R1 cells an enhanced ability to produce iNOS (**Figure 5-3**). I therefore wondered whether this important transcriptional regulator may play a role in the further downstream functional development of iNOS$^+$ production in comparison to MHCII$^+$ upregulation within monocyte subsets, during infection.

Culturing normalized numbers of bone marrow derived macrophages from *Sfpi1$^{+/-}$* or *Sfpi$^{+/+}$* mice with *L.m.* at an MOI of 1 or 10 or with LPS resulted in far greater amounts of iNOS in *Sfpi1$^{+/-}$* bone marrow derived macrophages as compared to their wild type counterparts. This was true in the percentage of iNOS$^+$ cells as well as in the MFI of iNOS generated (**Figure 5-10**). Thus, PU.1 inhibits iNOS expression within macrophages. Given that *Sfpi1$^{+/-}$* bone marrow is depleted of R2 monocytes, the cultures would contain a majority of macrophages derived from R1 monocytes. It could thus be suggested that PU.1 specifically inhibits the generation of iNOS within R1 monocyte-derived macrophages.

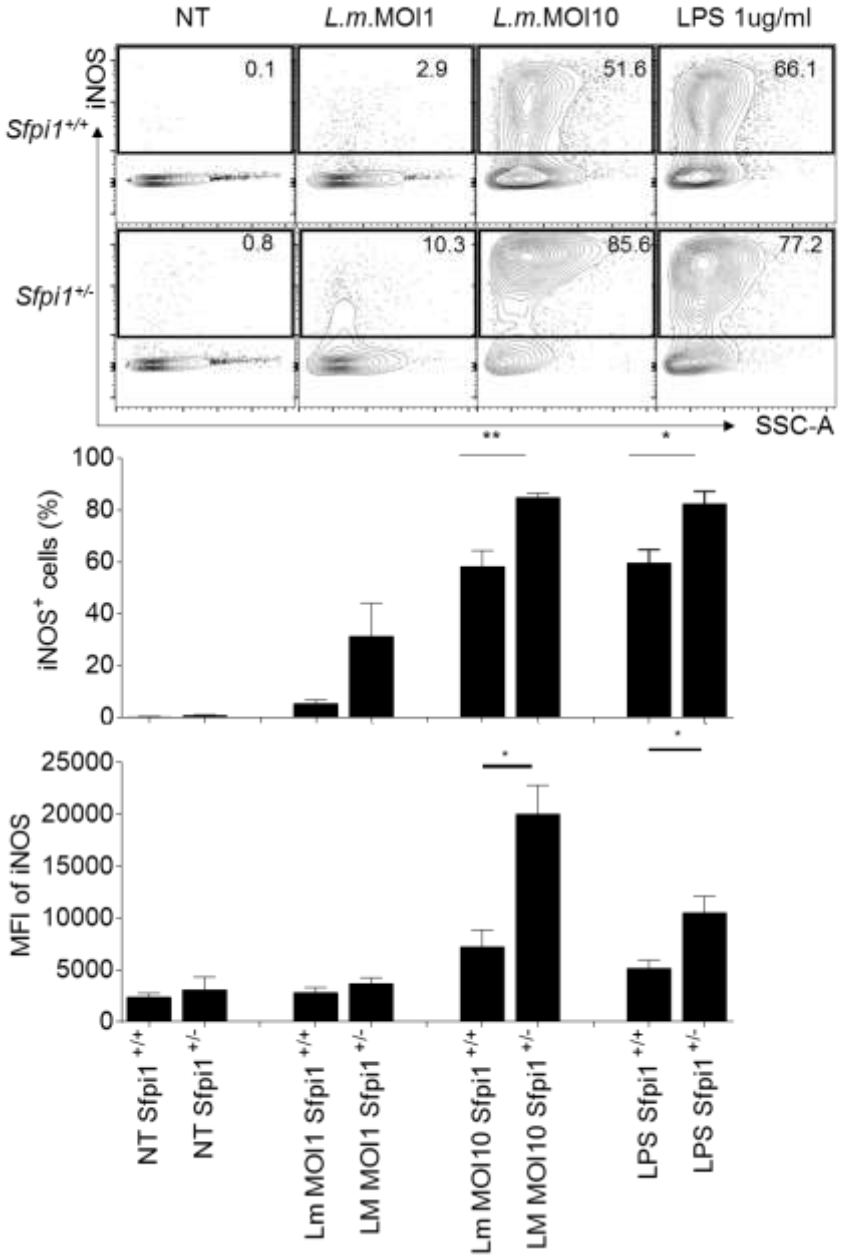


**Figure 5-10:*Sfpi1*$^{+/-}$ macrophages generate higher levels of iNOS**. 10,000 bone marrow derived macrophages were cultured in fresh medium with 20ng/ml M$^{-}$CSF and either *L.m.* (MOI 1 or 10 ) or LPS at 1ug/ml. Graphs show mean ± SEM data; n=3; *p<0.05, **p<0.005; Student's t-test. This experiment was performed by Giorgio Anselmi.

#### 5.2.3.3 *Sfpi1$^{+/-}$ BM generates iNOS$^{+}$ cells in vivo*

Having found an *in vitro* reliance on PU.1 to express iNOS by PU.1$^{lo}$ R1 monocytes, I wished to test this reliance *in vivo* through an adoptive transfer experiment where I injected whole BM from *Sfpi1$^{+/+}$* or *Sfpi1$^{+/-}$* mice (CD45.2) into congenic CD45.1 WT recipients (**Figure 5-11**a). Six hours later the recipients were injected with ΔActA Listeria and sacrificed at day 1.5 post infection. By harvesting cells from the spleen, I were able to analyse the CD45.2$^{+}$ cells and study their expression of iNOS in comparison to endogenous levels as an internal control for iNOS expression on CD45.1$^{+}$ cells. *Sfpi1$^{+/-}$* cells, being enriched in R1 monocytes, generated far more iNOS$^{+}$ cells that were CD11b$^{+}$Ly6C$^{hi}$ cells as compared to the *Sfpi1$^{+/+}$* cells **(Figure 5-11b)**. Thus, by circumventing any developmental abnormalities that may have explained the increased expression of iNOS in the hemizygous mice, I could show conclusively that PU.1 plays a significant cell-intrinsic role in the development of iNOS$^{+}$ cells.

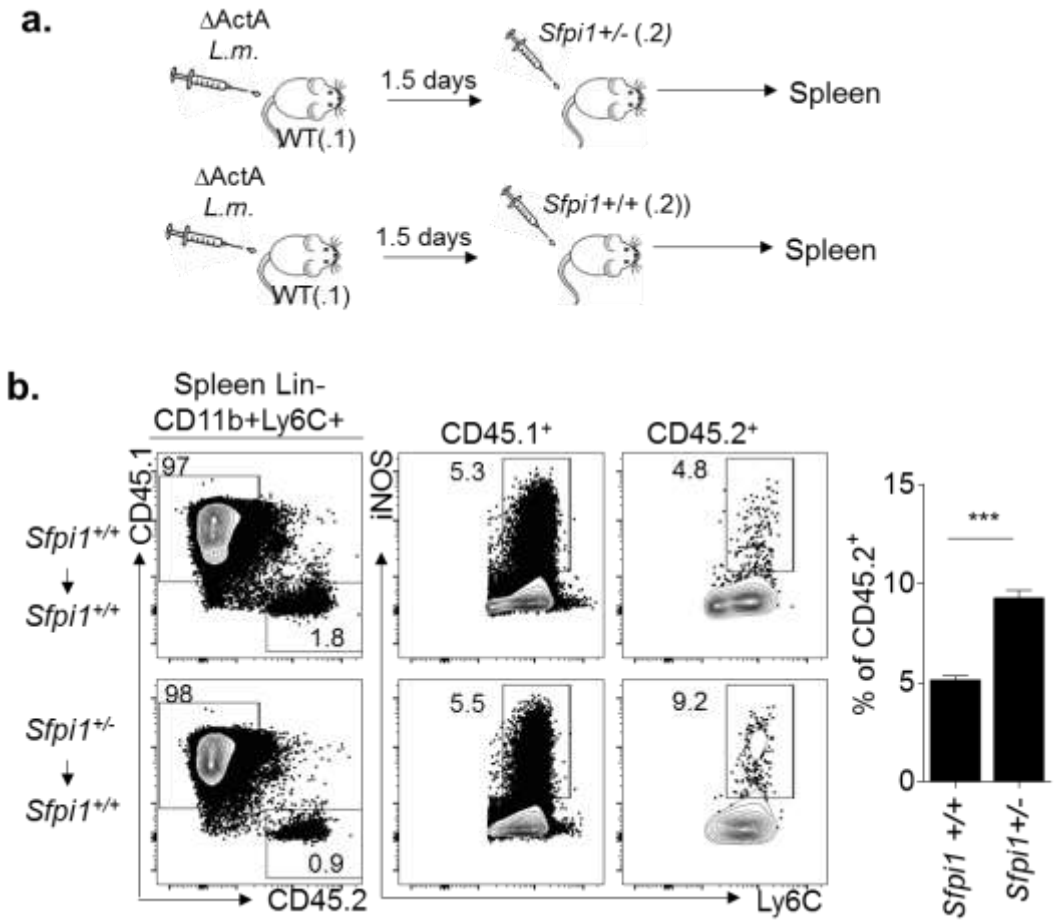


**Figure 5-11: *Sfpi1*$^{+/-}$ BM generates greater percentage of iNOS$^{+}$ cells**. a) Schematic diagram of experimental procedure. b) Representative FACS analysis of the spleens from *L.m.* infected WT recipients of *Sfpi1*$^{+/+}$ or *Sfpi1*$^{+/-}$ BM. Graphs show mean ± SEM; n=3; ***p,0.0005; Student's t-test.

### 5.2.3.4 *PU.1 plays a cell-intrinsic role in the generation of iNOS in monocytes*

In order to study the reliance of R1 monocytes on PU.1 for the expression of iNOS, I next performed an adoptive transfer experiment where *Sfpi1*$^{+/-}$ or *Sfpi1*$^{+/+}$ bone marrow monocytes were sorted with MACS beads and then injected into recipient WT ΔActA-*L.m.* infected mice (**Figure 5-12**a). Since *Sfpi1*$^{+/-}$ monocytes are devoid of both R2 monocytes and R3 pre-DCs, this experimental system would allow the adoptive transfer of mostly R1 monocytes into recipient mice. Additionally, to test for the competitive advantage of PU.1 in the generation of iNOS in an infected mouse model, I injected both *Sfpi1*$^{+/+}$ and *Sfpi1*$^{+/-}$ monocytes into the same infected recipient. I generated F1 mice from

a cross between CD45.2$^{+}$ and CD45.1$^{+}$ mice so that endogenous cells would be labelled with both markers. *Sfpi1*$^{+/+}$ bone marrow was taken from CD45.1$^{+}$ mice while the *Sfpi1*$^{+/-}$ mice were on a CD45.2 background. Thus, by injecting monocytes in a 1:1 proportion into the same recipient I were able to identify each genotype as well as the endogenous cells.

Adoptively transferred *Sfpi1*$^{+/-}$ monocytes generated a much higher percentage of iNOS$^{+}$ cells as compared to both the *Sfpi1*$^{+/+}$ monocytes and the endogenous recipient monocytes (**Figure 5-12b**). This corroborated with the data obtained from the previous adoptive transfer experiment with whole BM from *Sfpi1*$^{+/+}$ and *Sfpi1*$^{+/-}$ mice (**Figure 5-11**). Additionally, I could conclude that PU.1 was not only required for the development of R1 monocytes from its precursors at steady state but also played a central role in the expression of iNOS by these cells during *L.m.*.infection.

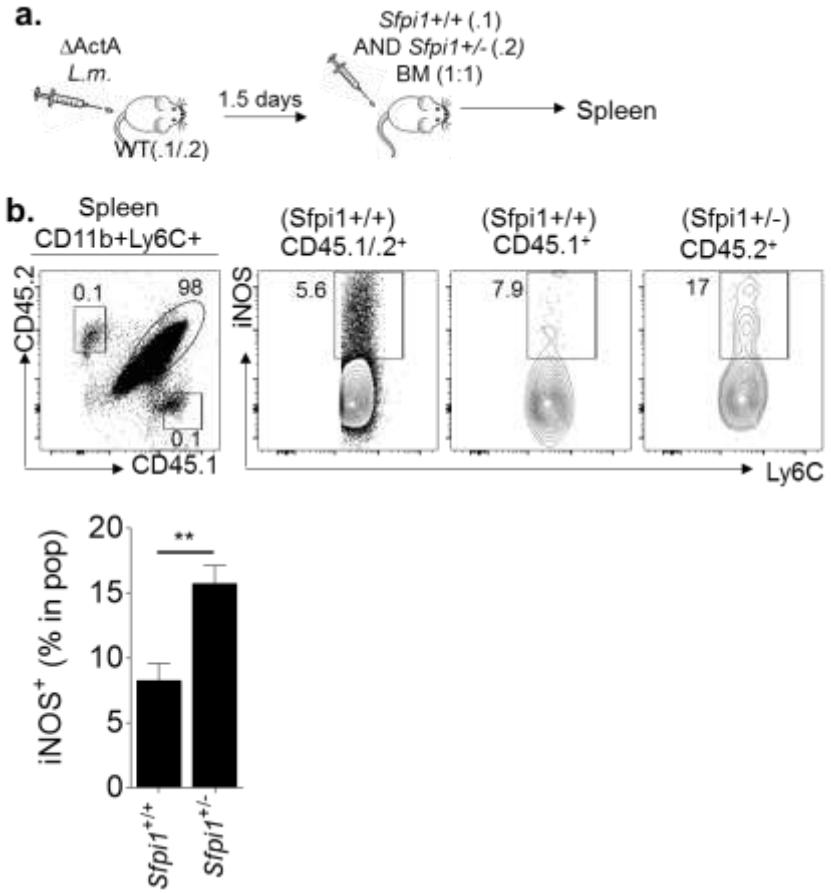


**Figure 5-12: *Sfpi1*$^{+/-}$ monocytes regulate iNOS production on cell intrinsic level** a) Schematic diagram of experiment setup b) Representative FACS plots of a recipient CD45.1/.2$^{+}$ spleen showing CD45.1$^{+}$(*Sfpi1*$^{+/+}$) Ly6C$^{hi}$monocytes and CD45.2$^{+}$(*Sfpi1*$^{+-/}$) Ly6C$^{hi}$ monocytes gated on Lin$^{-}$CD11b$^{+}$cells. Graph shows mean ± SEM; n=4, **p<0.005; Student's t-test.

## 5.3 Discussion and chapter overview

Inflammatory stimuli such as IFN-ɣ and TNF-α (Liew et al., 1990; Xie et al., 1993), TLR ligands (De Trez et al., 2009), co-stimulatory molecules and inflammatory cytokines (like IL-1β, IL-17, IL-18) induce the production of NO by macrophages. This is because iNOS production requires the concomitant activation of the STAT and NF-kB pathways that are stimulated by TLR and cytokine receptor signalling (Farlik et al., 2010). By providing appropriate stimuli, $iNOS^+$ cells are easily studied *in vivo* and *in vitro*.

While iNOS is responsible for important bactericidal activity to fight a number of infections, these cells can also prove pathological due to sustained exposure of neighbouring tissue to nitric oxide. In the case of chronic infection with the parasite *Trypanosoma brucei*, , iNOS-producing cells accumulate in large numbers in the liver, spleen and lymph nodes causing destruction to these organs (Guilliams et al., 2009).

By studying the induction of $iNOS^+$ cells *in vitro* in response to *L.m.* or LPS, I was able to draw on the separation between $iNOS^+$ cells and $MHCII^{hi}$ cells. iNOS induction and the expression of MHCII on $iNOS^+$ cells has been attributed to the action of IFNɣ produced by Th1 cells and NK cells in response to an infection (Kang et al., 2008; De Trez et al., 2009). In the case of our *in vitro* infection of flow cytometry assisted sorting of monocytes and pre-cDCs, I was able to decipher the precursor populations within $Ly6C^{hi}$ monocytes that were specialized to produce iNOS versus those that upregulated MHCII expression in response to *L.m.* infection or LPS – R1 ($Flt3^-CD11c^-$) cells had high mRNA expression levels of inflammation associated genes at steady state and were found to be the monocyte precursors with a predisposition to generate iNOS in response to infection with *L.m.* or LPS. R3 pre-cDCs did not produce iNOS and instead upregulated MHCII which was expected given their high expression of MHCII-associated genes. R2 displayed an intermediate phenotype generating both $iNOS^+$ cells (albeit at a lower percentage than R1) and upregulated MHCII. Thus, between the 2 $Ly6C^{hi}$ monocytes –

R1 and R2, R1 represents the precursors to inflammatory macrophages capable of generating iNOS$^{+}$ cells. Our *in vitro* and *in vivo* results hereby suggest that the occurrence of a DC-like phenotype in response to inflammation as reported by Zigmond et al, could be explained by the presence of R2 and R3 within the population gated as Lin$^{-}$ CD11b$^{+}$CD115$^{+}$Ly6C$^{hi}$ cells.

Additional experiments that could not be completed for this report include a thorough functional assessment of the resulting progeny of each of these precursor cells. Future work would include assessment of the ability of MHCII$^{hi}$ cells to prime CD4$^{+}$ T cells and a colony-forming-unit analysis of the cultures after overnight infections with *L.m.*.

An important finding was that PU.1 regulates the expression of iNOS. A culture of *Sfpi1*$^{+/-}$ bone marrow with M-CSF results in the enrichment of progeny from R1 monocytes as R2 monocytes are dramatically reduced in these mice. Upon infection with *L.m.* of normalized numbers of BMDMs., I noted that the *Sfpi1*$^{+/-}$ BMDMs produced higher levels and percentage of iNOS$^{+}$ cells. Such an experimental setup accommodated for any developmental differences that may occur as a result of PU.1 hemizygosity. I demonstrated that PU.1 directly influences the production of iNOS and the development of iNOS$^{+}$ cell precursors- R1 monocytes. The cell intrinsic role of PU.1 in the induction of iNOS expression was further demonstrated by mixed adoptive transfer experiments of *Sfpi1*$^{+/+}$ and *Spi1*$^{+/-}$ bone marrow into infected recipients.

The inhibitory role of PU.1 on iNOS generation that I describe both *in vivo* and *in vitro*, could be explained through PU.1 target miRNAs, namely miR146 and miR155 that have been found to inhibit iNOS production (Perske et al., 2010). Further details of this mechanism are alluded to later in the final conclusion of this thesis. PU.1 thus helps regulate the inflammatory response through various target genes.

The PU.1$^{hi}$ R2 monocytes that I describe, therefore, are suitably able to generate FcγRII/III$^{+}$CD209a$^{+}$ moDCs that are GM-CSF dependent while the PU.1$^{lo}$ R1 monocytes are pre-equipped to generate iNOS$^{+}$ phagocytes. Further studies are required to elucidate the effector role played by each of these populations in different inflammatory contexts.

**Are these cells the same as GM-CSF -induced FcγRII/III$^{+}$CD209a$^{+/-}$ cells?**

*L.m.* infection is cleared efficiently in *Csfr2r*$^{-/-}$ *Csf2rb2*$^{-/-}$ mice but not in *Ccr2*$^{-/-}$ mice (Greter et al., 2012) or in *Nos2*$^{-/-}$ mice (Serbina et al., 2003). This indicates that the cells responsible for controlling the pathogen are the Ccr2-dependent iNOS producing cells that are independent of GM-CSF. Our data shows that these iNOS$^{+}$ cells arise from the R1 Ly6C$^{hi}$monocytes and resemble the phenotype of the GM-CSF induced inflammatory macrophages (FcγRII/III$^{+}$CD209a$^{-}$Flt3$^{-}$CD115$^{+}$ cells) that also arise from R1 cells. This suggests that R1 cells are plastic and respond to different environmental cues to generate iNOS$^{+}$ or iNOS$^{-}$ cells.

# Chapter 6:

# Overview and Discussion

# 6 Discussion

## 6.1 Summary of findings

The study presented here differentiates between the 2 well characterized populations of inflammatory myeloid cells, namely iNOS-producing cells and mo-DCs. With the use of intricate *in vivo* and *in vitro* models of inflammation I was able to delineate characteristics from each population in order to better identify their distinctive functions, phenotypes and ontogeny.

Furthermore, I was able to decipher the precursor populations to iNOS$^{+}$ cells *(i.e.*, R1) and to MHCII$^{hi}$ cells that bear a more DC-like phenotype (*i.e.*, R2). I was able to establish novel surface marker expression patterns by which to distinguish them from other tissue-resident myeloid cells. Additionally, this study provided some clarity on the heterogeneity of the Ly6C$^{hi}$ monocytes that were previously considered to be homogenous and capable of becoming 'inflammatory macrophages'. Our t-SNE analysis highlighted various sub-populations within the conventional gating strategy of Ly6C$^{hi}$ monocytes that was encompassed within the novel R2 population. Bulk population analysis of this subset using cDC-associated markers like Flt3 and CD11c allowed the study of genetic and functional aspects of this novel R2 population. Single-cell analyses provided an in-depth view of the cells that truly express a unique transcriptional programme to other Ly6C$^{hi}$ monocytes and pre-cDCs. Highlighting the presence of pre-cDCs (R3) within conventional Ly6C$^{hi}$ monocyte gates also cautions against the inclusion of Flt3$^{+}$CD11c$^{+}$ cells in future studies. **Table 6-1** provides a comparison of the surface markers expressed on these novel populations with precursor populations for monocytes and cDCs.

**Table 6-1: Comparion of novel Ly6C$^{hi}$ sub-population surface markers**

| Steady state bone marrow | R1 | R2 | R3 | Pre-DCP | cMop* | CDP* | MDP* |
|---|---|---|---|---|---|---|---|
| CX3CR1 | lo | lo | lo | - | + | - | + |
| SIRPa | + | + | + | - | + | + | + |
| CD115 | + | + | + | - | + | + | + |
| Ly6C | + | + | + | lo | + | - | - |
| CD11b | + | + | + | - | - | - | - |
| FcgRII/III | + | + | - | - | | | |
| CD209a | - | + | + | +/- | | | |
| Flt3 | - | + | + | + | - | + | + |
| MHCII | - | +/- | +/- | + | - | - | - |
| CD11c | - | - | + | + | - | lo/neg | - |

*(Hettinger et al., 2013; Onai et al., 2007)

Finally, I show that the transcriptional regulator, PU.1, is responsible for delineating, the differential capacity of the Ly6C$^{hi}$ monocyte subsets to generate either iNOS$^{+}$ cells or mo-DCs under various conditions of inflammation.

The next section will discuss the significance and implications of these findings.

### *6.1.1 Ly6C$^{hi}$ monocyte gating strategy*

This study has revealed the presence of Flt3$^{+}$ cells within what was considered to be a homogenous population of bonafide Ly6C$^{hi}$ monocytes. These Flt3$^{+}$Ly6C$^{hi}$ monocytes are capable of generating mo-DCs within appropriate inflammatory environments and are GM-CSF-induced. Identifying the FcγRII/III$^{+}$CD209$^{+}$ cells within Flt3$^{+}$CD11c$^{-}$Ly6C$^{hi}$ monocytes in the blood at steady state proved particularly challenging. This was due to the small number of mo-DC precursor cells present and their relatively low expression of distinctive markers to identify them in the BM and blood by FACS analysis.

Single-cell analysis of BM progenitors has proved extremely useful in delineating the dynamic transcriptional programmes of progenitor cells. Although most work within the field of ontogeny is driven by an *a priori* definition of myeloid and lymphoid progenitors based on cell surface markers, single cell analyses have helped reveal the dynamic nature

of these cells and the stage of transcriptional divergence between various cell lineages (Ishizuka et al., 2016; Jaitin et al., 2015). In this study, our single cell qPCR studies allowed for a focused analysis of relevant surface markers and transcription factors that helped characterize the heterogeneity not only within Ly6C$^{hi}$ monocytes but also within the R2 population. Index-sorting of single-cells of the total population of Ly6C$^{hi}$ monocytes followed by RNA-Seq or microarray analysis might have enabled identification of unique markers and a more in-depth transcriptional characterisation of R1 and R2 without *a priori* gating for Flt3 and CD11c expression.

Additionally, this study was unable to identify a position in the developmental hierarchy for R2 among myeloid progenitors, precursors and differentiated cell populations, such as cMop, CDP and R1 Ly6C$^{hi}$ monocytes. R2 can be classified as a committed population of cells given that it does not express ckit. However, the exact transcriptional programme of these cells would have helped delineate whether R2 represented a transitional population of cells that co-expresses Flt3 and CD115, and whether they are a population that could give rise to R1 monocytes.

## 6.2 An improved definition of inflammatory myeloid cells

### *6.2.1 Phenotypic definition of monocyte-derived dendritic cells*

Ly6C$^{hi}$ monocytes differentiate into cells of various phenotypes during inflammation. As these cells egress into the tissue, they have been documented to become macrophages, DCs or myeloid-derived suppressor cells (MDSCs). Their phenotypic characterisation has continually been based on a mixture of markers such as CD11c and MHCII that are commonly expressed on a number of cells along with macrophage markers like CD64 (Tamoutounour et al., 2013), MertK, FcεRI (Plantinga et al., 2013), CD206 (Cheong et al., 2010) each of which have been characterised under different conditions of inflammation.

Here, I focus on a combination of FcγRII/III, which is expressed at high levels on monocytes and macrophages, and can be recognized by commercially available high affinity antibodies, along with CD209a, a marker that is expressed on *in vitro* derived GM-DCs as well as tissue DCs in humans. This report outlines a unique expression pattern to identify monocyte-derived macrophages and monocyte-derived dendritic cells as distinct cell types. While both are positive for a number of common markers that have previously been used to characterize inflammatory DCs and macrophages (such as CD206, CD115, FcεR1 and CD64), our study has shown that these inflammatory cells can be better characterized as FcγRII/III$^{+}$CD209a$^{-}$ inflammatory macrophages and FcγRII/III$^{+}$CD209a$^{+}$ mo-DCs.

Other than the expression of CD209a, our study did not highlight any other surface markers that distinctly differentiated between FcγRII/III$^{+}$CD209a$^{-}$ and FcγRII/III$^{+}$CD209a$^{+}$ cells. Performing microarrays on these populations could flag new markers that would help identify mo-DCs and inflammatory macrophages and provide a more functional understanding of the populations.

An important comparative study that would complement this approach would be with tissue-resident macrophages using markers such as CD169 and SIGN-R1 to outline the metallophilic and marginal zone macrophages, respectively. FcγRII/III$^{+}$CD209a$^{-}$ and FcγRII/III$^{+}$CD209a$^{+}$ cells are CCR2-dependent and recruited to the spleen in response to GM-CSF indicating that they do not arise from local proliferating macrophages. Ensuring that FcγRII/III$^{+}$CD209a$^{-}$ and FcγRII/III$^{+}$CD209a$^{+}$ cells have markers to distinguish them from tissue-resident macrophages may help further clarify future work.

### *6.2.2 Ontogenic perspective of mo-DCs and inflammatory macrophages.*

The origins of mo-DCs and inflammatory macrophages has been highly debated. Using relative expression levels of markers such as CD11b, CD11c, $CX_3CR1$ and MHCII, previous reports have indicated the absence of inflammatory myeloid cells in *Ccr2*$^{-/-}$ mice during inflammation. Inflammatory myeloid cells are thus suggested to originate from a *Ccr2*-dependent population. CCR2 is expressed on a number of cells including NK cells, T cells and pre-cDCs (Schlitzer et al., 2015). However, the reliance on the receptor for egress from the bone marrow lies mainly with Ly6C$^{hi}$ monocytes (Geissmann et al., 2003; Kurihara et al., 1997). Inflammatory macrophages and mo-DCs thus arise from Ly6C$^{hi}$ monocytes.

In order to answer the questions regarding the relationship of mo-DCs and iNOS+ cells with the cDC lineage, I used the most accurate mouse models available to track the expression of the cDC-lineage specific transcription factor- Zbtb46, within mo-DCs. The models included the reporter *Zbtb46*$^{gfp/+}$ mice and the fate mapping *Zbtb46*$^{CRE}$ *x ROSA*$^{lslYFP}$mice. While both mouse models showed that neither population expressed ZBTB46 to a significant degree, FcγRII/III$^{+}$CD209a$^{+}$ mo-DCs express slightly higher levels of ZBTB46-GFP than their CD209a$^{-}$ counterparts in *Zbtb46*$^{gfp/+}$ mice. The origin of these cells cannot be attributed to the cDC lineage however, as fate mapping analysis in the *Zbtb46*$^{CRE}$ *x ROSA*$^{lslYFP}$ mice showed that they had close to background levels of Zbtb46-YFP expression. Furthermore, *Zbtb46*$^{gfp/+}$reporter mice showed that GFP expression was not as high as in CD4$^{+}$ cDCs in the spleen.

By addressing the heterogeneity in the Ly6C$^{hi}$ monocyte population capable of generating FcγRII/III$^{+}$CD209a$^{+}$ mo-DCs, I was able to identify a Flt3$^{+}$CD11c$^{-}$ population that was able to give rise to the FcγRII/III$^{+}$CD209a$^{+}$ mo-DCs. This population was negative for reporter expression of the DC-specific Zbtb46 (Zbtb46-GFP$^{-}$ and Zbtb46-YFP$^{-}$*)* and in

spite of being $Flt3^{+}$, they were independent of Flt3L for their development. Thus, I conclude that the $Flt3^{+}CD11c^{-}$ $Ly6C^{hi}$ monocytes are not part of the cDC population and represent a distinct monocyte population.

These experiments would have been complemented by studies that addressed the progenitor populations that were responsible for giving rise to $Flt3^{+}CD11c^{-}$ R2 cells. While I noted that R2 are not $cKit^{+}$, colony formation experiments with CDP, cMop and MDP to test the origin of R2 cells would have better established the precise position within the monocyte lineage hierarchy to which R2 cells belong. I cannot confirm whether R2 is a divergent precursor population deriving from the MDP or whether the cMop diverges into *Nr4a1*-dependent $Ly6C^{lo}$ monocytes, $PU.1^{lo}$ $Ly6C^{hi}$ monocytes and $PU.1^{hi}$ $Ly6C^{hi}$ monocytes. This may need to be addressed in future studies. Among the various techniques used to fate map cells I attempted the use of reporter mice, fate-mapping via the use of the cre/loxp system and adoptive transfer experiments of congenically marked progenitor cells. Another technique that may be used is cellular barcoding which would outline the developmental path of R2 (**Figure 6-1**)

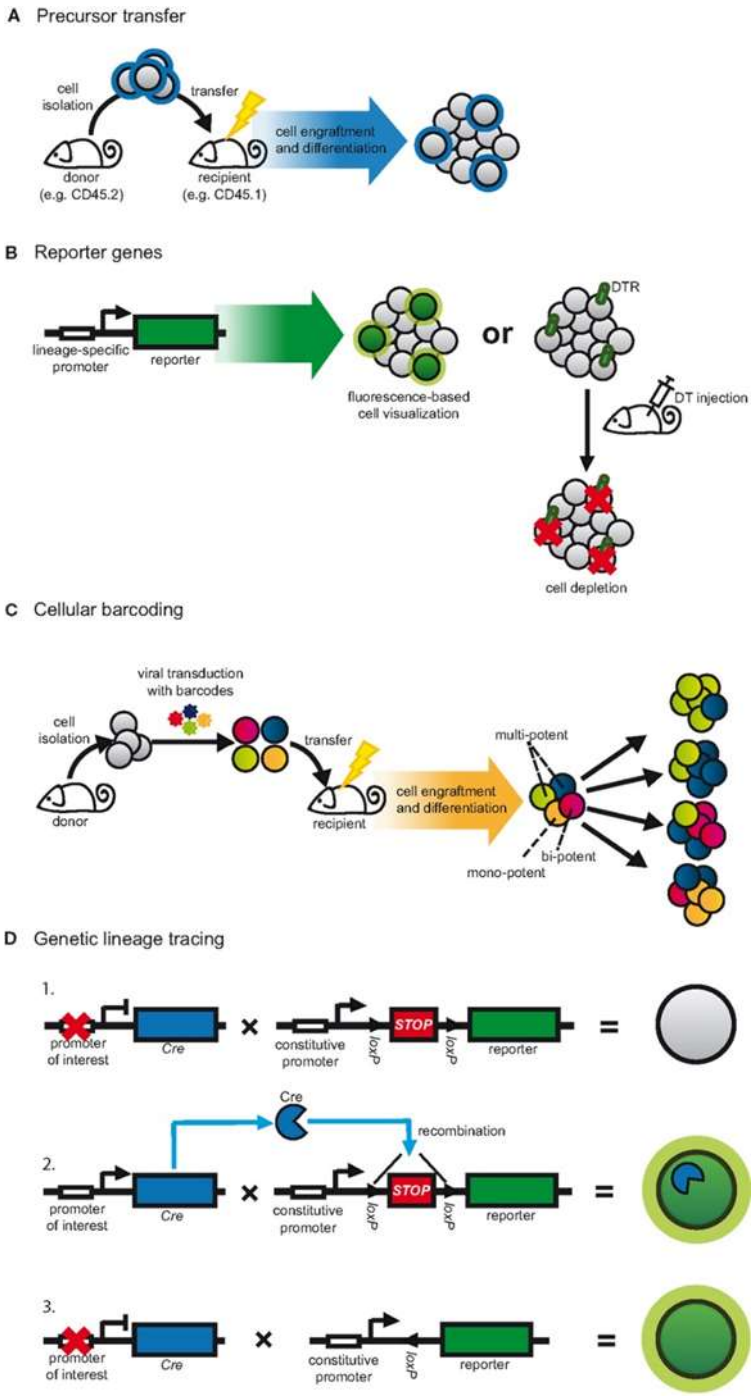


**Figure 6-1: Fate mapping strategies**. Reproduced from (Poltorak and Schraml, 2015). A number of techniques are used to more accurately define cDC populations. These include: A. Adoptive transfer experiments with pre-labelled cells that track transferred cells by the use of congenic markers, for example. B. and D. Tracking a lineage via fluorescent molecules encoded downstream of lineage-specific transcription factor promoters (eg. Zbtb46) (B) or via the cre - loxp system that ensures constitutive expression of the reporter gene via the action of cre recombinase (D). Bar-coding in C relies on *in vitro* viral transduction of progenitor populations with semi-random DNA sequences (barcodes). These progenitors are adoptively transferred into irradiated recipients and the differentiated progeny of each transduced cell can then be traced by RNA-Seq or microarray. This method does not rely on prior knowledge of lineage-specific transcription factors.

## 6.3 The functional role of mo–DCs and inflammatory macrophages

An aspect that remained outside the scope of this report is the functional description of the characterized mo-DCs and inflammatory macrophages. While the expression of MHCII in the R2 cells and their inflammatory progeny FcγRII/III$^{+}$CD209$^{+}$ mo-DCs might indicate the propensity of these cells to present antigen to T cells, I did not formally address this. Additionally, while FcγRII/III$^{+}$CD209a$^{-}$ cells were found to produce iNOS in response to an *L.m.* infection, I might have also tested the bactericidal capacity of these cells by checking for the number of colony forming units that survived the effector functions of the inflammatory macrophages or mo-DCs in culture. I might infer from our adoptive transfer experiments with *Sfpi1*$^{+/-}$ and *Sfpi1*$^{+/+}$ monocytes into *L.m.*-infected recipients, that PU.1$^{lo}$ R1 monocytes would perform greater levels of bactericidal activity due to a cell-intrinsic iNOS-producing advantage. Additional analyses might also include the production of chemokines and cytokines by these cells as mo-DCs have been reported to produce large amounts of CCL2, CCL6, CCL9, CCL24 in the lung in response to house dust-mite allergen (Plantinga et al., 2013).

### *6.3.1 The M1/M2 paradigm*

For the past 2 decades, alternatively-activated macrophages or M2 macrophages have been found to be important in the development of a tissue repair response. Several signals have been implicated in the development of an alternatively activated immune state namely signalling through the IL-4R, FcγR and TLRs (Wynn et al., 2013). Currently defined by activation through IL4-Ra signalling via IL-4 and IL-13, M2 macrophages are often associated with the expression of proteins like arginase1, chitinase-like proteins (eg. YM1, Ym2), and RELMa. These proteins have been found to directly influence tissue repair (RELMa via a negative feedback loop to control fibrosis) or through the alternative

activation of macrophages, fibroblast formation and matrix deposition (Chi3l1) (Zhou et al., 2015).

The origin of M2 cells is thought to be either from resident macrophages or circulating monocytes (Gundra et al., 2014). This origin influences the functional outcome of the monocytes in a way that supersedes the action of cytokine exposure. Peritoneal macrophages from naïve mice injected with IL-4 generate far fewer M2 macrophages that those in mice injected with IL-4 and thioglycollate- a model known to induce the recruitment of circulating monocytes. Monocyte-derived alternatively activated macrophages (AAMs) exclusively express high levels of RALDH2, PDL2 and CD206. Thus, monocyte-derived macrophages responding to IL-4 exhibit an M2 phenotype (Gundra et al., 2014).

Our study presents 2 types of monocyte-derived inflammatory cells that express PDL2 and CD206 among other surface markers. Whilst fitting the phenotype of monocyte-recruited M2 macrophages, it remains to be ascertained if one or both populations of GM-CSF-induced FcγRII/III$^{+}$ cells express M2-specific markers such as Raldh2, Chi3l3, arignase1 or is sensitive to IL-4 and IL-13 signalling.

### *6.3.2 Mo-DCs and inflammatory macrophages express PDL2*

PDL1 has been known to be expressed at steady state on a number of non-immune and immune cells including cDCs and this is enhanced under inflammation. In contrast, PDL2 is induced under inflammatory conditions on macrophages and cDCs both *in vitro* and *in vivo* (Yamazaki et al., 2002). Their common receptor Programmed Death receptor -1 PD-1 (Latchman et al., 2001) is expressed on activated T and NKT cells. PD-1 has an immune-receptor tyrosine switch motif (ITSM) site indicating that it could illicit both stimulatory and inhibitory signals. *Pdcd1*$^{-/-}$ (*PD-1*$^{-/-}$) mice develop spontaneous autoimmune diseases emphasizing the role of PD-1 in the induction of immune tolerance (Nishimura et al., 1999). PD-1 interactions with its ligands namely PDL1 and PDL2 have

been documented in several conditions including airway hyper-reactivity (AHR), transplantation, tumour immunology and infectious disease (Singh et al., 2011). PD-1 acts as a 'rheostat' in modulating the levels of T cell activation in these conditions (Nguyen and Ohashi, 2015).

PDL1 and PDL2 have very short cytoplasmic tails with no obvious signalling sequence indicating that they may not signal back into the APC expressing the ligand. PD1/PD-L1 interactions have been documented to illicit Treg responses and have been implicated in immune-evasion mechanisms used by cancerous cells and cells infected with murine cytomegalovirus (mCMV) (Benedict et al., 2008; Konishi et al., 2004). Engleman and colleagues noticed that blockade of PDL2 leads to a loss in polarization of *in vitro* anti-CD3 stimulated T cells (Davidson et al., 2013). Additionally, in the case of airway hypersensitivity reactions (AHR), PDL2 deficient mice have been found to have exacerbated AHR which was due to an increased production of IL-4 on iNKT cells (Akbari et al., 2010). PDL1 deficiency resulted in reduced AHR and increased levels of IFNg. This indicates the role of PDL2 in the blocking of Th2 responses while PDL1 mediates their induction (Akbari et al., 2010). Agarwal and colleagues also noticed that Flt3L administration induced the upregulation of PDL2 on $CD11b^{lo}CD11c^{hi}$ cDCs from OVA-sensitized mice, that in turn display regulatory properties (Shao et al., 2009). PD1 has been found to be highly expressed on synovial fluid T cells in patients with rheumatoid arthritis indicating that PD-1 may exert tolerogenic effects in inflammatory tissue (Hatachi et al., 2003). Thus, PDL2 and PDL1 exhibit immune regulatory functions and influence the polarization of T cells by APCs.

In this study, I noted an almost perfect divide in the expression of PDL2 and PDL1. $FcγRII/III^{+}CD209^{+}$ and $FcγRII/III^{+}CD209^{-}$ cells expressed high levels of PDL2 while $CD4^{+}$ cDCs and $FcγRII/III^{-}$ $CD11b^{+}MHCII^{+}$ cells expressed high levels of PDL1. The divergent expression of each ligand on the $FcγRII/III^{+}$ cells and the cDCs in response to

GM-CSF could indicate a differential ability to polarize T cells towards a Th1 versus Th2 phenotype. Further work is required to test the requirement for the disparate expression of PD-1 ligands on mo-DCs, inflammatory macrophages and tissue-resident cDCs.

### 6.4 The role of PU.1 in the development of FcγRII/III$^{+}$CD209a$^{+}$ mo-DCs

PU.1 is an example of a master transcriptional regulator in hematopoietic development, especially in the myeloid compartment. Lineage commitment is directed by master transcriptional regulators like PU.1, that are capable of creating 'poised' regions/ enhancers in the genome where the chromatin is unwound (Garber et al., 2012). Various stimuli drive the activation of specific transcription factors that bind to these poised enhancer regions (Garber et al., 2012). This occurs in a cell-type specific manner and induces a unique phenotype and function. Poised enhancers can be indicative of past lineage commitment or can arise at the stage of cell fate choice. PU.1 is constitutively expressed in macrophages (Ghisletti et al., 2010) and interacts with multiple transcription factors (such as C/EBPa, IRF4, IRF8 etc.) depending on cell fate decisions, which in turn may be regulated by environmental stimuli. Lavin et al. showed that differentiated peritoneal macrophages could acquire the transcriptional phenotype of lung macrophages when transplanted into the lung (Lavin et al., 2014).

The data in this thesis suggests that the role of PU.1 is considerably important with regards to the differentiation of inflammatory macrophages and mo-DCs from progenitor cells. Considering that relative levels of the master transcription factor shows clear differences between R1 and R2, it might be inferred that the elevated levels of PU.1 in R2 might be a unique cell fate choice that is made within the BM and becomes more pronounced in the blood and tissue. Indeed, the levels of PU.1 could not be distinctly discriminated within the bone marrow. PU.1 might act in a cell-specific way in R2, binding to regions in the chromatin to enhance the expression of genes such as *Ciita*, *CD209a,* and *FcγRII/III*. An important point of discussion would be to understand how

PU.1 is regulated and the mechanism by which it exerts its effects on inflammatory macrophages and mo-DCs.

### *6.4.1 The regulation of PU.1*

A number of studies investigating the role of PU.1 has been performed on fetal liver progenitors as removal of the gene is embryonically or post-natally lethal (McKercher et al., 1996; Scott et al., 1994). Overexpression of PU1 in hematopoietic fetal liver cells results in an exaggerated production of Mac-$1^{+}$ cells (DeKoter and Singh, 2000). However, extrapolating embryonic hematopoietic studies to our understanding of adult hematopoiesis can be misleading as removal of transcription factors such as AML-1 have shown different results in adult hemaotpoietic progenitors versus fetal liver progenitors (Ichikawa et al., 2004).

PU.1 is present in similar amounts in HSCs, myeloid and lymphoid progenitors as evidenced in *Pu.1*$^{gfp}$ mice (Back et al., 2004; Carotta et al., 2010; Nutt et al., 2005). Overexpression of the transcription factor plays a myeloid lineage instructive role, not at the point of myeloid commitment, but further downstream in myeloid differentiation (Dakic et al., 2005), through both positive selection for the myeloid lineage as well as negative regulation of other lineages, for example, by inhibiting GATA1-dependent erythroid cell development (Arinobu et al., 2007; Stopka et al., 2005). Inducible ablation of PU.1 in the *MxCre* dependent *Sfpi1* deleting mice have an expansion of aberrantly developed granulocytes in the spleen (Dakic et al., 2005). PU.1 thus influences myeloid development toward a monocytic lineage (which includes the propensity to generate cDCs) while dampening the selection of granulocytes.

PU.1 is able to regulate the transcription of about 3000 genes including those that code for cytokines (GM-CSF, G-CSF, M-CSF), their receptors (GM-CSFR, M-CSFR, Flt3) (Dakic et al., 2007) as well as cell-surface integrins used as markers of differentiation (CD11b, CD68, etc.) between various immune cells. Intriguingly, the protein-protein

complexes generated with PU.1 and its co-factors/co-regulators, can dramatically alter the transcriptional outcome of PU.1-regulated genes (Burda et al., 2010). Mo-DCs and inflammatory macrophages and their precursors that I describe rely on a number of these receptors for their development and are phenotypically characterised using a number of the markers that are regulated by PU.1. It is therefore crucial to understand how PU.1 regulates cell fate choice in these myeloid populations.

Within the myeloid lineage, PU.1 has been found to play a role in the development of DCs- cultured *Sfpi1*$^{-/-}$ embryonic thymocytes (Guerriero et al., 2000) and mice inducibly knocked-out for PU.1 (Carotta et al., 2010) are unable to give rise to CD11c$^{+}$ cells. This is possibly due to the direct transcriptional regulation of the Flt3 gene by PU.1 (Carotta et al., 2010). The role of PU.1 in the development of myeloid cells under inflammation, however has not been previously analysed.

Here I show that PU1 has a positive effect on the development of GM-DCs (Chapter 4) and a negative effect on iNOS$^{+}$ phagocytes (Chapter 5). In spite of the known ability of PU.1 to regulate the transcription of growth factor receptor, GM-CSFR (Hohaus et al., 1995), *Sfpi1*$^{-/-}$ thymocyte cultures are supported by GM-CSF (Guerriero et al., 2000) and CMPs from *Mx*$^{Cre}$*xSfpi1*$^{fl/fl}$ mice (Dakic et al., 2005) are still able to able to respond to GM-CSF. Thus, in our study, the loss of GM-CSF responsive FcγRII/III$^{+}$CD209a$^{+}$ cells in *Sfpi1*$^{+/-}$ mice is possibly due to the reliance of their precursor population on PU.1 rather than a loss in expression of GM-CSFR.

The inhibitory role of PU.1 on iNOS generation that I describe both *in vivo* and *in vitro*, could be explained through PU.1 target miRNAs, namely miR146 and miR155 that have been found to inhibit iNOS production (Perske et al., 2010). MiR146 and miR155 target the transcription of molecules downstream of the TLR signalling pathway such as IRAK1, TRAF6 and IFN response signalling (which play a crucial role in the induction

of *Nos2*) whilst being dependent on NF-κB thus generating a negative feedback loop to regulate the strength of the immune responses (Ivashkiv and Donlin, 2013; Taganov et al., 2006). Additionally, ectopic expression of miR146 in HSCs directs the development of functional macrophages (Ghani et al., 2011). Thus, PU.1 may exert its influence on the generation of iNOS in macrophages via miRNAs. PU.1 itself is regulated post-transcriptionally by miR-155 that binds with the 3' untranslated region of PU.1. miR155 is encoded by the BIC gene and binds over 400 mRNAs thus regulating a number of functions in the hematopoiesis of B cells, T cells, macrophages and granulocytes (Burda et al., 2010). A third mechanism by which PU.1 regulates cell fate decisions is by its concentration within a cell. It has been shown that high PU.1 concentration leads to a more monocyte/DC lineage commitment while lower concentrations are required for B cell development (Burda et al., 2010). This may also be the mechanism by which PU.1 regulates the development of R2 monocytes over R1 monocytes given its higher expression of transcriptional regulator.

The $PU.1^{hi}$ R2 monocytes that I describe in this study are suitably able to generate $Fc\gamma RII/III^{+}CD209a^{+}$ moDCs while the $PU.1^{lo}$ R1 monocytes are pre-equipped to generate $iNOS^{+}$ phagocytes. Studying the co-factors that interact with PU.1 that may be expressed more highly in one or the other population would provide a deeper mechanistic understanding of how the levels of PU.1 affect these populations. Further studies are required to decipher the effector role played by R1 and R2 in different inflammatory contexts and whether PU.1 continues to direct their function.

### 6.5 The role of GM-CSF in inflammation and cancer

GM-CSF is known to promote the development of myeloid precursors, as well as promote the differentiation of monocytes into macrophages and iNOS-producing cells during inflammation. Steady state influence of GM-CSF has been studied in great detail with the use of $Csf2r^{-/-}$ and $Csf2rb2^{-/-}$ mice (Greter et al., 2012). The quantity, timing and context

of the provision of GM-CSF influences the impact that the growth factor has on various cells and inflammatory outcomes. For example, GM-CSF is known to have an inhibitory effect on the differentiation of pDCs from murine hematopoietic cells (Gilliet et al., 2002). However, administration of GM-CSF to IFNα-producing cells results in their terminal differentiation (Ghirelli et al., 2010). Such studies emphasize the importance of the timing of GM-CSF.

Studies on the role of GM-CSF during inflammation have highlighted the pro-inflammatory influence of the growth factor in disease models such as EAE (Croxford et al., 2015) and airway hypersensitivity (Zhou et al., 2014). *Kras*$^{G12D}$ and *p48*$^{CRE}$ *x* *Kras*$^{LSLG12D}$ mutant mice develop pancreatic epithelial cell neoplastic lesions and have elevated levels of GM-CSF within the pancreas. This was noticed in pancreatic lesions from patients as well (Pylayeva-Gupta et al., 2012). GM-CSF orchestrates the recruitment of myeloid cells into the tumour via the $CD8^+$ T cells. Allogeneic cancer cells that are genetically engineered to overexpress GM-CSF (GVAX) are being used in a number of cancer immunotherapies in combination with T-cell checkpoint inhibitors such as anti-PD1/PD-L1 blockade and anti-CTLA4 in PhaseI and II clinical trials (Soares et al., 2015). This has had moderately good results in cancers such as melanoma and pancreatic ductal adenocarcinoma as it promotes strong effector T cell responses within the tumour (Pylayeva-Gupta et al., 2012; Soares et al., 2015).

In spite of the improved success of these therapies, the exact mechanisms of action and the cells involved in the response to excess levels of GM-CSF is not known. Given the strong response of the FcγRII/III$^+$CD209$^+$ and FcγRII/III$^+$CD209$^-$ cells to GM-CSF, it would be interesting to study if these cells appear in the tumour and if so, what their influence on such solid tumours would be.

## 6.6 Conclusion

By exploring the heterogeneity within the Ly6C$^{hi}$ monocyte population, this study has presented the existence of a unique precursor population of cells that has the ability to generate mo-DCs. Additionally, this study establishes characteristics for inflammatory macrophages and mo-DCs that not only distinguish these populations from each other with phenotypic and ontogenic perspectives but also helps distinguish them from cDCs in the tissue during inflammation (**Figure 6-2**). Myeloid populations have been confused for one another due to the use of promiscuous myeloid markers and loose nomenclature. In combination with a number of previous studies on myeloid cells in inflammation, this thesis delineates macrophages, classical dendritic cells, inflammatory-DCs and iNOS-producing macrophages in infections with intracellular bacteria and inflammatory settings of increased levels of GM-CSF (such as pre-clinical models of MS, pancreatic cancer, head and neck cancer *etc.*) (Bayne et al., 2012; Croxford et al., 2015; Hong, 2016; Van De Laar et al., 2012) .

By using single-cell analysis and a multi-dimensional reduction approach to study the Ly6C$^{hi}$ monocytes at steady state, my collaborators and I were also able to outline a unique transcriptional programme for the precursors to mo-DCs. Furthermore, I find that PU.1 is the master transcriptional regulator that is responsible for the cell fate choice between R1 and R2. Understanding this ontogenic and transcriptional diversity in the development of iNOS$^{+}$ macrophages and mo-DCs firstly provides a basis for understanding the conflicting data of previous reports and also part of the groundwork needed to improve the targeting of the most appropriate monocytic cells in future studies and immune therapies. Thus, these results can have potentially far-reaching consequences in the context of infection and cancer.

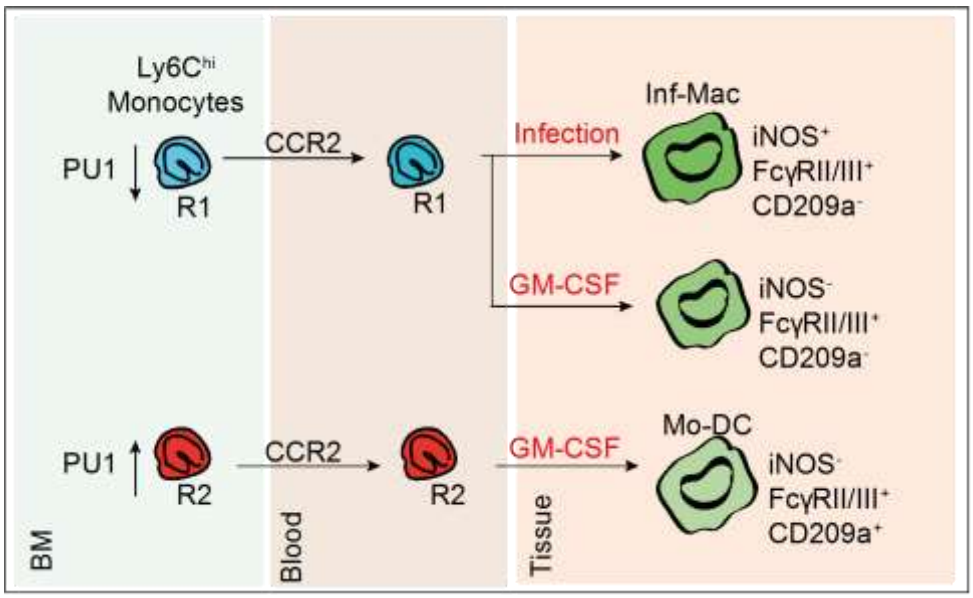


**Figure 6-2:Graphical summary**. R1 and R2 are Ly6C$^{hi}$ monocytes that egress from the bone marrow to the blood via CCR2. They differ in their expression of PU.1- R1 expresses lower levels while R2 expresses higher levels of the transcriptional regulator. R1 exhibits plasticity in responding to infection and elevated levels of GM-CSF by generating inflammatory macrophages and upregulating FcγRII/III and in the case of infection, iNOS. R2 on the other hand responds to GM-CSF by upregulating both FcγRII/III and CD209a thus generating mo-DCs.

# References


Abram, C.L., Roberge, G.L., Hu, Y., and Lowell, C.A. (2014). Comparative analysis of the efficiency and specificity of myeloid-Cre deleting strains using ROSA-EYFP reporter mice. J. Immunol. Methods *408*, 89–100.

Adolfsson, J., Borge, O.J., Bryder, D., Theilgaard-Mönch, K., Åstrand-Grundström, I., Sitnicka, E., Sasaki, Y., and Jacobsen, S.E.W. (2001). Upregulation of Flt3 expression within the bone marrow Lin-Sca1+c-kit+ stem cell compartment is accompanied by loss of self-renewal capacity. Immunity *15*, 659–669.

Akashi, K., Traver, D., Miyamoto, T., and Weissmann, I.L. (2000). A clonogenic common myeloid progenitor that gives rise to all myeloid lineages. Lett. to Nat. *404*, 193–197.

Akbari, O., Stock, P., Singh, A.K., Lombardi, V., Lee, W.-L., Freeman, G.J., Sharpe, A.H., Umetsu, D.T., and Dekruyff, R.H. (2010). PD-L1 and PD-L2 modulate airway inflammation and iNKT-cell-dependent airway hyperreactivity in opposing directions. Mucosal Immunol. *3*, 81–91.

Alaniz, R.C., Sandall, S., Thomas, E.K., and Wilson, C.B. (2004). Increased dendritic cell numbers impair protective immunity to intracellular bacteria despite augmenting antigen-specific CD8+ T lymphocyte responses. J. Immunol. *172*, 3725–3735.

Anderson, K.L., Perkin, H., Surh, C.D., Venturini, S., Maki, R.A., and Torbett, B.E. (2000). Transcription Factor PU.1 Is Necessary for Development of Thymic and Myeloid Progenitor-Derived Dendritic Cells. J. Immunol. *164*, 1855–1861.

Arinobu, Y., Mizuno, S., Chong, Y., Shigematsu, H., Iino, T., Iwasaki, H., Graf, T., Mayfield, R., Chan, S., Kastner, P., et al. (2007). Reciprocal Activation of GATA-1 and PU . 1 Marks Initial Specification of Hematopoietic Stem Cells into Myeloerythroid and Myelolymphoid Lineages. Cell Stem Cell *1*, 416–427.

Askenase, M.H., Han, S.-J.J., Byrd, A.L., Morais da Fonseca, D., Bouladoux, N., Wilhelm, C., Konkel, J.E., Hand, T.W., Lacerda-Queiroz, N., Su, X. zhuan, et al. (2015). Bone-Marrow-Resident NK Cells Prime Monocytes for Regulatory Function during Infection. Immunity *42*, 1130–1142.

Auffray, C., Fogg, D.K., Narni-Mancinelli, E., Senechal, B., Trouillet, C., Saederup, N., Leemput, J., Bigot, K., Campisi, L., Abitbol, M., et al. (2009). CX3CR1+ CD115+ CD135+ common macrophage/DC precursors and the role of CX3CR1 in their response to inflammation. J. Exp. Med. *206*, 595–606.

Autenrieth, S.E., Warnke, P., Wabnitz, G.H., Lucero Estrada, C., Pasquevich, K.A., Drechsler, D., Günter, M., Hochweller, K., Novakovic, A., Beer-Hammer, S., et al. (2012). Depletion of Dendritic Cells Enhances Innate Anti-Bacterial Host Defense through Modulation of Phagocyte Homeostasis. PLoS Pathog. *8*, e1002552.

Bachem, A., Güttler, S., Hartung, E., Ebstein, F., Schaefer, M., Tannert, A., Salama, A., Movassaghi, K., Opitz, C., Mages, H.W., et al. (2010). Superior antigen cross-presentation and XCR1 expression define human CD11c $^{+}$ CD141 $^{+}$ cells as homologues of mouse CD8 $^{+}$ dendritic cells. J. Exp. Med. *207*, 1273–1281.

Back, J., Dierich, A., Bronn, C., Kastner, P., and Chan, S. (2004). PU.1 determines the self-renewal capacity of erythroid progenitor cells. Blood *103*, 3615–3623.

Bain, C.C., Scott, C.L., Uronen-Hansson, H., Gudjonsson, S., Jansson, O., Grip, O., Guilliams, M., Malissen, B., Agace, W.W., and Mowat, A.M. (2013). Resident and pro-inflammatory macrophages in the colon represent alternative context-dependent fates of the same Ly6Chi monocyte precursors. Mucosal Immunol. *6*, 498–510.

Bain, C.C., Hawley, C.A., Garner, H., Scott, C.L., Schridde, A., Steers, N.J., Mack, M., Joshi,

A., Guilliams, M., Mowat, A.M.I., et al. (2016). Long-lived self-renewing bone marrow-derived macrophages displace embryo-derived cells to inhabit adult serous cavities. Nat. Commun. *7*, ncomms11852.

Bakri, Y., Sarrazin, S., Mayer, U.P., Tillmanns, S., Nerlov, C., Boned, A., and Sieweke, M.H. (2005). Balance of MafB and PU.1 specifies alternative macrophage or dendritic cell fate. Blood *105*, 2707–2716.

Barreda, D.R., Hanington, P.C., and Belosevic, M. (2004). Regulation of myeloid development and function by colony stimulating factors. Dev. Comp. Immunol. *28*, 509–554.

Bayne, L.J., Beatty, G.L., Jhala, N., Clark, C.E., Rhim, A.D., Stanger, B.Z., and Vonderheide, R.H. (2012). Tumor-Derived Granulocyte-Macrophage Colony-Stimulating Factor Regulates Myeloid Inflammation and T Cell Immunity in Pancreatic Cancer. Cancer Cell *21*, 822–835.

Beckerman, K.P., Rogers, H.W., Corbett, J.A., Schreiber, R.D., McDaniel, M.L., and Unanue, E.R. (1993). Release of nitric oxide during the T cell-independent pathway of macrophage activation. Its role in resistance to Listeria monocytogenes. J. Immunol. *150*, 888–895.

Bedoui, S., and Greyer, M. (2014). The role of dendritic cells in immunity against primary herpes simplex virus infections. Front. Microbiol. *5*, 533.

Benedict, C. a, Loewendorf, A., Garcia, Z., Blazar, B.R., and Janssen, E.M. (2008). Dendritic cell programming by cytomegalovirus stunts naive T cell responses via the PD-L1/PD-1 pathway. J. Immunol. *180*, 4836–4847.

Bernard, A., Lamy, L., and Alberti, I. (2002). the Two-Signal Model of T-Cell Activation After 30 Years. Transplantation *73*, 31–35.

Biswas, A., Bruder, D., Wolf, S.A., Jeron, A., Mack, M., Heimesaat, M.M., and Dunay, I.R. (2015). Ly6C(high) monocytes control cerebral toxoplasmosis. J. Immunol. *194*, 3223–3235.

Bogovski, P., and Bogovski, S. (1981). Animal Species in which N-nitroso compounds induce cancer. Int. J. Cancer *27*, 471–474.

Bogunovic, M., Ginhoux, F., Helft, J., Shang, L., Hashimoto, D., Greter, M., Liu, K., Jakubzick, C., Ingersoll, M. a, Leboeuf, M., et al. (2009). Origin of the lamina propria dendritic cell network. Immunity *31*, 513–525.

Bradley, T.R., and Metcalf, D. (1966). The growth of mouse bone marrow cells in vitro. Aust. J. Exp. Biol. Med. Sci. *44*, 287–299.

Bretscher, P., and Cohn, M. (1970). A theory of self-nonself discrimination. Science (80-. ). *169*, 1042–1049.

Briseño, C.G., Haldar, M., Kretzer, N.M., Wu, X., Theisen, D.J., Kc, W., Durai, V., Grajales-Reyes, G.E., Iwata, A., Bagadia, P., et al. (2016). Distinct Transcriptional Programs Control Cross-Priming in Classical and Monocyte-Derived Dendritic Cells. Cell Rep. *15*, 1–13.

Burda, P., Laslo, P., and Stopka, T. (2010). The role of PU.1 and GATA-1 transcription factors during normal and leukemogenic hematopoiesis. Leukemia *24*, 1249–1257.

Carotta, S., Dakic, A., D'Amico, A., Pang, S.H.M., Greig, K.T., Nutt, S.L., and Wu, L. (2010). The transcription factor PU.1 controls dendritic cell development and Flt3 cytokine receptor expression in a dose-dependent manner. Immunity *32*, 628–641.

Caton, M.L., Smith-Raska, M.R., and Reizis, B. (2007). Notch-RBP-J signaling controls the homeostasis of CD8- dendritic cells in the spleen. J. Exp. Med. *204*, 1653–1664.

Caux, C., Massacrier, C., Vandervliet, B., Dubois, B., Durand, I., Cella, M., Lanzavecchia, A., and Banchereau, J. (1997). CD34+ Hematopoietic Progenitors From Human Cord Blood Differentiate Along Two Independent Dendritic Cell Pathways in Response to Granulocyte-Macrophage Colony-Stimulating Factor Plus Tumor Necrosis Factor a: II. Functional Analysis.

Blood *90*, 1458–1470.

Cha, J.H., Chang, M.Y., Richardson, J.A., and Eidels, L. (2003). Transgenic mice expressing the diphtheria toxin receptor are sensitive to the toxin. Mol. Microbiol. *49*, 235–240.

Cheong, C., Matos, I., Choi, J.-H., Dandamudi, D.B., Shrestha, E., Longhi, M.P., Jeffrey, K.L., Anthony, R.M., Kluger, C., Nchinda, G., et al. (2010). Microbial Stimulation Fully Differentiates Monocytes to DC-SIGN/CD209+ Dendritic Cells for Immune T Cell Areas. Cell *143*, 416–429.

Choi, Y.E., Yu, H.N., Yoon, C.H., and Bae, Y.S. (2009). Tumor-mediated down-regulation of MHC class II in DC development is attributable to the epigenetic control of the CIITA type I promoter. Eur J Immunol *39*, 858–868.

Chow, A., Huggins, M., Ahmed, J., Hashimoto, D., Lucas, D., Kunisaki, Y., Pinho, S., Leboeuf, M., Noizat, C., van Rooijen, N., et al. (2013). $CD169^{+}$ macrophages provide a niche promoting erythropoiesis under homeostasis and stress-SOM. Nat. Med. *19*, 429–436.

Clausen, B.E., Burkhardt, C., Reith, W., Renkawitz, R., and Förster, I. (1999). Conditional gene targeting in macrophages and granulocytes using LysMcre mice. Transgenic Res. *8*, 265–277.

Cobb, J.P., Hotchkiss, R.S., Swanson, P.E., Chang, K., Qiu, Y., Laubach, V.E., Karl, I.E., and Buchman, T.G. (1999). Inducible nitric oxide synthase (iNOS) gene deficiency increases the mortality of sepsis in mice. Surgery *126*, 438–442.

Cook, A.D., Braine, E.L., and Hamilton, J.A. (2004). Stimulus-Dependent Requirement for Granulocyte-Macrophage Colony-Stimulating Factor in Inflammation. J. Immunol. *173*, 4643–4651.

Cross, M., Mangelsdorf, I., Wedel, A., and Renkawitz, R. (1988). Mouse lysozyme M gene: isolation, characterization, and expression studies. Proc. Natl. Acad. Sci. U. S. A. *85*, 6232–6236.

Croxford, A.L., Lanzinger, M., Hartmann, F.J., Schreiner, B., Mair, F., Pelczar, P., Clausen, B.E., Jung, S., Greter, M., and Becher, B. (2015). The Cytokine GM-CSF Drives the Inflammatory Signature of CCR2(+) Monocytes and Licenses Autoimmunity. Immunity *43*, 502–514.

Crozat, K., Tamoutounour, S., Vu Manh, T.-P.T.-P., Fossum, E., Luche, H., Ardouin, L., Guilliams, M., Azukizawa, H., Bogen, B., Malissen, B., et al. (2011). Cutting edge: expression of XCR1 defines mouse lymphoid-tissue resident and migratory dendritic cells of the CD8α+ type. J. Immunol. *187*, 4411–4415.

Cuello, C., Correa, P., Haenszel, W., Gordillo, G., Brown, C., Archer, M., and Tannenbaum, S. (1976). Gastric cancer in Colombia. I. Cancer risk and suspect environmental agents. J. Natl. Cancer Inst. *57*, 1015–1020.

Dakic, A. (2005). PU.1 regulates the commitment of adult hematopoietic progenitors and restricts granulopoiesis. J. Exp. Med. *201*, 1487–1502.

Dakic, A., Wu, L., and Nutt, S.L. (2007). Is PU.1 a dosage-sensitive regulator of haemopoietic lineage commitment and leukaemogenesis? Trends Immunol. *28*, 108–114.

Daro, E., Pulendran, B., Brasel, K., Teepe, M., Pettit, D., Lynch, D.H., Vremec, D., Robb, L., Shortman, K., McKenna, H.J., et al. (2000). Polyethylene Glycol-Modified GM-CSF Expands CD11bhighCD11chigh But Not CD11blowCD11chigh Murine Dendritic Cells In Vivo: A Comparative Analysis with Flt3 Ligand. J. Immunol. *165*, 49–58.

Davidson, M.G., Alonso, M.N., Kenkel, J.A., Suhoski, M.M., GonzÃ¡lez, J.C., Yuan, R., and Engleman, E.G. (2013). In Vivo T Cell Activation Induces the Formation of CD209+ PDL-2+ Dendritic Cells. PLoS One *8*, e76258.

Davies, L.C., Jenkins, S.J., Allen, J.E., and Taylor, P.R. (2013). Tissue-resident macrophages.

Nat. Immunol. *14*, 986–995.

Doherty, P.C., and Zinkernagel, R.M. (1975). A biological role for the major histocompatibility antigens. Lancet (London, England) *1*, 1406–1409.

Dorner, B.G., Dorner, M.B., Zhou, X., Opitz, C., Mora, A., Güttler, S., Hutloff, A., Mages, H.W., Ranke, K., Schaefer, M., et al. (2009). Selective Expression of the Chemokine Receptor XCR1 on Cross-presenting Dendritic Cells Determines Cooperation with CD8+ T Cells. Immunity *31*, 823–833.

Dranoff, G., Jaffee, E., Lazenby, A., Golumbek, P., Levitsky, H., Brose, K., Jackson, V., Hamada, H., Pardoll, D., and Mulligan, R.C. (1993). Vaccination with irradiated tumor cells engineered to secrete murine granulocyte-macrophage colony-stimulating factor stimulates potent, specific, and long-lasting anti-tumor immunity. Proc. Natl. Acad. Sci. U. S. A. *90*, 3539–3543.

Dubrot, J., Duraes, F. V, Potin, L., Capotosti, F., Brighouse, D., Suter, T., LeibundGut-Landmann, S., Garbi, N., Reith, W., Swartz, M.A., et al. (2014). Lymph node stromal cells acquire peptide-MHCII complexes from dendritic cells and induce antigen-specific $CD4^+$ T cell tolerance. J. Exp. Med. *211*, 1153–1166.

Edelson, B.T., Bradstreet, T.R., KC, W., Hildner, K., Herzog, J.W., Sim, J., Russell, J.H., Murphy, T.L., Unanue, E.R., and Murphy, K.M. (2011). Batf3-dependent CD11b(low/-) peripheral dendritic cells are GM-CSF-independent and are not required for Th cell priming after subcutaneous immunization. PLoS One *6*, e25660.

Epelman, S., Lavine, K.J., Beaudin, A.E., Sojka, D.K., Carrero, J.A., Calderon, B., Brija, T., Gautier, E.L., Ivanov, S., Ansuman, T., et al. (2014). Embryonic and adult-derived resident cardiac macrophages are maintained through distinct mechanisms at steady state and during inflammation. Immunity *40*, 91–104.

Fancke, B., Suter, M., Hochrein, H., and Keeffe, M.O. (2016). M-CSF : a novel plasmacytoid and conventional dendritic cell poietin. Blood *111*, 150–160.

Farlik, M., Reutterer, B., Schindler, C., Greten, F., Vogl, C., Müller, M., and Decker, T. (2010). Nonconventional initiation complex assembly by STAT and NF-kB transcription factors regulates nitric oxide synthase expression. Immunity *33*, 25–34.

Fenyk-Melody, J.E., Garrison, A.E., Brunnert, S.R., Weidner, J.R., Shen, F., Shelton, B.A., and Mudgett, J.S. (1998). Experimental autoimmune encephalomyelitis is exacerbated in mice lacking the NOS2 gene. J. Immunol. *160*, 2940–2946.

Fujimoto, K., Karuppuchamy, T., Takemura, N., Shimohigoshi, M., Machida, T., Haseda, Y., Aoshi, T., Ishii, K.J., Akira, S., and Uematsu, S. (2011). A New Subset of CD103+CD8α+ Dendritic Cells in the Small Intestine Expresses TLR3, TLR7, and TLR9 and Induces Th1 Response and CTL Activity. J. Immunol. *186*, 6287–6295.

van Furth, R., Cohn, Z.A., Hirsch, J.G., Humphrey, J.H., Spector, W.G., and Langevoort, H.L. (1972). The mononuclear phagocyte system: a new classification of macrophages, monocytes, and their precursor cells. Bull. World Health Organ. *46*, 845–852.

Gao, Q., Jiang, Y., Ma, T., Zhu, F., Gao, F., Zhang, P., Guo, C., Wang, Q., Wang, X., Ma, C., et al. (2010). A critical function of Th17 proinflammatory cells in the development of atherosclerotic plaque in mice. J. Immunol. *185*, 5820–5827.

Gao, Y., Nish, S.A., Jiang, R., Hou, L., Licona-Limón, P., Weinstein, J.S., Zhao, H., and Medzhitov, R. (2013). Control of T helper 2 responses by transcription factor IRF4-dependent dendritic cells. Immunity *39*, 722–732.

Garber, M., Yosef, N., Goren, A., Raychowdhury, R., Thielke, A., Guttman, M., Robinson, J., Minie, B., Chevrier, N., Itzhaki, Z., et al. (2012). A High-Throughput Chromatin Immunoprecipitation Approach Reveals Principles of Dynamic Gene Regulation in Mammals.

Mol. Cell *47*, 810–822.

Geijtenbeek, T.B.H., Torensma, R., van Vliet, S.J., van Duijnhoven, G.C.F., Adema, G.J., van Kooyk, Y., and Figdor, C.G. (2000). Identification of DC-SIGN, a novel dendritic cell-specific ICAM-3 receptor that supports primary immune responses. Cell *100*, 575–585.

Geissmann, F., Jung, S., Littman, D.R.D.R., Ajuebor, M.N., Flower, R.J., Hannon, R., Christie, M., Bowers, K., Verity, A., Perretti, M., et al. (2003). Blood monocytes consist of two principal subsets with distinct migratory properties. Immunity *19*, 71–82.

Ghani, S., Riemke, P., Schönheit, J., Lenze, D., Stumm, J., Hoogenkamp, M., Lagendijk, A., Heinz, S., Bonifer, C., Bakkers, J., et al. (2011). Macrophage development from HSCs requires PU.1-coordinated microRNA expression. Blood *118*, 2275–2284.

Ghirelli, C., Zollinger, R., Soumelis, V., Siegal, F., Kadowaki, N., Shodell, M., Liu, Y., Rothenfusser, S., Tuma, E., Endres, S., et al. (2010). Systematic cytokine receptor profiling reveals GM-CSF as a novel TLR-independent activator of human plasmacytoid predendritic cells. Blood *115*, 5037–5040.

Ghisletti, S., Barozzi, I., Mietton, F., Polletti, S., De Santa, F., Venturini, E., Gregory, L., Lonie, L., Chew, A., Wei, C.L., et al. (2010). Identification and Characterization of Enhancers Controlling the Inflammatory Gene Expression Program in Macrophages. Immunity *32*, 317–328.

Gilliet, M., Boonstra, A., Paturel, C., Antonenko, S., Xu, X.-L., Trinchieri, G., O'Garra, A., and Liu, Y.-J. (2002). The development of murine plasmacytoid dendritic cell precursors is differentially regulated by FLT3-ligand and granulocyte/macrophage colony-stimulating factor. J. Exp. Med. *195*, 953–958.

Ginhoux, F., Tacke, F., Angeli, V., Bogunovic, M., Loubeau, M., Dai, X.-M., Stanley, E.R., Randolph, G.J., and Merad, M. (2006). Langerhans cells arise from monocytes in vivo. Nat. Immunol. *7*, 265–273.

Ginhoux, F., Liu, K., Helft, J., Bogunovic, M., Greter, M., Hashimoto, D., Price, J., Yin, N., Bromberg, J., Lira, S. a, et al. (2009). The origin and development of nonlymphoid tissue CD103+ DCs. J. Exp. Med. *206*, 3115–3130.

Gosselin, D., Link, V.M., Romanoski, C.E., Fonseca, G.J., Eichenfield, D.Z., Spann, N.J., Stender, J.D., Chun, H.B., Garner, H., Geissmann, F., et al. (2014). Environment Drives Selection and Function of Enhancers Controlling Tissue-Specific Macrophage Identities. Cell *159*, 1327–1340.

Grajales-Reyes, G.E., Iwata, A., Albring, J., Wu, X., Tussiwand, R., Kc, W., Kretzer, N.M., Briseño, C.G., Durai, V., Bagadia, P., et al. (2015). Batf3 maintains autoactivation of Irf8 for commitment of a CD8α+ conventional DC clonogenic progenitor. Nat. Immunol. *16*, 708–717.

Granger, D.L., Hibbs, J.B., Perfect, J.R., and Durack, D.T. (1990). Metabolic fate of L-arginine in relation to microbiostatic capability of murine macrophages. J. Clin. Invest. *85*, 264–273.

Green, L.C., Ruiz de Luzuriaga, K., Wagner, D.A., Rand, W., Istfan, N., Young, V.R., and Tannenbaum, S.R. (1981). Nitrate biosynthesis in man. Proc Natl Acad Sci U S A *78*, 7764–7768.

Greter, M., Helft, J., Chow, A., Hashimoto, D., Mortha, A., Agudo-Cantero, J., Bogunovic, M., Gautier, E.L., Miller, J., Leboeuf, M., et al. (2012). GM-CSF Controls Nonlymphoid Tissue Dendritic Cell Homeostasis but Is Dispensable for the Differentiation of Inflammatory Dendritic Cells. Immunity *36*, 1031–1046.

Guermonprez, P., Helft, J., Claser, C., Deroubaix, S., Karanje, H., Gazumyan, A., Darasse-Jèze, G., Telerman, S.B., Breton, G., Schreiber, H. a, et al. (2013). Inflammatory Flt3l is essential to mobilize dendritic cells and for T cell responses during Plasmodium infection. Nat. Med. *19*, 730–738.

Guerriero, A., Langmuir, P.B., Spain, L.M., and Scott, E.W. (2000). PU.1 is required for myeloid-derived but not lymphoid-derived dendritic cells. Blood *95*, 879–885.

Guilliams, M., Movahedi, K., Bosschaerts, T., Vandendriessche, T., Chuah, M.K., Acosta-sanchez, A., Ma, L., Moser, M., Jo, A., Ginderachter, V., et al. (2009). IL-10 Dampens TNF/Inducible Nitric Oxide Synthase-Producing Dendritic Cell-Mediated Pathogenicity during Parasitic Infection. J Immunol *182*, 1107–1118.

Guilliams, M., Ginhoux, F., Jakubzick, C., Naik, S.H., Onai, N., Schraml, B.U., Segura, E., Tussiwand, R., and Yona, S. (2014). Dendritic cells, monocytes and macrophages: a unified nomenclature based on ontogeny TL - 14. Nat. Rev. Immunol. *14*, 571–578.

Gundra, U.M., Girgis, N.M., Ruckerl, D., Jenkins, S., Ward, L.N., Kurtz, Z.D., Wiens, K.E., Tang, M.S., Basu-Roy, U., Mansukhani, A., et al. (2014). Alternatively activated macrophages derived from monocytes and tissue macrophages are phenotypically and functionally distinct. Blood *123*, 110–123.

Gutiérrez-Martínez, E., Planès, R., Anselmi, G., Reynolds, M., Menezes, S., Adiko, A.C., Saveanu, L., and Guermonprez, P. (2015). Cross-Presentation of Cell-Associated Antigens by MHC Class I in Dendritic Cell Subsets. Front. Immunol. *6*, 363.

Hacker, C., Kirsch, R.D., Ju, X.-S., Hieronymus, T., Gust, T.C., Kuhl, C., Jorgas, T., Kurz, S.M., Rose-John, S., Yokota, Y., et al. (2003). Transcriptional profiling identifies Id2 function in dendritic cell development. Nat. Immunol. *4*, 380–386.

Hamilton, J.A. (2002). GM-CSF in inflammation and autoimmunity. Trends Immunol. *23*, 403–408.

Hanada, K., Tsunoda, R., and Hamada, H. (1996). GM-CSF-induced in vivo expansion of splenic dendritic cells and their strong costimulation activity. J. Leukoc. Biol. *60*, 181–190.

Hanna, R.N., Carlin, L.M., Hubbeling, H.G., Nackiewicz, D., Green, A.M., Punt, J.A., Geissmann, F., and Hedrick, C.C. (2011). The transcription factor NR4A1 (Nur77) controls bone marrow differentiation and the survival of Ly6C- monocytes. Nat. Immunol. *12*, 778–785.

Hatachi, S., Iwai, Y., Kawano, S., Morinobu, S., Kobayashi, M., Koshiba, M., Saura, R., Kurosaka, M., Honjo, T., and Kumagai, S. (2003). CD4+ PD-1+ T cells accumulate as unique anergic cells in rheumatoid arthritis synovial fluid. J. Rheumatol. *30*, 1410–1419.

Helft, J., Böttcher, J., Chakravarty, P., Zelenay, S., Huotari, J., Schraml, B.U., Goubau, D., and Reis e Sousa, C. (2015). GM-CSF Mouse Bone Marrow Cultures Comprise a Heterogeneous Population of CD11c+MHCII+ Macrophages and Dendritic Cells. Immunity *42*, 1197–1211.

Hettinger, J., Richards, D.M., Hansson, J., Barra, M.M., Joschko, A.-C., Krijgsveld, J., and Feuerer, M. (2013). Origin of monocytes and macrophages in a committed progenitor. Nat. Immunol. *14*, 821–830.

Hildner, K., Edelson, B.T., Purtha, W.E., Diamond, M.M.S., Matsushita, H., Kohyama, M., Calderon, B., Schraml, B.U., Unanue, E.R., Diamond, M.M.S., et al. (2008). Batf3 Deficiency Reveals a Critical Role for CD8a+ Dendritic Cells in Cytotoxic T Cell Immunity. Science *1144*, 1097–1100.

Hohaus, S., Petrovick, M.S., Voso, M.T., Sun, Z., Zhang, D.E., and Tenen, D.G. (1995). PU.1 (Spi-1) and C/EBP alpha regulate expression of the granulocyte-macrophage colony-stimulating factor receptor alpha gene. Mol. Cell. Biol. *15*, 5830–5845.

Holtschke, T., Löhler, J., Kanno, Y., Fehr, T., Giese, N., Rosenbauer, F., Lou, J., Knobeloch, K.P., Gabriele, L., Waring, J.F., et al. (1996). Immunodeficiency and chronic myelogenous leukemia-like syndrome in mice with a targeted mutation of the ICSBP gene. Cell *87*, 307–317.

Hong, I.-S. (2016). Stimulatory versus suppressive effects of GM-CSF on tumor progression in multiple cancer types. Exp. Mol. Med. *48*, e242.

Huang, H., Chan, J., Wittner, M., Jelicks, L.A., Morris, S.A., Factor, S.M., Weiss, L.M., Braunstein, V.L., Bacchi, C.J., Yarlett, N., et al. (1999). Expression of Cardiac Cytokines and Inducible Form of Nitric Oxide Synthase (NOS2) inTrypanosoma cruzi-infected Mice. J. Mol. Cell. Cardiol. *31*, 75–88.

Ichikawa, M., Asai, T., Saito, T., Yamamoto, G., Seo, S., Yamazaki, I., Yamagata, T., Mitani, K., Chiba, S., Hirai, H., et al. (2004). AML-1 is required for megakaryocytic maturation and lymphocytic differentiation , but not for maintenance of hematopoietic stem cells in adult hematopoiesis. *10*, 299–304.

Inaba, K., Inaba, M., Romani, N., Aya, H., Deguchi, M., Ikehara, S., Muramatsu, S., and Steinman, R.M. (1992). Generation of large numbers of dendritic cells from mouse bone marrow cultures supplemented with granulocyte/macrophage colony-stimulating factor. J. Exp. Med. *176*, 1693–1702.

Ishizuka, I.E., Chea, S., Gudjonson, H., Constantinides, M.G., Dinner, A.R., Bendelac, A., and Golub, R. (2016). Single-cell analysis defines the divergence between the innate lymphoid cell lineage and lymphoid tissue – inducer cell lineage. Nat. Immunol. *17*, 269–276.

Issaad, C., Croisille, L., Katz, A., Vainchenker, W., and Coulombel, L. (1993). A Murine Stromal Cell Line Allows the Proliferation of Very Primitive Human CD34 +. Blood *81*, 2916–2924.

Ito, T., Nishiyama, C., Nakano, N., Nishiyama, M., Usui, Y., Takeda, K., Kanada, S., Fukuyama, K., Akiba, H., Tokura, T., et al. (2009). Roles of PU.1 in monocyte- and mast cell-specific gene regulation: PU.1 transactivates CIITA pIV in cooperation with IFN-γ. Int. Immunol. *21*, 803–816.

Ivashkiv, L.B., and Donlin, L.T. (2013). Regulation of type I interferon responses. Nat. Rev. Immunol. *14*, 36–49.

Jaitin, D.A., Kenigsberg, E., Keren-shaul, H., and Elefant, N. (2015). Massively parallel single cell RNA-Seq for marker-free decomposition of tissues into cell types. Science *343*, 776–779.

Jakubzick, C., Gautier, E.L., Gibbings, S.L., Sojka, D.K., Schlitzer, A., Johnson, T.E., Ivanov, S., Duan, Q., Bala, S., Condon, T., et al. (2013). Minimal differentiation of classical monocytes as they survey steady-state tissues and transport antigen to lymph nodes. Immunity *39*, 599–610.

Jiao, X., Lo-Man, R., Guermonprez, P., Fiette, L., Deriaud, E., Burgaud, S., Gicquel, B., Winter, N., and Leclerc, C. (2002). Dendritic Cells Are Host Cells for Mycobacteria In Vivo That Trigger Innate and Acquired Immunity. J. Immunol. *168*, 1294–1301.

Jiao, Z., Bedoui, S., Brady, J.L., Walter, A., Chopin, M., Carrington, E.M., Sutherland, R.M., Nutt, S.L., Zhang, Y., Ko, H.-J., et al. (2014). The Closely Related CD103+ Dendritic Cells (DCs) and Lymphoid-Resident CD8+ DCs Differ in Their Inflammatory Functions. PLoS One *9*, e91126.

Kang, S.-J., Liang, H.-E., Reizis, B., and Locksley, R.M. (2008). Regulation of hierarchical clustering and activation of innate immune cells by dendritic cells. Immunity *29*, 819–833.

Karsunky, H., Merad, M., Cozzio, A., Weissman, I.L., and Manz, M.G. (2003). Flt3 ligand regulates dendritic cell development from Flt3+ lymphoid and myeloid-committed progenitors to Flt3+ dendritic cells in vivo. J. Exp. Med. *198*, 305–313.

Kashiwada, M., Pham, N.-L.L., Pewe, L.L., Harty, J.T., Rothman, P.B., and Dc, W. (2011). NFIL3 / E4BP4 is a key transcription factor for CD8a+ dendritic cell development. Blood *117*, 6193–6197.

Kaufmann, S.H.E. (2008). Immunology's foundation: the 100-year anniversary of the Nobel Prize to Paul Ehrlich and Elie Metchnikoff. Nat. Immunol. *9*, 705–712.

Kingston, D., Schmid, M. a, Onai, N., Obata-onai, A., Baumjohann, D., Markus, G., Dc, W., and Manz, M.G. (2009a). The concerted action of GM-CSF and Flt3-ligand on in vivo dendritic cell homeostasis The concerted action of GM-CSF and Flt3-ligand on in vivo dendritic cell homeostasis. *114*, 835–843.

Kingston, D., Schmid, M.A., Onai, N., Obata-Onai, A., Baumjohann, D., Manz, M.G., Shortman, K., Liu, Y., Valladeau, J., Saeland, S., et al. (2009b). The concerted action of GM-CSF and Flt3-ligand on in vivo dendritic cell homeostasis. Blood *114*, 835–843.

Kitamura, N., Yokoyama, H., Yashiro, T., Nakano, N., Nishiyama, M., Kanada, S., Fukai, T., Hara, M., Ikeda, S., Ogawa, H., et al. (2012). Role of PU.1 in MHC class II expression through transcriptional regulation of class II transactivator pI in dendritic cells. J. Allergy Clin. Immunol. *129*, 814–824.e6.

Kobari, L., Dubart, A., Le Pesteur, F.F., Vainchenker, W., and Sainteny, F.F. (1995). Hematopoietic-Promoting activity of the murine stromal cell line MS-5 is not related to the expression of themajor hematopoietic cytokines.

Kondo, M., Weissman, I.L., and Akashi, K. (1997). Identification of Clonogenic Common Lymphoid Progenitors in Mouse Bone Marrow. Cell *91*, 661–672.

Konishi, J., Yamazaki, K., Azuma, M., Kinoshita, I., Dosaka-Akita, H., and Nishimura, M. (2004). B7-H1 expression on non-small cell lung cancer cells and its relationship with tumor-infiltrating lymphocytes and their PD-1 expression. Clin. Cancer Res. *10*, 5094–5100.

Kurihara, T., Warr, G., Loy, J., and Bravo, R. (1997). Defects in macrophage recruitment and host defense in mice lacking the CCR2 chemokine receptor. J. Exp. Med. *186*, 1757–1762.

Van De Laar, L., Coffer, P.J., and Woltman, A.M. (2012). Regulation of dendritic cell development by GM-CSF: Molecular control and implications for immune homeostasis and therapy. Blood *119*, 3383–3393.

Laiosa, C. V., Stadtfeld, M., Xie, H., de Andres-Aguayo, L., and Graf, T. (2006). Reprogramming of Committed T Cell Progenitors to Macrophages and Dendritic Cells by C/EBPa and PU.1 Transcription Factors. Immunity *25*, 731–744.

Latchman, Y., Wood, C.R., Chernova, T., Chaudhary, D., Borde, M., Chernova, I., Iwai, Y., Long, A.J., Brown, J.A., Nunes, R., et al. (2001). PD-L2 is a second ligand for PD-1 and inhibits T cell activation. Nat. Immunol. *2*, 261–268.

Lavin, Y., Winter, D., Blecher-gonen, R., David, E., Keren-shaul, H., and Merad, M. (2014). Tissue-Resident Macrophage Enhancer Landscapes Are Shaped by the Local Microenvironment. Cell *159*, 1312–1326.

Lavine, K.J., Epelman, S., Uchida, K., Weber, K.J., Nichols, C.G., Schilling, J.D., David, M., Randolph, G.J., Mann, D.L., Lavine, K.J., et al. (2016). Correction for Lavine et al., Distinct macrophage lineages contribute to disparate patterns of cardiac recovery and remodeling in the neonatal and adult heart. Proc Natl Acad Sci U S A *113*, E1414.

LeibundGut-Landmann, S., Waldburger, J.-M., Reis e Sousa, C., Acha-Orbea, H., and Reith, W. (2004). MHC class II expression is differentially regulated in plasmacytoid and conventional dendritic cells. Nat. Immunol. *5*, 899–908.

Lenzo, J.C., Turner, A.L., Cook, A.D., Vlahos, R., Anderson, G.P., Reynolds, E.C., and Hamilton, J. a (2012). Control of macrophage lineage populations by CSF-1 receptor and GM-CSF in homeostasis and inflammation. Immunol. Cell Biol. *90*, 429–440.

León, B., López-Bravo, M., and Ardavín, C. (2007). Monocyte-Derived Dendritic Cells Formed at the Infection Site Control the Induction of Protective T Helper 1 Responses against Leishmania. Immunity *26*, 519–531.

Lesokhin, A.M., Hohl, T.M., Kitano, S., Cortez, C., Hirschhorn-Cymerman, D., Avogadri, F.,

Rizzuto, G. a., Lazarus, J.J., Pamer, E.G., Houghton, A.N., et al. (2012). Monocytic CCR2 + myeloid-derived suppressor cells promote immune escape by limiting activated CD8 T-cell infiltration into the tumor microenvironment. Cancer Res. *72*, 876–886.

Lewis, K.L., Caton, M.L., Bogunovic, M., Greter, M., Grajkowska, L.T., Ng, D., Klinakis, A., Charo, I.F., Jung, S., Gommerman, J.L., et al. (2011). Notch2 receptor signaling controls functional differentiation of dendritic cells in the spleen and intestine. Immunity *35*, 780–791.

Liaskou, E., Zimmermann, H.W., Li, K.-K., Oo, Y.H., Suresh, S., Stamataki, Z., Qureshi, O., Lalor, P.F., Shaw, J., Syn, W., et al. (2013). Monocyte subsets in human liver disease show distinct phenotypic and functional characteristics. Hepatology *57*, 385–398.

Lichanska, A.M., Browne, C.M., Henkel, G.W., Murphy, K.M., Ostrowski, M.C., McKercher, S.R., Maki, R.A., and Hume, D.A. (1999). Differentiation of the mononuclear phagocyte system during mouse embryogenesis: the role of transcription factor PU.1. Blood *94*, 127–138.

Liew, F.Y., Li, Y., Millott, S., and Millott, S. (1990). Tumor necrosis factor-alpha synergizes with IFN-gamma in mediating killing of Leishmania major through the induction of nitric oxide. J. Immunol. *145*, 4306–4310.

Liu, K., Waskow, C., Liu, X., Yao, K., Hoh, J., and Nussenzweig, M. (2007). Origin of dendritic cells in peripheral lymphoid organs of mice. Nat. Immunol. *8*, 578–583.

Lloberas, J., Soler, C., and Celada, A. (1999). The key role of PU.1/SPI-1 in B cells, myeloid cells and macrophages. Immunol. Today *20*, 184–189.

Loschko, J., Rieke, G.J., Schreiber, H.A., Meredith, M.M., Yao, K.H., Guermonprez, P., and Nussenzweig, M.C. (2016a). Inducible targeting of cDCs and their subsets in vivo. J. Immunol. Methods *434*, 32–38.

Loschko, J., Schreiber, H.A., Rieke, G.J., Esterházy, D., Meredith, M.M., Pedicord, V.A., Yao, K.-H., Caballero, S., Pamer, E.G., Mucida, D., et al. (2016b). Absence of MHC class II on cDCs results in microbial-dependent intestinal inflammation. J. Exp. Med. *213*, 517–534.

Vander Lugt, B., Khan, A.A., Hackney, J.A., Agrawal, S., Lesch, J., Zhou, M., Lee, W.P., Park, S., Xu, M., DeVoss, J., et al. (2014). Transcriptional programming of dendritic cells for enhanced MHC class II antigen presentation. Nat. Immunol. *15*, 161–167.

MacDonald, K.P.A., Rowe, V., Bofinger, H.M., Thomas, R., Sasmono, T., Hume, D.A., and Hill, G.R. (2005). The colony-stimulating factor 1 receptor is expressed on dendritic cells during differentiation and regulates their expansion. J. Immunol. *175*, 1399–1405.

Madisen, L., Mao, T., Koch, H., Zhuo, J., Berenyi, A., Fujisawa, S., Hsu, Y.-W.A., Garcia, A.J., Gu, X., Zanella, S., et al. (2012). A toolbox of Cre-dependent optogenetic transgenic mice for light-induced activation and silencing. Nat. Neurosci. *15*, 793–802.

Mashayekhi, M., Sandau, M.M., Dunay, I.R., Frickel, E.M., Khan, A., Goldszmid, R.S., Sher, A., Ploegh, H.L., Murphy, T.L., Sibley, L.D., et al. (2011). CD8α(+) dendritic cells are the critical source of interleukin-12 that controls acute infection by Toxoplasma gondii tachyzoites. Immunity *35*, 249–259.

Mass, E., Ballesteros, I., Farlik, M., Halbritter, F., Günther, P., Crozet, L., Jacome-galarza, C.E., Händler, K., Klughammer, J., Kobayashi, Y., et al. (2016). Specification of tissue-resident macrophages during organogenesis. Science *353*, aaf4238-1-aaf4238-12.

Matthews, W., Jordan, C.T., Wiegand, G.W., Pardoll, D., and Lemischka, I.R. (1991). A receptor tyrosine kinase specific to hematopoietic stem and progenitor cell-enriched populations. Cell *65*, 1143–1152.

Mayer, C.T., Ghorbani, P., Nandan, A., Dudek, M., Arnold-Schrauf, C., Hesse, C., Berod, L., Stüve, P., Puttur, F., Merad, M., et al. (2015). Selective and ef fi cient generation of functional Batf3-dependent CD103 1 dendritic cells from mouse bone marrow. Blood *124*, 3081–3092.

McKenna, H.J., Stocking, K.L., Miller, R.E., Brasel, K., De Smedt, T., Maraskovsky, E., Maliszewski, C.R., Lynch, D.H., Smith, J., Pulendran, B., et al. (2000). Mice lacking flt3 ligand have deficient hematopoiesis affecting hematopoietic progenitor cells, dendritic cells, and natural killer cells. Blood *95*, 3489–3497.

McKercher, S.R., Torbett, B.E., Anderson, K.L., Henkel, G.W., Vestal, D.J., Baribault, H., Klemsz, M., Feeney, A.J., Wu, G.E., Paige, C.J., et al. (1996). Targeted disruption of the PU.1 gene results in multiple hematopoietic abnormalities. EMBO J. *15*, 5647–5658.

Medvinsky, A., and Dzierzak, E. (1996). Definitive hematopoiesis is autonomously initiated by the AGM region. Cell *86*, 897–906.

Mellman, I., Turley, S.J., and Steinman, R.M. (1998). Antigen processing for amateurs and professionals. Trends Cell Biol. *8*, 231–237.

Meredith, M.M., Liu, K., Darrasse-Jeze, G., Kamphorst, A.O., Schreiber, H.A., Guermonprez, P., Idoyaga, J., Cheong, C., Yao, K.-H., Niec, R.E., et al. (2012). Expression of the zinc finger transcription factor zDC (Zbtb46, Btbd4) defines the classical dendritic cell lineage. J. Exp. Med. *209*, 1153–1165.

Mortha, A., Chudnovskiy, A., Hashimoto, D., Bogunovic, M., Spencer, S.P., Belkaid, Y., and Merad, M. (2014). Microbiota-Dependent Crosstalk Between Macrophages and ILC3 Promotes Intestinal Homeostasis. Science *343*, 1249288.

Mucenski, M.L., McLain, K., Kier, A.B., Swerdlow, S.H., Schreiner, C.M., Miller, T.A., Pietryga, D.W., Scott, W.J., and Potter, S.S. (1991). A functional c-myb gene is required for normal murine fetal hepatic hematopoiesis. Cell *65*, 677–689.

Müller, A.M., Medvinsky, A., Strouboulis, J., Grosveld, F., and Dzierzak, E. (1994). Development of hematopoietic stem cell activity in the mouse embryo. Immunity *1*, 291–301.

Nahrendorf, M., Pittet, M.J., and Swirski, F.K. (2010). Monocytes: Protagonists of infarct inflammation and repair after myocardial infarction. Circulation *121*, 2437–2445.

Naik, S.H., Metcalf, D., Nieuwenhuijze, A. Van, Wicks, I., Wu, L., Keeffe, M.O., and Shortman, K. (2006). Intrasplenic steady-state dendritic cell precursors that are distinct from monocytes. Nat. Immunol. *7*, 663–671.

Naik, S.H., Perie, L., Swart, E., Gerlach, C., van Rooij, N., de Boer, R.J., and Schumacher, T.N. (2013). Diverse and heritable lineage imprinting of early haematopoietic progenitors. Nature *496*, 229–232.

Narni-Mancinelli, E., Campisi, L., Bassand, D., Cazareth, J., Gounon, P., Glaichenhaus, N., and Lauvau, G. (2007). Memory CD8+ T cells mediate antibacterial immunity via CCL3 activation of TNF/ROI+ phagocytes. J. Exp. Med. *204*, 2075–2087.

Nascimento, M., Huang, S.C., Smith, A., Everts, B., Lam, W., Bassity, E., Gautier, E.L., Randolph, G.J., and Pearce, E.J. (2014). Ly6Chi monocyte recruitment is responsible for Th2 associated host-protective macrophage accumulation in liver inflammation due to schistosomiasis. PLoS Pathog. *10*, e1004282.

Nguyen, L.T., and Ohashi, P.S. (2015). Clinical blockade of PD1 and LAG3 — potential mechanisms of action. Nat. Publ. Gr. *15*, 45–56.

Nishimura, H., Nose, M., Hiai, H., Minato, N., and Honjo, T. (1999). Development of lupus-like autoimmune diseases by disruption of the PD-1 gene encoding an ITIM motif-carrying immunoreceptor. Immunity *11*, 141–151.

Notta, F., Zandi, S., Takayama, N., Dobson, S., Gan, O.I., Wilson, G., Kaufmann, K.B., Mcleod, J., Laurenti, E., Dunant, C.F., et al. (2015). Distinct routes of lineage development reshape the human blood hierarchy across ontogeny. Science *351*, 1–16.

Nutt, S.L., Metcalf, D., D'Amico, A., Polli, M., and Wu, L. (2005). Dynamic regulation of PU.1

expression in multipotent hematopoietic progenitors. J. Exp. Med. *201*, 221–231.

Ogawa, M., Matsuzaki, Y., Nishikawa, S., Hayashi, S.-I., Kunisada, T., Sudo, T., Kina, T., Nakauchi, H., and Nishikawa, S.-I. (1991). Expression and Function of c-kit in Hemopoietic Progenitor Cells. J. Exp. Med. *174*, 63–71.

Ohyagi, H., Onai, N., Sato, T., Yotsumoto, S., Liu, J., Akiba, H., Yagita, H., Atarashi, K., Honda, K., Roers, A., et al. (2013). Monocyte-Derived Dendritic Cells Perform Hemophagocytosis to Fine-Tune Excessive Immune Responses. Immunity *39*, 584–598.

Okabe, Y., and Medzhitov, R. (2014). Tissue-specific signals control reversible program of localization and functional polarization of macrophages. Cell *157*, 832–844.

Olekhnovitch, R., Ryffel, B., Müller, A.J., and Bousso, P. (2014). Collective nitric oxide production provides tissue-wide immunity during Leishmania infection. J. Clin. Invest. *124*, 1711–1722.

Onai, N., Obata-Onai, A., Schmid, M. a, Ohteki, T., Jarrossay, D., and Manz, M.G. (2007). Identification of clonogenic common Flt3+M-CSFR+ plasmacytoid and conventional dendritic cell progenitors in mouse bone marrow. Nat. Immunol. *8*, 1207–1216.

Onai, N., Kurabayashi, K., Hosoi-Amaike, M., Toyama-Sorimachi, N., Matsushima, K., Inaba, K., and Ohteki, T. (2013). A clonogenic progenitor with prominent plasmacytoid dendritic cell developmental potential. Immunity *38*, 943–957.

Paolicelli, R.C., Bolasco, G., Pagani, F., Maggi, L., Scianni, M., Panzanelli, P., Giustetto, M., Ferreira, T.A., Guiducci, E., Dumas, L., et al. (2011). Synaptic pruning by microglia is necessary for normal brain development. Science *333*, 1456–1458.

Perez, C., Coeffier, E., Moreau-Gachelin, F., Wietzerbin, J., and Benech, P.D. (1994). Involvement of the transcription factor PU.1/Spi-1 in myeloid-restricted expression of an interferon-inducible gene encoding the human high-affinity Fc gamma receptor. Mol.Cell.Biol. *14*, 5023–5031.

Plantinga, M., Guilliams, M., Vanheerswynghels, M., Deswarte, K., Branco-Madeira, F., Toussaint, W., Vanhoutte, L., Neyt, K., Killeen, N., Malissen, B., et al. (2013). Conventional and Monocyte-Derived CD11b+ Dendritic Cells Initiate and Maintain T Helper 2 Cell-Mediated Immunity to House Dust Mite Allergen. Immunity *38*, 322–335.

Pluznik, D.H., and Sachs, L. (1966). The induction of clones of normal mast cells by a subsetance from conditioned medium. *563*, 553–563.

Poltorak, M.P., and Schraml, B.U. (2015). Fate mapping of dendritic cells. Front. Immunol. *6*, 199.

Poulin, L.F., Reyal, Y., Uronen-Hansson, H., Schraml, B.U., Sancho, D., Murphy, K.M., Håkansson, U.K., Moita, L.F., Agace, W.W., Bonnet, D., et al. (2012). DNGR-1 is a specific and universal marker of mouse and human Batf3-dependent dendritic cells in lymphoid and nonlymphoid tissues. Blood *119*, 6052–6062.

Poussin, M.A., and Goldfine, H. (2010). Evidence for the involvement of ActA in maturation of the Listeria monocytogenes phagosome. Cell Res. *20*, 109–112.

Pylayeva-Gupta, Y., Lee, K.E., Hajdu, C.H., Miller, G., and Bar-Sagi, D. (2012). Oncogenic Kras-Induced GM-CSF Production Promotes the Development of Pancreatic Neoplasia. Cancer Cell *21*, 836–847.

Qian, F., Deng, J., Lee, Y.G., Zhu, J., Karpurapu, M., Chung, S., Zheng, J.-N., Xiao, L., Park, G.Y., and Christman, J.W. (2015). The transcription factor PU.1 promotes alternative macrophage polarization and asthmatic airway inflammation. J. Mol. Cell Biol.

Randolph, G.J., Inaba, K., Robbiani, D.F., Steinman, R.M., and Muller, W.A. (1999). Differentiation of Phagocytic Monocytes into Lymph Node Dendritic Cells In Vivo. Immunity

*11*, 753–761.

Rio, M., Bölter, J., Ballmaier, M., Dittrich-Breiholz, O., Kracht, M., Jung, S., Förster, R., Bo, J., Fo, R., Del Rio, M.-L., et al. (2008). CX3CR1+c-kit+ Bone Marrow Cells Give Rise to CD103+ and CD103- Dendritic Cells with Distinct Functional Properties. J. Immunol. *181*.

del Rio, M.-L., Rodriguez-Barbosa, J.-I., Kremmer, E., and Förster, R. (2007). CD103- and CD103+ bronchial lymph node dendritic cells are specialized in presenting and cross-presenting innocuous antigen to CD4+ and CD8+ T cells. J. Immunol. *178*, 6861–6866.

Ross, I.L., Yue, X., Ostrowski, M.C., and Hume, D.A. (1998). Interaction between PU . 1 and Another Ets Family Transcription Factor Promotes Macrophage-specific Basal Transcription Initiation *. Journalof Biol. Chem. *273*, 6662–6669.

Sabin, F., Doan, C., and Cunningham, R. (1925). Discrimination of two types of phagocytic cells in the connective tissues by the supravital technique. Contrib. Embryol. (Am) *16*, 125–162.

Sallusto, B.F., and Lanzavecchia, A. (1994a). Dendritic cell use macropinocytosis and the mannose receptor to concetrate macromolecules in the major histocompatibility complex classII compartment: downregulation by cytokines and bacterial products. J. Exp. Med. *179*.

Sallusto, F., and Lanzavecchia, A. (1994b). Efficient presentation of soluble antigen by cultured human dendritic cells is maintained by granulocyte/macrophage colony-stimulating factor plus interleukin 4 and downregulated by tumor necrosis factor alpha. J. Exp. Med. *179*, 1109–1118.

Sánchez, M.J., Holmes, A., Miles, C., and Dzierzak, E. (1996). Characterization of the first definitive hematopoietic stem cells in the AGM and liver of the mouse embryo. Immunity *5*, 513–525.

Satpathy, A.T., KC, W., Albring, J.C., Edelson, B.T., Kretzer, N.M., Bhattacharya, D., Murphy, T.L., and Murphy, K.M. (2012a). Zbtb46 expression distinguishes classical dendritic cells and their committed progenitors from other immune lineages. J. Exp. Med. *209*, 1135–1152.

Satpathy, A.T., Wu, X., Albring, J.C., and Murphy, K.M. (2012b). Re(de)fining the dendritic cell lineage. Nat. Immunol. *13*, 1145–1154.

Satpathy, A.T., Briseño, C.G., Lee, J.S., Ng, D., Manieri, N.A., Kc, W., Wu, X., Thomas, S.R., Lee, W.-L., Turkoz, M., et al. (2013). Notch2-dependent classical dendritic cells orchestrate intestinal immunity to attaching-and-effacing bacterial pathogens. Nat. Immunol. *14*, 937–948.

Schiavoni, G., Mattei, F., Sestili, P., Borghi, P., Venditti, M., Morse, H.C., Belardelli, F., and Gabriele, L. (2002). ICSBP is essential for the development of mouse type I interferon-producing cells and for the generation and activation of CD8alpha(+) dendritic cells. J. Exp. Med. *196*, 1415–1425.

Schlitzer, A., Sivakamasundari, V., Chen, J., Sumatoh, H.R. Bin, Schreuder, J., Lum, J., Malleret, B., Zhang, S., Larbi, A., Zolezzi, F., et al. (2015). Identification of cDC1- and cDC2-committed DC progenitors reveals early lineage priming at the common DC progenitor stage in the bone marrow. Nat Immunol *16*, 718–728.

Schraml, B.U., Van Blijswijk, J., Zelenay, S., Whitney, P.G., Filby, A., Acton, S.E., Rogers, N.C., Moncaut, N., Carvajal, J.J., and Reis E Sousa, C. (2013). Genetic tracing via DNGR-1 expression history defines dendritic cells as a hematopoietic lineage. Cell *154*, 843–858.

Schreiber, H. a, Loschko, J., Karssemeijer, R. a, Escolano, A., Meredith, M.M., Mucida, D., Guermonprez, P., and Nussenzweig, M.C. (2013). Intestinal monocytes and macrophages are required for T cell polarization in response to Citrobacter rodentium. J. Exp. Med. *210*, 2025–2039.

Schulz, C., Gomez Perdiguero, E., Chorro, L., Szabo-Rogers, H., Cagnard, N., Kierdorf, K., Prinz, M., Wu, B., Jacobsen, S.E.W., Pollard, J.W., et al. (2012). A lineage of myeloid cells independent of Myb and hematopoietic stem cells. Science *336*, 86–90.

Scott, C.L., Bain, C.C., Wright, P.B., Sichien, D., Kotarsky, K., Persson, E.K., Luda, K., Guilliams, M., Lambrecht, B.N., Agace, W.W., et al. (2014). CCR2(+)CD103(-) intestinal dendritic cells develop from DC-committed precursors and induce interleukin-17 production by T cells. Mucosal Immunol. *8*, 327–339.

Scott, E.W., Simon, M.C., Anastasi, J., and Singh, H. (1994). Requirement of transcription factor PU.1 in the development of multiple hematopoietic lineages. Science *265*, 1573–1577.

Segura, E., and Amigorena, S. (2013). Inflammatory dendritic cells in mice and humans. Trends Immunol. *34*, 440–445.

Segura, E., Touzot, M., Bohineust, A., Cappuccio, A., Chiocchia, G., Hosmalin, A., Dalod, M., Soumelis, V., and Amigorena, S. (2013). Human Inflammatory Dendritic Cells Induce Th17 Cell Differentiation. Immunity *38*, 336–348.

Serbina, N. V, Salazar-Mather, T.P., Biron, C. a, Kuziel, W. a, and Pamer, E.G. (2003). TNF/iNOS-producing dendritic cells mediate innate immune defense against bacterial infection. Immunity *19*, 59–70.

Serbina, N. V, Jia, T., Hohl, T.M., and Pamer, E.G. (2008). Monocyte-mediated defense against microbial pathogens. Annu. Rev. Immunol. *26*, 421–452.

Shao, Z., Bharadwaj, A.S., McGee, H.S., Makinde, T.O., and Agrawal, D.K. (2009). Fms-like tyrosine kinase 3 ligand increases a lung DC subset with regulatory properties in allergic airway inflammation. J. Allergy Clin. Immunol. *123*, 917–924.e2.

Singh, A.K., Stock, P., and Akbari, O. (2011). Role of PD-L1 and PD-L2 in allergic diseases and asthma. Allergy *66*, 155–162.

Soares, K.C., Rucki, A.A., Wu, A.A., Olino, K., Xiao, Q., Chai, Y., Wamwea, A., Bigelow, E., Lutz, E., Liu, L., et al. (2015). PD-1/PD-L1 blockade together with vaccine therapy facilitates effector T-cell infiltration into pancreatic tumors. J. Immunother. *38*, 1–11.

Sprangers, S., Vries, T.J. De, and Everts, V. (2016). Monocyte Heterogeneity : Consequences for Monocyte-Derived Immune Cells. J. Immunol. Res. *2016*, 1–10.

Stanley, E.R., and Heard, P.M. (1977). Factors Regulating Macrophage Production and Growth. J. Biol. Chem. *252*, 4305–4312.

Stanley, E.R., Hansen, G., Woodcock, J., and Metcalf, D. (1975). Colony stimulating factor and the regulation of granulopoiesis and macrophage production. Fed. Proc. *34*, 2272–2278.

Steinman, R., and Cohn, Z. (1973). Identification of a novel cell type in peripheral lymphoid organs of mice. I. Morphology, quantitation, tissue distribution. J. Exp. Med. *137*, 1142–1162.

Steinman, R.M., and Witmer, M.D. (1978). Lymphoid dendritic cells are potent stimulators of the primary mixed leukocyte reaction in mice Immunology : October *75*, 5132–5136.

Stenger, S., Thüring, H., Röllinghoff, M., and Bogdan, C. (1994). Tissue expression of inducible nitric oxide synthase is closely associated with resistance to Leishmania major. J. Exp. Med. *180*, 783–793.

Stopka, T., Amanatullah, D.F., Papetti, M., and Skoultchi, A.I. (2005). PU.1 inhibits the erythroid program by binding to GATA-1 on DNA and creating a repressive chromatin structure. EMBO J. *24*, 3712–3723.

Storozynsky, E., Woodward, J.G., Frelinger, J.G., and Lord, E.M. (1999). Interleukin-3 and granulocyte-macrophage colony-stimulating factor enhance the generation and function of dendritic cells. Immunology *97*, 138–149.

Tacke, R., Hilgendorf, I., Garner, H., Waterborg, C., Park, K., Nowyhed, H., Hanna, R.N., Wu, R., Swirski, F.K., Geissmann, F., et al. (2015). The transcription factor NR4A1 is essential for the development of a novel macrophage subset in the thymus. Sci. Rep. *5*, 10055.

Taganov, K.D., Boldin, M.P., Chang, K.-J., and Baltimore, D. (2006). NF-kappaB-dependent induction of microRNA miR-146, an inhibitor targeted to signaling proteins of innate immune responses. Proc. Natl. Acad. Sci. U. S. A. *103*, 12481–12486.

Tamoutounour, S., Henri, S., Lelouard, H., de Bovis, B., de Haar, C., van der Woude, C.J., Woltman, A.M., Reyal, Y., Bonnet, D., Sichien, D., et al. (2012). CD64 distinguishes macrophages from dendritic cells in the gut and reveals the Th1-inducing role of mesenteric lymph node macrophages during colitis. Eur. J. Immunol. *42*, 3150–3166.

Tamoutounour, S., Guilliams, M., MontananaSanchis, F., Liu, H., Terhorst, D., Malosse, C., Pollet, E., Ardouin, L., Luche, H., Sanchez, C., et al. (2013). Origins and functional specialization of macrophages and of conventional and monocyte-derived dendritic cells in mouse skin. Immunity *39*, 925–938.

Tamura, T., Nagamura-Inoue, T., Shmeltzer, Z., Kuwata, T., and Ozato, K. (2000). ICSBP directs bipotential myeloid progenitor cells to differentiate into mature macrophages. Immunity *13*, 155–165.

Tamura, T., Tailor, P., Yamaoka, K., Kong, H.J., Tsujimura, H., O'Shea, J.J., Singh, H., and Ozato, K. (2005). IFN regulatory factor-4 and -8 govern dendritic cell subset development and their functional diversity. J Immunol *174*, 2573–2581.

Tordjman, R., Ortéga, N., Coulombel, L., Plouët, J., Roméo, P.-H., and Lemarchandel, V. (1999). Neuropilin-1 Is Expressed on Bone Marrow Stromal Cells: A Novel Interaction With Hematopoietic Cells. Blood *94*, 2301–2309.

Torti, N., Walton, S.M., Murphy, K.M., and Oxenius, A. (2011). Batf3 transcription factor-dependent DC subsets in murine CMV infection: Differential impact on T-cell priming and memory inflation. Eur. J. Immunol. *41*, 2612–2618.

De Trez, C., Magez, S., Akira, S., Ryffel, B., Carlier, Y., and Muraille, E. (2009). iNOS-producing inflammatory dendritic cells constitute the major infected cell type during the chronic Leishmania major infection phase of C57BL/6 resistant mice. PLoS Pathog. *5*, e1000494.

Tussiwand, R., Everts, B., Grajales-Reyes, G.E., Kretzer, N.M., Iwata, A., Bagaitkar, J., Wu, X., Wong, R., Anderson, D.A., Murphy, T.L., et al. (2015). Klf4 Expression in Conventional Dendritic Cells Is Required for T Helper 2 Cell Responses. Immunity *42*, 916–928.

Varol, C., Landsman, L., Fogg, D.K., Greenshtein, L., Gildor, B., Margalit, R., Kalchenko, V., Geissmann, F., and Jung, S. (2007). Monocytes give rise to mucosal, but not splenic, conventional dendritic cells. J. Exp. Med. *204*, 171–180.

Vremec, D., J. Lieschke, G., R. Dunn, A., Robb, L., Metcalf, D., and Shortman, K. (1997). The influence of granulocyte/macrophage colony-stimulating factor on dendritic cell levels in mouse lymphoid organs. Eur. J. Immunol. *27*, 40–44.

Waldburger, J.M., Suter, T., Fontana, a, Acha-Orbea, H., and Reith, W. (2001). Selective abrogation of major histocompatibility complex class II expression on extrahematopoietic cells in mice lacking promoter IV of the class II transactivator gene. J. Exp. Med. *194*, 393–406.

Waskow, C., Liu, K., Darrasse-Jèze, G., Guermonprez, P., Ginhoux, F., Merad, M., Shengelia, T., Yao, K., and Nussenzweig, M. (2008). The receptor tyrosine kinase Flt3 is required for dendritic cell development in peripheral lymphoid tissues. Nat. Immunol. *9*, 676–683.

Witmer-Pack, M.D., Hughes, D.A., Schuler, G., Lawson, L., McWilliam, A., Inaba, K., Steinman, R.M., and Gordon, S. (1993). Identification of macrophages and dendritic cells in the osteopetrotic (op/op) mouse. J. Cell Sci. *104*.

Wu, L., D'Amico, A., Winkel, K.D., Suter, M., Lo, D., and Shortman, K. (1998). RelB is essential for the development of myeloid-related CD8a- dendritic cells but not of lymphoid-related CD8a+ dendritic cells. Immunity *9*, 839–847.

Wynn, T.A., Chawla, A., and Pollard, J.W. (2013). Macrophage biology in development, homeostasis and disease. Nature *496*, 445–455.

Xie, Q.W., Whisnant, R., and Nathan, C. (1993). Promoter of the mouse gene encoding calcium-independent nitric oxide synthase confers inducibility by interferon gamma and bacterial lipopolysaccharide. J. Exp. Med. *177*, 1779–1784.

Xu, Y., Zhan, Y., Lew, A.M., Naik, S.H., and Kershaw, M.H. (2007). Differential Development of Murine Dendritic Cells by GM-CSF versus Flt3 Ligand Has Implications for Inflammation and Trafficking. J. Immunol. *179*, 7577–7584.

Yamazaki, T., Akiba, H., Iwai, H., Matsuda, H., Aoki, M., Tanno, Y., Shin, T., Tsuchiya, H., Pardoll, D.M., Okumura, K., et al. (2002). Expression of programmed death 1 ligands by murine T cells and APC. J. Immunol. *169*, 5538–5545.

Yona, S., Kim, K.-W., Wolf, Y., Mildner, A., Varol, D., Breker, M., Strauss-Ayali, D., Viukov, S., Guilliams, M., Misharin, A., et al. (2013). Fate mapping reveals origins and dynamics of monocytes and tissue macrophages under homeostasis. Immunity *38*, 79–91.

Yoon, H., and Boss, J.M. (2010). PU.1 binds to a distal regulatory element that is necessary for B cell-specific expression of CIITA. J. Immunol. *184*, 5018–5028.

Yoshida, H., Hayashi, S.-I., Kunisada, T., Ogawa, M., Nishikawa, S., Okamura, H., Sudo, T., Shultz, L.D., and Nishikawa, S.-I. (1990). The murine mutation osteopetrosis is in the coding region of the macrophage colony stimulating factor gene. Nature *345*, 442–444.

Zhan, Y., Carrington, E.M., van Nieuwenhuijze, A., Bedoui, S., Seah, S., Xu, Y., Wang, N., Mintern, J.D., Villadangos, J.A., Wicks, I.P., et al. (2011). GM-CSF increases cross-presentation and CD103 expression by mouse CD8+ spleen dendritic cells. Eur. J. Immunol. *41*, 2585–2595.

Zhong, W., Fei, M., Zhu, Y., and Zhang, X. (2009). Transcriptional profiles during the differentiation and maturation of monocyte-derived dendritic cells, analyzed using focused microarrays. Cell. Mol. Biol. Lett. *14*, 587–608.

Zhou, Q., Ho, a. W.S., Schlitzer, a., Tang, Y., Wong, K.H.S., Wong, F.H.S., Chua, Y.L., Angeli, V., Mortellaro, a., Ginhoux, F., et al. (2014). GM-CSF-Licensed CD11b+ Lung Dendritic Cells Orchestrate Th2 Immunity to Blomia tropicalis. J. Immunol. *193*, 496–509.

Zhou, Y., Peng, H., Sun, H., Peng, X., Tang, C., Gan, Y., Chen, X., Mathur, A., Hu, B., Slade, M.D., et al. (2015). Chitinase 3–like 1 Suppresses Injury and Promotes Fibroproliferative Responses in Mammalian Lung Fibrosis. *6*, 1–28.

Zigmond, E., Varol, C., Farache, J., Elmaliah, E., Satpathy, A.T., Friedlander, G., Mack, M., Shpigel, N., Boneca, I.G., Murphy, K.M., et al. (2012). Ly6C hi monocytes in the inflamed colon give rise to proinflammatory effector cells and migratory antigen-presenting cells. Immunity *37*, 1076–1090.

Zinkernagel, R.M., and Doherty, P.C. (1974). Restriction of in vitro T cell-mediated cytotoxicity in lymphocytic choriomeningitis within a syngeneic or semiallogeneic system. Nature *248*, 701–702.